To Investigate the Subcellular Localisation of CBP (CREB-Binding Protein) and its Interacting Proteins

Thesis submitted for the degree of Doctor of Philosophy at the
University of Leicester

By
Colm M. Ryan BA (Mod) (Trinity College Dublin)

Department of Biochemistry,
University of Leicester
August 2006

UMI Number: U490770

All rights reserved

INFORMATION TO ALL USERS
The quality of this reproduction is dependent upon the quality of the copy submitted.

In the unlikely event that the author did not send a complete manuscript
and there are missing pages, these will be noted. Also, if material had to be removed,
a note will indicate the deletion.

UMI®
Dissertation Publishing

UMI U490770
Published by ProQuest LLC 2013. Copyright in the Dissertation held by the Author.
Microform Edition © ProQuest LLC.
All rights reserved. This work is protected against
unauthorized copying under Title 17, United States Code.

ProQuest®

ProQuest LLC
789 East Eisenhower Parkway
P.O. Box 1346
Ann Arbor, MI 48106-1346

Declaration

Unless otherwise acknowledged, the experimental work in this thesis has been carried out by the author in the Department of Biochemistry at the University of Leicester and the School of Pharmacy, University of Nottingham between October 2002 and August 2006. The work has not been submitted for any other degree at these or any other university

Signed: Colm Ry Date: 03/07/2007

Colm M Ryan

To Investigate the Subcellular Localisation of CBP and its Interacting Proteins

Colm M. Ryan

Synopsis

CBP (Creb-binding Protein) is a histone acetyltransferase that plays an essential role in RNA-polymerase II-dependent transcription. CBP is a dynamic component of PML bodies, which contain more than 50 proteins many of which have been shown to be SUMOylated. The CBP homologue, p300 was shown to be SUMOylated and CBP sequence is predicted to contain putative SUMO modification sites. Here we show that CBP is SUMOylated *in vivo* and *in vitro* and deletion of the putative SUMO sites abolishes SUMOylation. In addition we show that SUMOylation affects the subcellular localisation and co-activator function of CBP.

CBP acetylation of non-histone proteins such as p53, ACTR and Impα has been postulated to regulate their activity. The research described shows the interaction between CBP and the nuclear transport proteins CAS, Impα and the nucleoporin Nup93. We show that increasing global acetylation levels using HDAC inhibitors (HDACi) leads to a perturbation in the subcellular localisation of CAS, while the number of CBP-associated PML bodies increases. In addition, we demonstrate that CBP association with Impα increases in response to HDACi treatment. These results give us a novel insight into the regulation of non-histone proteins by HDACi. In addition, these findings suggest a functional link between chromatin regulation, acetylation and nuclear transport.

Mislocalisation of CBP from PML bodies has been implicated in the pathology of many diseases such as Huntington's disease and Acute Myeloid leukaemia expressing the fusion protein MOZ-TIF2. CBP mislocalisation has also been implicated in Kennedy's disease, a late onset neurodegenerative disorder, which expresses a mutant form of the Androgen Receptor (AR) with an expanded polyglutamine region. Reports in the literature suggest that the mislocalisation of CBP in Kennedy's disease may play a crucial role in its pathology. Here we describe experiments, which show that both CBP and PML are mislocalised in cells expressing AR with an expanded polyglutamine tract. Furthermore, we demonstrate that ARQ77-dependent transcriptional repression cannot be rescued by overexpression of CBP in a neuronal and non-neuronal cell line. These results shed new light on the potential role of CBP and PML in Kennedy's disease.

Dedicated to my parents Nicholas and Mary

Acknowledgements

This thesis would not have been possible without the help of many people who taught me so much. Firstly, my supervisor, David, for all his help, guidance and support during the last four years. He was not only my scientific mentor but was also a great friend too. Without his encouragement and commitment I would be back in Tipp long ago! I will be forever indebted to my lab colleagues and friends, Karin and Hilary, who gave up huge amounts of their time to teach me and to assist me in whatever problems I encountered. They thought me how to be a scientist and also let me annoy them constantly, both in the lab, and on all those coffee and lunch breaks. I would also like to thank Cristina, Ta and all the other lab members past and present for whose help I am grateful. Many thanks to my committee members, Dr. Andrew Fry and Prof. Bill Brammar, who taught me how to be critical of my own work. Thank you to the Department of Biochemistry, University of Leicester for my stipend, the BBSRC for my fees and AICR for funding me for the last year or so.

I would like to give a special thanks to a group of people who supported me throughout these last four years. My parents, Mary and Nicholas, without whose support and love I could not have survived. My brother Eoin and sister Nicki whose fun and laughter lifted my spirits on dark days. To Paul, who annoyed me and kept me company on many a rainy night in Gypsy lane and in the Dunkey! To Nanna and Granddad and the rest of my family for whose love this would not have been possible. To Lorna, whose love and support kept me going through the good and bad times, to you I will be eternally grateful. Finally, thanks to Jonas, for letting me stay when nobody would have me!, to Keith for food and enzymes!, to all the Willis group for letting me steal their enzymes and reagents!, to all the guys in Leicester and especially to www.football365.com, the website who should be awarding my thesis for all the time I spent on it!

TABLE OF CONTENTS

Title Page i

Declaration ii

Synopsis iii

Dedication iv

Acknowledgements v

Table of Contents vi

CHAPTER 1 1

INTRODUCTION 1

1.1 Nuclear organisation, dynamics and gene regulation 2

1.1.1 Introduction 2

  1.1.2 Transcription 3

  1.1.3 Chromatin and chromosomes 4

  1.1.4 Nucleosomes and histones 5

  1.1.5 The histone code hypothesis 7

  1.1.6 Histone post-translational modifications and chromatin remodelling 9

  1.1.7 Regulation of gene activity by chromosome dynamics 16

  1.1.8 Interchromatin domain and transcriptional control 18

  1.1.9 Nuclear bodies, transcriptional regulation and chromatin dynamics 18

1.1.10 SUMOylation is a key regulator of protein function 28
1.1.11 Acetylation and deacetylation of non-histone proteins 33
1.2.1 CBP – structure, function and subcellular localisation 36
1.2.2 CBP and Disease 43
1.2.3 Interaction between transcription-associated proteins, the NPC and nuclear transport proteins 47
1.2.4 The nuclear periphery and the NPC in the regulation of gene expression 50
1.3 Project aims 52

CHAPTER 2 **54**

MATERIALS AND METHODS **54**

2.1.1 General suppliers 55
2.1.2 Bacterial reagents 55
2.1.3 Molecular biology reagents 55
2.1.4 Tissue culture and transient transfection reagents 56
2.1.5 Protein chemistry, Western blotting and immunofluorescence reagents 56
2.1.6 Assay reagents 56

2.2 Bacterial preparation and culture **57**

2.2.1 Culture of *E. coli* DH5α 57
2.2.2 Preparation of *E. coli* competent cells 57
2.2.3 Transformation of competent *E. coli* 58
2.2.4 Long term storage of bacterial cultures 58
2.2.5 Composition of solutions and media used for bacterial methods 59

2.3 Molecular biology techniques **60**

2.3.1 Small scale plasmid DNA preparation 60

2.3.2 Large scale plasmid DNA preparation 60

2.3.3 Caesium Chloride Purification of Plasmid DNA 61

2.3.4 Spectrophotometric quantification of DNA 62

2.3.5 Phenol/chloroform extraction and ethanol precipitation of DNA 62

2.3.6 Agarose gel electrophoresis 63

2.3.7 Purification of DNA fragments from agarose gel slices 63

2.3.8 Restriction digest of DNA 63

2.3.9 Removal of 5' terminal phosphate groups from cleaved plasmid DNA 64

2.3.10 Ligation of DNA fragments 65

2.3.11 Polymerase Chain Reaction (PCR) 65

2.3.12 Annealing of single-stranded oligonucleotides 67

2.3.13 Polynucleotide Kinase treatment of DNA 67

2.3.14 Solutions 68

2.4 Cell culture **68**

2.4.1 Maintenance of cell lines 68

2.4.2 Transient transfection – Transfast method 69

2.4.3 Calcium phosphate-mediated transfection of adherent cells 69

2.5 Biochemical Techniques **70**

2.5.1 Preparation of cell-free extracts for Western blotting 70

2.5.2 Co-Immunoprecipitation 71

2.5.3 SDS-polyacrylamide gel electrophoresis (PAGE) 72

2.5.4 Western blotting 72

2.5.5 Protein assay 73

2.5.6 Harvesting adherent cells for reporter assays 73

2.5.7 Luciferase assays 74

2.5.8 Indirect Immunofluorescence 74

2.5.9 Live-Cell Imaging 76

2.5.10 Stripped FCS for nuclear receptor transfections 76

2.5.11 Small-scale bacterial expression of GST-tagged proteins 77

2.5.12 Large-scale bacterial expression of GST-tagged proteins 77

2.5.13 Purification of GST-tagged proteins 78

2.5.14 *In vitro* transcription and translation of expression vector-encoded cDNA 79

2.5.15 GST-pulldown of mammalian expressed protein 79

2.5.16 *In vitro* protein SUMOylation assay 79

2.5.17 Fixing and amplifying radioactive SDS-PAGE gels 80

2.5.18 Exposure of radioactive gels to x-ray film and phosphorimager plates 80

2.5.19 Solutions 80

2.6 Yeast methods 82

2.6.1 Yeast strains and culture conditions 82

2.6.2 Yeast transformation 82

2.6.3 Preparation of a yeast cell free lysate 83

2.6.4 Quantitative β-galactosidase activity assay 83

2.6.5 Composition of solutions and media used for Yeast methods 84

CHAPTER 3 85

EFFECT OF SUMO CONJUGATION ON THE SUBCELLULAR LOCALISATION AND COACTIVATOR FUNCTION OF CBP 85

3.1 Introduction 86

3.2 CBP foci colocalise with PML bodies *in vivo* 88

3.3 Live-cell imaging of YFP-CBP 90

3.4 GFP-SUMO-1, but not GFP-SUMO-1 Glycine97Alanine mutant colocalises with CBP in PML bodies 90

3.5 Endogenous CBP colocalises with PIAS-1, PIAS-xα and PIASγ In PML bodies 92

3.6 CBP is SUMOylated *in vivo* 94

3.7 CBP is SUMOylated between amino acids 998-1087 *in vitro* 101

3.8 Sequences outside the amino acids 998-1087 are essential for CBP SUMOylation *in vitro* 104

3.9 The acetyltransferase MOZ is modified by SUMO-1 and SUMO-2 *in vitro* 107

3.10 SUMOylation affects the subcellular localisation of CBP 108

3.11 Sequences outside CBP 998-1087 are necessary for formation of nuclear foci 111

3.12 Overexpression of PML IV recruits CBP and CBPΔ998-1087 into nuclear foci 117

3.13 SUMOylation state affects the ability of CBP to associate with SUMO foci 120

3.14 Overexpression of SUMO-1 has no clear effect on the subcellular localisation of CBP and CBPΔ998-1087 120

3.15 CBPΔ998-1087 moderately increases AML1 reporter activity in COS-1 cells 122

3.16 Discussion 125

CHAPTER 4 **132**

CBP INTERACTION WITH NUCLEAR TRANSPORT PROTEINS AND MODULATION BY HDAC INHIBITORS **132**

4.1 Introduction 133

4.2 CBP-SID interacts with the nuclear export factor CAS and the nucleoporin Nup93 135

4.3 Mutations in the SID disrupt the interaction with CAS 137

4.4 Construction of CAS-NΔ244-253 140

4.5 Expression analysis of yeast 2-hybrid constructs 142

4.6 Deletion of a conserved leucine-rich motif in CAS-N abrogates binding to CBP-SID 142

4.7 Endogenous and overexpressed CAS proteins are expressed in the nucleus and cytoplasm of mammalian cells 143

4.8 CAS proteins localise to the nucleus and cytoplasm of mammalian cells 145

4.9 Overexpressed CAS colocalises with CBP in COS-1 cells 147

4.10 HDAC inhibitors (HDACi) perturb the subcellular localisation of endogenous and overexpressed CAS proteins 150

4.11 TSA and NaB causes an increase in the number of CBP associated PML bodies 151

4.12 The interaction between CAS and CBP is indirect 155

4.13 Co-immunoprecipitations do not detect an interaction between CBP and CAS *in vivo* 164

4.14 HDACi treatment of COS-1 cells induces accumulation of Impα at the nuclear periphery 166

4.15 CBP overexpression leads to the accumulation of endogenous Impα at the nuclear periphery 166

4.16 Association of CBP and Impα *in vivo* 169

4.17 Colocalisation of overexpressed CBP and Impα at the nuclear periphery is increased on TSA treatment 172
4.18 Chapter summary 174

CHAPTER 5 **181**

TO INVESTIGATE THE EFFECT OF ARPOLYQ EXPRESSION ON THE SUBCELLULAR LOCALISATION OF CBP AND ITS INTERACTING PROTEINS **181**

5.1 Introduction 182
5.2 AR polyQ expression perturbs the subcellular localisation of endogenous CBP and PML in a ligand dependent manner 183
5.3 FLAG-ARwt and GFP-ARwt activate transcription of a reporter gene construct 191
5.4 CBP does not rescue ARQ-mediated repression 191
5.5 CBP does not rescue ARQ77-mediated transcriptional repression in SY-5Y cells 193
5.6 AR-mediated ligand-dependent activation of a GAL4-responsive reporter 195
5.7 Discussion 200

CHAPTER 6 CONCLUDING REMARKS **203**

Appendix: Oligonucleotides and antibodies **209**

References **217**

Publication List **250**

TABLE OF FIGURES

CHAPTER 1 1

Figure 1.1 Schematic representation of chromatin structure 6

Figure 1.2 Crystal structure of a nucleosome 8

Figure 1.3 Schematic depicting all the known human histone modifications 10

Figure 1.4 Schematic representation of SUMO conjugation 15

Figure 1.5 Schematic representation of the nucleus 20

Figure 1.6 Schematic showing the domain structure of PML and the various isoforms 24

Figure 1.7 Schematic depicting some of the PML body 29

Table 1.1 Table showing the effect of acetylation on some of the known non-histone proteins 34

Figure 1.8 Domain structure of CBP and its interacting proteins 38

Figure 1.9 Ribbon diagrams depicting the NMR structure of CBP-SID (Blue) complexed with SRC-1 AD1 (Red) 41

Table 1.2 Table showing a proportion of the diseases associated with dysregulation of CBP 44

Figure 1.10 Schematic representation of the classical NLS-mediated import pathway 49

CHAPTER 3 85

Figure 3.1 Endogenous CBP colocalises with PML bodies 89

Figure 3.2 Live-cell imaging of YFP-CBP in HEK293 91

Figure 3.3 CBP co-localises with GFP-SUMO-1 fusion proteins 93

Figure 3.4 Endogenous CBP colocalises with PIAS proteins 95

Figure 3.5 SUMOplot of CBP sequence 96

Figure 3.6 CBP contains 27 putative SUMO conjugation sites 97

Figure 3.7 CBP is SUMOylated in COS-1 cells 99

Figure 3.8 YFP-CBP is SUMOylated in HEK293 cells *in vivo* 100

Figure 3.9 CBP is SUMOylated between amino acids 998-1087 102

Figure 3.10 Schematic of CBP C-terminal deletions 105

Figure 3.11 Sequences outside CBP amino acids 998-1087 are essential for SUMOylation 106

Figure 3.12 The acetyltransferase MOZ is SUMOylated *in vitro* 109

Figure 3.13 Expression analysis of YFP-CBP fusion proteins 110

Figure 3.14 YFP-CBP and YFP-CBPΔ998-1087 partially colocalise with PML bodies 112

Figure 3.15 Expression of CBP C-terminal deletions in COS-1 and HEK293 cells 114

Figure 3.16 Deletion of CBP C-terminus affects its subcellular localisation 115

Figure 3.17 FLAG-CBP 1-1100 displays various phenotypes in COS-1 cells 116

Figure 3.18 FLAG-CBP 1-507 is a diffuse nuclear protein 118

Figure 3.19 FLAG-PML IV recruits YFPCBP and partially recruits YFPCBPΔ997-1087 into nuclear bodies 119

Figure 3.20 YFP-CBP but not YFPCBP Δ998-1087 colocalises with endogenous SUMO-1 121

Figure 3.21 Overexpression of FLAG-SUMO-1 has no effect on the ability of YFP-CBP or YFP-CBPΔ998-1087 to colocalises with SUMO-1 foci 123

Figure 3.22 SUMOylation affects CBP mediated AML-1-dependent transcription 124

CHAPTER 4 **132**

Figure 4.1 CBPSID interacts with the nuclear export factor CAS and Nic96 136

Figure 4.2 Mutations in CBP-SID disrupt interaction with CAS 138

Figure 4.3 Western blot analysis of Y2-H CAS-N fusion constructs 141

Figure 4.4 A conserved leucine rich motif is necessary for the interaction between CAS-N and CBPSID 144

Figure 4.5 Western Blot analysis of endogenous and overexpressed CAS 146

Figure 4.6 Endogenous CAS and YFP-CAS proteins display cytoplasmic and nuclear localisation 148

Figure 4.7 Overexpressed CAS colocalises with endogenous and overexpressed CBP in COS-1 cells 149

Figure 4.8 TSA perturbs the subcellular localisation of endogenous CBP and CAS proteins 152

Figure 4.9 NaB perturbs the subcellular localisation of endogenous CBP and CAS proteins 153

Figure 4.10 TSA perturbs the subcellular localisation of overexpressed CAS 154

Figure 4.11 Endogenous CBP and PML colocalise after treatment with HDACi 156

Figure 4.12 Quantification of PML bodies HDACi treated COS-1 cells 158

Figure 4.13 SDS-PAGE gels showing expression of GST-fusion proteins and |35S|-labelled *in vitro* translated SRC1, CAS, CAS-N, Impα and RANQ69L 160

Figure 4.14 The interaction between CBP-SID and nuclear transport proteins is undetectable via GST-pulldown 161

Figure 4.15 The interaction between overexpressed CAS and GST-SID is undetectable 163

Figure 4.16 Interaction between CBP and CAS 165

Figure 4.17 TSA perturbs the subcellular localisation of endogenous CBP and Impα 167

Figure 4.18 NaB perturbs the subcellular localisation of endogenous CBP and Impα 168

Figure 4.19 Overexpression of CBP leads to the accumulation of endogenous Impα at the nuclear periphery 170

Figure 4.20 CBP associates more strongly with Impα in TSA treated cells 171

Figure 4.21 CBP and Impα colocalisation at the nuclear periphery is increased on TSA treatment 173

Figure 4.22 Full view crystal structure of CSE1 177

Figure 4.23 Partial viewcrystal structure of CSE1 178

CHAPTER 5 181

Figure 5.1 Subcellular localisation of GFP-ARwt and endogenous CBP in COS-1 cells 185

Figure 5.2 Subcellular localisation of GFP-ARQ and endogenous CBP in COS-1 cells 186

Figure 5.3 GFP-ARQ perturbs the subcellular localisation of endogenous CBP in COS-1 cells 187

Figure 5.4 Subcellular localisation of GFP-ARwt, GFP-ARQ and endogenous PML in COS-1 cells 189

Figure 5.5 GFP-ARQ expression perturbs PML bodies in COS-1 cells 190

Figure 5.6 FLAG-ARwt and GFP-ARwt activate the MMTV-luc reporter in HEK293 cells 192

Figure 5.7 FLAG-ARQ represses AR-dependent MMTV-luc reporter activity in COS-1 cells 194

Figure 5.8 FLAG-ARQ represses AR-dependent MMTV-luc reporter activity in SY-5Y cells 196

Figure 5.9 FLAG-ARQ represses GAL4-AD1-dependent transcription in SY-5Y cells 198

Figure 5.10 FLAG-ARQ represses GAL4-AD1-dependent transcription in COS-1 cells 199

CHAPTER 6 CONCLUDING REMARKS 203

Figure 6.1 Schematic showing the interactions between CBP, nuclear transport proteins and the NPC 206

Figure 6.2 Model of the mechanism of action of the wild-type AR and mutant AR polyQ 208

Appendix: Oligonucleotides and antibodies 209

Figure A.1 Schematic of mutagenesis using PCR 210

Figure A.2 List of primers used in the cloning of YFP-CAS, VP16-AAD-CASΔ244-253 and HIS-CBPΔ998-1087 211

Table A.3 Table of all primers used and their sequences 212

Table A.1 Table showing the antibodies used for all applications 213

Table A.2 Table showing the sources of all plasmids used 215

Chapter 1

Introduction

1.1 Nuclear organisation, dynamics and gene regulation

1.1.1 Introduction

Life on earth is highly diverse, ranging from the simple single-cell prokaryotes to the amazingly complex multicellular mammals. The simplest and the most complex organisms share common features in which metabolic processes are tightly regulated ensuring that cells grow, divide and even die when they should. Within each and every cell, is a plethora of molecular machinery performing the functions necessary for survival. The very blueprint for existence is contained within these cells in the form of genes made up of deoxyribonucleotides. Indeed, the mechanisms involved in reading the blue-print of life have to be tightly controlled to ensure that each cell within each organism performs its exact function on time, every time. In addition, there are many layers of complexity that ensure that genes are turned on and off at the correct time. The position of chromosomes within their own territories or relative to the nuclear periphery acts as a method of regulating gene activity. Not only is the position of the chromosomes important; another layer of complexity exists in the form of histone modifications, which regulate the accessibility of the chromosomes to proteins which control gene expression. The proteins regulating these cellular processes can sometimes be found associated with a myriad of non-membranous nuclear bodies which add yet another layer of complexity by sequestering them until required. These and many more proteins and signalling pathways combine to regulate gene expression that ultimately control cell growth, metabolism and division.

1.1.2 Transcription

Eukaryotic transcription is a multi-step process that is much more complex than prokaryotic transcription. In the eukaryotic cell nucleus there are three distinct RNA polymerases. RNA polymerase I (RNAPI) is found primarily in the nucleolus and is responsible for the transcription of the rRNA genes. RNAPIII is a nuclear enzyme that is involved in the transcription of small RNAs such as tRNA and 5S rRNA while RNAPII transcribes mRNA.

Genes transcribed by RNAPII generally contain common core-promoter elements that are recognised by RNAPII and associated factors and also gene-specific regulatory elements that are recognised by additional transcription factors (Roeder, 1996). However, RNAPII is unable to initiate transcription on its own, it needs additional factors such as the general transcription factors (GTFs) of which at least six have been identified (TFIIA, TFIID, TFIID, TFIIE, TFIIF and TFIIH). The first putative step in the transcription of mRNA occurs when a transcription factor binds its cognate response element and recruits activators or in the case of some transcription factors, leads to the dissociation of co-repressors. This is followed by the recruitment of TFIID which recognises the TATA box, the most common core-promoter element which is located approximately 25 base pairs (bp) upstream from the transcription start site. TFIID consists of the TATA-box binding protein (TBP) which makes contact with the minor groove of DNA and ~10 TBP associated factors (TAFs). TFIID bound to the promoter is stabilised by TFIIA and together this allows the assembly of the RNAPII holoenzyme complex which occurs in a stepwise manner. TFIIB, a single polypeptide, that can bind sequences upstream and downstream of the TATA-box, makes contact with TBP and TFIIA. This is followed by the binding of the pre-formed RNAPII-TFIIF complex which causes the melting of the DNA at the promoter to expose the template strand through the helicase activity of TFIIF. Binding of TFIIH is the next step in the pathway. TFIIH consists of 9 subunits, two of the largest subunits XPB and XPD have helicase activity and are important in nucleotide excision repair, while another subunit phosphorylates RNAPII C-terminal domain (CTD) which is an essential step in promoter clearance and elongation. Finally different regulatory factors such as Srb-Mediator, Srb10-CDK and the ATPase-dependent chromatin remodeler, Swi-Snf, bind to complete the formation of the pre-initiation complex. This results in promoter clearance and the beginning of elongation with the dissociation of RNAPII from the transcription factors and other complexes that are required for initiation (Roeder, 1996; Molecular Biology of the cell, 4th edition Garland science). However, an alternative pathway for preinitiation complex formation was uncovered by several laboratories that purified a pre-assembled holoenzyme complex. In addition, many chromatin remodelling factors and HATs also co-purified suggesting that the whole pre-initiation complex may form and then activate transcription (Thomas *et al.*, 2006). This is the basis of eukaryotic transcription but DNA is not free to be accessed by the transcription machinery at any time – it is a tightly regulated process.

1.1.3 Chromatin and chromosomes

The human genome sequence predicted that there are approximately 30,000 genes which are spread throughout 3.2 billion base pairs of DNA packaged into a nucleoprotein structure called chromatin. The chromatin must be accessible to proteins that mediate recombination, replication, repair, mitotic condensation and transcriptional regulators that mediate the activation or repression of target genes. All this must occur within the nucleus which has an average volume of 600-1500 μm^3 (Spector, 2003). To enable all the DNA to fit within the nucleus, 146bp of DNA is wrapped 1.65 times around two molecules of each core histone; H2A, H2B, H3 and H4, that form an octamer and comprise the basic repeating unit of chromatin, the nucleosome. Each nucleosome is spaced 180-200bp along eukaryotic DNA which form the 10nm chromatin fibre or 'beads on a string' conformation. The remaining 50bp of linker DNA allows the incorporation of linker histones such as H1 or H5 allowing the chromatin to be further compacted into the 30nm solenoid chromatin fibre providing a 30-40 fold compaction of chromatin. Beyond this the structure of chromatin is poorly understood, although it is hypothesised that the 30nm fibre can form transcriptionally active loops from the central chromosome structure which is classically referred to as 'euchromatin'. The antithesis of this is 'heterochromatin', another level of compaction that sees the chromatin condensed into a transcriptionally inactive 700nm fibre. As the chromosomes prepare for mitosis the chromatin is condensed into 1400 nm fibres, which are best represented by the 'typical' mitotic chromosome (Figure 1.1). The mitotic chromosome is 50,000 times shorter than its fully extended length. However, the primary determinant of DNA accessibility is the nucleosome, due to its role as the principal packager of DNA within the eukaryotic nucleus (Alberts *et al.,* 1998).

1.1.4 Nucleosomes and histones

Histones were discovered by Albrecht Kossel in 1884 who named them after the German word "Histon", of unknown origin (Eisenstein *et al.,* 2005). Unsurprisingly, it was not until the 1990s the role of histones in DNA packing was elucidated. The four histones that comprise the nucleosome octamer, H2A, H2B, H3 and H4 are highly conserved proteins that share a very similar structural motif of 3 α-helices separated by loops. Histones form pairs with identical copies of themselves forming dimers or 'histone-fold pairs'. These are defined by H3-H4 and H2A-H2B histone pairs, which associate to form a large protein octamer or nucleosome. The H3-H4 tetramer interaction is mediated by a 4-helix bundle between the two H3 molecules while H2A-H2B interacts with the H3-H4 tetramer through a homologous 4-helix bundle between H2B and H4. The nucleosome core particle forms through association of the H3-H4 tetramer with DNA followed by the association of two separate H2A-H2B dimers. Histones H2B, H3 and H4 interact with DNA through alpha-helices which cause a net positive charge to accumulate at the

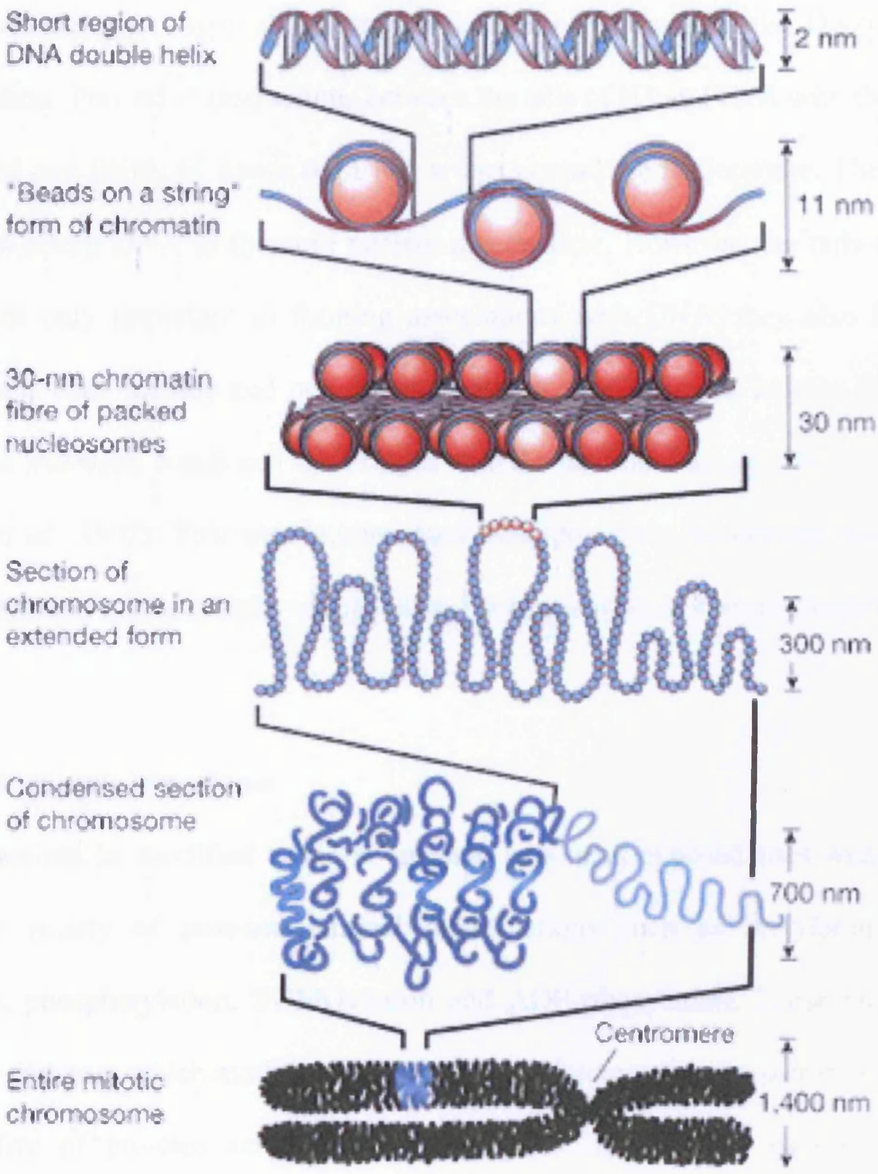
Short region of DNA double helix
2 nm
"Beads on a string" form of chromatin
11 nm
30-nm chromatin fibre of packed nucleosomes
30 nm
Section of chromosome in an extended form
300 nm
Condensed section of chromosome
700 nm
Centromere
Entire mitotic chromosome
1,400 nm

Figure 1.1 Schematic representation of chromatin structure (taken from Felsenfeld *et al.,* 2003)

point of interaction with the negatively charged phosphate groups of DNA (Figure 1.2). Also, the amine group on the main chain of histone proteins can interact with the DNA backbone via hydrogen bonding. Two other interactions between the tails of H3 and H2A with the DNA occur at the entry and exit points of where the DNA wraps around the nucleosome. These interactions are believed to clamp DNA to the core nucleosome particle. However, the tails of histones H3 and H4 are not only important in forming associations with DNA, they also form extensive interactions with other histone and non-histone proteins. For example, histone H3 K16 to N25 makes multiple hydrogen bonds and salt bridges with the basic and acidic side chains of H2A and H2B (Luger *et al.,* 1997). Post-translational modifications of the N-terminal tails and globular regions of histones is a major mode of regulating the association of histones with DNA and other proteins.

1.1.5 The histone code hypothesis

Histones can be modified at the N-terminal tails or at exposed sites within the globular regions by a variety of post-translational modifications such as acetylation, methylation, ubiquitination, phosphorylation, SUMOylation and ADP-ribosylation. These modifications are carried out by enzymes which modify the chromatin architecture thereby increasing or decreasing the accessibility of proteins involved in transcription, DNA repair and recombination to chromatin. Some modifications can lead to a compaction of chromatin structure which blocks access or causes the dissociation of proteins from sites within the chromatin. A proportion of these modifications are compatible with each other, for example, acetylation of H3 Lysine 14 (H3 K14), methylation of H3 Lysine 4 (H3 K4) and phosphorylation of H3 Serine 10 (H3 S10) are synonymous with transcriptional activation, however, these modifications are not present when H3 Lysine 9 (H3 K9) is methylated, a mark of transcriptional inhibition (Santos-Rosa *et al.,* 2005). Therefore, Jenuwein and Allis (2001) proposed the 'histone code' hypothesis which

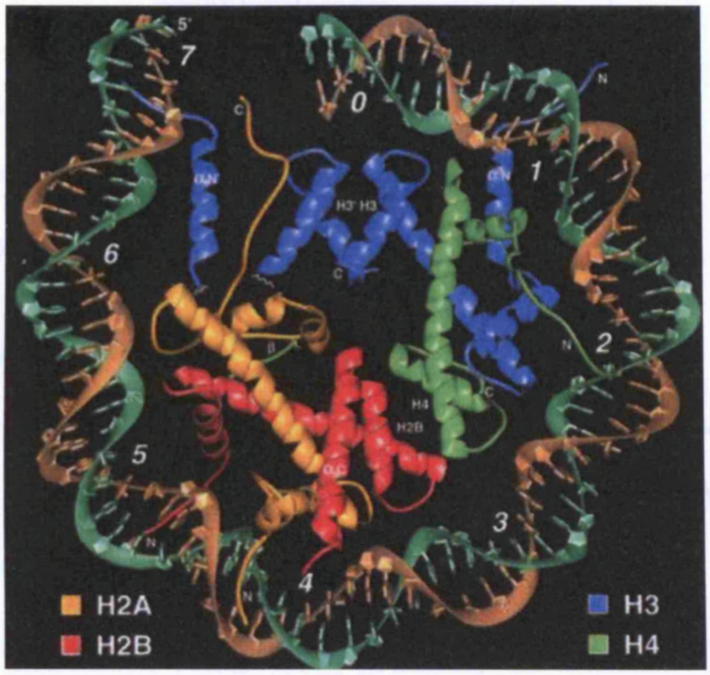
5'
7
0
1
6
2
5
3
4
H3' H3
H4
H2B
H2A
H2B
H3
H4

Figure 1.2 Crystal structure of a nucleosome. Histones are shown in light green, blue, pink and yellow ribbon model while DNA is shown as green and brown ribbons (taken from Luger *et al.,* 1997)

postulated that certain marks on histones are 'read' by other proteins such as bromodomain containing proteins, which recognise acetylated lysine residues and proteins with a chromodomain, that can recognise methylated residues, thus leading to a potentiation or inhibition of downstream processes depending on the mark. Figure 1.3 shows all the known post-translational modifications of human histones.

1.1.6 Histone post-translational modifications and chromatin remodelling

In this section I will give a brief overview of how the main post-translational modifications affect histone and ultimately chromatin structure. The effect of post-translational modifications on the regulation of non-histone proteins is discussed later.

Acetylation of histones is synonymous with transcriptional activation and is carried out by a group of enzymes known as histone acetyltransferases (HATs). Acetylation of the ε-amino group of lysine residues on histone tails increases the space between the nucleosome and the DNA thus preventing repressive modifications and leading to the recruitment of transcription activators. HATs can be organised into families based on sequence similarity of their HAT domains. The p300/CBP family are global transcriptional coactivators that contain a bromodomain and are primarily responsible for the acetylation of lysine residues on the N-terminal tails of all 4-core histones (this will be discussed in more detail later). Other HAT families include the Gcn5/pCAF family which are coactivators for a subset of transcription factors and the MOZ, YBF2, SAS2, TIP60 (MYST) family so called because of high conservation between the 370 amino acids in the MYST domain (Troke *et al.*, 2006). Interestingly, while both the CBP/p300, Gcn5/pCAF and MYST family members contain a bromodomain, only MYST family members have a chromodomain, allowing the recognition of methylated residues (Santos-Rosa *et al.*, 2005).

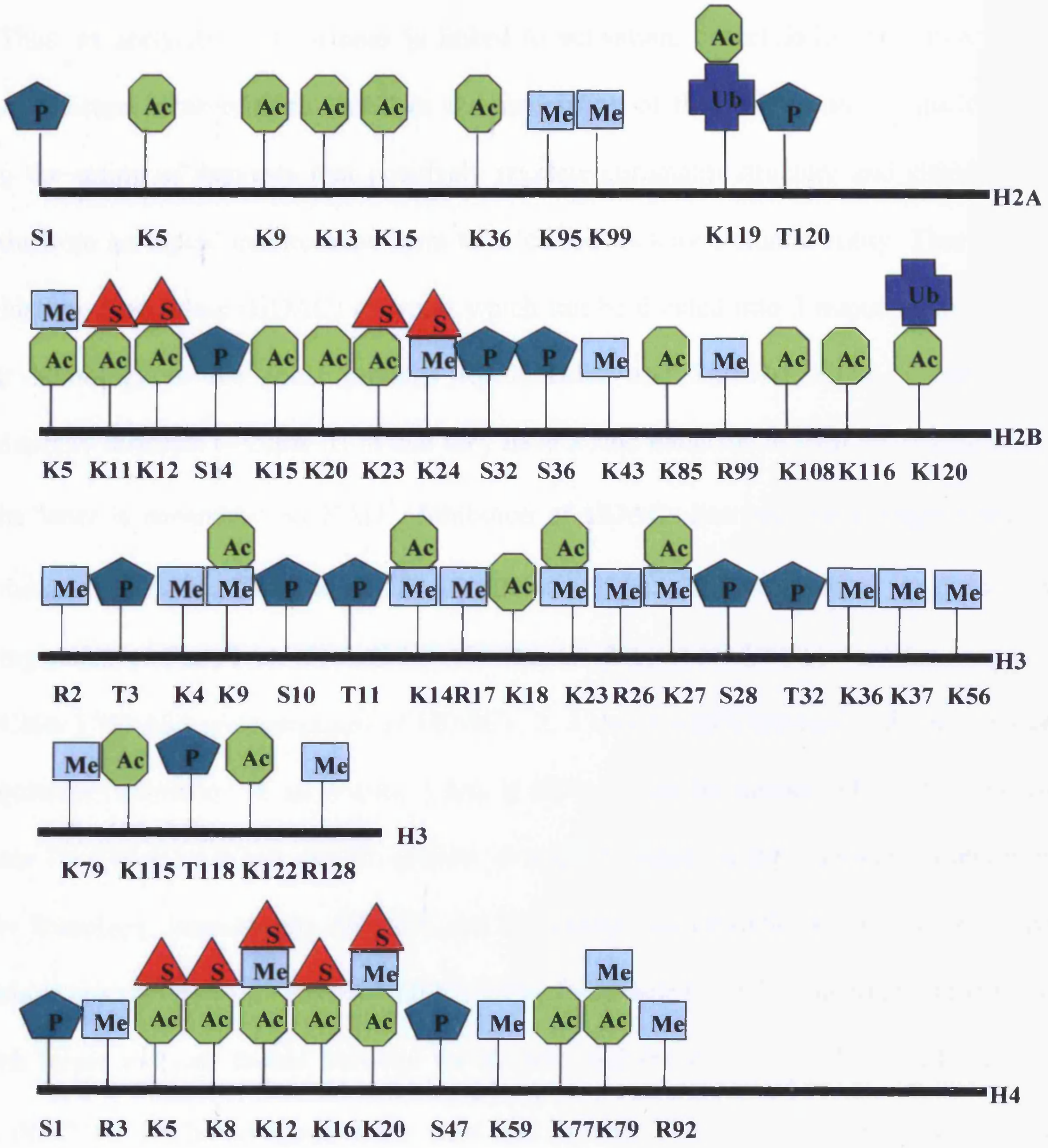
P
Ac
Me
Ub
S
H2A
S1 K5 K9 K13 K15 K36 K95 K99 K119 T120
H2B
K5 K11 K12 S14 K15 K20 K23 K24 S32 S36 K43 K85 R99 K108 K116 K120
H3
R2 T3 K4 K9 S10 T11 K14 R17 K18 K23 R26 K27 S28 T32 K36 K37 K56
H3
K79 K115 T118 K122 R128
H4
S1 R3 K5 K8 K12 K16 K20 S47 K59 K77 K79 R92

Figure 1.3 Schematic depicting all the known human histone modifications. P-Phosphate, Me-Methyl, Ac-Acetyl , Ub-Ubiquitin, S-SUMO (SUMO residues only mapped in *S.cerevisiae).* Reconstructed from Peterson *et al.* (2004) and www.abcam.com.

Thus, as acetylation of histones is linked to activation, deacetylation is a byword for repression. Histone deacetylation increases the association of the DNA with the nucleosome, blocking the action of enzymes that positively regulate chromatin structure and changing the chromatin from an 'open' euchromatic form to a 'closed' heterochromatic entity. There are 18 known histone deacetylase (HDAC) enzymes which can be divided into 3 major families based on their homology to the yeast proteins Rpd3, Hda1 and Sir2/Hst. Class 1 and II are mechanistically different to Class III in that they have a zinc molecule at their enzymatic pocket while the latter is dependent on NAD^+. Inhibition of HDACs has become a major focus for cancer therapy and most of the known HDAC inhibitors (HDACi) are known to target the zinc-containing pocket of Class I and Class II HDACs (Santos-Rosa *et al.*, 2005).

Class 1 HDACs are comprised of HDAC1, 2, 3 and 8 which localise to the nucleus and are ubiquitously expressed in all tissues. Class II HDACs can be further subdivided into two subclasses IIa (HDAC 4,5,7,9) and IIb (HDAC 6 and 10) based on their domain structure and sequence homology. Interestingly, HDAC6 and 10 contain two catalytic domains which makes them unique among HDACs. Class II HDACs differ from their Class I counterparts in that they are much larger and can shuttle between the nucleus and the cytoplasm. The third class, the sirtuins (SIRT1-7) are homologous to the yeast Sir2 protein. They require NAD^+ in their active site and their catalytic activity is inhibited by nicotinamide (NAM) (Lin *et al.*, 2006). However, HDACs not only are involved in the deacetylation of histones they also regulate the deacetylation of many non-histone proteins such as p53 (Luo *et al.*, 2001). This will be discussed in more detail later.

Methylation is defined as the replacement of a hydrogen atom with a methyl group and has emerged as a post-translational modification of histones to rival acetylation. While lysine residues can only be mono-acetylated, the side-chain nitrogen atoms of lysine residues can be mono-, di- or tri-methylated and arginine residues can accept either one or two methyl groups. This leads to a greater level of combinatorial complexity compared to lysine acetylation alone. Also, while acetylation generally precedes transcriptional activation, the many combinations of methyl modifications in addition to the other histone modifications can have pleiotropic effects on chromatin structure in accordance with the histone code hypothesis. For example, methylation of H3 K4 is associated with activation and results in the recruitment of Isw1p ATP-dependent chromatin remodelling protein to chromatin (Santos-Rosa *et al.,* 2003). However, Tri-methylation of H3 K9 results in the formation of heterochromatin and serves as a mark for the recruitment of the heterochromatic formation protein HP1 (Nielsen *et al.*, 2001).

The proteins that catalyse the methylation of arginine residues are the protein arginine methyltransferases (PRMTs) which share sequence homology within their catalytic domain but not outside. They can be divided into two families; type 1 which include the co-activator-associated R-methyltransferase 1 (CARM1) and PRMT1 proteins and are responsible for the asymmetric dimethylation of arginine (Strahl *et al.*, 2001). Type II PRMTs include the PRMT7 and PRMT5 proteins and catalyse the symmetric dimethylation of arginines. Arginine methylation is generally viewed as a mark of activation and many of the type II PRMTs associate with ATPase-chromatin remodelling complexes (Lee *et al.*, 2005).

Lysine methylation is carried out by a group of enzymes which have high sequence homology within the Su(var), Enhancer of zeste and trithorax (SET) domain. Different members of this family methylate different lysine substrates; SET7/9 catalyse the mono-methylation of H3 K4 while SET8 can switch between mono-methylation of H4 K20 to di-methylation at the onset of mitosis depending on cell signals (Rice *et al.*, 2002).

However, like acetylation, methylation is a reversible process. Cuthbart *et al.,* (2004) discovered that the methyl group on arginines could be converted into citrulline by a deimination process. They identified PADI4 as the enzyme responsible for the deimination of methylated arginines on H3 and H4. Further work carried out by Shi *et al.* (2004) determined that histone lysine methylation could be reversed by lysine demethylase, LSD1, an FAD-dependent amine oxidase.

The ubiquitination of protein targets was originally believed to target proteins for degradation. Ubiquitin is conjugated onto its target by means of E1 – ubiquitin maturation enzymes, E2 – ubiquitin conjugation enzymes and E3 and E4 ubiquitin ligases which regulate the specificity of the reaction (Pickert, 2001). Polyubiquitination has been shown to target proteins for degradation via the ubiquitin-proteosome pathway; however, monoubiquitation of histones has been shown to affect their methylation state. A proteomic screen to identify the mechanism of histone H3 methylation in *S. cervisiae* and subsequent studies identified mono-ubiquitination of H2B K123 by RAD6 as being essential for the methylation of H3 K4 (Schneider *et al.*, 2004; Dover *et al.*, 2002). Just like acetylation and methylation monoubiquitination is a reversible process. The *S. cervisiae*, Ubp8, which catalyses the deubiquitination of H2B, is a component of the SAGA HAT complex. Studies have shown that mono-ubiquitination of H2B results in the association of the SAGA complex which subsequently deubiquitinates H2B and initiates transcription (Henry *et al.*, 2003; Daniel *et al.*, 2004).

Of course other histone modifications play crucial roles in regulating chromatin structure such as phosphorylation and SUMOylation. Interestingly, phosphorylation of serine residues can lead to completely different downstream effects in agreement with the 'histone code'. For example, during hormonal or mitogenic activation of mammalian cells, H3 S10 is phosphorylated which blocks the methylation of H3 K9 and is coupled to the acetylation of H3 K9 and H3 K14 which are linked to transcriptional activation (Jenuwein *et al.*, 2001). However, at the onset of mitosis, members of the aurora AIR-Ip11 kinase family catalyse the phosphorylation of H3 S10 leading to chromatin condensation (Zeitlin *et al.*, 2001). Other modifications at the onset of mitosis, such as H3 S28 and H3 T11, have also been shown to be important in mitotic condensation (Santos-Rosa *et al.*, 2005). Thus, it appears that phosphorylation of histone tail residues can lead to the activation of transcription or condensation of chromatin but other modifications which act synergistically must be taken into account.

Small ubiquitin-like modifier (SUMO) is an 11kDa protein that is homologous to ubiquitin but rather than target proteins for degradation it has been shown to regulate their subcellular localisation and activity (this will be discussed in more detail later). SUMO is conjugated onto the lysine residue that is part of the ψKXE motif (ψ - any large hydrophobic amino acid, K – Lysine, X – any amino acid, E – glutamic acid). It is conjugated onto its target proteins by E1, E2 and E3 SUMO enzymes. The E1 enzymes (SAE1/2) catalyse the maturation of SUMO which then forms a thioester bond with the E2 enzyme Ubc9. Ubc9 makes contact with the ψKXE motif and catalyses the formation of an isopeptidase bond between SUMO and the lysine residue. Unlike ubiquitin, there is only one known SUMO E2 conjugation enzyme, Ubc9, but more and more E3 ligases are being uncovered (Figure 1.4). Due tc the lack of any ψKXE motif within the histone sequences, it was thought unlikely that histones could be SUMOylated. However, as we know of only one E2 conjugation enzyme it seems likely that there may be other SUMO ligases which are specific for histone SUMOylation. The first report of histone SUMOylation came from Shiio and Eisenman (2003) who showed the SUMOylation of histones *in vitro* and in mammalian cells via co-immunoprecipitation. In addition they found that SUMOylation of H4 was a repressive mark and led to a decrease in H4 acetylation and recruitment of HP1 to heterochromatin. Nathan *et al.*, (2006) mapped SUMO sites on H2B to K6 or K7 and showed that, even after deletion of 5 putative SUMO sites in H4, there was still residual SUMOylation. Furthermore, they observed a dynamic interplay between SUMOylation and acetylation suggesting that SUMO acts as a repressive mark by preventing the onset of transcription.

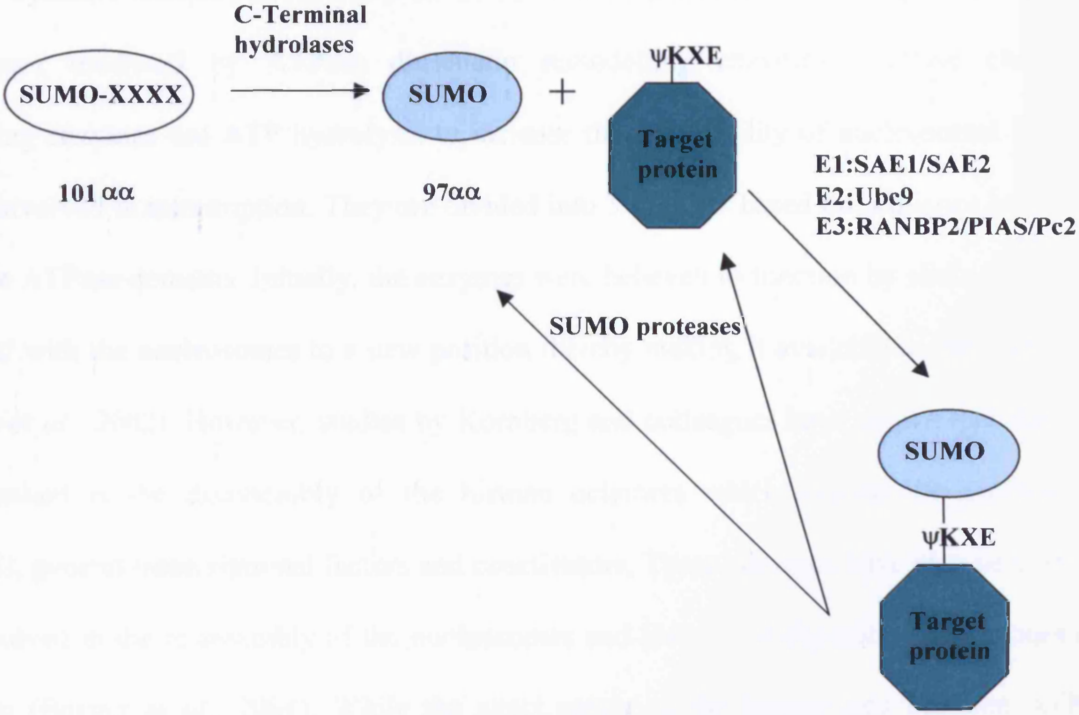
C-Terminal hydrolases
SUMO-XXXX
101 αα
SUMO
97αα
+
ψKXE
Target protein
E1:SAE1/SAE2
E2:Ubc9
E3:RANBP2/PIAS/Pc2
SUMO proteases
SUMO
ψKXE
Target protein

Figure 1.4 Schematic representation of SUMO conjugation. Including the maturation, conjugation and deconjugation of SUMO onto its target protein.

A dynamic interplay exists between histone modifications and the change in position of nucleosomes mediated by ATPase chromatin remodelling enzymes. ATPase chromatin remodelling enzymes use ATP hydrolysis to increase the accessibility of nucleosomal DNA to proteins involved in transcription. They are divided into 3 families based on sequence homology within the ATPase domains. Initially, the enzymes were believed to function by sliding the DNA associated with the nucleosomes to a new position thereby making it available to other enzymes (Narlikar *et al.,* 2002). However, studies by Kornberg and colleagues have shown that the more likely method is the disassembly of the histone octamers which expose the promoter to RNAPolII, general transcriptional factors and coactivators. These enzymes have also been shown to be involved in the re-assembly of the nucleosomes and also in the deposition of histones into chromatin (Boeger *et al.,* 2004). While the exact nature of the interactions between ATPase chromatin remodellers and histone modifying enzymes remains to be elucidated it appears that they can work in synergy to change chromatin structure. In addition, many HATs, HDACs and methyltransferases can be found in complexes with ATPase chromatin remodelling enzymes. For example, the chromo-ATPase/helicase-DNA binding domain (CHD) proteins 1 and 2, associate with the nucleosome-remodelling complex which has repressive activity (Tong *et al.,* 1998).

1.1.7 Regulation of gene activity by chromosome dynamics

Gene regulation at the histone level has been firmly established as a mode of regulating gene expression. However, the study of the position of the chromosomes within the nucleus is bringing to light another mode of regulating the expression of genes. At the beginning of the last century a series of elegant experiments carried out by the German biologist Theodore Boveri, on the nucleus of the horse nematode, *Ascaris megalocephala*, detailed the layout of chromosomes in the interphase nucleus (reviewed in Baxter *et al.,* 2002). These experiments revealed that chromosomes are arranged non-randomly in interphase nuclei and this reflects their position at mitosis (Baxter *et al.,* 2002). Further work by many groups using probes for individual chromosomes found that chromosomes occupy a defined, non-overlapping space within the interphase nucleus, thus the term chromosome territory (CT) was coined (Trask *et al.,* 1988). Therefore, the nucleus can be divided into 2 subcompartments: the chromosome territory and the remaining space, the interchromatin domain (ICD), which contains macromolecular complexes required for transcription, replication and repair (Cremer *et al.,* 2001).

The movement of chromosomes within the CTs with respect to gene regulation has become the cause of some controversy. Cremer *et al,* (2001) suggested that inactive genes are located at the periphery of CTs or may extend in loops outside to the ICD and active gene-rich regions concentrate at the interior of CTs. Mahy *et al.* (2002), on studies with human chromosome 11p13 and the syntenic region in the mouse, which contain ubiquitously expressed genes and tissue-specific genes, found that all expressed genes were located within the CT compared to a similar locus from 11p15. However, the bulk of evidence points towards the movement of transcriptionally active chromosome regions to move towards the periphery of the CT. Studies of the chromosome 1 territory, 1q21, which contains genes involved in keratinocyte development, are found towards the periphery of chromosome 1 territory during ketatinocyte development when they are active but not in lymphoblasts where they are transcriptionally inactive (Williams *et al.,* 2002). Similar results were observed in studies of the gene-rich major histocompatibility complex (MHC) which resides at human chromosome 6p21.3 (Volpi *et al.,* 2000). They showed that the MHC was located to the periphery of the CT or to large chromosomal loops which extended into the ICD. In addition, induction of the MHC class II genes resulted in an increased incidence of the MHC gene cluster at external chromosomal loops. Thus, the general consensus is that CTs are relatively porous, allowing transcriptional activators, which reside in the ICD, access to the internal or peripheral genes depending on the signals received (Dundr and Misteli, 2001).

1.1.8 Interchromatin domain and transcriptional control

Cook and colleagues put forward the hypothesis that transcription occurs at specific sites within the ICD termed "transcription factories" (Bartlett *et al.*, 2006). These factories which are ~50nm in diameter not only contain RNAPII but also associate with a whole host of transcription factors, chromatin remodelling factors and coactivators. Fakan and colleagues found that transcription sites were distributed throughout the nucleoplasm with a preference for the periphery of condensed chromatin (Fakan, 1994). In addition, it is believed that transcription sites are associated with perichromatin fibrils, which represent nascent transcripts due to their RNAase sensitivity. Work carried out by Pombo *et al.* (1999) using a mixture of electron microscopy and Br-UTP labelling of HeLa nuclei revealed that there are approximately 10,000 non-nucleolar transcription sites, 8000 of which are thought to be RNAPII sites and each site contains 5-6 active polymerases. Therefore, how are transcription factories associated with CTs and how does this association affect transcription? Osborne *et al.* (2004) using a combination of 3D-FISH, immunofluorescence and chromosome conformation assays of a 40MB region of chromosome 7, proposed a model whereby chromosome loops extend into the CT and into the ICD where they associate with transcription factories and active genes are transcribed.

1.1.9 Nuclear bodies, transcriptional regulation and chromatin dynamics

Using immunofluorescence microscopy the sub-nuclear localisation of general transcription factors (GTFs), coactivators and chromatin remodelling factors has been analysed. Grande *et al.* (1997) examined the subcellular localisation of the glucocorticoid receptor (GR), the transcription factors OCT1 and E2F, the chromatin-remodelling factor, BRG1 and also TFIIH and TFIIE. They found that these proteins were finely distributed throughout the nucleoplasm and were excluded from the nucleolus. Surprisingly, apart from TFIIH, little colocalisation was observed between any of the factors and active sites of transcription. It is now believed that this lack of colocalisation is due to the transient nature of the interaction between components of the transcription machinery and RNAPII (Spector, 2003). However, many of these proteins not only display a diffuse punctate nuclear staining they associate with other nuclear domains such the Oct/PTF/transcription domain (OPT) domain, Cajal bodies, nuclear speckles and promyelocytic leukemia (PML) bodies which have been shown to affect the subcellular localisation and function of transcription factors, DNA replication and repair enzymes, and other proteins of differing cellular functions (Figure 1.5).

Low-levels of pre-mRNA splicing factors are found dispersed throughout the nucleoplasm but are found highly-concentrated in sites variously referred to as 'nuclear speckles', 'SC35 domains' and Interchromatin granule clusters (ICGs) (Hall *et al.*, 2006). There are ~10-30 ICGs per cell and they range in size from 20-25nm in diameter. Like many nuclear domains, ICGs were originally proposed to function as storage sites for modification and/or assembly of pre-mRNA splicing factors which would allow the movement of these factors to active genes (Hall *et al.*, 2006). However, recently it has come to light that ICGs are associated in a euchromatic centre around which many genes are clustered (Shopland *et al.*, 2003). In addition, it was demonstrated that poly (A) RNA was enriched in the ICGs, while the gene corresponding to the RNA is found adjacent to the ICG. Interestingly, perichromatin granules, active sites of transcription, have been found adjacent to ICGs. Hendzel *et al.* (1998) using immunofluorescence and electron microscopy demonstrated that transcriptionally active chromatin was enriched adjacent to ICGs. But, if splicing also occurs at the periphery of the ICG then why must mRNA still pass through the ICG prior to export? Recent evidence using

COL1A1 mRNA showed that it was efficiently spliced before entry into the ICG. However, a splice-defective mutant of COL1A1

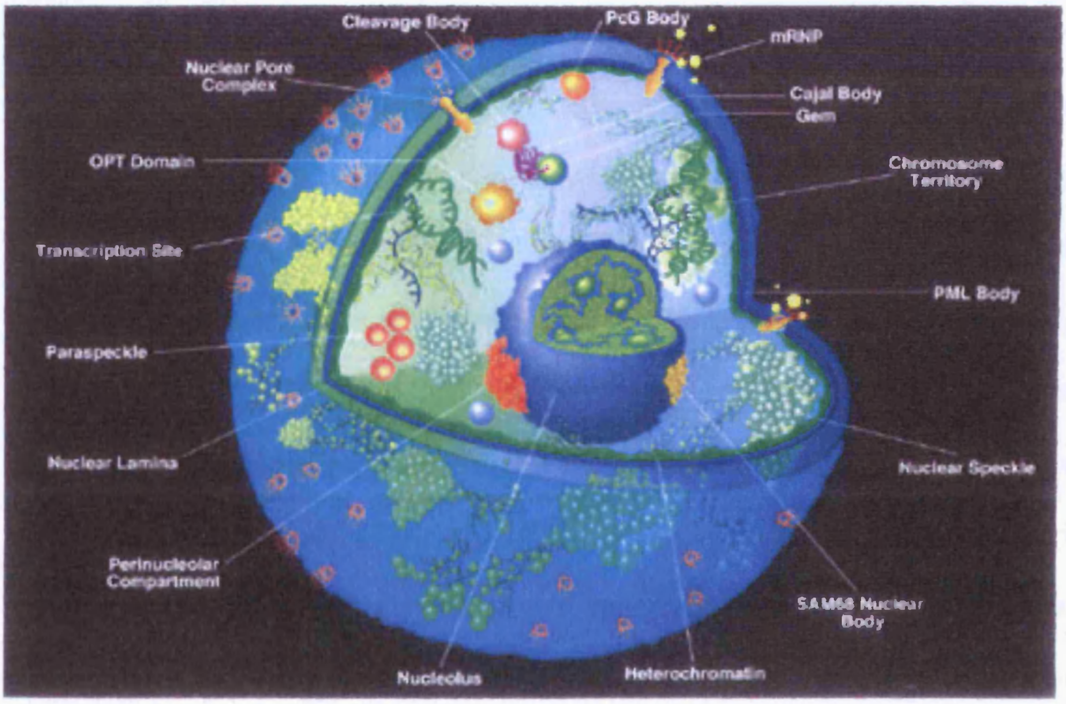
Cleavage Body
PcG Body
mRNP
Nuclear Pore Complex
Cajal Body
Gem
OPT Domain
Chromosome Territory
Transcription Site
PML Body
Paraspeckle
Nuclear Lamina
Nuclear Speckle
Perinucleolar Compartment
SAM68 Nuclear Body
Nucleolus
Heterochromatin

Figure 1.5 Schematic representation of the nucleus, showing all the known compartments and bodies (taken from Spector, 2003).

mRNA fails to export to the cytoplasm and is concentrated at ICGs (Johnson *et al.,* 2000). Furthermore, many factors such as REF/Aly which is involved in mRNA export, are concentrated at the ICGs. Allied to this is the discovery that nonsense mediated decay proteins, Y14 and RPNS1, associate with the ICGs (Kataoka *et al.,* 2000, and Mayeda *et al.,* 1999). Therefore, it is hypothesised that ICGs act as checkpoints linking specific pre-mRNA transcription, splicing and export to the rapid recycling of RNA metabolic complexes which allows the expression of highly active genes (Hall *et al.,* 2006).

Cajal bodies were first discovered by Ramon y Cajal in 1903 as nucleolar accessory bodies in neurons. They are ~1.0µm to 2.0µm structures which cap the nucleolus and number one to five per cell nucleus but their number is cell-type specific. They are not found in all cell types but are prominent in highly proliferative cells and neurons. While the exact function of Cajal bodies has not yet been elucidated they are associated with gene clusters encoding U4, U11 and U12 snRNAs (Jacobs *et al.,* 1999). Cajal bodies are enriched in small guide RNAs that play a key role in the maturation of snoRNPs and snRNPs (Cioce *et al.,* 2005). In addition, they contain factors involved in mRNA splicing, pre-rRNA processing and histone mRNA 3' end formation. Interestingly, associated with Cajal bodies are "gemini of Cajal bodies" or Gems, which contain proteins essential for snRNP assembly. Cajal bodies are believed to be involved in the storage and modification of snRNP, the assembly of pre-splicing complexes and the delivery of snRNPs to the nucleolus (Zimber *et al.,* 2004). Cajal bodies have also been shown to have other functions in the cell: certain factors involved in the cellular stress response such as p53 are found to associate with Cajal bodies after cellular stress (Cioce *et al.,* 2005). Also, Cajal bodies have been implicated as key integrators of several cell proliferation based phenomena such as histone biogenesis and cell cycle progression (Cioce *et al.,* 2005). Thus, Cajal bodies seem to be a focal point for many proteins involved in various cellular functions.

The OPT was found in discrete nuclear foci along with a diffuse nuclear staining in ~30% of HeLa cells (Pombo *et al.*, 1998). Oct1 and PTF form a complex which is involved in the transcription of snRNAs. Interestingly, this domain is located close to the nucleolus and contains RNAPII, TBP and transcripts generated from RNAPII and RNAPIII. It is often found associated with chromosome 6p21 and chromosome 7 and thus it is hypothesised that the OPT plays a role in recruiting genes to a particular region of the nucleus where the appropriate factors are contained, thereby facilitating the expression of genes (Pombo *et al.*, 1998).

The polycomb group genes (PcG) were first identified in Drosophila as negative regulators of homeotic genes (Lorente *et al.,* 2006). There are two separate PcG protein complexes, PRC2 which includes EED, YY1 SU(Z)12 and the methyltransferase EZH2 and PRC1 consisting of HPH, HPC and the ubiquitin ligases RING1 and BMI1. Several groups have shown that the DNA binding components of PcG complexes such as YY1 recruits the PRC2 which methylates H3 K27. This mark is 'read' by the PRC1 complex which contains E3 ubiquitin ligase activity and is postulated to play a role in the maintenance of heterochromatic silencing. Interestingly a subset of PcG proteins such as the heterochromatin associated BMI1 and HPC2, associate in discrete nuclear foci called PcG bodies. These are ~0.2 to 1.5μm in diameter and are found in the interchromatin space and are highly concentrated at the border of pericentric heterochromatin. Recently, a new component of the PcG bodies was recently identified, Pc2, which has SUMO E3 ligase activity. Pc2 SUMOylates the transcriptional co-repressor CtBP and CtBP2 which results in the recruitment of the E2 SUMO ligase, Ubc9 into PcG bodies (Kagey *et al.*, 2003). These results point to a possible role for PcG bodies as centres where proteins involved in transcriptional silencing can assemble. Furthermore, the fact that histone SUMOylation is associated with silencing (Nathan *et al.*, 2006) may suggest a possible link between SUMO, PcG bodies and heterochromatin formation and silencing.

Perhaps the best studied of the non-membranous nuclear domains are the PML bodies, also known as ND10 bodies or PML oncogenic domains (PODs) (Jensen *et al.*, 2001). PML bodies non-membranous nuclear structures that range in size from 0.5 to 1.0 μm in diameter and number between 5-30 bodies per cell (Luciani *et al.*, 2006). PML bodies were first identified in patients with acute promyelocytic leukemia (APL) which is associated with the t(15,17) translocation creating a fusion between the *promyelocyte* gene and the *retinoic acid receptor alpha* gene resulting in the expression of an aberrant fusion protein, PML-RARα. APL is characterised by expression of PML-RARα which results in a block in myeloid cell differentiation. Expression of PML-RARα leads to (1) the recruitment of co-repressors to the RARα promoter and (2) the fragmentation of PML bodies into hundreds of tiny dots (microspeckles) in the nucleus and cytoplasm of APL cells (Jensen *et al.*, 2001).

The PML protein itself contains 3 cysteine-rich zinc-binding domains: a RING finger, two B-boxes containing an additional 2 zinc fingers and a coiled-coil domain which together form the RBCC motif (or tripartite motif, TRIM) (Figure 1.6). RING finger family members mediate the interaction between ubiquitin E2 conjugation enzyme and E3 ligases. Interestingly, the PML RING finger was shown to interact with the E2 SUMO ligase Ubc9 which promoted the SUMOylation of PML. Deletion of the conserved zinc fingers in the cysteine-rich B-boxes results in the disruption of PML body formation *in vivo*. Furthermore, substitution of the SUMO motif within the B-Box prevents the recruitment of the 11S proteasomal subunit to PML bodies (Lallemand-Breitenbach *et al.*, 2001). The coiled-coil domain is principally involved in mediating homo-dimerisation of PML and hetero-dimerisation with PML-RARα. Deletion of the coiled-coil domain prevented the formation of PML bodies *in vivo* and also abrogated its tumour suppressor function (Fagioli *et al.*, 1998). PML also has a C-terminal nuclear localisation signal

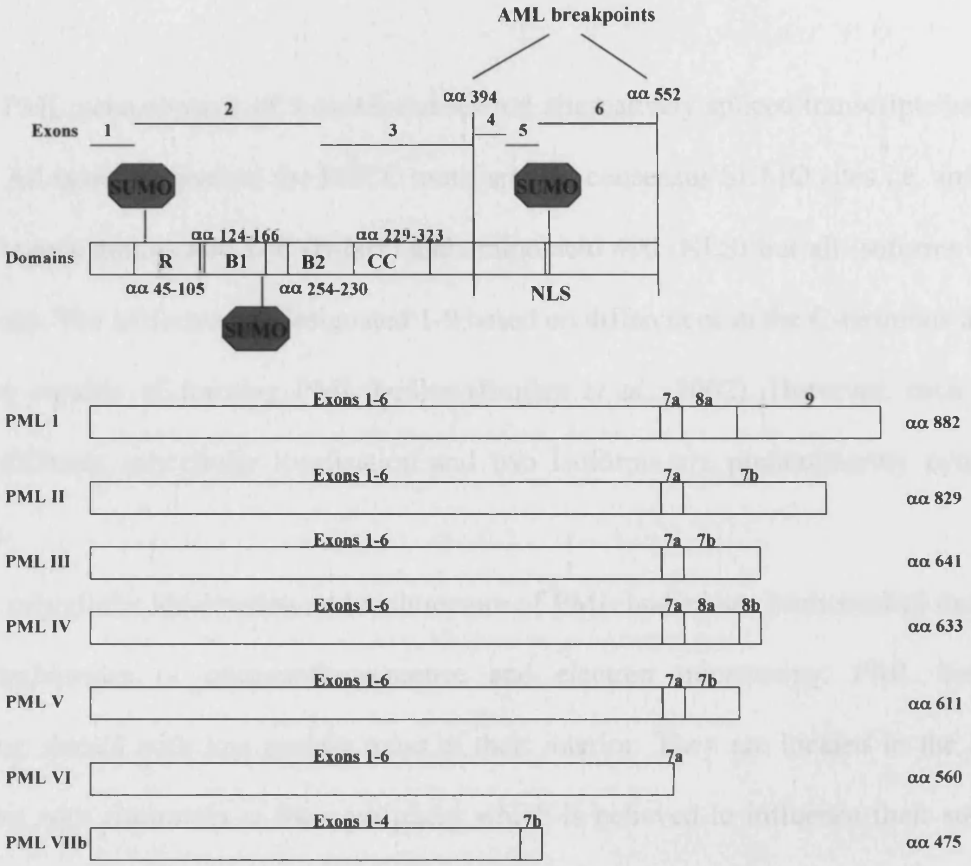
AML breakpoints
αα 394
αα 552
Exons
1
2
3
4
5
6
SUMO
SUMO
αα 124-166
αα 229-323
Domains
R
B1
B2
CC
αα 45-105
αα 254-230
NLS
SUMO
PML I
Exons 1-6
7a
8a
9
αα 882
PML II
Exons 1-6
7a
7b
αα 829
PML III
Exons 1-6
7a
7b
αα 641
PML IV
Exons 1-6
7a
8a
8b
αα 633
PML V
Exons 1-6
7a
7b
αα 611
PML VI
Exons 1-6
7a
αα 560
PML VIIb
Exons 1-4
7b
αα 475

Figure 1.6 Schematic showing the domain structure of PML and the various isoforms. R- RING finger, B1/2 – B-boxes, CC – coiled-coil domain, NLS – nuclear localisation signal.

and deletion of this prevents nuclear accumulation of PML and PML body formation (Le *et al.*, 1996).

The PML gene consists of 9 exons and several alternatively spliced transcripts have been discovered. All isoforms contain the RBCC motif and the consensus SUMO sites i.e. amino acid 65 (RING finger), amino acid 160 (B-box) and amino acid 490 (NLS) but all isoforms differ at the C-terminus. The isoforms are designated 1-9 based on differences in the C-terminus and most isoforms are capable of forming PML bodies (Borden *et al.*, 2002). However, each isoform displays a different subcellular localisation and two isoforms are predominantly cytoplasmic (Figure 1.6).

The subcellular localisation and architecture of PML bodies has been studied extensively using a combination of immunofluorescence and electron microscopy. PML bodies are spherical/ring shaped with less protein mass at their interior. They are located in the ICD and make contact with chromatin at their periphery which is believed to influence their subcellular localisation (Dellaire *et al.*, 2001). While PML is the only known structural protein of the bodies, other proteins such as Sp100 and DAXX are postulated to play a role in the structure and function of PML bodies. Furthermore, SUMO has been shown to play a major role in regulating the function of PML bodies and associated proteins, which will be discussed in more detail later. PML body size and movement has been shown to change during certain conditions such as viral infection, genotoxic stress, heat-shock treatment and S-phase of the cell-cycle, which restricts their movement in the ICD. During these conditions the bodies break-up or "bleb" to form microstructures with constrained diffusion but eventually fuse to form parental bodies. In addition, Dellaire *et al.* (2006) showed that the increase in PML body number during S-phase was due to changes in chromatin structure. Interestingly, parental PML bodies can be divided into three classes based on their movement within the cell. Using Sp100 as a marker for PML bodies they found that one class did not exhibit any movement, class II exhibited limited movement, while class III moved rapidly in an ATP-dependent manner (Muratani *et al.,* 2002). They hypothesised that class III PML bodies may be able to rapidly relocate to certain nuclear compartments during cellular stress or when needed for rapid transcription or emergency DNA repair.

However, the exact function of PML bodies is unknown. Studies of the subcellular localisation of PML bodies and their association with other nuclear structures has provided some insight into their function. PML bodies have been found adjacent to and associate with Cajal bodies and ICGs (Borden, 2002). Recently, Sun *et al.* (2005) demonstrated that the link between PML bodies and ICGs may be mediated by coilin (a component of Cajal bodies) and PIASγ (a PML body component). However, PML bodies do not associate with any known splicing factors and do not contain RNA. Taken together these results suggest that PML bodies could play some sort of role in RNA-processing events.

PML bodies have been implicated in the cellular stress response. Treatment of cells with UV-irradiation or genotoxic agents induces the accumulation of p53 in PML bodies where it is acetylated by CBP or phosphorylated by Chk-2 (Bernardi *et al.,* 2004). Furthermore, PML-/- cells fail to induce p53-dependent expression in response to genotoxic cells suggesting that PML bodies are important regulators of DNA damage and apoptosis.

PML bodies have also been implicated in DNA replication as PML bodies associate with replication sites in late S-phase but at no other time during replication (Grande *et al.,* 1996). In addition, proteins involved in DNA repair have been shown to interact with PML bodies. Interestingly, in has come to light that a proportion of PML bodies termed, ALT-associated PML bodies (APB) play an important role in the alternative lengthening of telomeres (ALT) in a subset of cells. Telomere length is shortened every time a cell divides and the cell enters a state of replicative senescence after a defined number of cell divisions. Tumour cells overcome this by activating telomerase which maintains telomere length. However, ~10% of tumour cells devoid of telomerase can maintain telomere length using an alternative mechanism – ALT. PML bodies associate with proteins involved in DNA metabolism such as BLM, Mre11 and NBS1. Mutations in these genes are associated not only with genomic instability but also with ALT (Nabetani *et al.*, 2004).

However, it is the role that PML bodies play in gene regulation that has stirred up the most interest. The association of PML bodies with RNA and transcription sites has provoked some controversy. La Morte *et al.* (1998) demonstrated that PML bodies contained nascent RNA but this was refuted by evidence provided by Boisvert *et al.* (2000). However, PML bodies have been shown to associate with RNAPII and active sites of transcription at their periphery (Spector, 2003). Also, using Br-UTP incorporation and staining for PML bodies it has been shown that PML bodies associate with ~7% of transcription sites and this increases to ~42% on interferon treatment. Interferon treatment increases the number of PML bodies but it is not known exactly how the association between PML body number and transcription correlate (Fuchsova *et al.*, 2002). Furthermore, PML bodies have been implicated in transcription mainly due to their association with a large number of transcription factors and coactivators such as p53, CBP, p300 and Rb (Borden, 2002). Interestingly, PML bodies have been found to associate non-randomly with the gene-rich MHC class II locus on chromosome 6 and many of the genes at this locus are regulated by the PML body-associated protein sp100 (Shiels *et al.*, 2001).

PML bodies have been postulated to provide a centre where transcription factors, coactivators or co-repressors can form into active complexes which are then able to relocate to active transcription sites (Best *et al.*, 2002). Contrary to this report, is the recent finding that a subset of PML bodies contain the heterochromatin protein 1 (HP1) and ATRX which are involved in the maintenance of heterochromatin. Due to the association of PML bodies with satellite DNA, HP1, ATRX and DAXX at G2-phase of the cell cycle, Luciani *et al.* (2006)

proposed that a subset of PML bodies function to re-establish heterochromatic state on late-replicated satellite DNA.

Thus, it appears that there may be different classes of PML bodies carrying out diverse cellular functions, which may be tissue-specific, cell cycle-dependent or in response to cellular stresses.

1.1.10 SUMOylation is a key regulator of protein function

The post-translational modification of non-histone proteins is an important way of regulating their function. Many proteins that associate with nuclear bodies and in particular PML bodies are SUMOylated (Figure 1.7). SUMOylation is coming to light as a very important post-translational modification of proteins and has been shown to regulate their subcellular localisation and transcriptional activity.

Ubiquitin family members and the ubiquitin-like proteins such as NEDD8 and SUMO have added an extra degree of complexity to the proteasomal system of protein degradation/stability. While the formation of multimeric ubiquitin chains targets proteins for degradation, SUMOylation of the same lysine residues has been shown to oppose the action of ubiquitin (Johnson, 2004). SUMO shares only 20% sequence homology with ubiquitin however the C-terminal ubiquitin-like domain is almost completely super-imposable on the ubiquitin 3-D structure (Johnson, 2004). 4 SUMO paralogues are expressed in vertebrates, designated SUMO-1, -2, -3, -4. SUMO-1 (Smt3c, PIC1, GMP1, sentrin, Ubl1) is 50% homologous to SUMO-2 and SUMO-3 which differ from each other in only 3 N-terminal residues whose function is unknown (Saitoh *et al.*, 2000, Tatham *et al.*, 2001). SUMO-1 forms monomeric chains and mainly exists conjugated onto its target proteins while SUMO-2/-3 can form multimeric chains and is mainly found in large free pools which are conjugated onto their targets after stress such as acute heat-

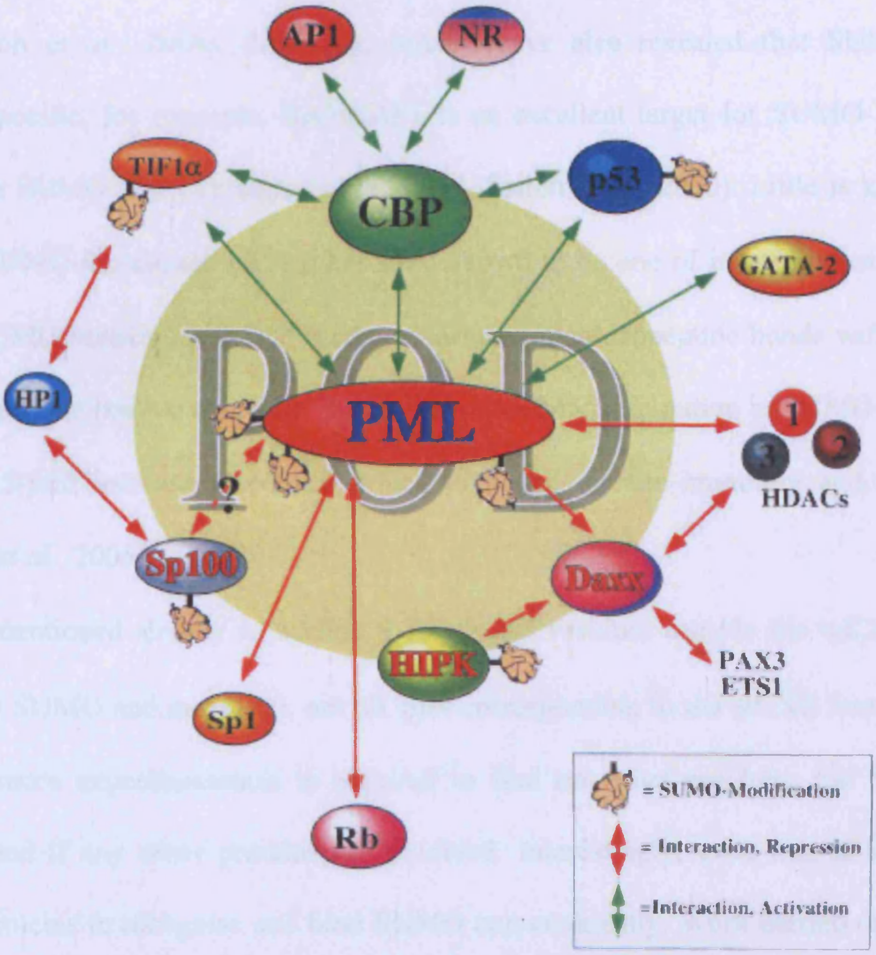
AP1
NR
TIF1α
CBP
p53
GATA-2
POD
PML
HP1
1
3
2
HDACs
?
Sp100
Daxx
HIPK
PAX3
ETS1
Sp1
Rb
= SUMO-Modification
= Interaction, Repression
=Interaction, Activation

Figure 1.7 Schematic depicting some of the PML body. Including associating proteins and the role of SUMO in regulating their function taken from Lin *et al.,* 2001. POD – PML oncogenic domain.

shock (Saitoh *et al.,* 2000). Proteomic screens have also revealed that SUMO targets are paralogue specific, for example, RANGAP1 is an excellent target for SUMO-1 but is a poor substrate for SUMO-2/-3 (Vertegaal *et al.,* 2004, Saitoh *et al.,* 2000). Little is known about the intronless SUMO-4 although NF-κB has been shown to be one of its substrates. It differs from the other SUMO paralogues in that it cannot form covalent isopeptide bonds with substrates due to a unique proline residue at residue 90. However, an M55V mutation in SUMO-4 was shown to result in a 5-fold increase in NF-κB which is linked to auto-immunity and type 1 diabetes (Owerbach *et al.,* 2005).

As mentioned already in section 1.1.6, lysine residues outside the ψKXE motif can be modified by SUMO and moreover, not all sites corresponding to the ψKXE motifs are modified. Therefore, more experimentation is required to find out what regulates the SUMOylation of substrates and if any other proteins are involved. Interestingly, even less is known about the ability of proteins to recognise and bind SUMO non-covalently. Work carried out by Song *et al.* (2004) demonstrated that the minimal SUMO interaction motif consensus was V/I-X-V/I-VI, where X is any amino acid. Many proteins contain this motif including the mismatch repair protein, TDG, which can be modified and interact non-covalently with SUMO. TDG interaction with PML bodies was shown to be mediated by the recognition of TDG for SUMOylated PML (Takahashi *et al.,* 2005).

New families of SUMO E3 ligases which increase the efficiency of conjugation have recently been discovered. The PIAS (Protein Inhibitor of Activated STAT) family, the largest family of SUMO E3 ligases, are similar to ubiquitin E3 RING ligases and were originally identified as inhibitors of activated STAT proteins. Kotaja *et al.* (2002) *elucidated* the mechanism of action of the PIAS family members by identifying their ability to act as E3 SUMO ligases. PIAS members aid the E2 SUMO ligase Ubc9 in the conjugation of SUMO to the target protein. However, while the exact mode of how these two proteins act cooperatively is unknown, structural studies with another SUMO E3 ligase, Nup358/RanBP2, revealed that it acts as an E3 ligases to RanGAP1 by binding both Ubc9 and SUMO-1 to position SUMO-E2-thioester in an energetically optimal position enhancing conjugation of SUMO-1 to RANGAP1 (Reverter *et al.*, 2005). Further studies revealed that different PIAS members display substrate specificity e.g. PIAS1 and PIASxβ acts as an E3 ligase in the SUMOylation of p53 and c-Jun (Schmidt *et al.*, 2002), while PIAS3 promotes the SUMOylation of IRF-1 (Nakagawa *et al.*, 2002). RANBP2 also known as Nup358, is a nucleoporin SUMO E3 ligase that is situated in the basket of the nuclear pore complex. It is neither a HECT- nor RING-type E3 ligase and was originally identified as an E3 ligase for RANGAP1, SUMOylation of which is essential for its association with the nuclear rim (Saitoh *et al.*, 2006). Furthermore, it acts as an E3 ligase for hnRNP C and M proteins thereby decreasing their binding to nucleic acids (Vassileva *et al.*, 2004). These and other results suggest that RANBP2 plays an important role in the SUMOylation of substrates in and around the nuclear pore complex.

Seven enzymes have been identified which act as SUMO isopeptidases, designated SUMO protease 1-3 and 5-8 (SENP), based on homology to the yeast Ulp1, the first identified SUMO protease (Li *et al.*, 1999). They have a dual role in the SUMO pathway: they are responsible for the initial processing of the SUMO polypeptide prior to conjugation and they also promote the deconjugation of SUMO from higher molecular weight proteins (Di Bacco *et al.*, 2006). All have divergent N-termini and localise to different subcellular localisations. These include SENP1 which localises to nuclear foci and the nuclear rim, SENP3, which localises to the nucleolus while SENP6 is cytoplasmic (Johnson, 2004).

SUMO has emerged as a major player in regulating the subcellular localisation of many cellular proteins. As already mentioned, PML contains 3 SUMO sites which are essential for the proper formation of PML bodies (Kamitani *et al.*, 1998). PML mutated for the SUMO sites forms mutant aggregates in PML-/- cells and moreover, many of the PML body associated proteins such as Sp100, DAXX, CBP and SUMO-1 fail to colocalise with these aggregates (Johnson, 2004). Interestingly, arsenic trioxide, which is used to treat patients expressing the PML-RARα fusion protein, promotes the hyper-SUMOylation of PML and leads to the formation of PML bodies. However, virus infection generally leads to the deconjugation of SUMO from PML and ultimately, PML body break-up (Muller *et al.,* 1999). Other proteins associating with PML bodies have been shown to be SUMOylated, for example, Sp100 (Sternsdorf *et al.,* 1997), p53 (Rodriguez *et al.,* 1999) and CBP (Kuo *et al.,* 2005) which will be discussed in more detail later. SUMOylation of many PML body proteins is essential for there localisation to these structures. For example, mutation of SUMO sites within the orphan receptor LRH-1 led to its release from PML bodies which facilitated its association with chromatin (Chalkiadaki *et al.,* 2005). In addition, a study by Best *et al.* (2002) on the SUMO protease, SuPr-1, suggested that co-activators are recruited into the PML bodies where they form into active complexes, which are de-SUMOylated and free to dissociate from the PML bodies and associate with their targets. They showed that SuPr-1 bound to SUMO-modified PML stimulated c-jun mediated transcription by redistributing co-activators associated with PML bodies. This included CBP which was dispersed once SuPr-1 had hydrolysed the SUMO modified PML.

Not only does SUMO modification of histones negatively regulate transcription but SUMOylation of some transcription factors and coactivators results in the recruitment of HDACs. Yang *et al.,* (2004) demonstrated that SUMOylation of the Ets1 family member, the Elk-1 transcription factor, resulted in the recruitment of HDAC-2 to the Elk-1 promoter. This recruitment led to a decrease in histone acetylation and transcriptional repression of Elk-1-responsive genes. SUMOylation of the CBP paralogue, p300, at a domain termed the cell-cycle regulatory domain 1 (CRD1) led to the recruitment of HDAC6 and transcriptional repression (Girdwood *et al.,* 2003).

1.1.11 Acetylation and deacetylation of non-histone proteins

Acetylation of lysine residues is a widespread phenomena in eukaryotes. Since, 1964 in experiments carried out by Allfrey *et al.,* (1964) acetylation of histones has been shown to be an essential regulator of gene expression. However, it was not until 1997 that the acetylation of non-histone proteins was found to be an equally important regulator of protein function (Gu *et al.,* 1997). Interestingly, like most other post-translational modifications this is a reversible modification and acetylation can compete with other modifications such as methylation, SUMOylation and ubiquitination. As previously discussed, there are 3 families of histone acetyltransferases, or protein acetyltransferases, CBP/p300, Gcn5/pCAF and MYST, some of which display substrate specificity although there appears to be a functional redundancy among certain family members. There are 18 potential histone or protein deacetylases, HDAC1 to HDAC11 and SIRT1 to SIRT7, which can all deacetylate non-histone proteins *in vitro* if not *in vivo*.

Acetylation and deacetylation of non-histone proteins can affect the stability, DNA binding potential, subcellular localisation or the association with other proteins (Table 1.1). The first non-histone protein to be identified as a target for protein acetylation was the transcription factor p53 (Gu *et al.,* 1997). Acetylation of p53 by p300/CBP within the DNA binding motif enables p53 to bind to its cognate sequence. Interestingly, deacetylation of p53 by HDAC1 results in the MDM2-mediated degradation of p53 as the lysine residues that are targets for acetylation overlap with the ubiquitination sites (Ito *et al.,* 2002). p53 is also a target for SIRT1 deacetylation, which decreases the affinity of p53 for the cell-cycle regulator p21 causing the cells to re-enter the cell-cycle after DNA repair (Luo *et al.,* 2001; Vaziri *et al.,* 2001). However, acetylation can have pleiotropic affects on the ability of proteins to associate with DNA. Acetylation of the sequence specific transcription factor Ying Yang by CBP and p300, within its zinc finger-binding domain greatly decreases its DNA binding potential. However, acetylation

Protein	**Function of acetylation**	**Reference**
YY1	Decreases DNA binding	Yao *et al.*, 2001
GATA1	Increases DNA binding	Boyes *et al.*, 1998
p53	Increases DNA binding and transcriptional activity	Gu *et al.*, 1997 Luo *et al.*, 2004
STAT3	Increases transcriptional activity	Wang *et al.*, 2005
Androgen Receptor	Increases transcriptional activity	Fu *et al.*, 2000 Gaughan *et al.*, 2002
HIF1α	Decreases transcriptional activation	Jeong *et al.*, 2002
Smad7	Increases protein stability	Gronroos *et al.*, 2002
EKLF	Promotes protein-protein interaction	Zhang *et al.*, 2001
Importin α	Unknown	Bannister *et al.*, 2000
Ku70	Disrupts protein-protein interaction	Cohen *et al.*, 2004

Table 1.1 Table showing the effect of acetylation on some of the known non-histone proteins.

and deacetylation of regions outside the zinc fingers control its transcriptional activity (Yao *et al.*, 2001). In addition to transcription factors, many other proteins are targets of acetylation such as α-tubulin, Ku70, HDAg and importin alpha (which will be discussed in more detail later). Dynamic microtubules at the leading edge of cells where tubulin subunits are added or subtracted are hypoacetylated while stable microtubules have high levels of acetylated lysine residues. The deacetylation of tubulin is mediated by HDAC6 and SIRT2 but the acetyltransferase responsible for the acetylation has yet to be identified (Hubbert *et al.,* 2002; North *et al.,* 2003). Ku70, an essential component of the non-homologous end-joining pathway (NHEJ), plays an essential role in apoptosis by binding to the pro-apoptotic factor Bax and preventing its translocation to the mitochondria. At the onset of apoptosis, acetylation of ku70 by CBP and p/CAF disrupts the ku70-Bax interaction, allowing Bax to translocate to the mitochondria. Deacetylation of Ku70 by SIRT1 causes the sequestration of Bax from the mitochondria and inhibits apoptosis (Cohen *et al.,* 2004).

The abnormal activity of HATs and HDACs is associated with tumorigenesis, as an imbalance in acetylation can lead to changes in chromatin structure, protein-protein interactions and protein stability. In recent years, the use of HDAC inhibitors (HDACi) in the treatment of solid and liquid tumours has come to the fore (Lin *et al.,* 2006). There are a large number of structurally diverse HDACi which have been synthetically synthesised or derived from natural compounds. They are divided into six classes based on differences in their structure: hydroxamic acids-derived compounds, cyclic tetrapeptides, short-chain fatty acids, synthetic pyridyl carbamate derivatives, synthetic benzamide derivatives and ketones (Hess-Stumpp *et al.,* 2005). While their mode of action has not yet been fully elucidated, crystallographic studies have revealed that trichostatin A (TSA) and suberoylanilide hydroxamic acid (SAHA) inhibit HDACs by binding to the catalytic pocket of HDACs and chelating the indispensable zinc ion (Lindemann *et al.,* 2004). Interestingly, HDACi have only a limited effect on a subset of genes due to changes in histone acetylation (Drummond *et al.,* 2005). Although many of these genes encode proteins involved in tumorigenesis or tumour suppression, there is increasing evidence that epigenetic modifications of histones may not be the primary mechanism for HDACi-mediated growth suppression or apoptosis in cancer (Lin *et al.,* 2006).

So, what effects do HDACi have on non–histone protein localisation, stabilisation, protein-protein interactions and how does this affect cellular function? Roy *et al.* (2005) recently demonstrated that TSA-mediated acetylated p53 induced cell-cycle arrest and apoptosis in prostate cancer cells. Further studies revealed TSA induced the disruption of Ku70-Bax complex which resulted in neuroblastoma apoptosis (Subramanian *et al.,* 2005). HDACi have also been shown to induce the dephosphorylation of signalling kinases such as Akt through the disruption of HDAC-PP1 complexes which are upstream activators of signalling kinases (Chen *et al.,* 2005). This sensitises cancer cells to other apoptotic agents such as Gleevec and Herceptin and also radiation therapy by lowering the apoptotic threshold (Yu *et al.,* 2003; Fuino *et al.,* 2003). Therefore, targeting the acetylation state of non-histone proteins with HDACi will hopefully lead to novel therapeutic targets in cancer therapy.

1.2.1 CBP – structure, function and subcellular localisation

The acetyltransferase CBP, was first identified as a protein that binds to the cAMP response element binding protein (CREB) (Chivria *et al.,* 1993). The functionally related p300 was discovered as a consequence of its interaction with the adenoviral E1A protein (Eckner *et al.,* 1994). Both CBP and p300 are involved in many cellular processes including differentiation, proliferation and apoptosis. The CBP gene was mapped to the chromosomal region 16p13.3, which is implicated in Rubenstein-Taybi syndrome. This results in the loss of a single allele thereby leading to severe developmental defects (Petrij *et al.*, 1995). In addition certain types of acute myeloid leukaemia with the translocation t(8;16)(p11,p13) give rise to fusion proteins consisting of CBP and the acetyltransferase MOZ. The 16p13.3 region shows sequence homology to 22q13 where p300 resides (Eckner *et al.,* 1994).

CBP and p300 share a number of conserved domains. CBP can interact with a variety of proteins such as the basal transcription machinery, co-activators, transcription factors, histones and other non-histone nuclear proteins (Figure 1.8). Recruitment of CBP to the promoters of target genes leads to the acetylation and methylation of histone tail residues, mediated by CBP and other co-activators which in turn results in the recruitment of RNAPII and the concomitant start of transcription. CBP preferentially acetylates H2B K12, K15, H3 K14, K18 and H4 K5, K8 which increases the accessibility of transcription factors and GTFs for DNA. Its ability to acetylate histone tails and other proteins is mediated by its HAT domain. The HAT domain contains a coenzyme A binding site (CoA) and plant homeodomain (PHD) zinc fingers which are an integral part of the enzymatic core. The PHD zinc fingers (CH2) have a cysteine 4- histidine 3 motif which is most commonly found in proteins which associate with chromatin. However, while the PHD zinc fingers are indispensable for HAT activity, their exact function is unknown (Kalkhoven *et al.,* 2002). The bromodomain is located proximal to the HAT domain and is responsible for the recognition of acetylated lysine residues. It is postulated that this allows the tethering of CBP to target promoters, moreover the bromodomain was found to cooperate with the PHD zinc fingers in binding to hyperacetylated histones (Kalkhoven *et al.,* 2002; Manning *et al.,* 2001; Ragvin *et al.,* 2004). Although, HATs are defined as histone acetyltransferases, Sterner *et al.* (1979) showed that the non-histone protein HMG1 was a substrate for acetylation, which was subsequently shown to be carried out by CBP (Munshi *et al.* 1998). An increasing number of transcription factors have been shown to be acetylated by p300/CBP for example acetylation of ACTR leads to its dissociation from nuclear receptors and to the attenuation of transcription. Furthermore, it was reported that CBP acetylates the nuclear import factor importinα which is

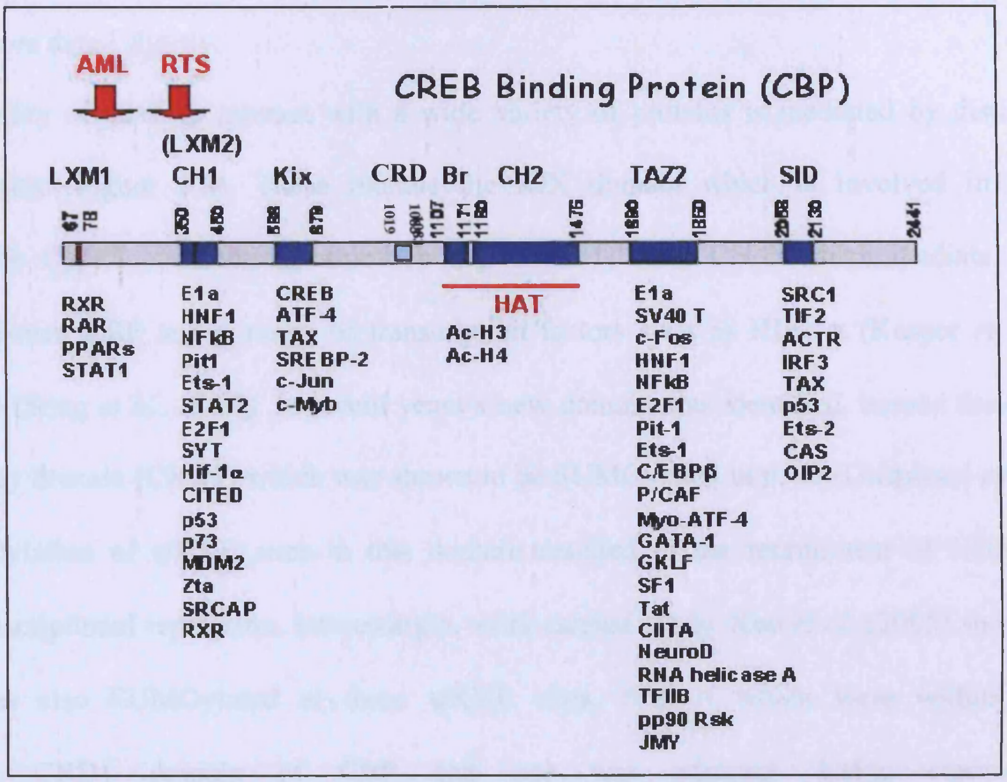
AML
RTS
CREB Binding Protein (CBP)
(LXM2)
LXM1
CH1
Kix
CRD
Br
CH2
TAZ2
SID
67
78
350
450
588
679
1019
1080
1107
1171
1180
1475
1680
1850
2058
2130
2441
HAT
RXR
RAR
PPARs
STAT1
E1a
HNF1
NFkB
Pit1
Ets-1
STAT2
E2F1
SYT
Hif-1α
CITED
p53
p73
MDM2
Zta
SRCAP
RXR
CREB
ATF-4
TAX
SREBP-2
c-Jun
c-Myb
Ac-H3
Ac-H4
E1a
SV40 T
c-Fos
HNF1
NFkB
E2F1
Pit-1
Ets-1
C/EBPβ
P/CAF
Myo-ATF-4
GATA-1
GKLF
SF1
Tat
CIITA
NeuroD
RNA helicase A
TFIIB
pp90 Rsk
JMY
SRC1
TIF2
ACTR
IRF3
TAX
p53
Ets-2
CAS
OIP2

Figure 1.8 Domain structure of CBP and its interacting proteins. AML – acute myeloid leukemia, RTS – Rubenstein-Taybi syndrome, CRD – cell cycle regulatory domain, Br – bromodomain, SID – SRC1 interaction domain, HAT – histone acetyltransferase.

involved in the import of many nuclear components (Bannister *et al.* 2000). This will be discussed in more detail shortly.

The ability of CBP to interact with a wide variety of proteins is mediated by distinct globular domains (Figure 1.8). These include the KIX domain which is involved in the interaction with CREB, cysteine/histidine-rich regions CH-1 and CH-3 which mediate the interaction between CBP and a range of transcription factors such as HIF-1α (Kasper *et al.*, 2005) and p53 (Song *et al.*, 2002). In recent years a new domain was identified, termed the cell cycle regulatory domain (CRD1) which was shown to be SUMOylated in p300 (Girdwood *et al.*, 2003). SUMOylation of ψKXE sites in this domain resulted in the recruitment of HDAC6 leading to transcriptional repression. Interestingly, work carried out by Kuo *et al.* (2005) showed that CBP was also SUMOylated at three ψKXE sites, two of which were within the corresponding CRD1 domain of CBP and one was adjacent. Using chromatin immunoprecipitation assays (ChIP) they demonstrated that DAXX recognised SUMOylated CBP which mediated the recruitment of HDACs to target promoters. However, as already discussed, SUMO has also been shown to affect the subcellular localisation of many proteins, which was not addressed in these studies.

CBP also has an SRC1 Interacting Domain (SID) which is essential for binding to the p160 coactivators (Sheppard *et al.* 2001) as well as the transcription factors Ets-2 and IRF3, and viral proteins such as Tax and E1A (Matsuda *et al.* 2004). These proteins share conserved leucine rich amphipathic α-helices that are crucial for interactions with the SID (Matsuda *et al.* 2004). The p160 family of coactivators mediate the binding between CBP and the nuclear receptors. Upon binding ligand nuclear receptors (NRs) undergo a conformational change that stimulates the interaction between the LXXLL (L-leucine, X-any amino acid) motif of the NRs and the p160 proteins (Heery *et al.*, 1997). This in turn results in the p160-mediated recruitment of HATs e.g. CBP to the promoter at the onset of transcription. In a comprehensive study of the sequential recruitment of transcription components to the ERα response element (ERE) on ligand binding, Metevier *et al.,* (2003) demonstrated that p160s and HATs were among the first factors to be recruited on ligand induction. The efficient interaction of NRs and cofactors is mitigated by a number of factors including the number of LXXLL motifs. CBP contains 3 LXXLL motifs within its SID domain which mediate only weak interactions with the estrogen, androgen and progesterone receptors but are essential for the interaction between CBP and SRC-1 and other proteins such as Ets-2 (Matsuda *et al.,* 2004). NMR studies have determined that complexes involving the p160, ACTR AD1 and CBP-SID involves largely hydrophobic interactions between three α-helices (Demarest *et al*., 2002). In both SRC1/CBP (Figure 1.9) and ACTR/CBP complexes, a tight 4 helix bundle is formed from three α-helices from CBP and a conserved leucine-rich α-helix present in the activation domain (AD1) of the p160 family members and other SID binding proteins (Demarest *et al*., 2002; Waters *et al*., 2006). Interestingly, neither domain adopts a stable folded structure in isolation (Waters *et al*., 2006). The SRC1-AD1/CBP-SID structure seems to be stabilised by a sequence containing repeats of the sequence QPGM/L (Matsuda *et al.,* 2004; Waters *et al.,* 2006). The interaction between CBP-SID and SRC-1 AD1 was abrogated by mutation of three leucine residues which form part of a conserved leucine rich motif in SRC-1 (Waters *et al.,* 2006). Interestingly, the conserved amphipathic α-helices within the p160 family members that mediate binding with CBP are also conserved in many other proteins. The transcription factor, Ets-2 contains 5 α-helices (Pointed domain; PNT) that are conserved with Ets-1 and helix 5 is similar in sequence with AD1 Aα1 consensus sequence of SRC-1. Deletion of the PNT domain or helix 5 completely abrogated binding between CBP and Ets-2 (Matsuda *et al.,* 2004). Therefore, it appears that the leucine-rich motifs within CBP, are essential for the interaction with p160 family members and also other transcription factors such as Ets-2.

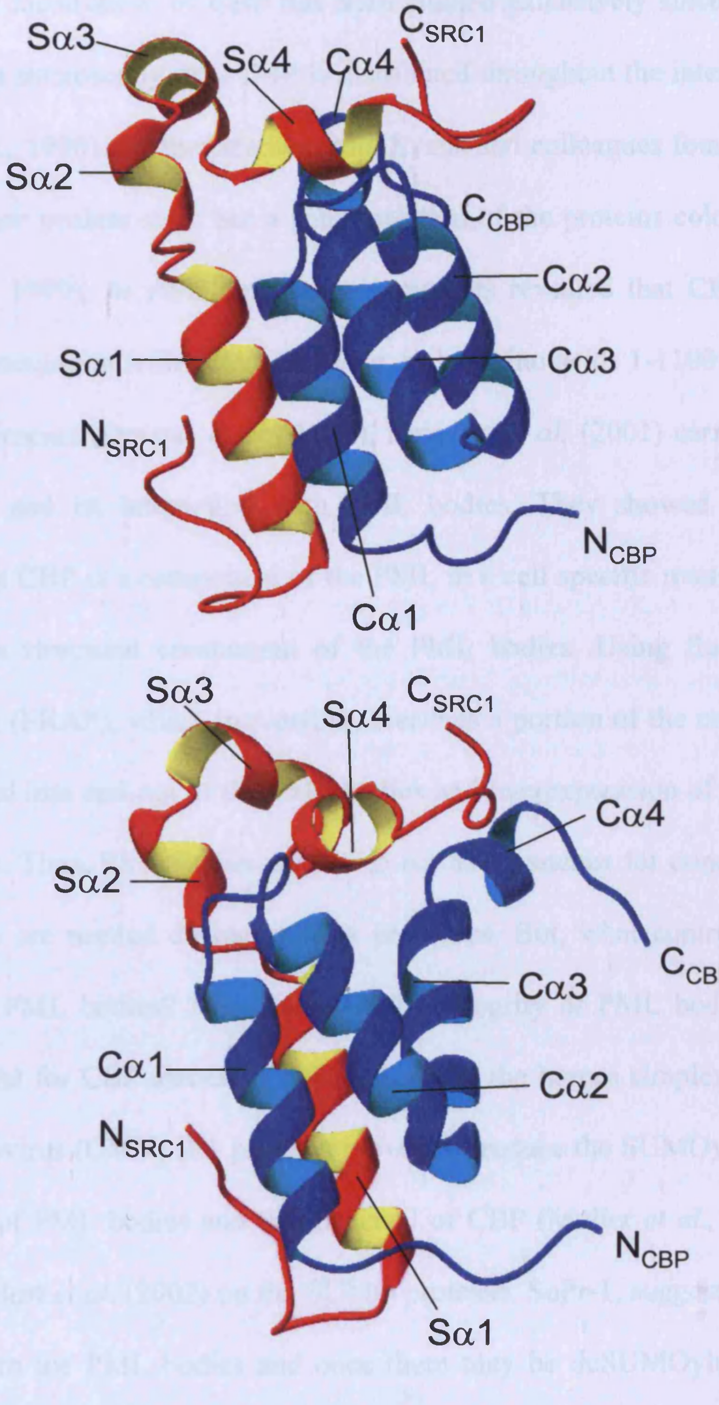
Sα3
C_SRC1
Sα4
Cα4
Sα2
C_CBP
Cα2
Sα1
Cα3
N_SRC1
N_CBP
Cα1
Sα3
C_SRC1
Sα4
Cα4
Sα2
C_CBP
Cα3
Cα1
Cα2
N_SRC1
N_CBP
Sα1

Figure 1.9 Ribbon diagrams depicting the NMR structure of CBP-SID (Blue) complexed with SRC-1 AD1(Red) (Waters *et al.*, 2006)

The subcellular localisation of CBP has been studied extensively since it was first shown, via immunoelectron microscopy, that CBP is distributed throughout the internal core of PML bodies (La Morte *et al.,* 1998). Further studies from Evans and colleagues found that endogenous CBP displays a diffuse nuclear stain but a subpopulation of the proteins colocalise with PML bodies (Doucas et al., 1999). *In vitro* mapping experiments revealed that CBP amino acids 311-521 mediated the association with PML. However, only amino acids 1-1100 of CBP were used in the mapping experiments (Doucas *et al.,* 1999). Boisvert *et al.* (2001) carried out a comprehensive study of CBP and its interaction with PML bodies. They showed by immunofluorescence microscopy that CBP is a component of the PML in a cell specific manner. In addition, CBP is a dynamic, not a structural component of the PML bodies. Using fluorescence recovery after photobleaching (FRAP), which irreversibly bleaches a portion of the nucleus, they demonstrated that CBP moved into and out of the PML bodies and overexpression of GFP-PML recruited CBP in PML bodies. Thus, PML bodies appear to act as an anchor for concentrating such factors as CBP until they are needed during cellular processes. But, what controls the ability of CBP to associate with PML bodies? It appears that the integrity of PML bodies and SUMOylation of PML is essential for CBP association. For example, the herpes simplex virus (HSV) ICP10 and the cytomegalovirus (CMV) IE1 proteins prevent or reduce the SUMOylation of PML leading to the disruption of PML bodies and the dispersal of CBP (Muller *et al.,* 1999). In addition, work carries out by Best *et al.* (2002) on the SUMO protease, SuPr-1, suggested that co-activators may be recruited into the PML bodies and once there may be deSUMOylated, at which point they leave in their desired co-activator complexes. They showed that SuPr-1 bound to SUMO-modified PML which stimulated c-jun mediated transcription by redistributing co-activators associated with PML bodies. This included CBP which was dispersed once SuPr-1 had hydrolysed the SUMO modified PML. However, they did not show whether SuPr-1 had any effect on CBP SUMOylation or if CBP redistribution was due directly to SUMO deconjugation of CBP by SuPr1 or indirectly by SUMO deconjugation of PML which affected its interaction with CBP. Thus, SUMOylation appears as a very important mechanism in regulating the association of proteins with PML bodies and also in regulating their structural integrity.

1.2.2 CBP and Disease

Disruption of CBP subcellular localisation and coactivator function has been implicated in many human diseases (Table 1.2). Rubenstein-Taybi syndrome (RTS), a congenital developmental disorder, is characterised by microdeletions, chromosomal translocations or point mutations in the CBP gene resulting in haploinsufficiency (Kalkhoven, 2004). The phenotypic characterisation of RTS is retarded growth and mental function, big toes and facial abnormalities. RTS phenotypes were also found in patients with mutations in the PHD zinc fingers, which abrogated HAT activity and also a Y1175C mutation within the bromodomain (Kalkhoven *et al.*, 2003; Kalkhoven, 2004; Bartsch *et al.*, 2002).

Translocations involving the CBP or p300 gene are implicated in the pathogenesis of a subset of patients with acute myeloid leukemia (AML). The translocations result in the fusion of CBP with either monocytic leukemia zinc finger protein (MOZ), monocytic leukemia related factor (MORF) or the mixed lineage leukemia protein (MLL),. The MOZ-CBP and MORF-CBP fusion proteins contain nearly all of the CBP protein and the HAT domain and zinc fingers of MOZ and MORF. Expression of these fusion proteins results in a block in myeloid cell differentiation due to deregulation of acetyltransferase activities and mislocalisation of binding proteins. Interestingly, Kitabayashi *et al.* (2001) demonstrated that deletion of the HAT domain of MOZ-CBP rescued myeloid cell differentiation. In MLL-CBP induced AML, almost all of CBP is fused to the portion of MLL which does not have any methyltransferase activity. However, while the loss of methyltransferase activity may have a role to play in the pathogenesis

Disease	
Rubenstein-Taybi syndrome	Disruption of *cbp* gene
AML (MOZ-CBP, MOZ-TIF2, MLL-CBP) fusion proteins	Mislocalisation/degradation of CBP leading to AML
Huntington's disease/Kennedy's disease	Mislocalisation of CBP to polyglutamine aggregates
Alzheimer's disease	Mislocalisation of CBP due to Presenilin mutations
AML (HOXA9-NUP98 fusion protein)	Recruitment of CBP via FG repeats of NUP98 is implicated in AML

Table 1.2 Table showing a proportion of the diseases associated with dysregulation of CBP.

of MLL, it appears that the HAT and bromodomains of CBP are the essential components needed for induction of leukemia (Lavau *et al.,* 2000).

Interestingly, CBP coactivator function and subcellular localisation are also affected by other aberrant fusion proteins and this has been implicated in the pathology of many forms of AML. For example, the MOZ-TIF2 fusion protein which is a reciprocal translocation derived from an inversion of chromosome 8, inv8(p11q13), fuses the N-terminal of MOZ, including the HAT domain to the C-terminus of TIF2, a p160 family member which interacts with CBP. Expression of MOZ-TIF2 leads to deregulation of CBP interacting proteins such as p53 and NRs, through the interaction between the TIF2 AD1 and CBP. Interestingly, the subcellular localisation of MOZ-TIF2 is distinct to that of MOZ or TIF2 and leads to the mislocalisation of CBP from PML bodies. In addition, deletion of the AD1 domain of TIF2 or the nucleosomal binding domain of MOZ rescues CBP function and releases the block in myeloid cell differentiation (Kindle *et al.,* 2005; Deguchi *et al.,* 2003).

Impairment of CBP function and localisation is not only implicated in many of the AML pathologies, it is also impaired in many neurodegenerative diseases such as Huntington's disease (HD), spinocerebellar ataxias (SCAs), dentatorubral-palidoluysian atrophy (DRPLA) and Kennedy's disease (spinal and bulbar muscular atrophy) which all have expanded polyglutamine repeats (CAG) within the causative proteins which either mislocalise or degrade CBP (Kalkhoven, 2004). In HD tissue culture models and post-mortem brains, the mutant Huntington protein (htt) localised to the nucleus where it formed inclusion bodies that colocalise with CBP (Steffan *et al.,* 2001; Nucifora *et al.,* 2001). In addition, mutant htt interacted with CBP and resulted in its degradation, although HDACs have been shown to arrest polyglutamine-dependent neurodegeneration in *Drosophila* and mice (Steffan *et al.,* 2001; Hockly *et al.,* 2003).

Kennedy's disease (X-linked spinal and bulbar muscular atrophy) is a late onset rare inherited disease that is characterised by progressive muscular weakness and atrophy. Like

Huntington's disease, Kennedy's disease is associated with an expansion of polymorphic CAG repeat sequence in the first exon of the gene encoding the androgen receptor (AR). The AR contains three defined domains: the activation domain (AD), the DNA-binding domain (DBD) and the ligand-binding domain (LBD). The AR normally regulates transcription in a ligand-dependent manner like other members of the steroid hormone receptor family. Unliganded, the AR resides in the cytoplasm and is kept in an inactive conformation by Heat Shock Proteins (HSP) and other chaperones. On binding ligand, the HSPs dissociate and the AR dimerises, translocates to the nucleus, whereupon it binds to an Androgen Response Element (ARE) and activates transcription (Tsai and O'Malley, 1994). In the normal population the CAG repeat region ranges from 12 to 30 but in patients with Kennedy's disease, the repeats range from 40 to 70 (Butler *et al*., 1998). A hallmark of Kennedy's disease is the aggregation of polyQ containing proteins in the affected cell populations, which leads to neurotoxicity. The mutant AR is not only expressed in neural tissue but is also highly expressed in other tissues, primarily in the prostates, kidneys and testes of diseased patients (Adachi *et al.,* 2005). McCampbell *et al.* (2001) demonstrated that CBP was mislocalised in mouse neuronal cells expressing the mutant AR and that GAL4-CBP dependent transcription could be impaired by expression of a constitutive AR bearing a 119 glutamine stretch (McCampbell *et al.,* 2000). In a *Drosophila* model of Kennedy's disease it was shown that retinal degeneration corresponded with altered acetylation levels and decreased transcription levels could not be rescued by CBP (Taylor *et al.,* 2003). However, contrasting reports suggest that CBP is not mislocalised by polyQ inclusions but is degraded by the ubiquitin proteasome pathway (Jiang *et al.,* 2003). Furthermore, oral administration of the HDACi, Sodium Butyrate, to transgenic SMBA mice, ameliorated neurological phenotypes and increased acetylation of histones (Minamiyama *et al.,* 2004).

1.2.3 Interaction between transcription-associated proteins, the NPC and nuclear transport proteins

While it is clear that CBP plays a direct role in transcription and in regulating the activity of specific non-histone proteins, there is evidence that CBP may play a role in nuclear transport. As already mentioned, CBP acetylates Impα, which is essential for the nucleocytoplasmic import of proteins containing a classic nuclear localisation signal (NLS). Bannister *et al.* (2000) demonstrated that Impα could be acetylated at lysine22 *in vitro* by CBP and *in vivo* by p300. Interestingly, CBP interacts with the HOXA9/NUP98 fusion protein which is expressed in the t(7:11) translocation of AML, via FG repeats of NUP98 (Kasper *et al.* 2002). FG (Phe-Glu) repeats have been identified in a number of other NPC component proteins and are believed to be essential for the movement of cargo across the nuclear membrane.

So how are proteins actively transported across the nuclear membrane? Eukaryotic cells are characterised by distinct nuclear and cytoplasmic compartments which are separated by a nuclear envelope, a double membrane and a continuous endoplasmic reticulum. Within the membrane are numerous Nuclear Pore complexes (NPC) for the purpose of nucleocytoplasmic transport. They have an 8-fold rotational symmetry, a central core structure, nuclear and cytoplasmic extensions and many different protein components (Nucleoporins, NUPs). The number of NPCs differs depending on the demand for nuclear transport, cell size, synthetic activity and proliferative activity.

Not only must all nuclear proteins be imported to the nucleus but tRNA, rRNA and mRNA are also exported to the cytoplasm. Therefore based on experimental evidence the classical NLS (nuclear localisation signal)-dependent import-export pathway was elucidated. The key actors are Importinβ (Impβ), which recognises and binds to the NPC, Impα which binds to the NLS containing protein, Ran which is a small GTPase and can switch between a GDP and a GTP form due to its mediators RANGAP1 and RANBP1 on the cytoplasmic side and RCC1 (guanine nucleoside exchange factor) on the nuclear side. This creates a RanGTP gradient across the nuclear membrane with a higher concentration of RanGTP in the nucleus versus the cytoplasm (Figure 1.10).

Another protein involved in nucleo-cytoplasmic transport is CAS (Cellular apoptosis susceptibility protein), a homologue of the yeast CSE1 (Chromosome Segregation Factor). CAS was first cloned in a screen to isolate cDNAs that cause MCF-7 breast cancer cells to become resistant to apoptosis. They found that CAS was highly expressed in human tumour cell lines and CAS antisense cDNA conferred resistance to a number of apoptosis inducing chemicals which led to cell cycle arrest in G2 or mitosis (Brinkmann *et al.,* 1995, Brinkmann *et al.,* 1996, Ogryzko *et al.,* 1997). Further studies showed that CAS shared 59% homology with the yeast chromosome segregation factor 1 (CSE1) and localised to microtubules and the mitotic spindle (Scherf *et al.,*1996). However, novel experiments carried out by Kutay *et al.* (1997) demonstrated that CAS is an essential exporter of Impα from the nucleus to the cytoplasm in a Ran-dependent manner. In addition, Cse1 was shown to be required for the nucleo-cytoplasmic shuttling of Impα (ySrp1) (Hood *et al.,* 1998). Structural studies have revealed that cargo-free Cse1 is in a compact state with the Impα and RANGTP occluded. Upon cargo binding, Cse1 undergoes a major conformational change to accommodate Impα and RANGTP (Cook *et al.,* 2005). Thus, many of the original observations made about the role CAS plays in cell-cycle progression and apoptosis have now been attributed to its role as a nuclear transport factor.

The binding of an NLS-containing protein to Impα results in their association with Impβ. This trimeric complex binds the NPC via Impβ and mediates the import of the protein into the nucleus. The trimeric complex is blocked at the NPC basket and released when Impβ binds RANGTP, which dissociates the complex and Impβ is returned to the cytoplasm in its RANGTP bound state. CAS shows a preference for free Impα over Impα bound to Impβ, so when the

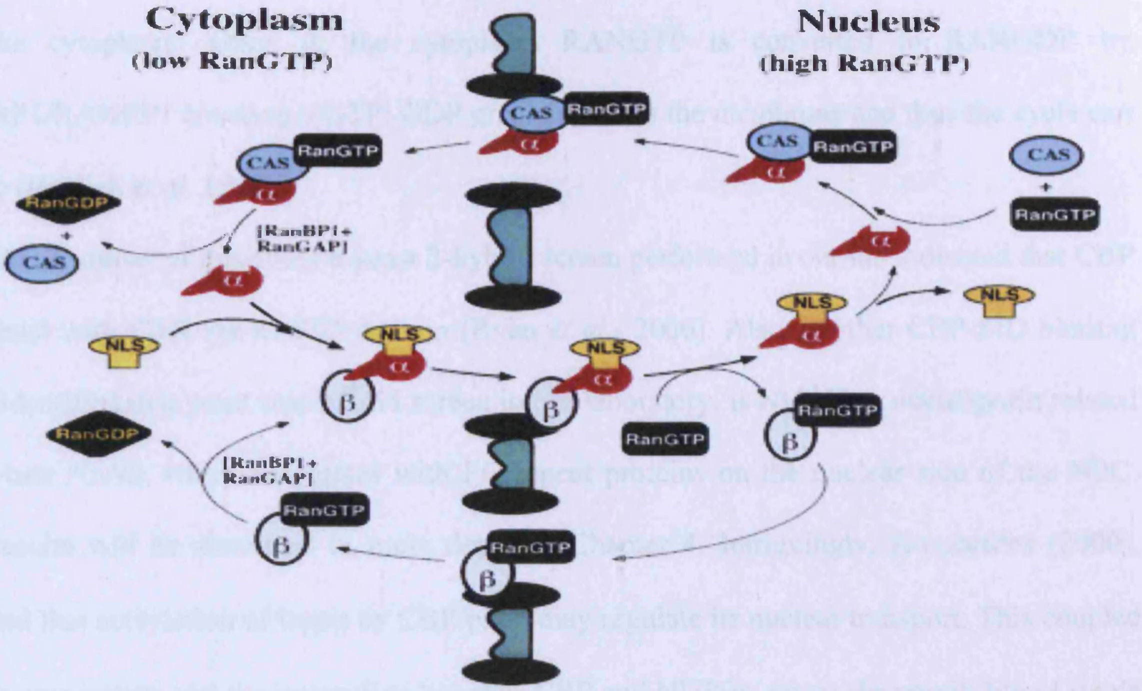
Cytoplasm
(low RanGTP)
Nucleus
(high RanGTP)
CAS
RanGTP
α
CAS
RanGTP
α
CAS
RanGTP
α
CAS
+
RanGTP
RanGDP
+
CAS
[RanBP1+
RanGAP]
α
α
NLS
NLS
NLS
α
β
NLS
α
β
NLS
α
RanGTP
β
RanGTP
RanGDP
[RanBP1+
RanGAP]
RanGTP
β
RanGTP
β

Figure 1.10 Schematic representation of the classical NLS-mediated import pathway (Gorlich and Kutay 1999).

trimeric complex is dissociated into its components; CAS binds impα and RANGTP and exports it to the cytoplasm. Once in the cytoplasm RANGTP is converted to RANGDP by RANGAP1/RANBP1 ensuring a GTP: GDP gradient across the membrane and thus the cycle can continue (Gorlich *et al.* 1999).

At the outset of this study a yeast 2-hybrid screen performed in our lab indicated that CBP can interact with CAS via its SID domain (Ryan *et al.,* 2006). Also, another CBP-SID binding protein identified in a yeast two-hybrid screen in our laboratory, is NUP93, a nucleoporin related to the yeast Nic96, which associates with FG repeat proteins on the nuclear side of the NPC. These results will be discussed in more detail in Chapter 4. Intriguingly, Kouzarides (2000), postulated that acetylation of Impα by CBP/p300 may regulate its nuclear transport. This coupled with our own results and the interaction between CBP and NUP98, raises the possibility of a role for CBP in nuclear transport.

1.2.4 The nuclear periphery and the NPC in the regulation of gene expression

In recent years new evidence has come to light implicating the NPC, nuclear transport proteins and the nuclear periphery in gene expression. The non-random arrangement of chromosomes in the nucleus is maintained by nuclear structure such as the nuclear lamina, the nuclear matrix and the nuclear pore complex. These are not only involved in the correct positioning of chromatin but they play a vital role in the regulation of gene expression.

The nuclear envelope is a lipid bilayer composed of the inner and outer membranes, the NPC and the nuclear lamina. The Lamins and associated proteins are the major components of the nuclear lamina, a filamentous network of proteins that form a mesh-like structure on the inner membrane (INM) of the nuclear envelope. The Lamins and associated proteins have been shown to interact with histones, DNA and chromatin-associated proteins. The widely held belief is that heterochromatin including telomeres, centromeres and repetitive DNA is located at the nuclear periphery while gene rich regions are located more centrally in the nucleus (Spector, 2003). For instance, the inactive heterochromatic X-chromosome is situated at the periphery of the nucleus in female mammalian cells but the active X-chromosome is located more internally (Boyle *et al.*, 2001; Belmont *et al.*, 1986). Evidence from experiments carried out in yeast, using a GAL4-transmembrane fusion protein, showed that transcriptional silencing occurs at the nuclear membrane (Andrulis *et al.*, 1998). However, as yeast does not contain any lamins, transcriptional silencing may occur by a different method. Furthermore, the nuclear periphery is also an anchoring site for transcription factors and associated proteins. The lamin-associated protein, LAP2α binds to the tumour suppressor Retinoblastoma protein (Rb). Interestingly, hypophosphorylated Rb is anchored at the envelope by LAP2α and the aberrant localisation of lamin or LAP2α results in the redistribution of Rb (Markiewicz *et al.*, 2002).

In addition to the lamina, the nuclear membrane also contains NPCs. NUP153 has been shown to bind DNA and NPC-associated proteins can also bind to and regulate chromatin structure and dynamics. For example, yKu70, the telomere-associated protein, binds to the NPC-associated protein Mlp2 which in turn binds NUP145. Interestingly, mutation of NUP145, yKu70 or Mlp2 prevents the association of telomeres at the nuclear envelope (Galy *et al.*, 2000; Laroche *et al.*, 1998). However, a new body of evidence suggests that the nuclear periphery and the NPC are not only involved in heterochromatic silencing, but they too can associate with the transcriptional machinery and both positively and negatively regulate transcription in yeast. Ishii *et al.* (2002) published a series of elegant experiments showing the ability of exportins, such as Cse1 and Srp1p, to act as potent boundary proteins that block the spread of heterochromatin in *S. cerevisiae*. Boundary elements are specialised DNA sequences that flank genes and can protect the genes from the spread of heterochromatin from a nearby region. They showed that nuclear transport proteins fused to a DNA binding domain could exhibit boundary activity, by tethering the boundary element to the NPC and thus blocking the spread of heterochromatin. Following from this, a genome-scale analysis was carried out to analyse the DNA-binding patterns for NUPs and related proteins. It was found that many nucleoporins such as Nic96 and the karyopherin Cse1 were found to preferentially associate with transcriptionally active genes in yeast. Furthermore, they demonstrated that the galactose genes (GAL) genes moved to the nuclear periphery upon galactose induction (Casolari *et al.,* 2004). However, activation of GAL genes requires transactivation by Gal4p and the recruitment of the chromatin remodeler SAGA, which contains the HAT, Sus1. This serves as an adaptor for the mediator complex which facilitates the assembly of the preinitiation complex, composed of the general transcription factors TBP and RNAPII. Interestingly, Cabal *et al.* (2006) have recently shown that members of the SAGA complex, Sus1 and Ada2 along with Sac3, a messenger RNA transport factor physically link Nup1 to activated GAL genes at the nuclear periphery. These results are in agreement with the 'gene gating' hypothesis originally put forward by Blobel (1985). He postulated that gene expression occurred at the NPC where the 'active' genes would be in close contact with the transcription machinery with easy access for mRNA to the cytoplasm. While all the yeast data suggests that the NPC, nuclear transport factors and the transcription machinery associate at the periphery to regulate gene expression it remains to be determined if this is the case in mammalian systems.

1.3 Project aims

Transcription is a complex process regulated at many levels from chromatin structure to the position of chromosomes in the nucleus. The control of transcription is regulated by transcription factors, coactivators, corepressors and associated proteins. Understanding the factors that control the function of these proteins will not only shed light on the mechanisms of transcription but will also give us valuable insight into the mechanisms of diseases which are associated with transcriptional misregulation.

The aim of this project was, firstly, to investigate if CBP was SUMOylated *in vitro* and *in vivo*. To map the SUMO sites and to determine how SUMOylation impacts on the subcellular localisation and transcriptional activity of CBP. The second objective was to investigate the interaction of CBP with CAS and Impα. In addition, we aimed to find out what role acetylation plays in regulating the subcellular localisation of Impα, CAS, CBP and PML. The final objective was to examine whether CBP and PML bodies were mislocalised in cells expressing AR with an expanded polyglutamine tract.

Chapter 2

Materials and Methods

2.1 Sources of materials

2.1.1 General suppliers

All general laboratory chemicals were of analytical grade and supplied by Fisher Chemicals or Sigma Chemical Company Ltd. unless otherwise stated. Phosphate buffered saline (PBS) was prepared using PBS tablets (1 tablet/100 ml distilled water) supplied by OXOID Ltd. Double deionised water, purified by passage through a Purite select/Neptune water purification system was used to make all solutions. The pH of solutions was measured using a Jenway 3510 pH meter. Where appropriate, sterilisation was achieved by filtration through a 0.22 micron filter or by autoclaving for 15 minutes at 121°C and 25 Ib/in^2 pressure.

2.1.2 Bacterial reagents

Tryptone and yeast extract for bacterial growth medium were purchased from OXOID Ltd. *E. coli* strain DH5α (Hanahan, 1983) was purchased from Stratagene.

2.1.3 Molecular biology reagents

All enzymes and their respective buffers were purchased from Roche, ABgene, New England Biolabs (NEB) or Invitrogen Life Technologies. dATP, dCTP, dGTP and dTTP were purchased from ABgene. 1 kb Plus DNA ladder was purchased from Invitrogen Life Technologies. QIAquick gel extraction kit (50), QIAprep mini and maxi DNA prep kits were obtained from QIAGEN Ltd. Oligonucleotides for sequencing and PCR applications were purchased from the Protein and Nucleic Acid Sequencing laboratory (PNACL), University of Leicester, Invitrogen or Biopolymer Synthesis and Analysis group, QMC, Nottingham.

2.1.4 Tissue culture and transient transfection reagents

HeLa, COS-1, HEK293, U2OS and SY-5Y cells were purchased from the European Collection of Cell Cultures (ECACC). All tissue culture reagents were purchased from Invitrogen Life Technologies and plastic-ware was obtained from Helena Biosciences. Transfast mammalian transfection kit was purchased from Promega Inc.

2.1.5 Protein chemistry, Western blotting and immunofluorescence reagents

30% (w/v) acrylamide mix was obtained from National Diagnostics. 10x Tris-glycine-SDS running buffer and Precision Protein Standards were purchased from Bio-Rad. Nitrocellulose transfer membrane was obtained from Schleicher and Schuell and FUJI medical x-ray film was used. Enhanced Chemiluminescence system (ECL Plus™) was purchased from Amersham Pharmacia Biotech. Complete Protease Inhibitor Cocktail tablets were obtained from Roche. All primary antibodies, Horseradish peroxidase (HRP) conjugated secondary antibodies, Protein A/G sepharose beads and lactacystin proteasome inhibitor were obtained from Autogen Bioclear UK Ltd., Sigma-Aldrich, USA, Abcam UK Ltd. and Novocastra Ltd., UK.

2.1.6 Assay reagents

Protein assay reagent was purchased from Bio-Rad Laboratories and bovine serum albumin (BSA) protein standard was purchased from First Link (UK) Ltd. All reagents for reporter assays were purchased from Applied Biosystems, Foster City, CA, and U.S.A.

2.2 Bacterial preparation and culture

2.2.1 Culture of *E. coli* DH5α

The bacterial strain *E. coli* DH5α was used for all protein expression and DNA manipulations. To obtain single colonies the bacteria were streaked onto agar plates containing the correct antibiotic and grown at 37 °C. Once single colonies had appeared, the plates could be stored for several weeks at 4 °C. Liquid cultures were grown by placing a single colony into liquid LB (with appropriate antibiotics) and incubated in universal screw-top tubes (Bibby Sterilin, Staffordshire, UK) or conical flasks at 37 °C @200rpm.

2.2.2 Preparation of *E. coli* competent cells

E. coli DH5α were made competent for DNA transformation using the Rubidium chloride - Calcium chloride method. Briefly, a single colony from an overnight LB plate was inoculated into 5 ml LB medium. After 16 hours growth at 37 °C the culture was diluted at 1:100 ratio in LB medium and grown at 37 °C to an optical density (at 600 nm) of 0.5. Following a 10 min incubation on ice in pre-chilled 50 ml Falcon tubes, the cells were harvested by centrifugation (10 min, 2400 rpm, 4 °C). The cell pellets were resuspended gently on ice in 20 ml each of ice-cold Buffer 1. After a second centrifugation (10 min, 2400 rpm, 4 °C) each cell pellet was resuspended in 2 ml ice-cold buffer 2 and the cell suspensions combined. Microfuge tubes were placed in dry ice to allow snap freezing of 200 µl cell suspension aliquots. Competent cells were stored at –80 °C. Transformation efficiency was checked using the pUC19 vector and the transformation serially diluted to allow determination of number of transformants: 1 µg DNA should give more than 1x10^{6} transformants.

The transformation efficiency of the competent cells could be determined by transforming with a known amount (e.g. 10 pg pSG5) of plasmid DNA and then calculating:

Number of colonies obtained x dilution factor x 1/amount of DNA used (μg)

If the transformation efficiency of the competent cells was $1x10^6$ - $1x10^7$, and if no bacterial colonies were obtained in a no DNA control then the competent cells were deemed suitable for use.

2.2.3 Transformation of competent *E. coli*

50 ml aliquots of competent cells prepared, as described in section 2.2.2, were used for each transformation. In the case of previously constructed plasmids, 1 ng of DNA was used to ensure a good yield of successfully transformed cells. When transforming ligation mixtures, 5-10 ml of the ligation mix was used (see section 2.3.10). Cells and DNA were mixed in a pre-chilled 1.5 ml microfuge tube and incubated on ice for 15 min. The transformation mixture was then heat shocked by incubation at 42 °C for 2 min, followed by incubation on ice for 2 min. 950 μl LB media was then added to the heat shocked cells and they were incubated for 1 hr at 37 °C. The cells were centrifuged at 3,000 *g* for 2 min and 900 μl supernatant was discarded. The remaining 100 μl supernatant was used to resuspend the cell pellet and this cell suspension was spread on LB agar plates containing 100 μg/ml ampicillin. The plates were then incubated at 37 °C overnight.

2.2.4 Long term storage of bacterial cultures

Bacterial cultures were maintained for long periods of time by transferring 0.8 ml of a turbid bacterial culture to a cryogenic storage tube. 0.2 ml sterile glycerol was then added to the culture, the contents were vortexed, flash frozen (IMS/dry ice) and stored at -70 °C.

2.2.5 Composition of solutions and media used for bacterial methods

To prevent degradation of the antibiotics at high temperatures, they were added to molten media at ~65 °C.

Kanamycin 1,000x stock solution: 50 mg/ml in H_2O

Ampicillin 1,000x stock solution: 100 mg/ml in 50% ethanol

Chloramphenicol 1000x stock solution: 10mg/ml in 100% ethanol

Buffer 1: (30 mM KCl; 100 mM RbCl; 10 mM $CaCl_2$, 50 mM $MgCl_2$, 15% glycerol; adjusted to pH 5.8 using 0.2 M glacial acetic acid

Buffer 2: (10 mM MOPS; 75 mM $CaCl_2$, 10 mM RbCl, 15% glycerol; adjusted to pH 6.5 using 1 M filter sterilised KOH)

Luria-Bertoni (LB) media: 1% (w/v) tryptone, 0.5% (w/v) yeast extract, 1% (w/v) NaCl (pH 7.0 NaOH). Solidified where required by the addition of 2% (w/v) bacteriological agar.

2.3 Molecular biology techniques

2.3.1 Small scale plasmid DNA preparation

QIAGEN QIAprep mini prep kits were used for the small-scale preparation of plasmid DNA. This DNA was primarily used to screen for plasmids containing the correct DNA inserts. Briefly, a single bacterial colony was picked and used to inoculate 5ml of LB containing the appropriate antibiotic and grown overnight in an orbital shaker at 37°C, 225 rpm. 1.5 ml of the overnight culture was pelleted by centrifugation in a microfuge tube at 4,000 *g* for 2 min. The remaining bacterial culture was stored at 4°C for later use. The pelleted cells were then resuspended and subjected to alkaline lysis. The plasmid DNA was absorbed onto a silica gel membrane, washed and eluted. This technique was carried out according to manufacturers instructions and details can be found in the QIAGEN QIAprep miniprep handbook.

2.3.2 Large scale plasmid DNA preparation

In order to obtain larger quantities (up to 500 μg) of high quality plasmid DNA suitable for transient transfections and *in vitro* transcription/translation experiments etc. the QIAGEN-tip 500 plasmid maxiprep kit was used according to manufacturer's instructions. A single colony, containing the plasmid of interest, was picked and used to inoculate 5 ml LB containing the appropriate antibiotic. The culture was grown in an orbital shaker at 37 °C, 225 rpm overnight. Isolation of the plasmid DNA was achieved by alkaline lysis of the cells, followed by immobilization of the plasmid DNA on QIAGEN anion-exchange resin, elution and precipitation in isopropanol. DNA precipitates were resuspended in 400 μl sterile H_2O and re-precipitated in 1 ml absolute ethanol, prior to being washed in 70% (v/v) absolute ethanol, dried under vacuum to remove residual ethanol and resuspended in the appropriate volume of sterile H_2O. Details of this technique and compositions of solutions used can be found in the QIAGEN maxiprep handbook.

2.3.3 Caesium Chloride Purification of Plasmid DNA

Caesium chloride gradients were used to purify ultra-pure, supercoiled plasmid DNA. An overnight 400 ml culture of transformed *E. coli* DH5α was harvested by centrifugation (15 min, 4000 g, 4 °C). The cell pellet was resuspended in 10 ml Cell Lysis Solution I before addition of 20 ml Solution II and a five-minute incubation on ice. 15 ml ice-cold Solution III was then added to neutralize the alkali lysis and the suspension incubated on ice for 10 mins. The plasmid-containing supernatant was collected by centrifugation of the cellular DNA and debris (12,000 g, 15 min, 4 °C), transferred to a fresh tube and precipitated using 50 ml ice-cold isopropanol. The DNA was collected by a further centrifugation (12,000 g, 15 min, 4 °C) and resuspended in 5.5 ml TE after air-drying for 30 minutes. 500 µl (10 mg/ml stock) ethidium bromide and 6 g $CsCl_2$ were added and, once the latter had dissolved completely, the solution was centrifuged (4,000 g, 5 min. R.T.) and the supernatant pipetted into a new tube. The tubes were then balanced to within 0.001 g of each other using 1.1 mg/ml $CsCl_2$. Once balanced, the solutions were pipetted into quick-seal tubes (Beckman Coulter Ltd., High Wycombe, Buckinghamshire), heat-sealed and centrifuged (100,000 rpm, Beckman Coulter Optima MAX ultracentrifuge, overnight, 20 °C). The lower (supercoiled) plasmid band was removed from the gradient using a 21gauge needle and the ethidium bromide was removed from the DNA by repeated extraction with equal volumes of water-saturated iso-butanol. The solution was then diluted with two volumes H_2O and the DNA precipitated with ethanol. Following three washes with 70% ethanol the DNA was resuspended in 500 µl sterile H_2O.

2.3.4 Spectrophotometric quantification of DNA

All DNA was quantified and qualified by spectrophotometry, restriction digest (section 2.3.8) or by comparison of various dilutions of DNA samples with molecular weight markers of known concentration following separation by agarose gel electrophoresis (section 2.3.6). The concentration of DNA sample was determined by optical density measurement at 260 nm using a UV spectrophotometer (Eppendorf). DNA concentration was calculated by using the following formula:

OD 260 nm x Dilution factor x 50 = Concentration of DNA in µg/ml

The purity of DNA sample was estimated by the ratio of OD260:OD280. The measurement at 280nm is a measurement of protein contamination in the sample. Pure DNA has an OD260/280 of between 1.7 and 1.9.

2.3.5 Phenol/chloroform extraction and ethanol precipitation of DNA

Phenol/chloroform extraction, followed by ethanol precipitation was performed on all DNA samples with a low A_{260nm}/A_{280nm} absorbance ratio (i.e. lower than 1.7). An equal volume of phenol was added to the DNA solution to extract the protein contaminant and the mixture was inverted ~5 times, followed by centrifugation at 13,000 *g* for 2 min. The top aqueous layer was transferred to a clean microfuge tube to which an equal volume of chloroform was added to remove residual phenol, inverted ~5 times and centrifuged at 13,000 *g* for 2 min. The top aqueous layer was transferred to a clean microfuge tube to which 0.1 volumes of 3 M sodium acetate (pH 5.2) and 3 volumes absolute ethanol were added to precipitate the DNA, vortexed for 10 sec. The sample was then thawed on ice and centrifuged at 13,000 *g* for 10 min and the supernatant discarded. The pellet was washed in 70% (v/v) absolute ethanol, centrifuged and the supernatant discarded as before. The resulting pellet was dried under vacuum to remove residual ethanol and resuspended in an appropriate volume of sterile H_2O.

2.3.6 Agarose gel electrophoresis

DNA was size fractionated on neutral agarose gels of between 0.8 and 2 % agarose (w/v) as appropriate to the size of the fragments being resolved. Gels containing 0.5 µg/ml ethidium bromide were made and run in 0.5 x TBE buffer as described in standard protocols (Sambrook *et al.*, 1989). DNA samples were loaded in a 0.5 x gel-loading buffer. Following electrophoresis, gels were visualised by transillumination with ultra violet light and photographed via Gel-Doc 2000 (Bio-Rad). The size (kb) and amount (ng) of DNA fragments was determined by comparison with a reference DNA molecular weight standard kb ladder.

2.3.7 Purification of DNA fragments from agarose gel slices

DNA fragments were purified from agarose gel slices using a QIAquick gel extraction kit according to manufacturer's instructions. The DNA was bound to the QIAquick membrane, washed and eluted in sterile H_2O.

2.3.8 Restriction digest of DNA

Plasmid DNA was digested with restriction endonucleases in order to generate compatible ends for cloning and to verify newly created plasmids. The reaction conditions were set up according to manufacturer's instructions. Typically, digests were set up in a 30 µl reaction volume consisting of:

DNA	x µl
restriction endonuclease (10 units/µl)*	2 µl
10x buffer	3 µl
sterile H_2O	x µl, to total volume of 30 µl

Digests were normally carried out at 37 °C for 3-4 hr unless advised otherwise in the manufacturers instructions.

* When two or more enzymes were used simultaneously the total reaction volume was increased proportionally to prevent the glycerol concentration exceeding 10 %, which can interfere with the activity/specificity of certain restriction endonucleases.

2.3.9 Removal of 5' terminal phosphate groups from cleaved plasmid DNA

In order to reduce the efficiency with which plasmid DNA cleaved by a single restriction endonuclease would re-ligate itself without any insert DNA, the 5' terminal phosphate groups were removed by treatment with calf intestinal alkaline phosphatase (CIAP). Restriction digests were set up and incubated as in section 2.3.8 and then 5 µl manufacturers 10 x CIAP buffer and 2 µl CIAP (1 unit/µl) were added to the digestion mixture and the final volume made up to 120 µl with sterile H_2O. This mixture was incubated at 37°C for 1 hr prior to incubation at 65°C for 10 min to inactivate the CIAP.

2.3.10 Ligation of DNA fragments

Recombinant plasmids were created by annealing cut fragments using T4 DNA ligase. All restriction digests in this study resulted in the production of compatible cohesive ends. Relative quantities of cut vector and digested inserts were determined by agarose gel electrophoresis (section 2.3.6) and cohesive end ligation reactions were set up so the vector:insert ratio was 1:1, 1:3 and 1:5. Ligations were set up as follows and incubated at 16° C for 24 hr:

vector	x μl
insert	x μl
5x T4 DNA ligation buffer	2 μl
T4 DNA ligase (5 units/μl)	1 μl
Sterile H_2O	x μl to a total volume of 10 μl

Vector only controls were set up as above except without the addition of insert DNA.

2.3.11 Polymerase Chain Reaction (PCR)

PCR was used to generate DNA fragments needed for the construction of recombinant plasmids and also to screen newly generated recombinant plasmids for the correct DNA inserts. For the synthesis of DNA to be used for cloning, a DNA polymerase enzyme with proofreading (3' to 5' exonuclease) activity KOD(XL)™ (Novagene) DNA polymerase was used in the following typical reaction mixture:

KOD (XL) 10x Buffer	5.0 µl
dNTP mixture (2 mM)	5.0 µl
forward PCR primer (100 µM)	1 µl
reverse PCR primer (100 µM)	1 µl
DNA template (100 ng/µl)	1 µl
KOD (XL) DNA polymerase	0.3µl
Sterile H_2O	36.7µl

The PCR mixture was subject to a pre-amplification denaturation step of 94 °C for 3 mins and then typical thermal cycling parameters were as follows: denaturation, 94 °C for 1 min, annealing, 45-65 °C for 30 secs and extension, 74 °C for 30 secs per kb of target DNA, for a total of 30-35 cycles and a final extension period of 5mins.

TAQ^{TM} polymerase was used to screen for bacterial cultures containing the appropriate DNA insert.

10x PCR buffer*	5 µl
dNTP mixture (2 mM)	5 µl
forward PCR primer (100 µM)	1 µl
reverse PCR primer (100 µM)	1 µl
bacterial culture*	5 µl
TAQ DNA polymerase (5 units/µl)	0.5 µl
Sterile H_2O	32.5 µl

TAQ polymerase does not have 3'->5' proofreading activity and has 4 times less fidelity than KOD.

*10X PCR reaction buffer: 100 mM Tris-HCl, 15 mM $MgCl_2$, 500mM KCl, pH 8.3 (20 °C)

*Bacteria transformed with the plasmid of interest were grown in LB culture and when turbid this was used directly in the PCR.

The PCR mixture was subject to a pre-amplification denaturation step of 94 °C for 5 min and then thermal cycling parameters were as follows: denaturation, 94 °C for 30 sec, annealing, 45 °C for 30 sec and extension, 72 °C for 1 min per kb of target DNA, for a total of 35 cycles and a final extension cycle of 72 °C for 5 mins.

2.3.12 Annealing of single-stranded oligonucleotides

Complimentary oligonucleotides for generation of FLAG-tag were diluted to 10 ng/µl and treated separately with Polynucleotide Kinase. They were then ethanol precipitated, resuspended in 10 µl H_2O each and combined. Annealing was catalysed by heating to 100 °C (2 min) and slow cooling (100 °C down to 40 °C over 30 min) using a Perkin Elmer DNA Thermal Cycler 480.

2.3.13 Polynucleotide Kinase treatment of DNA

5 µl DNA was phosphorylated in a 50 µl reaction volume using 2 µl Polynucleotide Kinase and 10 µl 5x T4 DNA ligase buffer (Roche) at 37 °C for 30 min.

2.3.14 Solutions

Agarose gel loading buffer (6x): 0.25% (w/v) bromophenol blue dye, 30 % (v/v) glycerol

Tris-borate-EDTA (TBE): 40 mM Tris base, 40 mM boric acid, 1 mM EDTA (pH 8.0)

Tris-EDTA (TE) buffer (1x): 10 mM Tris/HCl (pH 8.0), 1 mM EDTA

Cell Lysis Solution I: (25 mM Tris pH 8.0, 10 mM EDTA pH 8.0)

Cell Lysis Solution II: (0.2 M NaOH, 1% SDS)

Cell lysis Solution III: (60 ml 5 M potassium acetate, 11.5 ml glacial acetic acid, 28.5 ml H_2O)

2.4 Cell culture

2.4.1 Maintenance of cell lines

HEK293, U2OS, COS-1 and SY-5Y cells were routinely maintained in Dulbecco's modified Eagle's medium (DMEM) containing phenol red and supplemented with 10 % (v/v) heat inactivated (56 °C for 1 hr) fetal calf serum (FCS), 1% (v/v) 0.2 M L-glutamine and 1% Penicillin/Streptomycin antibiotics. Cells were grown in 100 mm tissue culture (TC) dishes at 37 °C in a humidified atmosphere containing 5 % CO_2. Cells were passaged at 100 % confluency for a maximum of 30 passages at which point the cells were discarded. To passage cells, the DMEM was aspirated and the cell layer washed twice with sterile PBS. 1 ml trypsin/EDTA was added (for all cell-lines except HEK293 only) to the cell layer and incubated at room temperature for 1 min prior to being aspirated and the cells returned to the 37 °C, 5 % CO_2 incubator for 10 min. Cells were then resuspended in the appropriate volume of DMEM and transferred to fresh 100 mm TC dishes (for maintenance) or 6-well plates (for transient transfections).

2.4.2 Transient transfection – Transfast method

The Transfast™ mammalian transfection kit was used for transient transfections by the Transfast liposomal transfection method according to the manufactuer's instructions. Briefly, the cells to be transfected were seeded at a density of $5x10^5$ cells/well in a 6 well dish in complete DMEM i.e. 10% HI FCS, 1% L-glutamine, 1% Pen/Strep until they were adherent. The plasmid DNA to be transfected was placed in a 1.5ml microcentrifuge tube to which 100µl of DMEM was added and vortexed for 10 secs. Following this 2µl of Transfast/µg DNA was added to the solution and vortexed for 10 secs. The DNA/DMEM/Transfast solution was then incubated in the hood for 15 mins. During the incubation period, the cells were taken from the incubator and the media was aspirated off the cells. They were equilibrated with 900 µl of fresh DMEM and returned to the incubator for 10-15 mins. After the 15 min incubation period had elapsed, the DNA/DMEM/Transfast was vortexed briefly and added to the cells in a dropwise fashion. The cells were replaced in the incubator for a period of 1 hour after which time the final volume of each well was made up to 3 ml with DMEM containing Hi-FCS 15%(v/v), 1% L-glutamine, 1% Pen/Strep and the cells were incubated for the desired period 12-48 hr.

2.4.3 Calcium phosphate-mediated transfection of adherent cells

For reporter assays, adherent cells were seeded at $1\text{-}2x10^5$ cells/well in 6-well plates overnight prior to transfection (TPP, c/o Helena Biosciences) with 2 ml phenol red-free medium (GIBCO) supplemented with 5 % DCSS. Phenol-red free media was used as phenol-red dye bears structural similarity to androgen and can mimic its effect. Unless otherwise stated, the quantities of transfected plasmids per well were as follows: 100 ng β-galactosidase reporter pCH110, 500 ng luciferase reporter, 100 ng expression vectors for transcription factors and other proteins of interest. Empty vector (pcDNA3.0PT) was used to standardise the quantity of DNA in each well in the experiment. 1-4 hr prior to transfection, cells were washed with sterile 1x PBS and fresh medium was added (2 ml for 6-well plate experiments. Transfections were carried out using the CalPhosTM Mammalian Transfection Kit (Clontech, Basingstoke, U.K.) with some modifications: for 6-well plate experiments, a 100 µl/well DNA mastermix containing sterile water, DNA and 12.5 % (v/v) 2 M calcium chloride solution was prepared for each transfection condition. This was added dropwise to an equivalent volume 2x Hepes Buffered Saline (HBS) solution while vortexing gently. After a 20 min incubation at room temperature the solution was mixed by pipetting and 200 µl was added dropwise to the 2 ml medium present in each well. 8-16 hr later the medium was removed, the cells were washed twice with 1x PBS and fresh medium was added. For experiments involving the Androgen receptor, 30 mins to 24 hours before harvesting, depending on the experiment, 10^{-8} M Mibolerone, an Androgen analogue, or vehicle was added. The cells were then lysed at the appropriate time (24 hours to 48 hours).

2.5 Biochemical Techniques

2.5.1 Preparation of cell-free extracts for Western blotting

Cells were harvested by aspirating the DMEM and scraping the cell layer into 10ml sterile PBS which was transferred to a sterile 15ml Greiner tube. Centrifugation at 4000 rpm for 5 min at 4 ^{O}C was used to pellet the cells before discarding the supernatant. The pelleted cells were resuspended and lysed on ice in 1 x the pellet volume of the required cell lysis buffer containing protease inhibitors. Lysis was allowed to proceed for 30 mins with periodic vortexing to aid efficient lysis and then the cell debris was pelleted by centrifugation at 13,000 rpm, 4°C for 2 min. The cell-free extract (supernatant) was transferred to a fresh sterile 1.5 ml microfuge tube. Cell-free extracts and cell debris pellets were stored at –20 ^{O}C.

2.5.2 Co-Immunoprecipitation

Co-immunoprecipitation (Co-IP) was used to identify putative protein-protein interactions and post-translational modifications. Cells were seeded in 100 mm dishes and transfected at 60 % confluency with one or two DNA constructs (section 2.4.2). 48 hr post-transfection the cells were lysed in Co-IP buffer for 30 mins with vortexing at regular intervals and the protein concentration determined. For pre-clearing, 20 µl of protein A/G agarose beads were added to each sample and placed on a moving wheel at 4 °C for 30mins. These were then spun down by centrifugation at 2500 g, 4 ^{O}C for 5 mins. To bind the protein of interest, 20 µl of primary antibody and 20 µl of protein A/G sepharose beads were added to the supernatant and the samples were placed on the wheel mixer for 2-24 hr during which time immune complexes will form. After this period elapsed, the samples were spun down by centrifugation at 2500 g, 4 ^{O}C for 5 mins. The supernatant was removed and placed in the –20 ^{O}C. The protein A/G sepharose beads bound to the immune complexes were washed in Co-IP buffer 3-4 times and the beads were spun down by centrifugation at 2500 g, 4 ^{O}C for 5 mins. The supernatant was removed and SDS-loading buffer (1X) was added and boiled for 5 mins. The samples were vortexed and spun down at 2500 g in a bench top centrifuge. The supernatant was then loaded on an SDS-polyacrylamide gel (8 %-12%) and Western blotting was carried out (section 2.5.4) to see if the antibody-protein complex bound a protein of interest. This procedure was also used to monitor post-translational modification such as SUMOylation and acetylation.

2.5.3 SDS-polyacrylamide gel electrophoresis (PAGE)

Cell extracts were analysed by one-dimensional polyacrylamide gel electrophoresis using either a mini-gel system (Protean II, Bio-Rad) or large gel system (Bio-Rad), according to the method described by Laemmli, 1970. Cell extracts (mammalian and yeast) and *in vitro* translated proteins were resuspended in the appropriate volume of SDS-loading buffer and boiled for 5 min, prior to being resolved on 8-12% SDS-polyacrylamide gels (table 2.2), depending on the sizes of the proteins to be resolved.

	Resolving Gel		**Stacking Gel**
%	**8%**	**12%**	**5%**
dH_2O	4.6 ml	3.3 ml	6.8 ml
30% acrylamide	2.7 ml	4.0 ml	1.7 ml
1.5 M Tris (pH 8.8)	2.5 ml	2.5 ml	1.25 ml (pH 6.8)
10% SDS	100 µl	100 µl	100 µl
10% APS	100 µl	100 µl	100 µl
TEMED	6 µl	4 µl	10 µl

Table 2.2 Preparation of polyacrylamide gels

2.5.4 Western blotting

Protein samples were separated by SDS-PAGE and transferred from the polyacrylamide gel to nitrocellulose membrane by electrophoresis using a wet transfer apparatus (Bio-Rad). Membranes were incubated in Ponceau S stain for 5 min and then washed in sterile H_2O to monitor protein transfer. Ponceau S stained membranes could be photocopied or photographed.

The following incubation steps were performed at room temperature on a rocking platform. Membranes were incubated in blocking buffer for 30 min at room temperature, to block non-specific antibody binding sites, prior to being incubated with primary antibody at 4 ^{O}C O/N. Primary antibodies were prepared in blocking buffer at dilutions indicated in table 2.3. Membranes were washed in PBS containing 0.1% Tween 20 (3 x 10 min) and incubated in the appropriate secondary antibody for 30 mins at room temperature. Horseradish peroxidase (HRP) conjugated secondary antibodies were prepared blocking buffer at dilutions specified in Table A1. Membranes were then washed as above and proteins were visualized using ECL according to manufacturers' instructions. For re-use with other primary antibodies, membranes could be stripped by incubation in stripping buffer for 15 min at 50 °C with occasional agitation, washed as above and then re-probed with antibodies or stored at 4 °C wrapped in moistened saran wrap.

2.5.5 Protein assay

The protein concentration of samples was measured using the Bio-Rad protein assay reagent according to manufacturer's instructions. Typically 2 µl of the sample was mixed with 200 µl protein assay reagent and 800 µl dH_2O in a cuvette, incubated at room temperature for 15-20 min and then its absorbance at 595 nm (A_{595nm}) was measured. Protein concentration was calculated using A_{595nm} values of diluted BSA standards of known concentrations.

2.5.6 Harvesting adherent cells for reporter assays

Transfected cells to be harvested for reporter assays were washed once with 1x PBS and harvested by scraping in 50 µl 1x Reporter Lysis Buffer (Applied Biosystems, Bedford, Ma., U.S.A.). Following vigorous vortexing, the cells were centrifuged at 2000 rpm for 5 mins and frozen at –20 °C.

2.5.7 Luciferase assays

Harvested cells stored at –20 °C in lysis buffer were centrifuged (8 min, 13,000 rpm, 4°C) directly from the freezer and placed on ice. Luciferase and β-galactosidase activities were determined using the Dual-Light System (Applied Biosystems, Bedford, MA, U.S.A). 5 μl of each cell extract was added in duplicate to a 96 well plate and 12.5 μl of buffer A was added to each well. A stock solution of buffer B (50 μl per sample + 600 μl for priming + Galactone-Plus 1:100) was made up in a universal tube and the green tube marked "1" from the Luminometer was placed in the solution. The red tube marked "2" from the Luminometer was placed in the Accelerator. The luciferase and the β-galactosidase were measured using a Berthold Orion microplate luminometer. The luciferase:β-galactosidase ratio for each tube was calculated and the average ratio and S.E.M. (standard error of the mean) for each transfection condition determined. Relative Luciferase Activity (RLA) was calculated by dividing the average luciferase:β-galactosidase ratio for each condition by that for wells containing reporter DNA alone.

2.5.8 Indirect Immunofluorescence

1-3 x 10^5 cells were seeded on 25 mm coverslips in 6 well tissue culture plates and when fully adherent, were transfected with appropriate plasmid DNA as described in Section 2.4.2. 24 or 48 hr post-transfection the following steps were performed at room temperature with the coverslip undisturbed in the well. The cells were gently washed twice with sterile PBS, taking care not to disrupt the cell layer on the coverslip, and fixed by incubation in 1.5 ml 4% (w/v) paraformaldehyde for 10 min. Cells were washed in PBS (3 x 5 min) to remove excess paraformaldehyde which could interfere with fluorescence and permeabilised by incubation with

1.5 ml 0.2% (v/v) Triton X-100 (in PBS) for 2 min, followed by washing in PBS as above. Cells were again washed as above and incubated in 1 ml Hoechst stain 33258 (1 µg/ml final concentration) for 5 min (this step was only included for epifluorescence microscopy). To block non-specific binding sites, cells were incubated in 1 ml PBS, 3 % BSA for 30 min. Primary antibodies were prepared in PBS with 3% BSA at dilutions specified in Table 2.4 to a final volume of 50-200 µl. To prevent the coverslip drying out, a large sheet of blue towel was soaked in water and placed on the bench. A 50 x 10 cm strip of paraflim was placed on top of the blue towel and 50 µl of primary antibody/slide was pipetted on. The slides were removed from the well and inverted with the cell side down on the primary antibody. When this step was completed for each slide, the slides were covered with a box creating a semi-humidified container. After 1hr the slides were replaced in the plate and washed as above. Alexa-488 or Alexa-594-conjugated secondary antibodies were prepared in PBS 3 % BSA at 1/400 dilution and 100 µl was pipetted onto a new strip of parafilm. Control cells were incubated in secondary antibody only, to determine background fluorescence. The slides were inverted as above and covered with an aluminium foil box for 30 mins. The slides were once again replaced in the wells and washed in PBS. After washing each coverslip was carefully removed from its well, drained of excess solution by dabbing one edge of the coverslip on a tissue and placed cell side down onto 10 µl mounting media (Section 2.8) spotted onto a microscope slide. The coverslips were secured on the microscope slides by applying a thin layer of clear nail varnish around the edge of the coverslip and allowed to dry. Slides were stored at 4°C, protected from light. Fluorescent cells were imaged using either a Zeiss LSM510 meta confocal microscope or an ORCA ER charge-coupled-device camera (Hamamatsu) attached to a Nikon TE300 inverted microscope.

2.5.9 Live-Cell Imaging

Cells of interest were seeded on 25 mm coverglass or 22 mm coverglass. The cells were transfected once all the cells had adhered to the coverglasses and successful transfection was observed on a Zeiss Axioskop 2 fluorescent microscope. Once the cells were deemed to have a high transfection efficiency, the heated stage was switched on (set at 37 ^{O}C) followed by Xenon bulb, Orbit controller, camera, Ludl wheel, computer. Openlab 3.06 software was opened and the automation GFP over time OR gfp/bf time lapse version 3.08 Mic3 Phase/GFP only Mic1. The metal ring used to hold the coverglass in place during imaging was cleaned with some IMS in the hood. A P10 tip was used to apply sterile grease onto the metal ring in the hood. The coverglass was removed from the 6 well plate using a sterile forceps and the bottom was cleaned using ethanol. The coverglass was placed in the bottom section of the ring and the top section was secured by gently pressing it into the grooves of the bottom ring. 400 µl-600 µl of CO_2 independent medium was carefully placed onto the coverglass using a p 1000 pipette. 300 µl-500 µl of mineral oil was then layered onto the medium. The ring containing the coverglass, medium and oil was placed in a 100mm dish, carried to the microscope and gently lowered into the hole in the centre of the heated stage. Oil was applied to the objective if required and the heated stage was slotted into the grooves of the microscope stage. Once this was completed, the cell layer was focused using brightfield and the automation was run using an an ORCA ER charge-coupled-device camera (Hamamatsu, Hamamatsu City, Japan) attached to a Nikon TE300 inverted microscope for the desired length of time making sure the cells did not dry out.

2.5.10 Stripped FCS for nuclear receptor transfections

One litre foetal calf serum (FCS) was stripped of all nuclear receptor ligands using a dextran-charcoal mix. 125 ml dextran-charcoal mix was added to each of eight 250 ml bottles and centrifuged (8,000 rpm, 20 min). The supernatant was carefully removed to leave the dextran-charcoal pellet and the 1 litre FCS split between four of the bottles. After careful mixing the FCS-charcoal-dextran solution was transferred to a 2 litre conical flask and incubated at 55 ^{O}C for 30 min with shaking. The mix was then returned to the four 250 ml bottles and centrifuged (8,000 rpm, 20 min, 4 ^{O}C). The supernatant was carefully removed and added to the remaining four bottles containing the dextran-charcoal mix pellet for the second round of stripping. The FCS-dextran-charcoal solution was mixed, incubated, and centrifuged, as already described. To remove trace charcoal from the DCSS (dextran/charcoal stripped serum), the solution was drawn through a 0.8 µm filter under vacuum. It was then transferred to a tissue culture hood, passed through a 0.2 µm filter, aliquoted into sterile plasticware in 25 ml volumes and frozen at -20 ^{O}C.

2.5.11 Small-scale bacterial expression of GST-tagged proteins

Bacterial colonies from a freshly transformed plate were inoculated into 2.5 ml LB Ampicillin medium. After 2 hr growth (37 ^{O}C) 1 ml was placed in two microfuge tubes. IPTG was added to one to a final concentration of 500 µM (induced culture), and an equal volume of water was added to the other (control culture). The remaining 0.5 ml was kept at 4 ^{O}C for future inoculation of large-scale cultures. After a further 3 hr growth (37 ^{O}C) the cells were harvested by centrifugation (4,000 rpm, 5 min) and the pellets resuspended in 50 µl SDS-PAGE sample buffer. After boiling, 20 µl was loaded onto a SDS-PAGE mini-gel. Induced cultures were run alongside the appropriate control culture and the presence of an induced protein band of the correct size determined after staining.

2.5.12 Large-scale bacterial expression of GST-tagged proteins

The remaining 0.5 ml from bacterial cultures showing good protein induction during small-scale expression analysis were used to inoculate 10 ml LB-Ampicillin medium (overnight, 37 ^{O}C, 220 rpm). A 200 µl sample was removed to a microfuge tube (uninduced). IPTG was added to a final concentration of 500 µM and the cultures were incubated for a further 3 hr. A second 200 µl sample was then taken which represented the induced fraction. The cells were harvested by centrifugation (50 ml volume, 4,000 rpm, 10 min, 4 ^{O}C) and the pellet was frozen.

2.5.13 Purification of GST-tagged proteins

Induced bacterial pellets from 50 ml culture aliquots were resuspended in NDTN Buffer and sonicated (20 sec on / 40 sec off, 3 cycles, power 12, MSE Soniprep 150, Sanyo). Cell debris was removed by centrifugation (4,000 rpm, 5 min, 4 ^{O}C), the supernatant transferred to a 15 ml falcon and a 20 µl sample removed. 100 µl glutathione sepharose beads were washed three times with an equal volume 0.5% milk powder in NDTN Buffer, collected by centrifugation (2,000 rpm, 2 min) and resuspended in 100 µl milk/NTN. 125 µl bead slurry was added to the cleared 5 ml bacterial supernatant and placed on a rotating wheel at 4 ^{O}C for 1 hr. The glutathione beads were collected by centrifugation (2,000 rpm, 2 min, 4 ^{O}C) and a 20 µl sample of the aspirated supernatant kept for later analysis. The beads were washed (5 min, rotating wheel, 4 ^{O}C) three times with NDTN, resuspended in 1 ml NDTN (20 µl sample taken) and stored at 4 ^{O}C. SDS-PAGE was used to determine the level of GST-fusion protein induction and the success of purification. Uninduced and induced cell pellets were resuspended in 50 µl SDS-PAGE sample buffer and boiled. The cell debris pellet was resuspended in 5 ml NDTN by pipetting and a 20 µl sample taken. This sample along with the post-sonication supernatant sample, glutathione bead-cleared supernatant sample and final bead:GST-fusion sample were mixed with SDS-PAGE sample buffer, boiled and run alongside 20 µl samples of uninduced and induced cell pellets. Relative levels of induced protein at each stage were determined by Coomassie staining of the

SDS-PAGE gel.

2.5.14 *In vitro* transcription and translation of expression vector-encoded cDNA

cDNAs cloned into expression vectors under the control of the T7 or Sp6 promoter were transcribed and translated *in vitro* in a coupled reaction using TNT. Coupled Reticulolysate System (Promega). Briefly, 1 μg expression plasmid (containing a T7/Sp6 promoter) was mixed with 25 μl rabbit reticulolysate, 2 μl TNT reaction Buffer, 1 μl T7/Sp6 RNA Polymerase, 2 μl amino acid mixture (minus Methionine), [35S]- Methionine (1.175 mCi/mmol, Amerham), 1μl RNasin. Ribonuclease Inhibitor (Promega) and nuclease-free water to 50 μl. The mixture was incubated for 90 min at 30 ^{O}C. Samples (1 μl and 0.1 μl) of each reaction were loaded onto an SDS-PAGE gel to determine the efficiency of translation. The rest of the IVT was stored at -80 ^{O}C.

2.5.15 GST-pulldown of mammalian expressed protein

Normalised levels of GST-tagged fusion proteins (as determined by SDS-PAGE) were incubated (4 hr, rotating wheel, 4 ^{O}C) with *in vitro* translated (IVT) protein in a 1 ml volume of NDTN. The beads were washed three times (5 min, rotating wheel, 4 °C), aspirated, dried under vacuum (Savant DNA Speed Vac. DNA120), resuspended in 20 μl SDS-PAGE sample buffer, boiled and run on an SDS-PAGE mini-gel.

2.5.16 *In vitro* protein SUMOylation assay

Reaction mixtures containing equal concentrations of [^{s}35] IVT protein (section 2.5.13), recombinant 0.1 μg SAE1/SAE2, 0.45 μg Ubc9, 1 μg SUMO1/2 (Alexis biochemicals) were incubated in SUMO conjugation buffer at 30 °C for 2 hours. The reactions were stopped by addition of 4X SDS-loading buffer and incubated at 95 °C for 5 mins. The proteins were resolved on 10 % SDS-PAGE gels.

2.5.17 Fixing and amplifying radioactive SDS-PAGE gels

The fixation of radioactive gels was carried out in 10 % (v/v) glacial acetic acid, 10 % methanol, 1 ml Glycerol and incubated for 30 mins at room temperature. The gels were washed twice in H_2O and placed for a further 1 hour in 20 ml of Amplify (Amersham). The gels were placed on filter paper, covered with saran wrap and dried down under vacuum at 80 °C for 2 hours.

2.5.18 Exposure of radioactive gels to x-ray film and phosphorimager plates

Dried gels were placed in X-Ray film cassettes and exposed to a phosphorimager plate for between 2 and 24 hours and processed using a Bio-rad Molecular imager FX phosphorimager. The gels were then exposed to X-ray film between 24 hours and 2 weeks depending on the intensity of the signal and the X-ray film was developed.

2.5.19 Solutions

Co-IP buffer: 150 mM NaCl, 50 mM Tris-Hcl pH 7.4, 1 % NP-40, 1.5 mM $MgCl_2$, EDTA-free Complete^{TM} supplemented with fresh protease inhibitors 1 mM NaF, 1 mM PMSF and leupeptin, aprotinin, pepstatin at 10 μg/μl each.

Tris-glycine-SDS PAGE running buffer (10x): 250 mM Tris base, 2 M glycine, 35 mM SDS

Tris-glycine-SDS transfer buffer (standard): 39 mM glycine, 48 mM Tris base, 0.037% (w/v) SDS, 20 % (v/v) methanol (pH 8.3)

Tris-glycine-SDS transfer buffer (for high molecular weight protein transfer): 380 mM glycine, 48 mM Tris base, 0.037% (w/v) SDS, 20% (v/v) methanol

SDS-PAGE loading buffer (4x): 62.5 mM Tris (pH 6.8), 10 % (v/v) glycerol, 2 % (w/v) SDS, 20 mM β-mercaptoethanol, 0.05 % (w/v) bromophenol blue

Coomassie® Blue staining solution: 10 % (v/v) acetic acid, 40 % (v/v) methanol, 0.25 % (w/v) Coomassie® Blue R-250

Destaining solution: 10 % (v/v) acetic acid, 40 % (v/v) methanol

Fix solution: 10 % (v/v) acetic acid, 10 % (v/v) methanol

RIPA buffer: 20 mM Tris (pH 8.0), 150 mM sodium chloride, 0.1 % (w/v) SDS, 1 % (v/v) NP40, 1 mM EDTA. 1 complete protease inhibitor cocktail tablet was added to 50 ml RIPA buffer.

NDTN buffer: 20 mM Tris-HCl pH 8.0, 200 mM NaCl (unless otherwise stated), 0.5 % (v/v) NP-40, 1 mM DTT, 1x ETDA-free Complete tablet (Roche) /25 ml buffer

Blocking buffer (for western blotting): 3 % (w/v) skimmed milk powder in PBS

SUMO conjugation buffer: 50 mM Tris pH 7.5, 10 mM $MgCl_2$, 5 mM ATP, 0.2 mM DTT

Dextran-charcoal mix: 10 g charcoal, 1 g Dextran T70, 10 ml 1 M Tris-HCl pH 7.4, made up to 1 litre with deionised water

Stripping buffer: 100 mM β-mercaptoethanol, 2 % (w/v) SDS, 62.5 mM Tris/HCl (pH 6.7)

Mounting media: 90% (v/v) sterile glycerol, 3% (w/v) n-propyl-gallate in PBS

2.6 Yeast methods

2.6.1 Yeast strains and culture conditions

The genotype of *Saccharomyces cerevisiae* reporter strain L40 is *trp1 leu2 his3 ade2 LYS2::(lexAop)$_{4x}$-HIS3 URA3::(lexAop)$_{8x}$-LacZ.* For two-hybrid screening, the yeast reporter strain L40 contains *lacZ* and *HIS3* as reporter genes downstream of the LexA binding site. Yeast strains were grown at 30 °C in YPD medium or in synthetic minimal medium with appropriate supplements.

2.6.2 Yeast transformation

A single colony of *S. cerevisiae* strain L40 from a fresh plate was inoculated into 25 ml YPD or inoculated at optical density $(OD)_{600}$ 0.01 and grown overnight at 30 °C with shaking until the culture reached an $OD_{600} = 0.8\text{-}1.0$ (equivalent to approximately $2x10^7$ cells /ml). The cells were pelleted by centrifugation at 3,000 g for 5 minutes at room temperature. Then the pellet was washed twice with distilled water and transferred to a 1.5 ml tube. The cells were pelleted at maximum speed for 15 second and the supernatant was removed. Subsequently, the pellet was resuspended in 250 µl 100 mM Lithium Acetate and the suspension was incubated at 30 °C for 15 mins. In parallel, carrier DNA, such as salmon sperm DNA which facilitates the transfer of plasmid DNA, was boiled for 5-10 minutes and quickly chilled on ice. For each transformation, 173 µl of transformation mix was aliquoted into each fresh 1.5 ml tube. 2 µl of transforming DNA and 23 µl of cell suspension was then distributed into the transformation mix, vortexed, and incubated at 30 °C for 30 minutes with shaking. After that, the cells were heat-shocked in a 42 °C water bath for 20 minutes. The transformants were spun down with maximum speed centrifugation for 15 second and the supernatant was discarded. The pellet was resuspended in 200 µl distilled water and plated onto SD medium plate lacking amino acid for selection. The plates were incubated at 30 °C for 2-4 days.

2.6.3 Preparation of a yeast cell free lysate

Transformed yeast colonies were used to inoculate 15 ml SD media lacking selective amino acids and incubated overnight at 30 °C. The overnight culture was centrifuged at 3,000 g for 5 minutes and the cells were washed and pelleted twice with distilled water. The cells were transferred to 1.5 ml tube, repelleted and resuspended in 150 µl breaking buffer. Acid-washed glass-beads (425-600 mm) were added into the cell suspension until the beads reached a level just below the meniscus of the liquid. The samples were vortexed vigorously for 30 seconds and placed on ice to cool; this step was repeated four times for each sample. Then, the samples were centrifuged at 13,000 rpm, for 15 mins at 4 °C. The protein extract was then collected into a fresh tube.

2.6.4 Quantitative β-galactosidase activity assay

5 to 50 µl of each yeast cell free lysate was adjusted to 500 µl with Z buffer. Samples

were vortexed and equilibrated at 30 °C for 5 mins. The reaction was initiated by addition of 100 ul of 4 mg/ml onitrophenylgalactoside (ONPG) in Z buffer and timed. The reactions were quenched by addition of 250 µl 1M Na_2CO_3 when a pale yellow color had developed; the stop time was recorded. The absorbance of the sample was read at OD420 nm. The protein concentration was determined by using Bradford reagent (BioRad). The enzyme activity was calculated according to the following formula:

Specific activity (nmol/ml/min) =

$$\frac{\text{OD420x0.85}}{\text{0.0045 x Protein conc x volume x time}}$$

2.6.5 Composition of solutions and media used for Yeast methods

Z buffer: 60 mM $Na_2HPO_4.7H_2O$, 40 mM $NaH_2PO_4.H_2O$, 10 mM KCl, 1 mM $MgSO_4.7H_2O$, 0.3 % β-mercaptoethanol, pH 7.0

Breaking Buffer: 0.4 M KCl, 50 mM Tris-Hcl, pH 7.9, 1 mM PMSF, 1 complete protease inhibitor cocktail tablet was added to 50 ml buffer

YPD: Bacto-yeast extract (10 g/L), bacto-peptone (20 g/L), glucose (20 g/L), bacto-agar 20 g/L (for plates only)

SD (synthetic dextrose minimal media): Bacto-yeast nitrogen base without amino-acids (6.7 g/L), glucose (20 g/L), drop-out mix (2 g/L), bacto-agar 20 g/L (plates only)

Transformation mix: 1.2 ml 50 % PEG, 180 µl 1.0 M LiAc, 250 µl carrier DNA, 100 µl distilled water

Chapter 3

Effect of SUMO conjugation on the subcellular localisation and coactivator function of CBP

3.1 Introduction

The nucleus contains a number of distinct structures which are not membrane bound such as Cajal bodies, interchromatin granules and PML bodies. PML bodies are matrix associated, multiprotein structures between 250-500nm in diameter and are present in the nucleus of most cell lines (Ascoli *et al.*, 1991). PML was originally identified as a fusion partner of retinoic acid receptor in the t(15,17) translocation resulting in the PML-RARα fusion which ultimately leads to acute promyelocytic leukemia (APL).

There are over 50 known proteins that associate with PML bodies; the majority of these associate transiently, such as p53, while PML and Sp100 are among the structural components. Functions of the associated proteins include transcription, DNA repair, mRNA stability, and mRNA transport (Borden, 2002). While the exact function of PML bodies is unknown they have been implicated in apoptosis, translation and cellular senescence. Several groups have suggested that PML bodies play a role in transcription due to the fact that they act as a repository for assemblies of transcription factors and chromatin remodelling factors. La Morte *et al.* (1998) demonstrated via immunoelectron microscopy that CBP and nascent RNA both associated with PML bodies in Hep-2 cells. However, other reports demonstrated, using both 3-D microscopy and electron microscopy, that PML bodies were not sites of transcription or RNA splicing although newly synthesised RNA was found adjacent to PML bodies (Boisvert *et al.*, 2000, Grande *et al.*, 1997). However, it may be that PML bodies associate with nascent RNA at certain times during the cell cycle, as yet this has not been investigated.

Boisvert *et al.* (2001) carried out a comprehensive study of CBP and its interaction with PML bodies. They showed by immunofluorescence microscopy that CBP is a component of PML bodies in a cell-type specific manner. However, CBP is a dynamic not a structural component of the PML bodies. By using FRAP (Fluorescence Recovery After Photobleaching) technology which irreversibly bleaches a defined area of the nucleus, they demonstrated that CBP moved into and out of the PML bodies. Furthermore, La Morte *et al.* (1998) demonstrated that CBP localised to the interior of PML bodies while PML was preferentially associated with the periphery. Thus, PML bodies may act as an anchor for concentrating such factors as CBP until they are needed during cellular processes.

Many proteins that associate with PML bodies are SUMOylated including Sp100 (Sternsdorf *et al.,* 1997), p53 (Rodriguez *et al.,* 1999) and PML itself (Boisvert *et al.,* 2001). SUMOylation of PML body proteins may be essential for their localisation to these structures. For example, mutation of SUMO sites within the orphan receptor LRH-1 led to its release from PML bodies and resulted in its association with chromatin (Chalkiadaki *et al.,* 2005). While ubiquitination often targets proteins for degradation, SUMOylation seems to stabilise the proteins and can alter the subcellular localisation or the transcriptional activity of the target protein. For example, mutation of conserved SUMO sites within TDG resulted in a decrease in its DNA and AP-1 binding affinity (Hardeland *et al.,* 2002). Also, SUMOylation of many transcription factors such as myocyte enhancer factor 2 (MEF2) resulted in a decrease in its ability to mediate transcription (Riquelme *et al.,* 2006).

Ishov *et al.* (1999) demonstrated that proper PML body formation required SUMOylation. Work carried out by Best *et al.* (2002) on the SUMO protease, SuPr-1, suggested that co-activators may be recruited into the PML bodies and once there they may be de-SUMOylated, at which point they leave in their desired co-activator complexes. They showed that SuPr-1 bound to SUMO-modified PML stimulated c-jun mediated transcription by redistributing co-activators associated with PML bodies. This included CBP which was dispersed once SuPr-1 had hydrolysed the SUMO modified PML. However they did not show whether SuPr-1 had any effect on CBP SUMOylation or if CBP redistribution was due directly to SUMO deconjugation of CBP by SuPr1 or indirectly by SUMO deconjugation of PML which affected its interaction with CBP. This may tie in with the observations made by Girdwood *et al.* (2002) who demonstrated that p300 is SUMOylated at two back-to-back ψKXE motifs within the previously described CRD1 and this leads to recruitment of HDAC6 and transcriptional repression.

This chapter describes work carried out to test the hypothesis that CBP is SUMOylated and to investigate whether SUMOylation of CBP affects its subcellular localisation, its ability to associate with PML bodies and its ability to function as a transcriptional coactivator.

3.2 CBP foci colocalise with PML bodies *in vivo*

At the outset of this work it was shown that the CBP paralogue p300 was SUMOylated within the CRD1. As CBP contains ~5 putative SUMO sites and associates with PML bodies, we hypothesised that SUMOylation regulated the subcellular localisation of CBP. Firstly, immunofluorescence microscopy studies were performed to test reagents and to confirm the reports in the literature which showed that CBP colocalised with PML bodies *in vivo* (Boisvert *et al.*, 2001). COS-1 and HEK293 cells were seeded, fixed, permeabilised and stained for endogenous CBP and an Alexa-488 conjugated secondary antibody while localisation of endogenous PML was observed with a mouse PML antibody (PG-M3; Sigma-Aldrich) and an Alexa-594 conjugated secondary antibody. Figure 3.1 shows that endogenous CBP is a nuclear protein with the majority of the population localising to discrete foci in both cell lines. Similarly, endogenous PML is a nuclear protein which also localises to nuclear foci or PML bodies. It is clear from the merge images that endogenous CBP and PML colocalise at PML bodies.

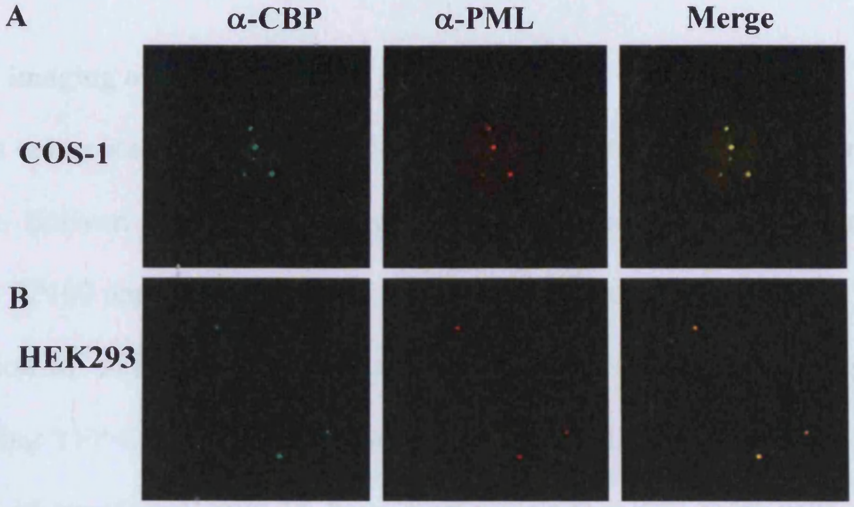

Figure 3.1 Endogenous CBP colocalises with PML bodies (A) COS-1 and (B) HEK293 cells were seeded on 22mm coverslips at 1 x 10^5 confluency prior to fixation in 4% paraformaldehyde. The cells were permeabilised and stained with antibodies raised against rabbit anti-CBP (green) and mouse anti-PML (red) followed by anti-mouse Alexa488 and anti-rabbit Alexa594 secondary antibodies.

3.3 Live-cell imaging of YFP-CBP

To aid us in our study of CBP, a YFP-CBP expression construct was generated (Phil Troke; unpublished). Boisvert *et al.* (2001) suggested that CBP was a dynamic component of PML bodies while SP100 and PML were relatively immobile in the nucleoplasm. Thus, we analysed the localisation of YFP-CBP over a 4-hour period using time-lapse imaging. An expression vector encoding YFP-CBP was transfected into HEK293 cells. YFP-CBP was nuclear diffuse in the majority of transfected cells 15 hours post-transfection and three cells with intermediate levels of fluorescence were selected for live-cell imaging. Using the Piezo drive and the GFP overtime automation we took five z-stacks, 2μm thick once every five minutes for a 4-hour period (Chapter 2 section 2.5.9). We noted that in each of the three selected cells, YFP-CBP accumulated in discrete nuclear foci, a subset of which localise to the nuclear periphery (Figure 3.2). Interestingly, a number of reports in the literature suggested that SUMOylation controlled the ability of proteins to associate in foci and with PML bodies, thus regulating their function such as LRH-1 and PML itself. But, it is important to note that SUMOylation does not affect the ability of all proteins to associate with PML bodies such as c-Myb (Dahle *et al.*, 2004) and SOX6 (Fernandez-Lloris *et al.*, 2006). However, we hypothesised that SUMOylation of CBP governed its ability to associate in discrete foci, which are likely to be PML bodies and furthermore, played an important role in regulating its coactivator function.

3.4 GFP-SUMO-1, but not GFP-SUMO-1 Glycine97Alanine mutant colocalises with CBP in PML bodies

To determine whether CBP co-localised with GFP-SUMO-1, COS-1 cells were transfected with GFP-SUMO-1 or GFP-SUMOG/A, a mutant form of SUMO that cannot be

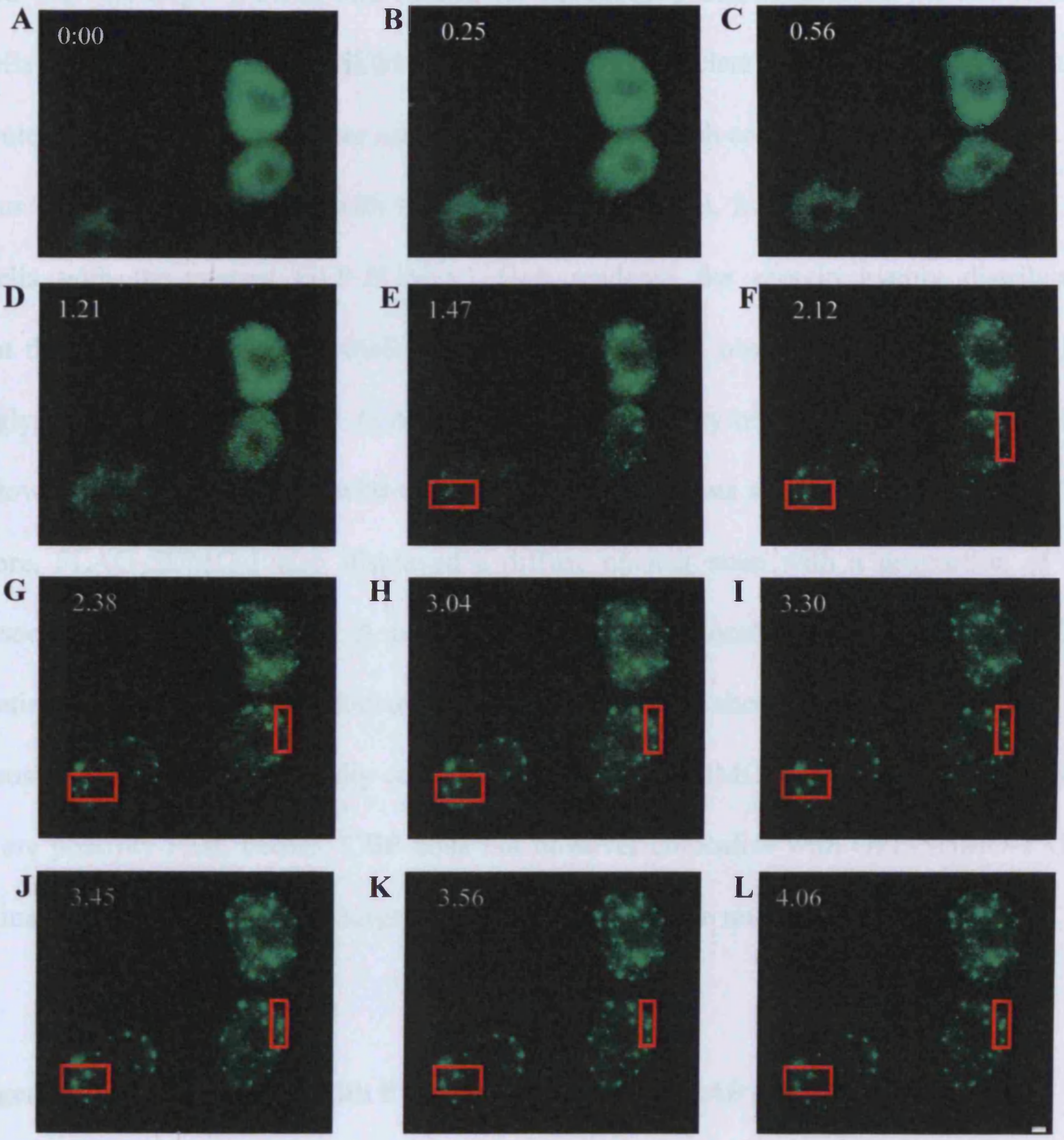
A
0:00
B
0.25
C
0.56
D
1.21
E
1.47
F
2.12
G
2.38
H
3.04
I
3.30
J
3.45
K
3.56
L
4.06

FIG 3.2 Live-cell imaging of YFP-CBP in HEK293

HEK293 cells were seeded on 25mm round coverslips and transfected after 24hours with an expression construct encoding YFP-CBP. 14 hours post-transfection the coverslip was placed on a heated stage and z-stacks (2μm) were taken once every 5 minutes for a 4 hour period. The images were deconvolved and merged to produce the composite images. Scale bar represents 1μM conjugated onto the target protein, and stained for endogenous CBP. Figure 3.3 A, shows that COS-1 cells transfected with GFP-SUMO-1 gave a diffuse nuclear stain but a subset of the SUMO protein accumulates in discrete nuclear foci many of which are PML bodies. A subset of endogenous CBP foci co-localised with these GFP-SUMO-1 foci. Interestingly, transfection of COS-1 cells with the mutant GFP-SUMO-1 G/A rendered the protein evenly distributed throughout the cell nucleus with a small number of nuclear foci observed in a subset of cells. Interestingly, expression of SUMO-1 G/A did not affect the ability of CBP to form nuclear foci, although low level fluroescence of wild-type SUMO-1 protein was still present (Figure 3.3 B). Furthermore, FLAG-SUMO-1 also displayed a diffuse nuclear stain with a proportion of the protein associating in nuclear bodies. A subset of these bodies colocalised with endogenous CBP foci indicating that not all SUMO-1 foci are PML bodies (data not shown).

Thus endogenous CBP partially co-localises with GFP-SUMO-1 in nuclear foci, a subset of which are possibly PML bodies. CBP does not however colocalise with GFP-SUMO-1 G/A due to its inability to conjugate to its target protein and associate in nuclear bodies.

3.5 Endogenous CBP colocalises with PIAS-1, PIAS-xα and PIASγ In PML bodies

As previously discussed, SUMO proteins are conjugated onto the target protein using E1, E2 and E3 SUMO ligases. *In vitro,* the E1 and E2 ligases are the minimum requirements for SUMO conjugation but *in vivo* E3 ligases boost SUMOylation of the target protein considerably. The PIAS (Protein Inhibitor of Activated STAT) family, the largest family of SUMO E3 ligases, were originally identified as inhibitors of activated STAT proteins. Interestingly CBP and p300 have been shown to form a ternary complex with PIAS3, but not PIASγ, and Smad3 during Smad-dependent transcription. However, the question as to whether PIAS-3 had any effect on the SUMOylation of p300, CBP or Smad2 has not been addressed (Long *et al.,* 2004).

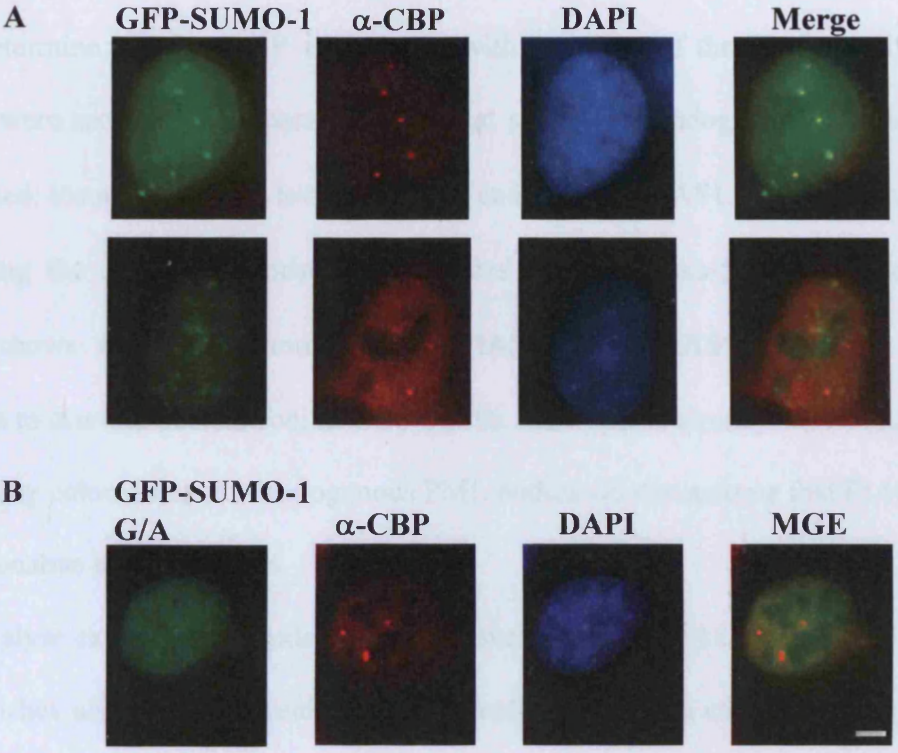
A
GFP-SUMO-1
α-CBP
DAPI
Merge
B
GFP-SUMO-1 G/A
α-CBP
DAPI
MGE

Figure 3.3 CBP co-localises with GFP-SUMO-1 fusion proteins. (A) COS-1 cells were seeded on 22mm coverslips at 1 x 10^5 confluency and transfected with expression plasmids encoding GFP-SUMO-1 or (B) GFP-SUMO-1 G/A. 48 hours post transfection, immunofluorescence labelling was performed using anti-CBP(A22) antibody and a TRITC conjugated secondary (1/200). Scale bar represents 1µM.

To determine whether CBP co-localises with members of the PIAS family of proteins, COS-1 cells were seeded, fixed, permeabilised and stained for endogenous CBP and an Alexa-488 conjugated secondary while localisation of endogenous PIAS1, PIASxα and PIASγ was observed using the appropriate primary antibodies and an Alexa-594 conjugated secondary. Figure 3.4 shows that endogenous PIAS1, PIASxα and PIASγ and CBP show strong colocalisation to discrete nuclear foci in COS-1 cells. As we have already shown that endogenous CBP completely colocalises with endogenous PML bodies we can assume that PIAS proteins and CBP foci colocalise in PML bodies.

To analyse expression of endogenous and overexpressed PIAS1, COS-1 cells were grown on 100mm dishes and either un-transfected or transfected with an expression plasmid encoding PIAS1. 48hrs post-transfection the cells were lysed and the lysates were resolved by SDS-PAGE. The blots were probed with anti-PIAS1 and an HRP-conjugated secondary and the bands observed migrated at the expected size for PIAS 1, ~68Kda. PIAS1 was detected in both the untransfected and the transfected samples but the expression levels were markedly higher in the transfected samples. While further experiments are needed to find out if CBP interacts with SUMO E3 ligases, it is of interest to note that PIAS1 was recently shown to promote the movement of the homeobox protein Msx1 from the nuclear interior to the nuclear periphery where it bound the MyoD promoter during myoblast differentiation (Lee *et al.*, 2006).

3.6 CBP is SUMOylated *in vivo*

Analysis of CBP primary sequence using SUMOplot (Abgent) software revealed that CBP contains 27 putative SUMOylation sites throughout its entire sequence, with 7 of these sites designated 'high probability' SUMO acceptor sites (Figure 3.5 and Figure 3.6). The majority of

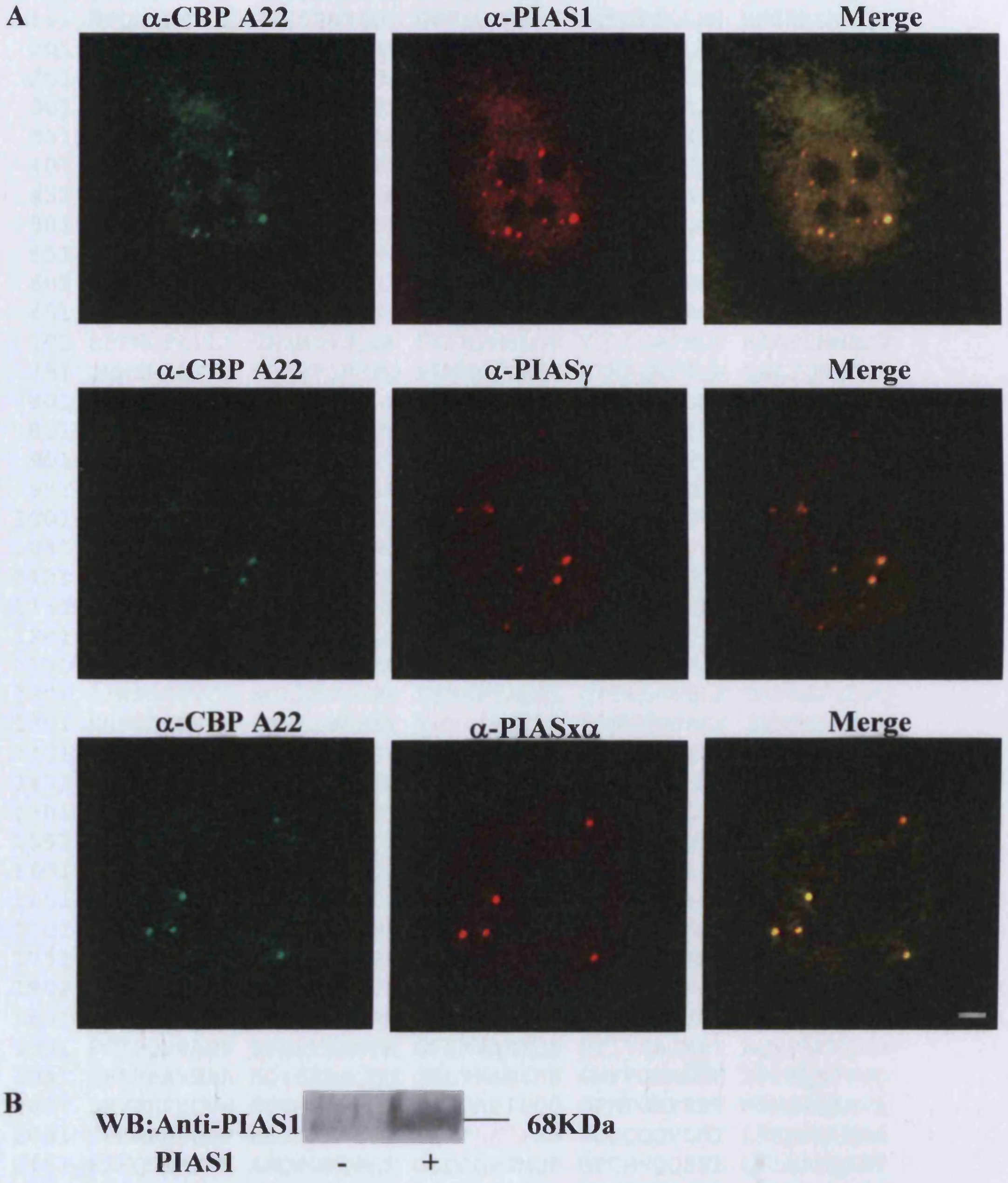
A
α-CBP A22
α-PIAS1
Merge
α-CBP A22
α-PIASγ
Merge
α-CBP A22
α-PIASxα
Merge
B
WB:Anti-PIAS1
68KDa
PIAS1
-
+

Figure 3.4 Endogenous CBP colocalises with PIAS proteins (A) COS-1 cells and were seeded on 22mm coverslips, fixed and immunostained for endogenous CBP and PIAS1, PIASγ and PIASxα proteins. Immunofluorescence labelling was carried out using anti-CBP(A22) and an Alexa-488 conjugated secondary while the appropriate PIAS antibody was used to recognise endogenous PIAS proteins in conjunction with an Alexa594 secondary antibody. (B) Western blot of whole cell lysates from COS-1 cells either non-transfected or transfected with PIAS1 and lysed after 48hrs. The blots were probed with anti-PIAS1 antibody. Scale bar represents 1μM.

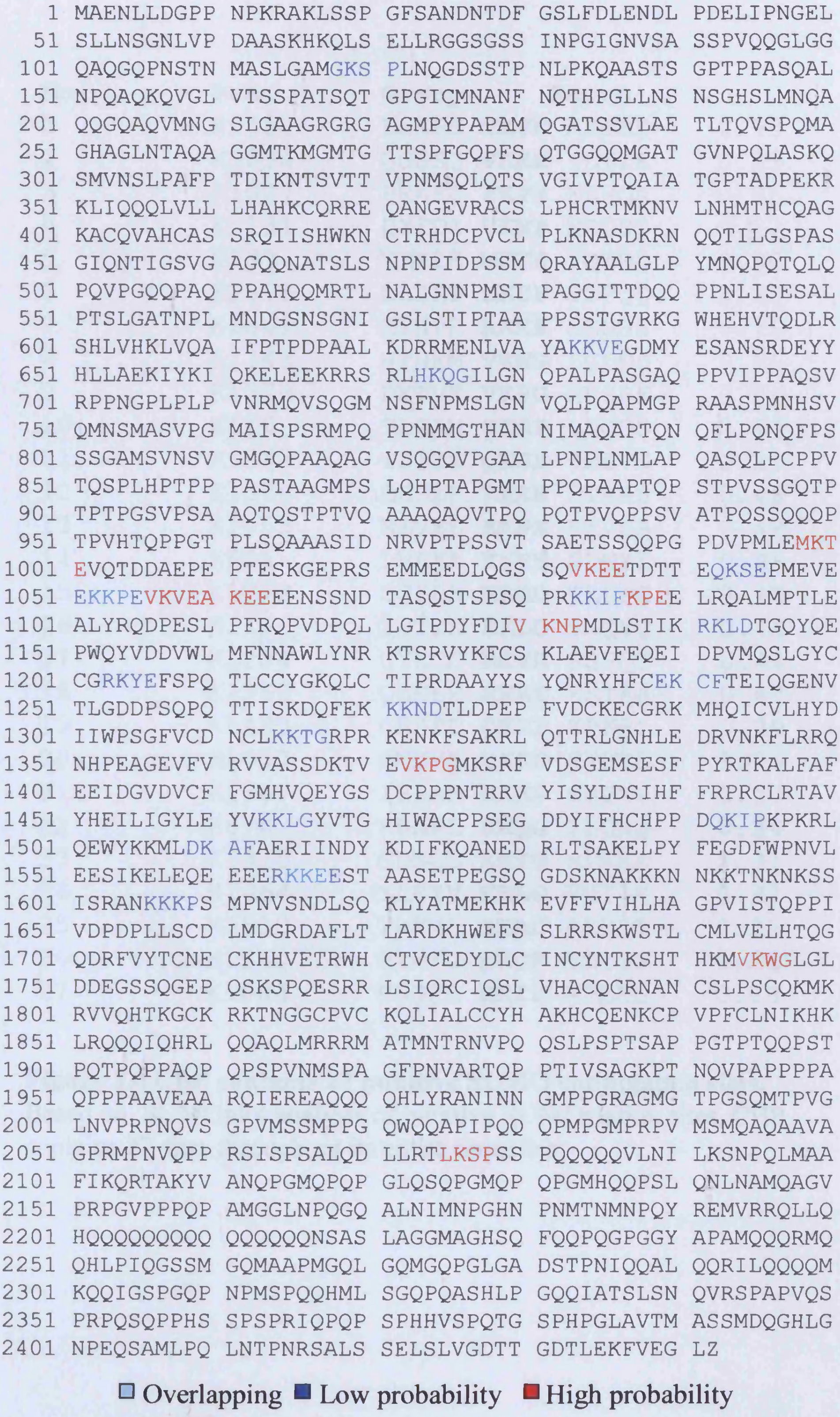

```
   1 MAENLLDGPP NPKRAKLSSP GFSANDNTDF GSLFDLENDL PDELIPNGEL
  51 SLLNSGNLVP DAASKHKQLS ELLRGGSGSS INPGIGNVSA SSPVQQGLGG
 101 QAQGQPNSTN MASLGAMGKS PLNQGDSSTP NLPKQAASTS GPTPPASQAL
 151 NPQAQKQVGL VTSSPATSQT GPGICMNANF NQTHPGLLNS NSGHSLMNQA
 201 QQGQAQVMNG SLGAAGRGRG AGMPYPAPAM QGATSSVLAE TLTQVSPQMA
 251 GHAGLNTAQA GGMTKMGMTG TTSPFGQPFS QTGGQQMGAT GVNPQLASKQ
 301 SMVNSLPAFP TDIKNTSVTT VPNMSQLQTS VGIVPTQAIA TGPTADPEKR
 351 KLIQQQLVLL LHAHKCQRRE QANGEVRACS LPHCRTMKNV LNHMTHCQAG
 401 KACQVAHCAS SRQIISHWKN CTRHDCPVCL PLKNASDKRN QQTILGSPAS
 451 GIQNTIGSVG AGQQNATSLS NPNPIDPSSM QRAYAALGLP YMNQPQTQLQ
 501 PQVPGQQPAQ PPAHQQMRTL NALGNNPMSI PAGGITTDQQ PPNLISESAL
 551 PTSLGATNPL MNDGSNSGNI GSLSTIPTAA PPSSTGVRKG WHEHVTQDLR
 601 SHLVHKLVQA IFPTPDPAAL KDRRMENLVA YAKKVEGDMY ESANSRDEYY
 651 HLLAEKIYKI QKELEEKRRS RLHKQGILGN QPALPASGAQ PPVIPPAQSV
 701 RPPNGPLPLP VNRMQVSQGM NSFNPMSLGN VQLPQAPMGP RAASPMNHSV
 751 QMNSMASVPG MAISPSRMPQ PPNMMGTHAN NIMAQAPTQN QFLPQNQFPS
 801 SSGAMSVNSV GMGQPAAQAG VSQGQVPGAA LPNPLNMLAP QASQLPCPPV
 851 TQSPLHPTPP PASTAAGMPS LQHPTAPGMT PPQPAAPTQP STPVSSGQTP
 901 TPTPGSVPSA AQTQSTPTVQ AAAQAQVTPQ PQTPVQPPSV ATPQSSQQQP
 951 TPVHTQPPGT PLSQAAASID NRVPTPSSVT SAETSSQQPG PDVPMLEMKT
1001 EVQTDDAEPE PTESKGEPRS EMMEEDLQGS SQVKEETDTT EQKSEPMEVE
1051 EKKPEVKVEA KEEEENSSND TASQSTSPSQ PRKKIFKPEE LRQALMPTLE
1101 ALYRQDPESL PFRQPVDPQL LGIPDYFDIV KNPMDLSTIK RKLDTGQYQE
1151 PWQYVDDVWL MFNNAWLYNR KTSRVYKFCS KLAEVFEQEI DPVMQSLGYC
1201 CGRKYEFSPQ TLCCYGKQLC TIPRDAAYYS YQNRYHFCEK CFTEIQGENV
1251 TLGDDPSQPQ TTISKDQFEK KKNDTLDPEP FVDCKECGRK MHQICVLHYD
1301 IIWPSGFVCD NCLKKTGRPR KENKFSAKRL QTTRLGNHLE DRVNKFLRRQ
1351 NHPEAGEVFV RVVASSDKTV EVKPGMKSRF VDSGEMSESF PYRTKALFAF
1401 EEIDGVDVCF FGMHVQEYGS DCPPPNTRRV YISYLDSIHF FRPRCLRTAV
1451 YHEILIGYLE YVKKLGYVTG HIWACPPSEG DDYIFHCHPP DQKIPKPKRL
1501 QEWYKKMLDK AFAERIINDY KDIFKQANED RLTSAKELPY FEGDFWPNVL
1551 EESIKELEQE EEERKKEEST AASETPEGSQ GDSKNAKKKN NKKTNKNKSS
1601 ISRANKKKPS MPNVSNDLSQ KLYATMEKHK EVFFVIHLHA GPVISTQPPI
1651 VDPDPLLSCD LMDGRDAFLT LARDKHWEFS SLRRSKWSTL CMLVELHTQG
1701 QDRFVYTCNE CKHHVETRWH CTVCEDYDLC INCYNTKSHT HKMVKWGLGL
1751 DDEGSSQGEP QSKSPQESRR LSIQRCIQSL VHACQCRNAN CSLPSCQKMK
1801 RVVQHTKGCK RKTNGGCPVC KQLIALCCYH AKHCQENKCP VPFCLNIKHK
1851 LRQQQIQHRL QQAQLMRRRM ATMNTRNVPQ QSLPSPTSAP PGTPTQQPST
1901 PQTPQPPAQP QPSPVNMSPA GFPNVARTQP PTIVSAGKPT NQVPAPPPPA
1951 QPPPAAVEAA RQIEREAQQQ QHLYRANINN GMPPGRAGMG TPGSQMTPVG
2001 LNVPRPNQVS GPVMSSMPPG QWQQAPIPQQ QPMPGMPRPV MSMQAQAAVA
2051 GPRMPNVQPP RSISPSALQD LLRTLKSPSS PQQQQQVLNI LKSNPQLMAA
2101 FIKQRTAKYV ANQPGMQPQP GLQSQPGMQP QPGMHQQPSL QNLNAMQAGV
2151 PRPGVPPPQP AMGGLNPQGQ ALNIMNPGHN PNMTNMNPQY REMVRRQLLQ
2201 HQQQQQQQQQ QQQQQQNSAS LAGGMAGHSQ FQQPQGPGGY APAMQQQRMQ
2251 QHLPIQGSSM GQMAAPMGQL GQMGQPGLGA DSTPNIQQAL QQRILQQQQM
2301 KQQIGSPGQP NPMSPQQHML SGQPQASHLP GQQIATSLSN QVRSPAPVQS
2351 PRPQSQPPHS SPSPRIQPQP SPHHVSPQTG SPHPGLAVTM ASSMDQGHLG
2401 NPEQSAMLPQ LNTPNRSALS SELSLVGDTT GDTLEKFVEG LZ
```

▢ Overlapping ■ Low probability 🟥 High probability motifs

Figure 3.5 SUMOplot of CBP sequence. SUMOplot analysis of putative SUMOylation sites within the entire CBP sequence.

No.	Pos.	Group	Score
1	K1057	EKKPE **VKVE** AKEEE	0.93
2	K1034	QGSSQ **VKEE** TDTTE	0.93
3	K1087	PRKKI **FKPE** ELRQA	0.85
4	K1131	DYFDI **VKNP** MDLST	0.82
5	K999	VPMLE **MKTE** VQTDD	0.80
6	K2076	DLLRT **LKSP** SSPQQ	0.80
7	K1061	EVKVE **AKEE** EENSS	0.79
8	K1745	HTHKM **VKWG** LGLDD	0.76
9	K1373	DKTVE **VKPG** MKSRF	0.76
10	K119	SLGAM **GKSP** LNQGD	0.57
11	K1043	TDTTE **QKSE** PMEVE	0.50
12	K1566	EEEER **KKEE** STAAS	0.48
13	K1053	MEVEE **KKPE** VKVEA	0.48
14	K634	LVAYA **KKVE** GDMYE	0.48
15	K1272	DQFEK **KKND** TLDPE	0.48
16	K1142	LSTIK **RKLD** TGQYQ	0.44
17	K1204	GYCCG **RKYE** FSPQT	0.44
18	K1565	QEEEE **RKKE** ESTAA	0.44
19	K1493	CHPPD **QKIP** KPKRL	0.39
20	K1052	PMEVE **EKKP** EVKVE	0.39
21	K1607	ISRAN **KKKP** SMPNV	0.37
22	K674	RRSRL **HKQG** ILGNQ	0.34
23	K1315	CDNCL **KKTG** RPRKE	0.31
24	K1464	YLEYV **KKLG** YVTGH	0.31
25	K1510	YKKML **DKAF** AERII	0.15
26	K1240	RYHFC **EKCF** TEIQG	0.15
27	K1084	PSQPR **KKIF** KPEEL	0.13

Figure 3.6 CBP contains 27 putative SUMO conjugation sites. Based on SUMOplot analysis of putative SUMOylation sites, CBP contains 27 sites throughout its entire sequence.

published data on the SUMOylation of non-histone proteins has determined that the minimum motif required for SUMOylation is ψKXE (Rodriguez *et al.*, 2001). However, the algorithm driving the SUMOplot resource does not take into account the inability of SUMO-1 to attach to sequences not conforming to the ψKXE motif, thus, SUMOplot results should be only taken as a very rough guide to finding potential SUMO sites. Based on the SUMOplot data and more importantly, the SUMOylation of p300 (Girdwood *et al.*, 2003) we carried out experiments to find out if CBP was SUMOylated *in vivo*. To detect whether CBP was SUMOylated, a co-immunoprecipitation was carried out. COS-1 cells were seeded on 100mm dishes and co-transfected with expression vectors encoding CBP and FLAG-SUMO-1, as COS-1 cells contain very small amounts of unconjugated endogenous SUMO (Melchior 2000). 48 hours post-transfection the cells were lysed and the Co-IPs were carried out using α-CBP(A22) as described in Materials and Methods (section 2.5.2), the samples were resolved by SDS-PAGE gels before Western blotting with α-CBP (A22) or α-SUMO-1. The top panel of Figure 3.7 shows that a number of CBP bands were observed from ~200kDa to ~300kDa in the input samples. However, it is clear that CBP is not immunoprecipitated in the control sample in which an unspecific LexA antibody is used in the IP reaction. SUMO-1 is not detected in the input lanes and is not immunoprecipitated unspecifically with a control antibody. Figure 3.7 B shows that CBP is detected in the input lanes and is immunoprecipitated by α-CBP (A22). Western blotting for SUMOylated forms of CBP detected a number of high molecular weight bands, one at ~250kDa and a doublet ~280-300kDa.

Similar results were found when HEK293 cells were transfected with expression vectors encoding YFP-HIS-CBP and FLAG-SUMO-1 (Figure 3.8). The Co-IPs were carried out as described in (section 2.5.2) and the samples were resolved by SDS-PAGE gels before western blotting with α-YFP or α-SUMO-1. Figure 3.8 shows that SUMO-1 or YFP-CBP does not bind

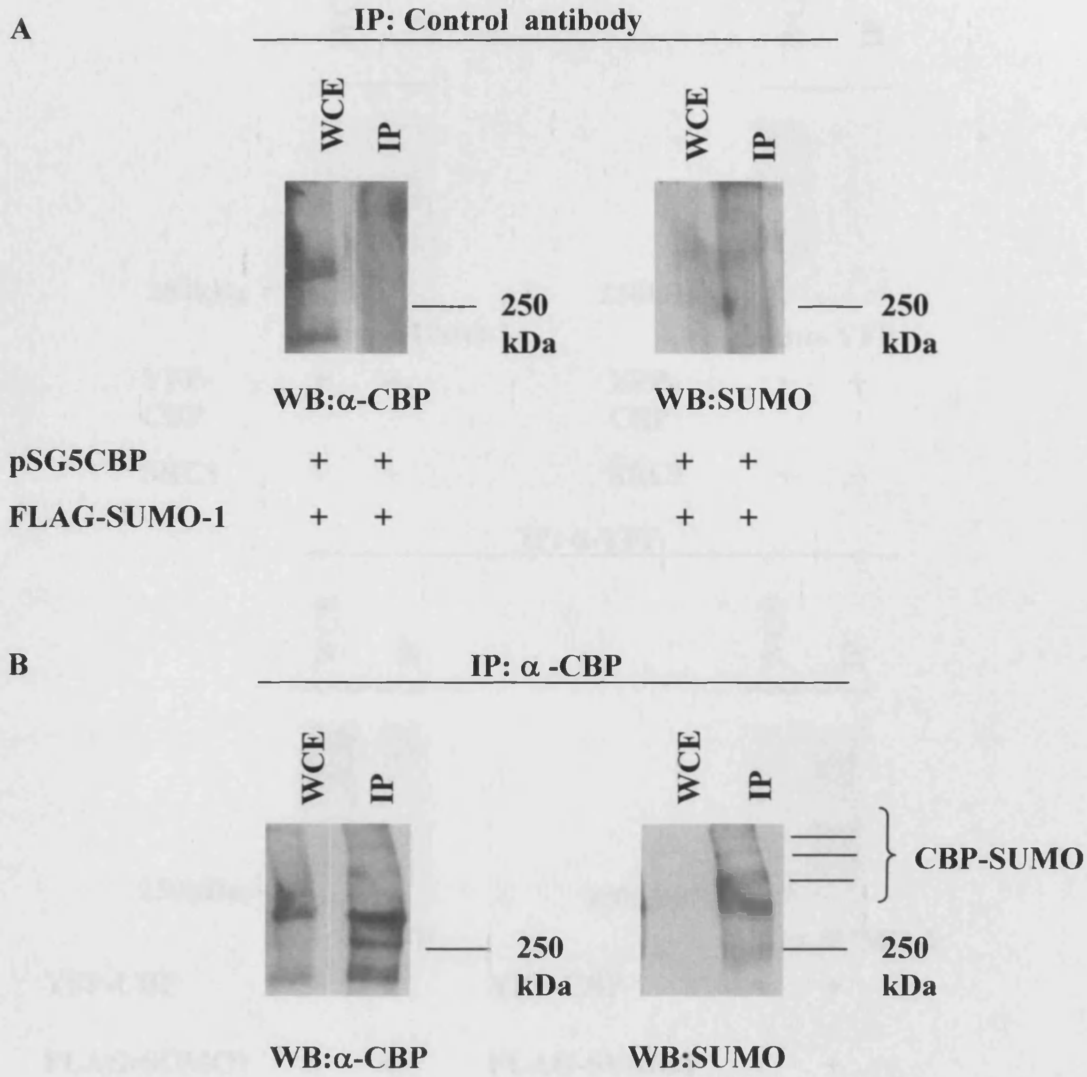
A
IP: Control antibody
WCE
IP
WCE
IP
250 kDa
250 kDa
WB:α-CBP
WB:SUMO
pSG5CBP + + + +
FLAG-SUMO-1 + + + +
B
IP: α -CBP
WCE
IP
WCE
IP
CBP-SUMO
250 kDa
250 kDa
WB:α-CBP
WB:SUMO

Figure 3.7 CBP is SUMOylated in COS-1 cells *in vivo*.
COS-1 cells were seeded in 100mm dishes, incubated for 24 hours and transfected with expression constructs for CBP and FLAGSUMO-1. 48 hours post-transfection the cells were lysed in 400µl of lysis buffer. 100µg of the protein extract was used to check for expression of all protein inputs. To immunoprecipitate CBP containing complexes, the lysates were incubated with antibodies raised against rabbit CBP coupled to protein A/G bound sepharose beads. After 2 hours incubation the immune complexes were isolated and washed X3 with lysis buffer. 100µg of the whole cell lysate along with the isolated protein complexes were separated via 6% SDS-PAGE and bound proteins were transferred to nitrocellulose membrane. After blocking, the membranes were incubated with antibodies raised against rabbit anti-CBP, rabbit anti-SUMO-1 followed by incubation with anti-rabbit HRP-conjugated secondary antibodies.

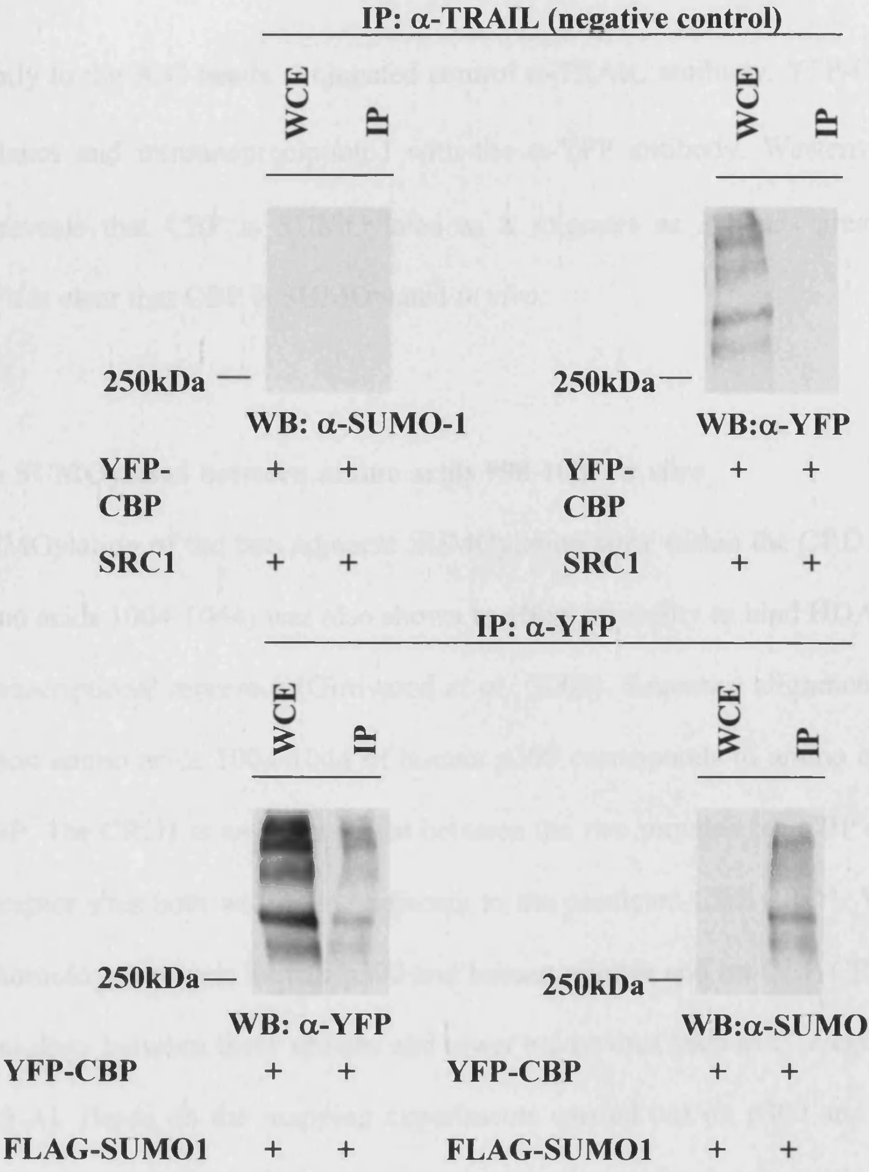
IP: α-TRAIL (negative control)
WCE
IP
WCE
IP
250kDa
WB: α-SUMO-1
250kDa
WB:α-YFP
YFP-CBP + +
SRC1 + +
YFP-CBP + +
SRC1 + +
IP: α-YFP
WCE
IP
WCE
IP
250kDa
WB: α-YFP
250kDa
WB:α-SUMO-1
YFP-CBP + +
FLAG-SUMO1 + +
YFP-CBP + +
FLAG-SUMO1 + +

Figure 3.8 YFP-CBP is SUMOylated in HEK293 cells *in vivo*.
HEK293 cells were seeded in 100mm dishes, incubated for 24 hours and transfected with expression constructs for YFP-CBP and FLAG-SUMO-1. 48 hours post-transfection the cells were lysed in 400μl of lysis buffer. 100μg of the protein extract was used to check for expression of all protein inputs. To immunoprecipitate CBP containing complexes, the lysates were incubated with antibodies raised against rabbit CBP coupled to protein A/G bound sepharose beads. An unspecific control α-TRAIL antibody was used in a control IP to ensure there was no unspecific association of CBP with the protein A/G beads. After 2 hours incubation the immune complexes were isolated and washed X3 with lysis buffer. 100μg of the whole cell lysate along with the isolated protein complexes were separated via 6% SDS-PAGE and bound proteins were transferred to nitrocellulose membrane. After blocking, the membranes were incubated with antibodies raised against rabbit anti-CBP, rabbit anti-SUMO-1 followed by incubation with anti-rabbit HRP.

unspecifically to the A/G beads conjugated control α-TRAIL antibody. YFP-CBP is detected in the input lanes and immunoprecipitated with the α-YFP antibody. Western blotting with α-SUMO-1 reveals that CBP is SUMOylated as it migrates as 3 bands greater than 250kDa. Therefore, it is clear that CBP is SUMOylated *in vivo*.

3.7 CBP is SUMOylated between amino acids 998-1087 *in vitro*

SUMOylation of the two adjacent SUMOylation sites within the CRD1 region of human p300 (amino acids 1004-1044) was also shown to affect its ability to bind HDAC6 and ultimately act as a transcriptional repressor (Girdwood *et al.*, 2003). Sequence alignment revealed that the CRD1 region amino acids 1004-1044 of human p300 corresponds to amino acids 1019-1082 of murine CBP. The CRD1 is well conserved between the two proteins but CBP contains 5 putative SUMO acceptor sites both within and adjacent to the predicted CBP CRD1. While there is high sequence homology between human p300 and human, mouse and rat CBP CRD1 domains, there is little homology between these species and lower eukaryotes such as *C. elegans* and *S. mansoni* (Figure 3.9 A). Based on the mapping experiments carried out on p300 and the other putative non-conserved SUMO acceptor sites outside the predicted CBP CRD1 we created CBPΔ998-1087 which deleted 5 putative ψKXE sites (Figure 3.9 B). Interestingly, these are the only ψKXE sites within the entire CBP sequence. Therefore we constructed two expression vectors for use in an *in vitro* SUMO assay, pSG5HIS-CBP wild-type and pSG5HIS-CBPΔ998-1087. In order to generate HIS-CBPΔ998-1087 two complementary primers were designed based on the CBP sequence which encompassed the 998-1087 sequence. A further two primers were designed: CBPHISF1 which was 3Kb 5' of the deletion and contained a HIS-tag and a unique Ksp1 site and 4474R which was 1Kb 3' of the deletion and encompassed a unique Xho1 site at amino acid position 1460 of CBP. The first PCR using CBPHIS1F and 994R generated ~3Kb fragment that

A

```
Human p300     971-qpsqevkmeakmevdqpepadtqpediseskvedc--------------kmestetee-995
Human CBP      992-vpvlemktetqaedtepdpgeskgeprsemmeedlqgasqvkeetdiaeqksepmeved-1050
Mouse CBP      993-vpmlemktevqtddaepepteskgeprsemmeedlqgssqvkeetdtteqksepmevee-1051
Rat CBP        993-vpmlemktevqtddaepdpaeskgeprsemmeedlqgssqvkeetdtteqksepmevee-1051
c.elegans CBP 985-Tplslfcygaamctiareqqywvfeqsstqynvtv------------terytycqkcfd-1031
S.mansoni CBP 975-dkvvevkplmrarftesgelsesfpyrlkavfafqeidgqdvcffglyvqeygsespqp-1033

Human p300      996-rstelkteikeeedqpstsatqsspapgqskkkifkpee-1054
Human CBP      1051-kkpevkvevkeeeesssngtasqstspsqprkkifkpee-1089
Mouse CBP      1052-kkpevkveakeeeenssndtasqstspsqprkkifkpee-1090
Rat CBP        1052-kkpevkveakeeeensangtasqstspsqprkkifkpee-1090
c.elegans CBP 1032-alppegislsenpndrnnmapktsfteqknsvidyepfe-1069
S.mansoni CBP 1034-nrrrvyvayldsvfffrpkqyrtdvyheilvgyllyakr-1071
```

B

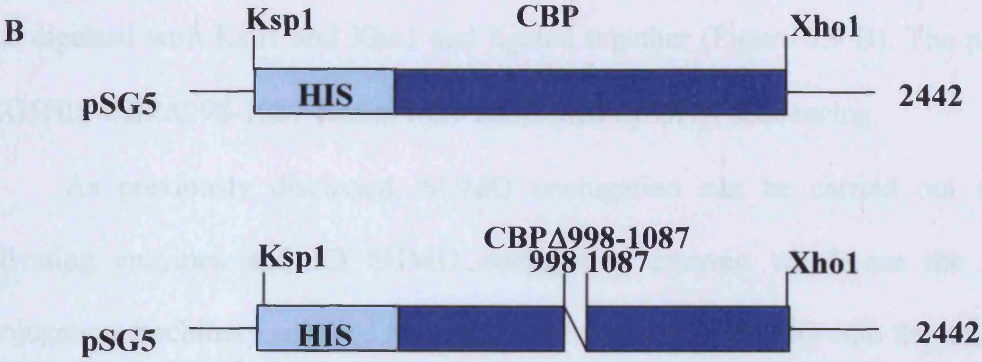

C

CBP	+	+	+	+
UBC9	-	+	-	+
Sae1/2	+	+	+	+
SUMO-1	+	+	-	-
SUMO-2	-	-	+	+

D

CBPΔ998-1087	+	+	+	+
UBC9	-	+	-	+
Sae1/2	+	+	+	+
SUMO-1	+	+	-	-
SUMO-2	-	-	+	+

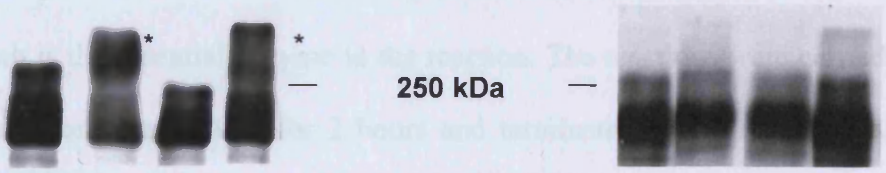

Figure 3.9 CBP is SUMOylated between amino acids 998-1087

(A) Sequence alignment of p300 and CBP from different species. CRD1 as defined by Girdwood et al., (2003) in blue, Putative SUMO sites in red (B) Schematic representation of pSG5-HIS-CBP and pSG5-HIS-CBPΔ998-1087 expression constructs (C) pSG5HIS-CBP and (D) pSG5HIS-CBPΔ997-1087 were in vitro translated in the presence of [^{35}S]-methionine to give full-length radio-labelled proteins. 5μl of the proteins were then used in an *in vitro* SUMO assay containing 0.1μg recombinant SAE1/SAE2, 1μg recombinant SUMO1/2, +/- 0.45μg recombinant Ubc9 as indicated. The reactions were then incubated at 30°C for 2 hours in the presence of 5mM ATP. The reactions were stopped by the addition of 4X SDS loading buffer and the proteins were resolved via 10% SDS-PAGE prior to visualisation. Asterisks indicate SUMOylated forms of the proteins was used in a recombinant PCR with a ~1Kb fragment from the reaction between CBP994F and CBP4474R. The fragments were purified from agarose gels prior to use in PCR reactions. The final ~5.0Kb fragment containing the deletion and pSG5CBP were digested with Kspl and Xhol, the resulting fragments were purified from an agarose gel and ligated together to produce pSG5HIS-CBPΔ998-1087. To synthesise wild-type HISCBP, a PCR reaction was set up using CBPHIS1F, 4474R and pSG5CBP as a template. The resulting ~5Kb fragment and pSG5CBP was digested with Kspl and Xhol and ligated together (Figure 3.9 B). The pSG5HIS-CBP and pSG5HIS-CBPΔ998-1087 clones were confirmed by DNA sequencing.

As previously discussed, SUMO conjugation can be carried out *in vitro* using E1 activating enzymes and E2 SUMO conjugating enzyme which are the minimum SUMO conjugation machinery required to catalyse the addition of SUMO onto the target protein. SUMO E3 ligases add a degree of specificity to SUMO conjugation *in vivo* but are not needed *in vitro.*

I carried out *in vitro* SUMO assays to determine if CBP was SUMOylated within the CRD1. HIS-CBP and HIS-CBPΔ998-1087 were prepared by IVT (section 2.5.14) and incubated with recombinant E1 ligases (SAE1/2), SUMO-1/SUMO-2 and with or without recombinant Ubc9 (E2 ligase) which is the essential enzyme in the reaction. The reactions were carried out in the presence of ^{35}S-methionine and ATP for 2 hours and terminated by addition of 4X SDS-loading buffer. The proteins were resolved via 10% SDS-PAGE and a change in the migration of the protein in the presence of Ubc9 indicated SUMOylation.

Figure 3.9 C shows that HIS-CBP migrates as multiple bands of ~250kDa in the absence of Ubc9. However, in the presence of Ubc9 and SUMO-1 or SUMO-2, it migrates as a higher species. HIS-CBPΔ998-1087 also migrates as multiple bands of ~250kDa but its migration is not impeded in the presence of Ubc9 and SUMO-1 or SUMO-2 (Figure 3.9 D).

These results show that there are SUMO acceptor sites within the deleted region. Interestingly, Kuo *et al*., (2005) recently demonstrated that CBP is SUMOylated by SUMO-1 at lysine residues 999/1034/1057. However, they did not determine if CBP was SUMOylated by SUMO-2 or whether SUMOylation affected the ability of CBP to associate with PML bodies.

3.8 Sequences outside the amino acids 998-1087 are essential for CBP SUMOylation *in vitro*

Having established that CBP is modified by SUMO-1 *in vivo* and both SUMO-1 and SUMO-2 *in vitro*, we examined if CBP could be SUMOylated outside the sequences 998-1087 and if sequences adjacent to the SUMO acceptor sequence were important for the conjugation of SUMO. Therefore, I generated a series of CBP C-terminal deletion mutants. All the mutants were made by digesting pCDNA3.1FLAG-CBP with two or three digesting restriction endonucleases which were re-ligated following gel purification to generate in-frame FLAG-tagged CBP C-terminal deletion constructs (Figure 3.10). These constructs were confirmed to be in frame by DNA sequencing.

The CBP C-terminal deletions and thymidine de-glycosylase (TDG), positive control for SUMOylation (Hardeland *et al.*, 2002) were *in vitro* translated in the presence of ^{35}S-methionine and the expression of the proteins was confirmed by SDS-PAGE (Figure 3.11). CBP 1-1901 has a predicted size of ~172kDa but it migrates at ~250kDa. However, CBP fragments 1-507, 1-1101 and 1-1458 migrate at ~50kDa, 110kDa and 135 kDa respectively which is very close to their predicted sizes of 46kDa, 100kDa and 130kDa (Figure 3.11).

Firstly, to determine if the C-terminal deletions were SUMOylated *in vitro*, the IVT fragments were incubated in the presence of E1 and SUMO-1/SUMO-2 with or without the E2 enzyme, Ubc9, which is the essential enzyme in the reaction. The reactions were allowed to proceed for 2 hours at 30°C and the reaction was stopped by the addition of 4X SDS loading buffer. The resulting protein complexes were resolved by SDS-PAGE and a change in the mobility of the substrate was analysed. Figure 3.11 A, shows that the positive control, TDG, in

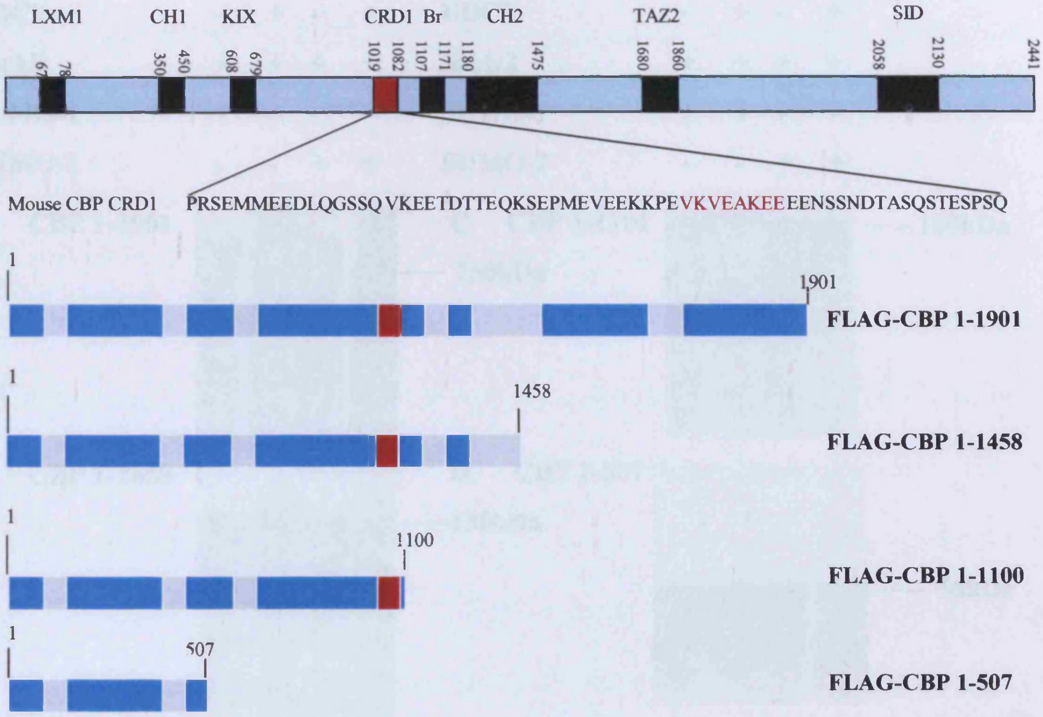
LXM1
CH1
KIX
CRD1
Br
CH2
TAZ2
SID
67
78
350
450
608
679
1019
1082
1107
1171
1180
1475
1680
1860
2058
2130
2441
Mouse CBP CRD1
PRSEMMEEDLQGSSQVKEETDTTEQKSEPMEVEEKKPEVKVEAKEEEENSSNDTASQSTESPSQ
1
1901
FLAG-CBP 1-1901
1
1458
FLAG-CBP 1-1458
1
1100
FLAG-CBP 1-1100
1
507
FLAG-CBP 1-507

Figure 3.10 Schematic of CBP C-terminal deletions
Schematic showing the domain structure of full-length CBP and predicted domain boundaries of the CBP C-terminal deletion mutants.

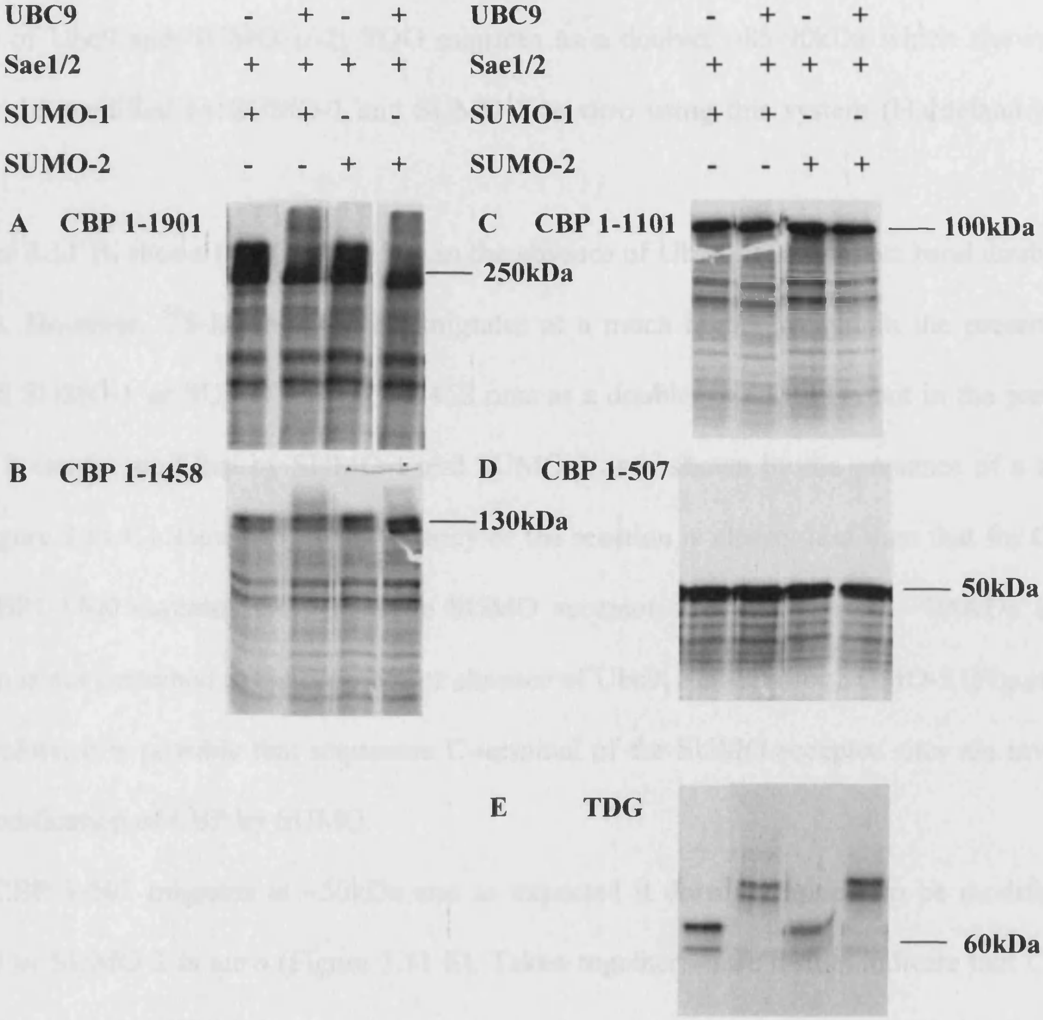
UBC9 - + - +
Sae1/2 + + + +
SUMO-1 + + - -
SUMO-2 - - + +
UBC9 - + - +
Sae1/2 + + + +
SUMO-1 + + - -
SUMO-2 - - + +
A CBP 1-1901
250kDa
C CBP 1-1101
100kDa
B CBP 1-1458
130kDa
D CBP 1-507
50kDa
E TDG
60kDa

Figure 3.11 Sequences outside CBP amino acids 998-1087 are essential for SUMOylation

(A) pSG5FLAG-CBP1-1901 , (B) pSG5FLAG-CBP1-1458, (C) pSG5FLAG-CBP1-1101, (D) pSG5FLAG-CBP1-507 (E) pSG5TDG were *in vitro* translated in the presence of [^{35}S]-methionine to give full-length radio-labelled proteins. 5μl of the proteins were then used in an *in vitro* SUMO assay containing 0.1μg recombinant SAE1/SAE2, 1μg recombinant SUMO1/2, +/- 0.45μg recombinant Ubc9 as indicated. The reactions were then incubated at 30°C for 2 hours in the presence of 5mM ATP. The reactions were stopped by the addition of 4X SDS loading buffer and the proteins were resolved via 10% SDS-PAGE prior to visualistion.

the absence of Ubc9 runs as a doublet very close to its predicted size of 75kDa. However, in the presence of Ubc9 and SUMO-1/-2, TDG migrates as a doublet ~85-90kDa which shows that TDG can be modified by SUMO-1 and SUMO-2 *in vitro* using this system (Hardeland *et al.*, 2002).

Figure 3.11 B, shows that CBP 1-1901 in the absence of Ubc9 runs as a two band doublet of ~250kDa. However, ^{35}S-labelled protein migrates at a much higher weight in the presence of Ubc9 and SUMO-1 or SUMO-2. CBP 1-1458 runs as a doublet of ~130kDa but in the presence of Ubc9 it can be modified by SUMO-1 and SUMO-2 as is shown by the presence of a higher band (Figure 3.11 C). However, the efficiency of the reaction is clearly less than that for CBP1-1901. CBP1-1100 contains the 5 putative SUMO acceptor sites and runs at ~100kDa but its migration is not perturbed in the presence or absence of Ubc9, SUMO-1 or SUMO-2 (Figure 3.11 D). Therefore, it is possible that sequences C-terminal of the SUMO acceptor sites are involved in the modification of CBP by SUMO.

CBP 1-507 migrates at ~50kDa and as expected it does not appear to be modified by SUMO-1 or SUMO-2 *in vitro* (Figure 3.11 E). Taken together, these results indicate that CBP is SUMOylated at the CRD1 but sequences proximal may be involved in E2/E3 binding and ultimately the conjugation of SUMO.

3.9 The acetyltransferase MOZ is modified by SUMO-1 and SUMO-2 *in vitro*

Results from a yeast 2-hybrid screen in our laboratory using the N-terminus of the acetyltransferase MOZ as bait identified SUMO-1, Ubc9 and PIAS3 as novel interacting proteins, suggesting that MOZ is modified by SUMO-1 *in vivo* and that the reaction is catalysed by Ubc9 and PIAS3 (N.Sirisriro and DMH; unpublished). To test this hypothesis full-length MOZ was *in vitro* translated in the presence of ^{35}S-methionine and used as a substrate in the *in vitro* SUMO assay with or without Ubc9 and PIAS-3 (Figure 3.12). In the absence of Ubc9, full-length MOZ is detected at ~250kDa with an additional higher molecular weight band at ~300kDa. In the presence of Ubc9 these bands are shifted to a single high molecular band >300kDa and inclusion of PIAS3 reduced the levels of SUMOylated MOZ suggesting that PIAS3 may compete with Ubc9 for MOZ binding. These results clearly show that other acetyltransferases such as the MYST family member, MOZ, can be SUMOylated by SUMO-1 and SUMO-2 *in vitro*.

3.10 SUMOylation affects the subcellular localisation of CBP

Previous reports showed that deletion of SUMO acceptor sites within a protein can abrogate its ability to associate with PML bodies (Ishov *et al.,* 1999). Furthermore, expression of specific SUMO proteases such as SuPr-1 demonstrated that loss of SUMO conjugation caused the loss of association between the transcription factor Sp3 and PML bodies (Best *et al.,* 2002). It has been shown in this study that SUMO-1 and SUMO-2 are conjugated to CBP at sites within amino acids 998-1087. Thus it was investigated whether SUMOylation of CBP is necessary for its ability to associate with PML bodies *in vivo*.

To aid this analysis we created full-length pSG5-YFP-HIS-CBP and pSG5-YFP-HIS-CBPΔ998-1087 constructs. pSG5-HIS-CBP and pSG5HIS-CBPΔ998-1087 were digested with Ksp1 and BamH1 which released HIS-CBP and HIS-CBPΔ998-1087 from pSG5 as 5'Ksp1-3'BamHI fragments. These were ligated into YFP-C3 and the resultant constructs were verified by DNA sequencing (Figure 3.13 A and B). To analyse expression of the constructs, COS-1 cells were seeded on 100mm dishes and transfected after 24 hours with expression vectors encoding YFP-HIS-CBPΔ998-1087 and YFP-HIS-CBP. 48 hours post-transfection the cells were lysed and the proteins were resolved via SDS-PAGE. The blots were then probed with rabbit anti-YFP specific antibodies followed by anti-rabbit HRP-conjugated secondary antibody. Figure 3.13 C

MOZ	+	+	+	+	+	+
UBC9	-	+	+	-	+	+
Sae1/2	+	+	+	+	+	+
SUMO-1	+	+	+	-	-	-
SUMO-2	-	-	-	+	+	+
PIAS3	-	-	+	-	-	+

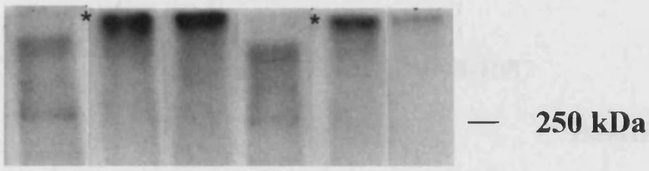

Figure 3.12 The acetyltransferase MOZ is SUMOylated *in vitro*

FLAG-MOZ was *in vitro* translated in the presence of [^{35}S]-methionine to give full-length radio-labelled MOZ protein. 5μl of the protein was then used in an *in vitro* SUMO assay containing 0.1μg recombinant SAE1/SAE2, 1μg recombinant SUMO1/2, +/- 0.45μg recombinant Ubc9 as indicated. 5μl of PIAS-3 was also added where indicated. The reactions were then incubated at 30°C for 2 hours in the presence of 5mM ATP. The reactions were stopped by the addition of 4X SDS loading buffer and the proteins were resolved via 10% SDS-PAGE prior to visualisation. Asterisks indicate SUMOylated forms of MOZ.

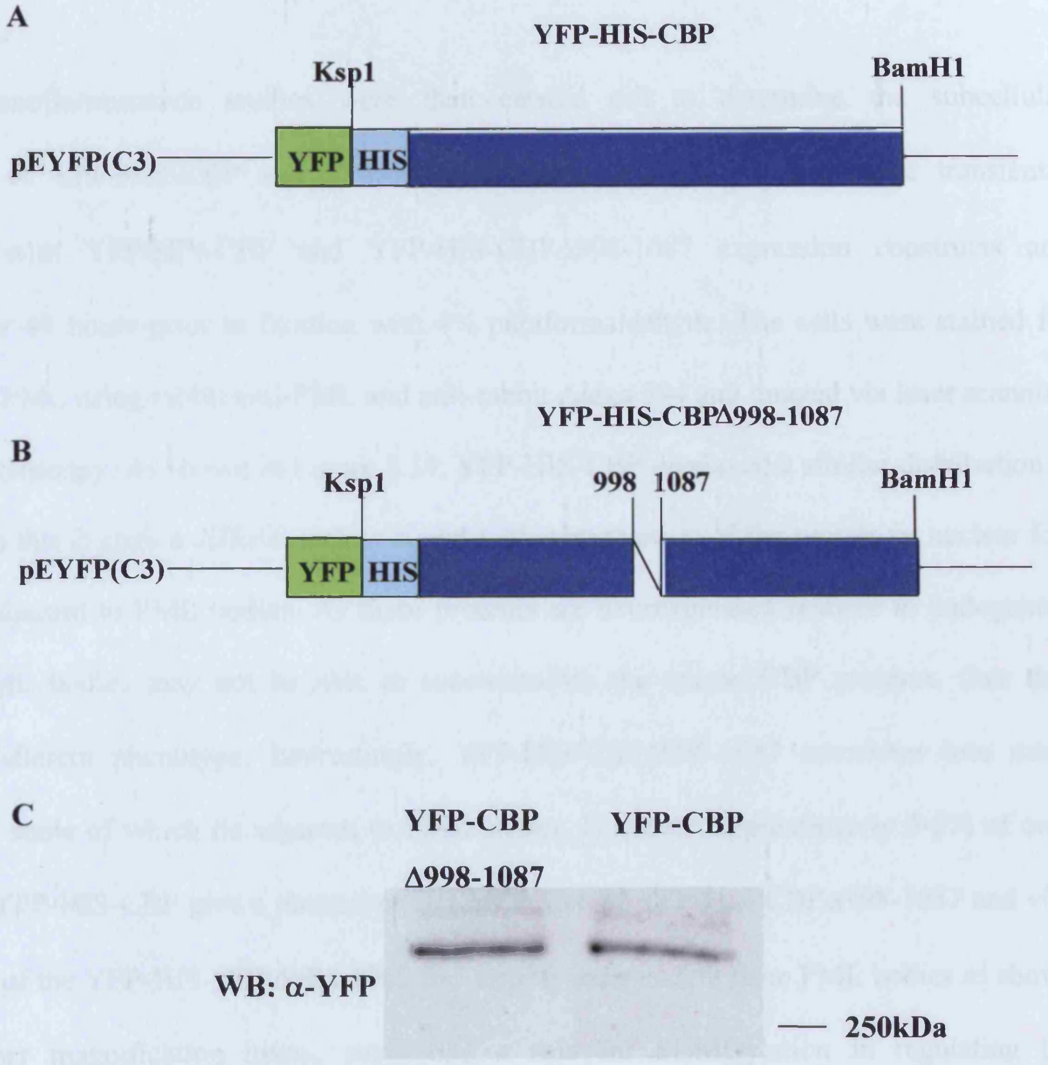
A
YFP-HIS-CBP
Ksp1
BamH1
pEYFP(C3)
YFP
HIS
B
YFP-HIS-CBPΔ998-1087
Ksp1
998
1087
BamH1
pEYFP(C3)
YFP
HIS
C
YFP-CBP Δ998-1087
YFP-CBP
WB: α-YFP
250kDa

Figure 3.13 Expression analysis of YFP-CBP fusion proteins
Schematic representation of (A) YFP-HIS-CBP and (B) YFP-HIS-CBPΔ998-1087 fusion proteins (C) COS-1 cells were seeded on 100mm dishes and transfected with either YFP-HIS-CBP or YFP-HIS-CBPΔ998-1087. 48 hours post-transfection the cells were lysed and the proteins resolved via SDS-PAGE. The blots were probed with rabbit anti-YFP followed by a rabbit conjugated-HRP secondary antibody.

shows that the two fusion proteins migrated at approximately 300kDa close to the predicted size of ~260kDa.

Immunofluorescence studies were then carried out to determine the subcellular localisation of YFP-HIS-CBP and YFP-HIS-CBPΔ998-1087. COS-1 cells were transiently transfected with YFP-HIS-CBP and YFP-HIS-CBPΔ998-1087 expression constructs and incubated for 48 hours prior to fixation with 4% paraformaldehyde. The cells were stained for endogenous PML using rabbit anti-PML and anti-rabbit Alexa 594 and imaged via laser scanning confocal microscopy. As shown in Figure 3.14, YFP-HIS-CBP displayed a similar distribution to YFP-CBP in that it gave a diffuse nuclear signal with a proportion of the protein in nuclear foci which are adjacent to PML bodies. As these proteins are overexpressed relative to endogenous proteins, PML bodies may not be able to accommodate the excess CBP proteins, thus they display a different phenotype. Interestingly, YFP-HIS-CBPΔ998-1087 associates into many smaller foci some of which lie adjacent to PML bodies. However, approximately 3-5% of cells expressing YFP-HIS-CBP give a phenotype similar to that of YFP-HIS-CBPΔ998-1087 and vice versa. Most of the YFP-HIS-CBPΔ998-1087 foci appear independent from PML bodies as shown in the higher magnification insets, suggesting a role for SUMOylation in regulating the subcellular localisation of CBP.

3.11 Sequences outside CBP 998-1087 are necessary for formation of nuclear foci

We have shown that deletion of the putative SUMO sites leads to a loss of CBP SUMOylation which in turn effects its subcellular localisation. Therefore we investigated which domains were important for the ability of CBP to associate in nuclear foci.

COS-1 and HEK293 cells were transfected with expression vectors encoding FLAG-CBP 1-507, FLAG-CBP 1-1100, FLAG-CBP 1-1458 and FLAG-CBP 1-1901. 48 hours post-

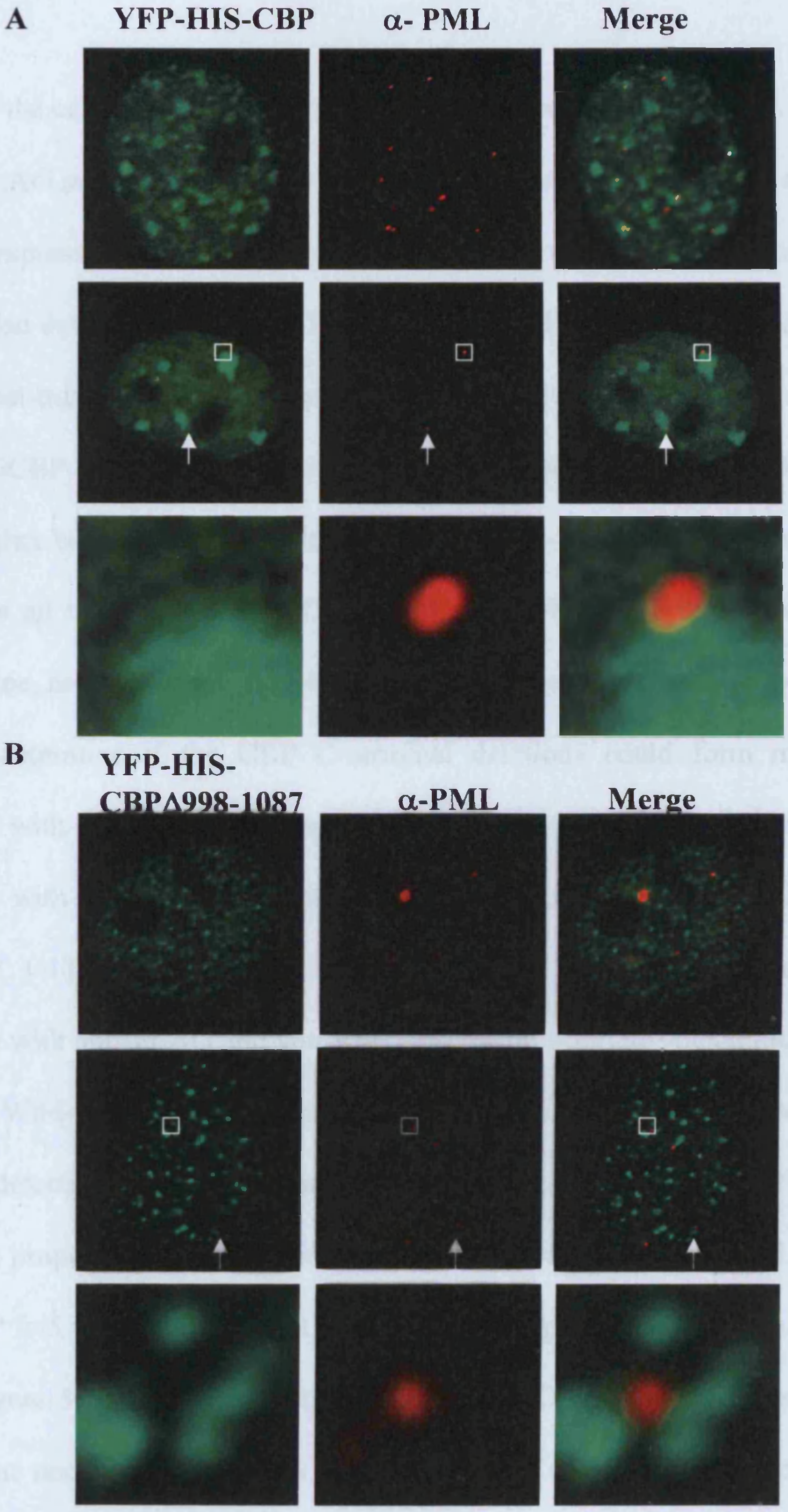

Figure 3.14 YFP-CBP and YFP-CBPΔ998-1087 partially colocalise with PML bodies COS-1 cells were seeded on 22mm coverslips at 1 x 10^5 confluency and transfected after 24 hours with an expression plasmids encoding (A)YFP-HIS-CBP and (B)YFP-HIS-CBPΔ998-1087. 48 hours post-transfection the cells were fixed in 4% paraformaldehyde, permeabilised and stained with antibodies raised against rabbit anti-PML (red) followed anti-rabbit Alexa594. Magnified insets correspond to the white square boxes. White arrows point to other CBP foci.

transfection the cells were lysed and the proteins resolved via SDS-PAGE. The blots were probed with anti-FLAG antibody and an HRP-conjugated secondary. Figure 3.15 shows that FLAG-CBP 1-507 was expressed in both cell lines and migrates at the expected size of ~50kDa. FLAG-CBP 1-1100 is also detected in both cell lines at 120kDa (HEK293) or 160kDa (COS-1) which could be due to post-translational modifications such as SUMO as this mutant contains SUMO acceptor sites. FLAGCBP 1-1901 migrates as a doublet of ~140kDa and ~250kDa in HEK293 cells but only the higher band is detected at high levels in COS-1 cells which is interesting as this mutant too contains all the putative SUMO sites. FLAG-CBP 1-1458 expression was not detected in either cell line, however it was translated *in vitro* to give a band of the expected size.

To determine if the CBP C-terminal deletions could form nuclear foci or if they colocalised with PML bodies, immunofluorescence studies were carried. COS-1 cells were transfected with expression plasmids encoding full-length FLAG-CBP, FLAG-CBP1-507, FLAG-CBP 1-1100, FLAG-CBP 1-1901. The cells were fixed and stained 48 hours post-transfection with anti-FLAG and anti-PML and the appropriate AlexaFluor conjugated secondary antibodies. Wild-type FLAG-CBP and all the mutants displayed a nuclear staining pattern with little or no detectable levels of the proteins in the cytoplasm. Full-length FLAG-CBP was nuclear with a large proportion of the protein associating in nuclear foci (Figure 3.16 A). Like YFP-CBP, FLAG-CBP foci were both adjacent to and overlapping with PML bodies. However, FLAG-CBP 1-1901 (Figure 3.16 B) which contains all the SUMO sites and all domains except the SID is diffuse in the nuclei of the majority of cells, hence, it is difficult to discern if it colocalises with the discrete foci of the PML bodies. Interestingly this phenotype is very similar to that observed for p300ΔSID which displays a nuclear diffuse staining pattern (Heery D.M. unpublished work). Figure 3.17 shows that FLAG-CBP1-1100 (+SUMO sites) is nuclear and diffuse but a small proportion (<20% of cells) of the proteins form nuclear foci which are intermingled with PML bodies not unlike those observed for full-length FLAG-CBP. However, FLAG-CBP1-507 (no

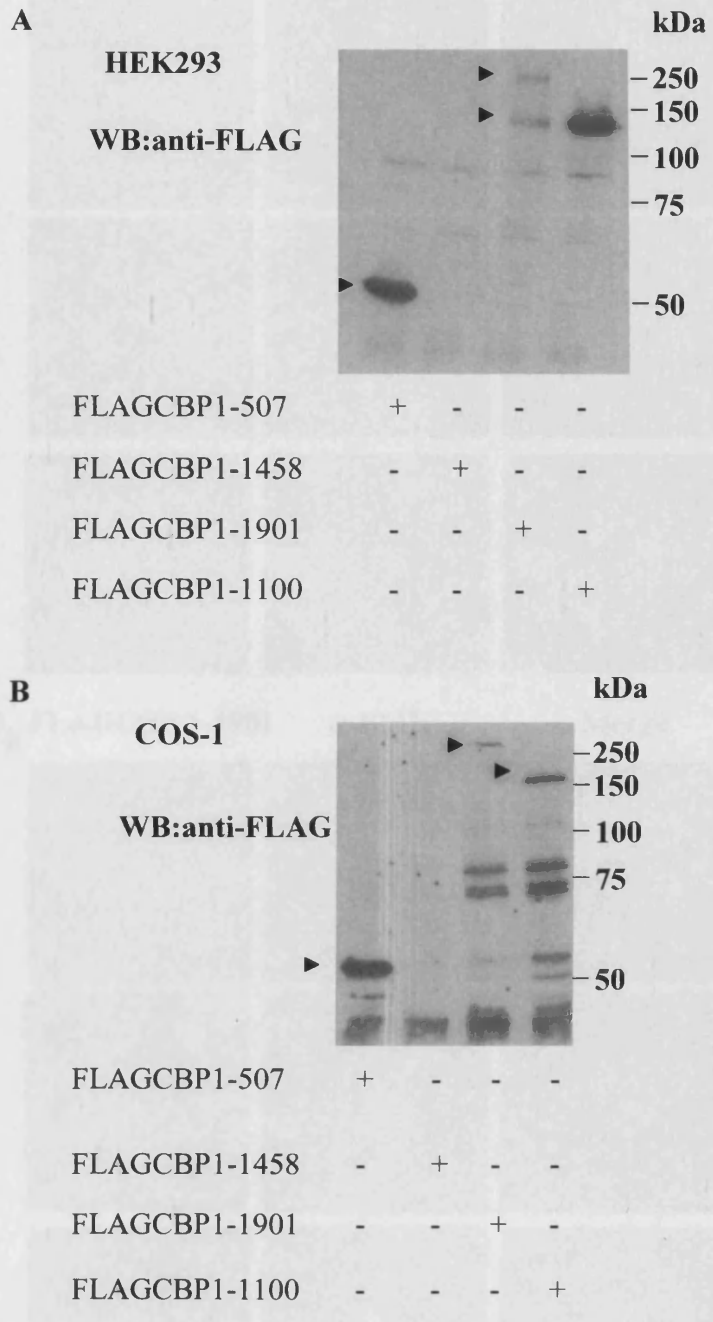
A
kDa
HEK293
WB:anti-FLAG
250
150
100
75
50
FLAGCBP1-507 + - - -
FLAGCBP1-1458 - + - -
FLAGCBP1-1901 - - + -
FLAGCBP1-1100 - - - +
B
kDa
COS-1
WB:anti-FLAG
250
150
100
75
50
FLAGCBP1-507 + - - -
FLAGCBP1-1458 - + - -
FLAGCBP1-1901 - - + -
FLAGCBP1-1100 - - - +

Figure 3.15 Expression of CBP C-terminal deletions in COS-1 and HEK293 cells

(A) HEK293 and (B) COS-1 cells were seeded on 100mm plates for 24 hours prior to being transfected with expression constructs encoding pSG5FLAG-CBP1-1901, pSG5FLAG-CBP1-1458, pSG5FLAG-CBP1-1101 and pSG5FLAG-CBP1-507. 48 hours post-transfection the cells were lysed and the proteins were resolved via 8% SDS-PAGE. The proteins were visualised by probing the blots with mouse anti-FLAG antibody followed by anti-mouse HRP conjugated secondary antibody.

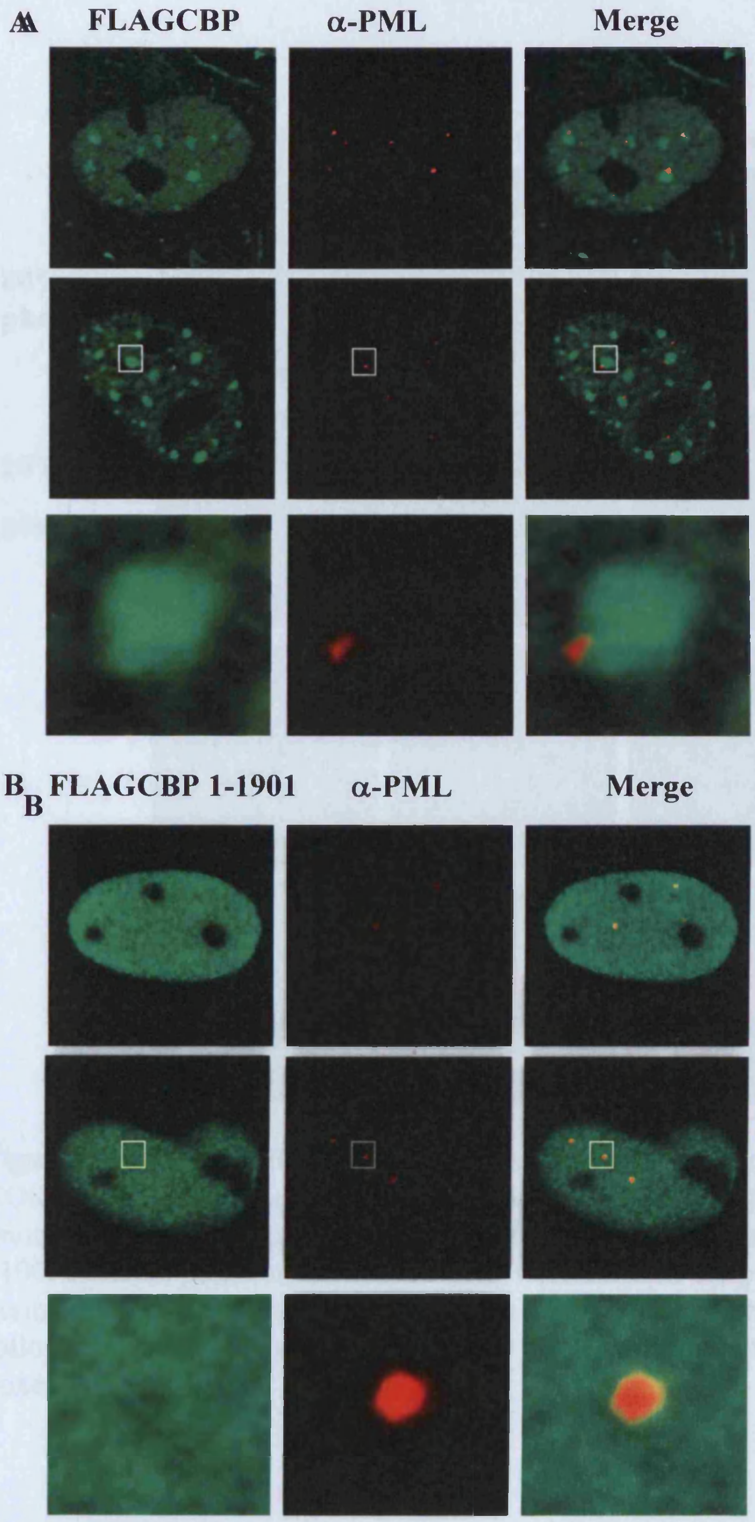

Figure 3.16 Deletion of CBP C-terminus affects its subcellular localisation
COS-1 cells were seeded on 22mm coverslips at 1 x 10^5 confluency and transfected after 24 hours with an expression plasmids encoding (A) FLAG-CBP and (B) FLAG-CBP1-1901. 48 hours post-transfection the cells were fixed in 4% paraformaldehyde, permeabilised and stained with antibodies raised against rabbit anti-PML (red) followed anti-rabbit Alexa594. Magnified insets correspond to the white square boxes.

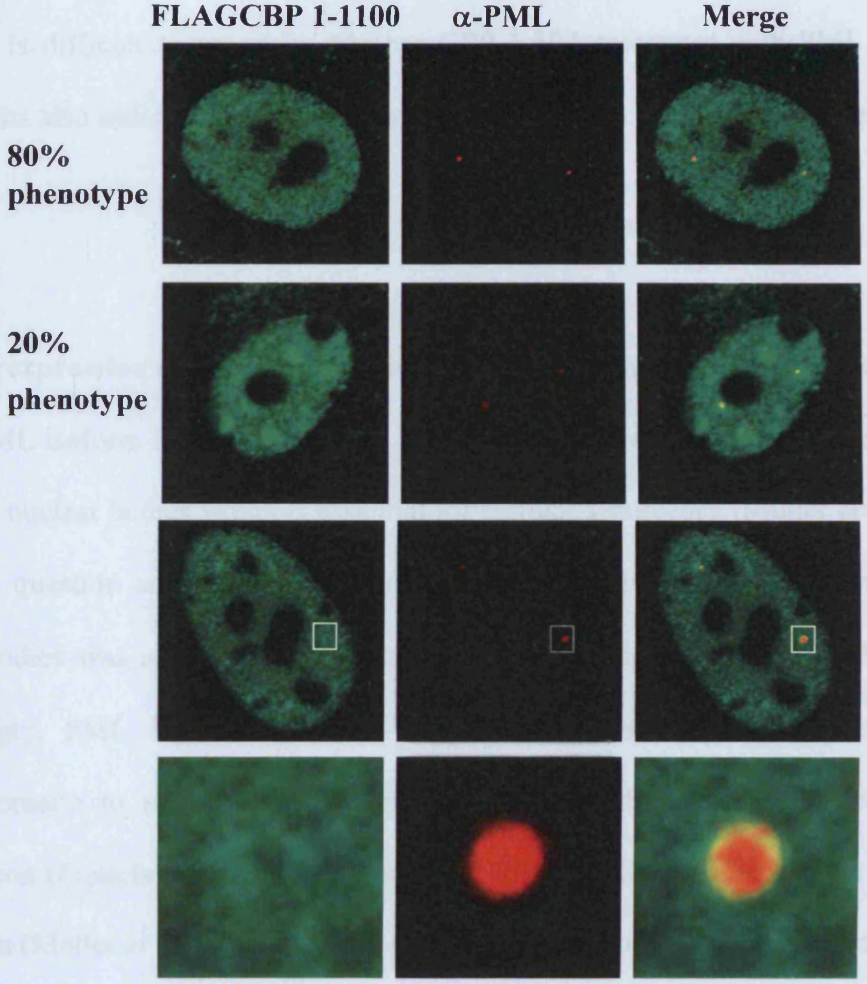
FLAGCBP 1-1100
α-PML
Merge
80% phenotype
20% phenotype

Figure 3.17 FLAG-CBP 1-1100 displays various phenotypes in COS-1 cells
COS-1 cells were seeded on 22mm coverslips at 1 x 10^5 confluency and transfected after 24 hours with an expression plasmid encoding FLAG-CBP1-1100. 48 hours post-transfection the cells were fixed in 4% paraformaldehyde, permeabilised and stained with antibodies raised against rabbit anti-PML (red) followed anti-rabbit Alexa594. Magnified insets correspond to the white square boxes.

SUMO sites) localised to the nucleus and displayed a diffuse pattern (Figure 3.18). As with CBP-1-1901 it is difficult to ascertain whether CBP-1-507 associates with PML bodies. However, these results also indicate that the CBP nuclear localisation signal (NLS) is between amino acids 1 and 507.

3.12 Overexpression of PML IV recruits CBP and CBPΔ998-1087 into nuclear foci

PML isoform IV, has previously been shown to mediate the recruitment of CBP and p53 into PML nuclear bodies which is essential for cellular senescence (Muller et al., 1999). We thus asked the question as to whether overexpression of PML isoform IV, a major component of nuclear bodies was able to alter the subcellular localisation of CBP or CBPΔ998-1087. PML Interestingly, PML IV recruits PML-associated repressor of transcription (PAROT) from heterochromatin to nuclear bodies thereby alleviating the repressive effects of PAROT on transcription (Fleischer *et al.,* 2006). Similarly, HIPK2 is recruited to nuclear bodies on PML IV expression (Moller *et al.,* 2003). COS-1 cells were transfected with expression plasmids encoding YFP-HIS-CBP, YFP-HIS-CBPΔ998-1087 and FLAG-PML IV. The cells were fixed and stained 48 hours post-transfection with anti-FLAG and Alexa-594 conjugated secondary antibody. As shown in Figure 3.19 A and B, expression of PML IV results in the recruitment of both YFP-CBP and YFP-CBPΔ998-1087 to nuclear bodies. However, it is clear that a proportion of YFP-CBPΔ998-1087 proteins remain independent of the nuclear bodies in microspeckles (Figure 3.19). Thus, it appears that PML IV-dependent recruitment of CBP into nuclear bodies is partially regulated by SUMOylation and furthermore it may regulate CBP coactivator function.

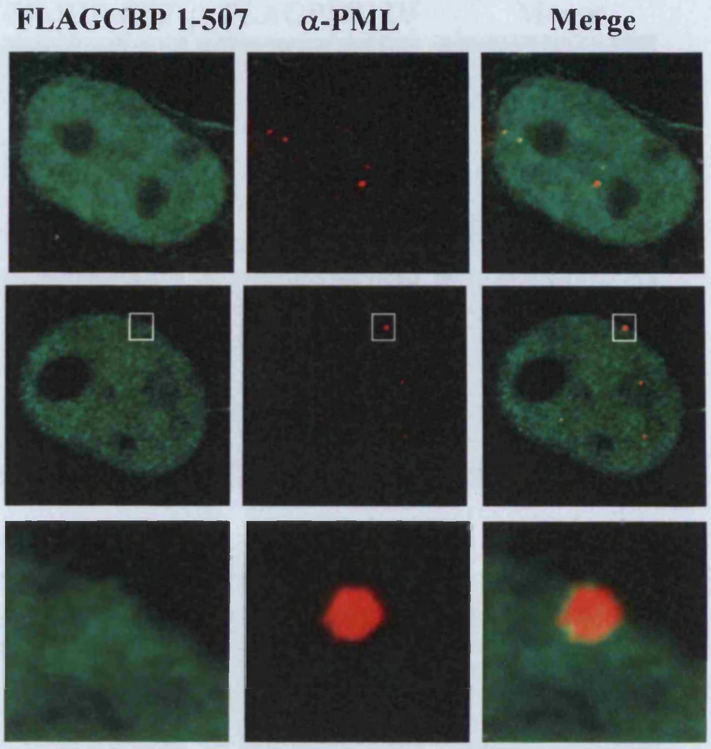

Figure 3.18 FLAG-CBP 1-507 is a diffuse nuclear protein
COS-1 cells were seeded on 22mm coverslips at 1 x 10^5 confluency and transfected after 24 hours with an expression plasmids encoding FLAG-CBP 1-507. 48 hours post-transfection the cells were fixed in 4% paraformaldehyde, permeabilised and stained with antibodies raised against rabbit anti-PML (red) followed by anti-rabbit Alexa594. Magnified insets correspond to the white square boxes.

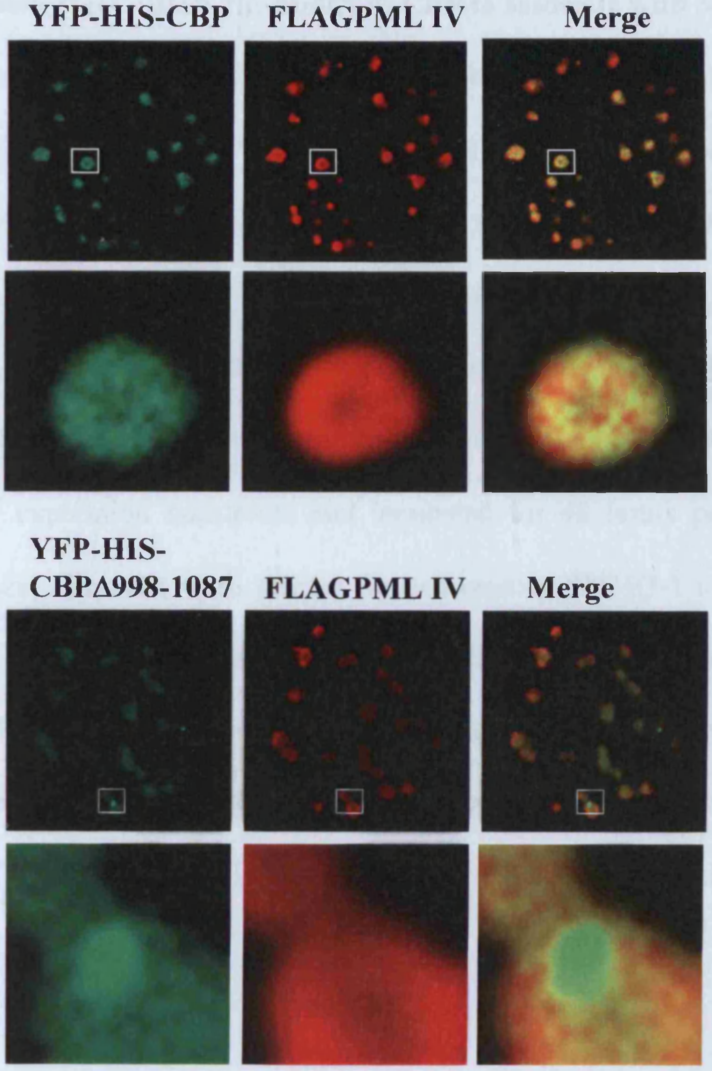
YFP-HIS-CBP
FLAGPML IV
Merge
YFP-HIS-CBPΔ998-1087
FLAGPML IV
Merge

Figure 3.19 FLAG-PML IV recruits YFPCBP and partially recruits YFPCBPΔ997-1087 into nuclear bodies
COS-1 cells were seeded on 22mm coverslips at 1 x 10^5 confluency and transfected after 24 hours with expression plasmids encoding FLAG-PMLIV, YFP-HIS-CBP or YFP-HIS-CBPΔ998-1087. 48 hours post-transfection the cells were fixed in 4% paraformaldehyde, permeabilised and stained with antibodies raised against mouse anti-FLAG (red) followed by anti-rabbit Alexa594. Magnified insets are represented by white square boxes

3.13 SUMOylation state affects the ability of CBP to associate with SUMO foci

As we had shown that SUMO affected the ability of CBP to associate with PML bodies we next determined whether CBP or CBPΔ998-1087 would colocalise with SUMO-1 *in vivo*. Staining cells with an anti-SUMO-1 antibody allows the visualisation of PML bodies, as they are the major form of SUMOylated proteins in the cell. Muller *et al.*, (1999) demonstrated that endogenous or overexpressed PML completely colocalises with SUMO-1 in nuclear foci. Therefore, COS-1 cells were transiently transfected with YFP-HIS-CBP and YFP-HIS-CBPΔ998-1087 expression constructs and incubated for 48 hours prior to fixation with 4% paraformaldehyde. The cells were stained for endogenous SUMO-1 using rabbit anti-SUMO-1 and anti-rabbit Alexa 594 and imaged via laser scanning confocal microscopy. As shown in Figure 3.20 YFP-HIS-CBP proteins form large distinct nuclear foci many of which lie adjacent or overlap with SUMO foci or PML bodies as shown by the higher magnification insets. Interestingly, YFP-HIS-CBPΔCRD1 associates into many smaller foci only some of which lie adjacent to PML bodies.

3.14 Overexpression of SUMO-1 has no clear effect on the subcellular localisation of CBP and CBPΔ998-1087

Experiments carried out by Chauchereau *et al.* (2003) showed that SUMOylation of Steroid Receptor Coactivator 1 (SRC-1) retarded its export from the nucleus and overexpression of SUMO-1 resulted in an increase in its nuclear retention. Similarly, GFP-SUMO-1 expression led to its complete colocalisation with topoisomerase-1 binding RS protein (Topors) in nuclear foci (Weger *et al.,* 2003). As overexpression of PML IV altered the subcellular localisation of YFP-CBP and YFP-CBPΔ998-1087 to different extents we wanted to examine if overexpression of SUMO-1 had a similar effect. Thus, we transfected COS-1 with expression plasmids encoding

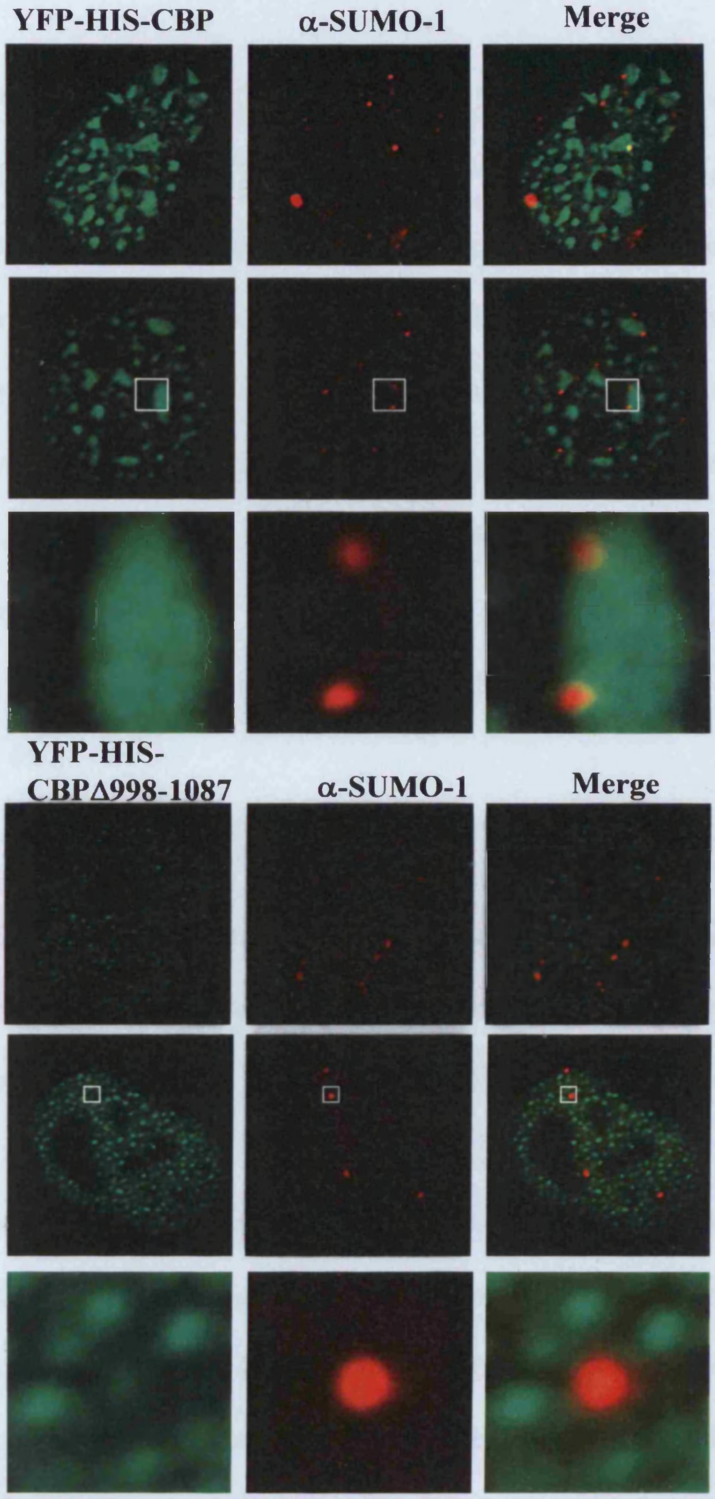
YFP-HIS-CBP
α-SUMO-1
Merge
YFP-HIS-CBPΔ998-1087
α-SUMO-1
Merge

Figure 3.20 YFP-CBP but not YFPCBP Δ998-1087 colocalises with endogenous SUMO-1

COS-1 cells were seeded on 22mm coverslips at 1 x 10^5 confluency and transfected after 24 hours with expression plasmids encoding YFP-HIS-CBP or YFP-HIS-CBPΔ998-1087. 48 hours post-transfection the cells were fixed in 4% paraformaldehyde, permeabilised and stained with antibodies raised against rabbit anti-SUMO-1 (red) followed by anti-rabbit Alexa594 secondary antibody. Magnified insets are represented by white boxes

YFP-HIS-CBP, YFP-HIS-CBPΔ998-1087 and FLAG-SUMO-1. The cells were fixed and stained 48 hours post-transfection with anti-FLAG and Alexa-594 conjugated secondary antibody. As shown in Figure 3.21, YFP-CBP gives the typical diffuse stain with a proportion of the proteins localising in nuclear aggregates which lay adjacent to FLAG-SUMO-1 proteins some of which localised in nuclear foci (PML bodies). However a subset of the FLAG-SUMO-1 proteins appeared to be nuclear diffuse. YFP-HIS-CBPΔ998-1087 formed a large number of small nuclear foci, which do not colocalise with FLAG-SUMO-1. This result is similar to the one observed when staining for endogenous PML.

In conclusion, SUMO-1 foci are distinct from YFP-HIS-CBPΔ998-1087, yet many colocalise with YFP-HIS-CBP foci.

3.15 CBPΔ998-1087 moderately increases AML1 reporter activity in COS-1 cells

Acute myeloid leukemia 1 (AML-1) is a transcription factor that plays an essential role in the development of haematopoietic lineages. CBP/p300 has been shown to be a potent coactivator of AML mediated transcriptional activation (Kitabayashi *et al.,* 1998). However, in certain circumstances, SUMOylation of transcription factors and coactivators has been shown to recruit HDACs to the promoters of target genes (Girdwood *et al.*, 2003; Yang *et al.*, 2004). Thus, we hypothesised that deletion of the SUMO conjugation sites in CBP might increase AML-1 reporter activity due to HDAC dissociation. To determine if deletion of CBP SUMO sites altered the ability of CBP to act as a transcriptional coactivator we carried out transcription reporter assays using pT109-luc which contains 3 AML-1 binding sites.

COS-1 cells were transfected with 500ng pT109-luc, 100ng of expression plasmids unless otherwise stated and either 250ng or 500ng of the CBP reporter constructs. As shown in Figure 3.22 transfection of 250 ng of YFP-CBP led to an increase in reporter activity when compared to

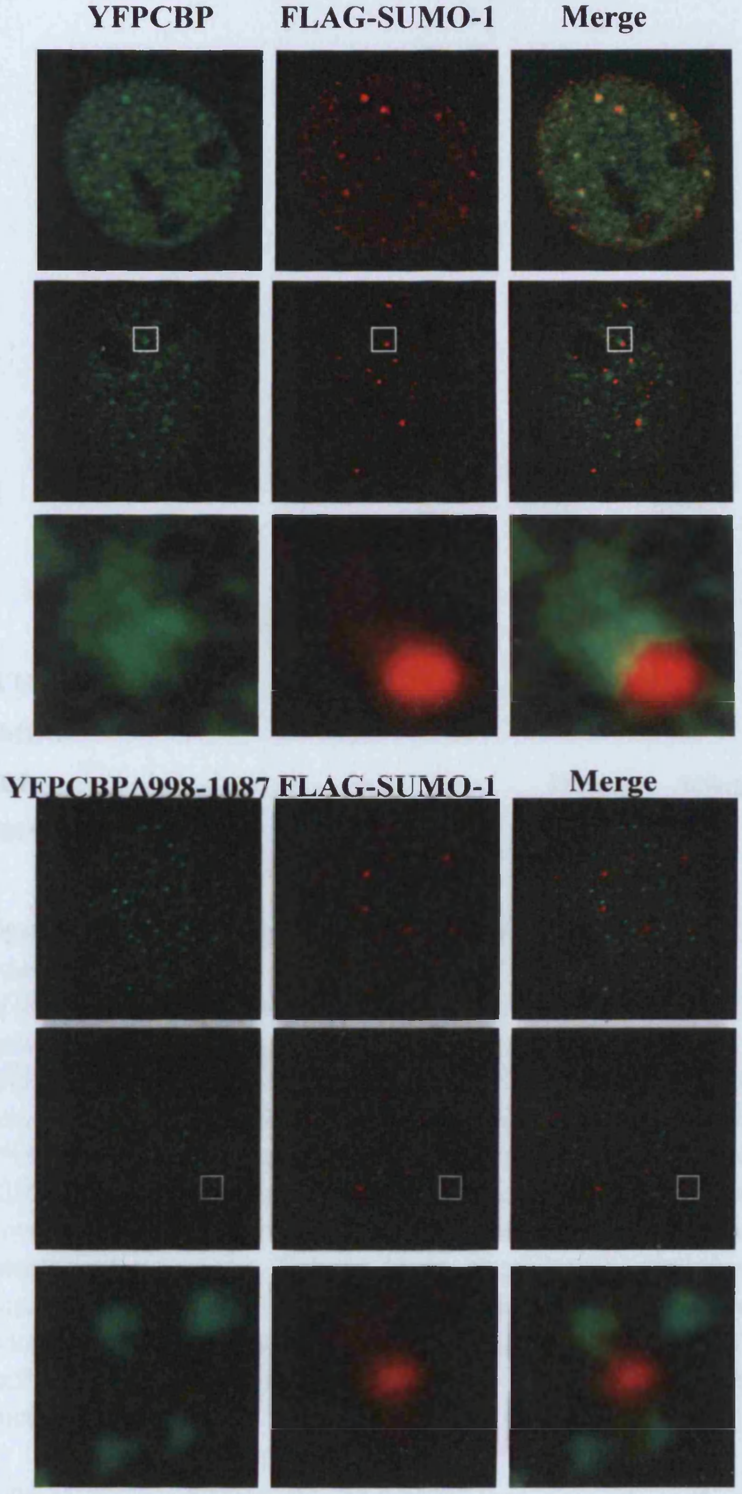

Figure 3.21 Overexpression of FLAG-SUMO-1 has no effect on the ability of YFP-CBP or YFP-CBPΔ998-1087 to colocalises with SUMO-1 foci.
COS-1 cells were seeded on 22mm coverslips at 1 x 10^5 confluency and transfected after 24 hours with expression plasmids encoding FLAG-SUMO-1 and YFP-HIS-CBP or YFP-HIS-CBPΔ998-1087. 48 hours post-transfection the cells were fixed in 4% paraformaldehyde, permeabilised and stained with antibodies raised against mouse anti-FLAG (red) followed by anti-mouse Alexa594 secondary antibody. Magnified insets are represented by white boxes.

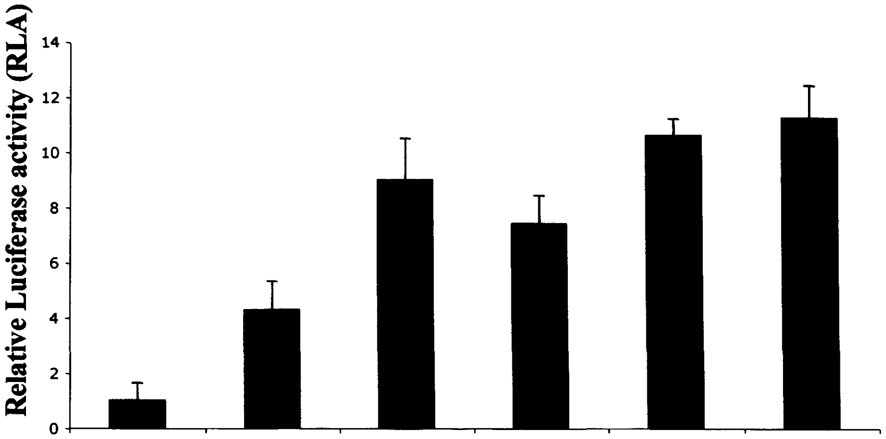

pT109	+	+	+	+	+	+
AML-1	-	+	+	+	+	+
CBP	-	-	**250ng**	**500ng**	-	-
CBPΔ998-1087	-	-	-	-	**250ng**	**500ng**

Figure 3.22 SUMOylation affects CBP mediated AML-1-dependent transcription

COS-1 cells were seeded and transfected with 500ng pT109-Luc luciferase reporter, 100ng pCH110 β-galactosidase reporter, 100ng pSG5-AML-1 and either pSG5-YFP-HIS-CBP or pSG5-YFP-HIS-CBPΔ998-1087 as shown. "-" indicates no DNA transfected, "+" or "number" indicate prescribed amount of DNA. 48 post-transfection the cells were harvested; extracts were assayed for luciferase activity using the luciferase assay system (Promega); and the data were normalised relative to β-galactosidase activities in the same extracts, as determined using the Galacto-Light chemiluminescence assay (Tropix). All measurements were done in triplicate, and each experiment repeated at least twice. Reporter activities are expressed as fold induction of the normalised luciferase activity relative to that due to reporters alone. Error bars show the calculated S.E.M.

reporter alone, or reporter + AML-1. While transfection of 500ng of YFP-CBP caused an increase in reporter activity it was less than that observed with 250ng YFP-CBP (these results were not statistically validated). This decrease in transcriptional activity is often observed when CBP is highly overexpressed, especially when observing the affects of CBP on nuclear receptor dependent transcription and is more commonly known as 'squelching'. Nevertheless, transfection of cells with either 250ng or 500ng of YFP-CBPΔ998-1087 led to a greater increase in reporter activity when compared to YFP-CBP. This result is in agreement with the published data not only for CBP (Yao *et al.*, 2005) but also p300 (Girdwood *et al.*, 2003) and the Ets-1 transcription factor Elk-1 (Yang *et al.*, 2004) which shows that deletion of putative SUMOylation sites led to a moderate increase in transcription. However, Yao *et al.* (2005) determined the effect of SUMOylation on CBP-mediated transcription by creating a GAL4-CBP fusion protein and observing the effects of SUMO mutations on a GAL4-responsive promoter. As CBP is a coactivator and not a transcription factor, tethering GAL4 to CBP may be an inappropriate model to use when observing the effects of post-translational modifications on CBP coactivator function.

3.16 Discussion

SUMOylation of nuclear proteins is believed to regulate their subcellular localisation and function. In addition, SUMOylation of PML body proteins has been shown to affect their ability to associate with PML bodies. SUMOylation also appears to play an important role in transcriptional repression by allowing the recruitment of HDACs to target promoters. Girdwood *et al.* (2003) demonstrated that SUMOylation of GAL4-p300 resulted in the recruitment of HDAC6 thereby repressing GAL4-mediated transcription. Therefore, as CBP is a transcriptional coactivator, a dynamic component of PML bodies and contains putative SUMO acceptor sites we investigated whether SUMOylation of CBP regulated its transcriptional activity and association with PML bodies.

Previous reports in the literature have shown that CBP colocalises with PML bodies (La Morte et al., 1998). In addition, FRAP experiments have shown that CBP is a dynamic component of PML bodies (Boisvert et al., 2000). Live-cell imaging experiments showed that YFP-CBP shows a dispersed distribution in the nucleus that concentrates into nuclear speckles over a time period of 2-4 hours. Interestingly, Muratani *et al.* (2002) have shown that PML bodies can be divided into three classes based on their relative mobility in cells. The first class are immobile, class II displayed limited movement while class III moved rapidly in an ATP-dependent manner. Our results indicate that CBP foci may have similar movements in mammalian cells allowing them to relocate to sites of action when needed.

SUMOylation of some nuclear proteins has been shown to control their ability to associate with PML bodies such as the orphan receptor LRH-1 (Chalkiadaki *et al.,* 2005). Thus, as CBP contains five putative SUMO acceptor sites, we investigated whether SUMOylation of CBP was involved in its association with PML bodies. Firstly, we carried out some preliminary immunofluorescence experiments in which we found that endogenous CBP colocalised with GFP-SUMO-1 foci but not with a GFP-SUMO-1 G/A which is unable to be conjugated onto its target protein. While endogenous SUMO foci completely colocalise with PML bodies (Muller *et al.,* 1998), only a subpopulation of overexpressed GFP-SUMO-1 foci colocalise with endogenous CBP foci at PML bodies.

The PIAS family of proteins contain SP-RING domains, which confer upon them the ability to act as SUMO E3 ligases. PIAS proteins have been shown to SUMOylate PML body-associated proteins, for example PIASγ increases the SUMOylation of the Wnt-responsive transcription factor LEF1, resulting in its recruitment into nuclear bodies (Sachdev *et al.,* 2001). Therefore, we carried out indirect immunofluorescence microscopy which showed that endogenous CBP foci colocalise with endogenous PIAS1, PIASxα and PIASγ at PML bodies. Interestingly, another PIAS family member PIAS3 has been shown to interact with CBP/p300 via its SP-RING domain however, it was not ascertained whether PIAS3 was directly involved in the SUMOylation of these proteins (Long *et al.,* 2004). These results suggest a possible role for the PIAS proteins in the SUMOylation of CBP and its recruitment into nuclear bodies although biochemical assays need to be carried out to confirm these observations.

In order to begin to investigate if CBP was SUMOylated *in vivo* we carried out Co-IPs with both untagged overexpressed CBP and YFP-tagged CBP. These results clearly showed that CBP was SUMOylated. Girdwood *et al.* (2003) showed that SUMOylation of p300 occurred at 2 lysine residues and CO-IPs revealed that SUMOylated p300 migrated as one high molecular weight band. This contrasts with our results whereby SUMOylated CBP migrates as a series of high molecular bands which may be due to the extra SUMO acceptor sites within CBP.

In order to determine whether CBP was directly SUMOylated, we carried out *in vitro* SUMO assays. *In vitro* SUMO assays, originally described by Desterro *et al.* (1999), enable the identification of potential SUMO sites using recombinant E1 and E2 SUMO ligases, recombinant SUMO proteins, the substrate protein and ATP, which drives the reaction. Based on homology with p300 and using the SUMOplot (Abgent) we identified 5 potential SUMOylation sites within and adjacent to the conserved CRD1. To aid us in our analysis we created expression constructs encoding HIS-CBP and HIS-CBPΔ998-1087 which deleted the putative SUMO sites. The CBP constructs were *in vitro* translated and used in an *in vitro* SUMO assay with or without the essential E2 SUMO ligase Ubc9. This revealed that full-length CBP was SUMOylated by SUMO-1 and SUMO-2 while the CBP SUMO mutant, HIS-CBPΔ998-1087 was not. These results are consistent with observations made by Girdwood *et al.* (2003) who showed that deletion of the conserved homologous region in p300 led to a loss of SUMOyation. Interestingly, during the course of this study, Kuo *et al.* (2005) demonstrated that CBP was SUMOylated by

SUMO-1 at K999, K1034 and K1057 *in vitro* thus confirming our findings that CBP was SUMOylated at sites between amino acids 998-1087. In addition, SUMO-2 is postulated to be conjugated onto target proteins in response to cellular stress, such as heat-shock, thereby protecting the protein from degradation. Our results suggest that CBP stability may be regulated by SUMO-2 in response to cellular stress although this observation needs to be investigated further.

We wanted to ascertain if any other sequences outside amino acids 998-1087 were SUMOylated *in vitro* or if they were important for the efficient SUMOylation of the identified SUMO sites between amino acids 998-1087. A series of FLAG-CBP C-terminal deletion mutants were generated and used in *in vitro* SUMO assays. This revealed that no sequences outside the amino acids 998-1087 were SUMOylated, however, sequences proximal were essential in the SUMOylation of CBP. This may be due to deletion of important Ubc9 docking sites which may be essential in the SUMOylation reaction. Alternatively, deletion of sequences C-terminal of the SUMO acceptor sites may have led to misfolding and the hiding of SUMO sites form the SUMO conjugation enzymes, ultimately preventing the SUMOylation reaction.

The experiments outlined here provide strong evidence that CBP is SUMOylated, therefore, we investigated whether SUMOylation affected the ability of CBP to associate with PML bodies and SUMO foci. Muller *et al.* (1998) demonstrated that endogenous CBP and SUMO-1 colocalised at PML bodies. To aid us in our analysis, we created YFP-HIS-CBP and YFP-HIS-CBPΔ998-1087 expression constructs. YFP-HIS-CBP was nuclear diffuse with a proportion of the proteins forming large nuclear bodies which were adjacent to PML bodies. These CBP foci appeared much larger then the YFP-CBP foci observed in the live-cell imaging experiment. This may be due to the fixation of cells which has been shown to disrupt some nuclear bodies such as RNAPII transcription factories (Guillot *et al.*, 2004), or PML bodies may only be able to accommodate a defined amount of CBP. Therefore, overexpression may result in the excess proteins congregating at the periphery of the bodies. Interestingly, Girdwood *et al.* (2003) demonstrated via live-cell imaging that p300 and SUMO-1 associated transiently, which may be another reason why only a proportion of the CBP foci colocalise with PML bodies. However, the majority of YFP-HIS-CBPΔ998-1087 proteins accumulated in much smaller foci, a large proportion of which were situated away from and were independent from PML bodies and SUMO foci. While there are no reports in the literature on the effect that SUMOylation has on CBP or p300, deletion of SUMO sites in other PML body-associated proteins gives similar results to those presented above. Mutation of SUMO sites within the transcription factor Sp3 resulted in its loss from PML bodies (Ross *et al.*, 2002). However, deletion of the SUMO sites in other PML body-associated proteins such as DAXX (Jang *et al.*, 2002) and Topors (Weger *et al.*, 2003) did not affect their ability to associate with PML bodies suggesting their association was mediated by adapter proteins.

While the results presented here suggest a potential role for SUMO in regulating the association of overexpressed CBP with PML bodies, we found that overexpression of PML isoform IV resulted in the complete recruitment of YFP-HIS-CBP but only the partial recruitment of YFP-HIS-CBPΔ998-1087 proteins into nuclear bodies. Fleischer *et al.* (2006) demonstrated that PML-associated repressor of transcription (PAROT) could be recruited into nuclear bodies by PML IV resulting in a decrease in its repressive function. Therefore, PML-mediated recruitment of CBP into nuclear bodies is partially dependent on SUMOylation which may play an essential role in regulating CBP function via its sequestration in nuclear bodies.

While SUMOylation was shown to play a partial role in regulating the association between CBP and PML bodies, we used our series of CBP C-terminal deletions to determine what domains were important in mediating the formation of CBP foci and in the association with PML bodies. Firstly, FLAG-CBP was similar to YFP-HIS-CBP in that a proportion of the proteins associated in nuclear foci some of which were adjacent to PML bodies. However, CBP amino acids 1901-2442 which include the SID domain are very important for the ability of CBP to associate in nuclear foci and ultimately in their localisation with PML bodies. This is similar to results from p300 in which deletion of the SID domain leads to the diffuse localisation of p300 (D.M. Heery unpublished data). This suggests that either the SID domain is important for the direct association with other CBP molecules or the SID domain may also bind to co-factors which mediate the formation of CBP foci and association with PML bodies. It appears that the latter statement is true, as work carried out by Doucas *et al.* (1999) demonstrated that amino acids 311-521 of CBP mediated the interaction with PML *in vitro*. This suggests that CBP must first associate into nuclear foci which is dependent on sequences outside amino acids 998-1087 and association of these foci with PML bodies is mediated by SUMO. While our results provide new insights into the association of CBP with PML bodies, further studies such as Co-IPs and FRET analysis are needed to fully elucidate the domains necessary for the interaction between CBP and PML bodies.

SUMOylation of transcription factors such as Elk-1 leads to the recruitment of HDACs and transcriptional repression (Yang *et al.,* 2004). SUMOylation of CBP and p300 has also been shown to recruit HDACs to target promoters and mutation of SUMO acceptor sites leads to an increase in co-activator-mediated transcriptional activation (Girdwood *et al.*, 2003, Yuo *et al.*, 2005). We used transcription reporter assays to determine if SUMOylation had any effect on CBP coactivator function. CBP has been shown to increase AML-1-dependent transcriptional activation which plays a crucial role in myeloid cell differentiation. Our results show that CBP increases AML1 reporter activity and deletion of SUMO acceptor sites results in a further increase. Based on the published data we suggest that SUMOylation of CBP may mediate the recruitment of HDACs and deletion of these sites would therefore lead to an increase in transcriptional activation. While our experiments were performed using CBP as a transcriptional coactivator, Girdwood *et al.* (2003) and Kuo *et al.* (2005) used GAL4-p300 and GAL4-CBP fusion constructs respectively to assess the effect of SUMO on a GAL4-reporter construct. However, we have also shown that SUMOylation leads to the accumulation of CBP in large nuclear foci. Therefore, it will be interesting to carry out Co-IPs and CHIP assays which will allow us to determine if SUMOylation of CBP recruits HDACs or other corepressor complexes to promoters or if sequestration of CBP in nuclear foci is the key to regulating CBP activity.

In summary, it appears that the SID domain plays an important role in mediating the accumulation of CBP in nuclear foci. However, the association of these foci with PML bodies appears to be regulated in part by SUMOylation. In addition, we have shown that deletion of the SUMOylation sites within CBP leads to an increase in AML1-mediated reporter activity. These results provide a novel insight into the mechanisms of how SUMOylation regulates CBP subcellular localisation and reporter activity.

Chapter 4

CBP interaction with nuclear transport proteins and modulation by HDAC inhibitors

4.1 Introduction

CBP interacts with a myriad of cellular proteins through multiple distinct domains such as the KIX domain and the SID. This enables CBP to play a crucial role in transcription by acting as a molecular scaffold for the GTFs and coactivators and also by acetylating the N-terminal tails of histones making the DNA more accessible to general transcription machinery and TFIID. Histone acetylation is generally correlated with transcriptional activation, whereas hypoacetylated histones are associated with transcriptional repression. Deacetylation of the N-terminal histone tails is carried out by HDACs potentially allowing the DNA to associate more tightly with the core histones. This acts as a barrier to recruitment of the transcriptional machinery.

Transcription is altered in many cancer cells, leading to changes in cell growth and differentiation. In recent years HDAC inhibitors (HDACi) have been utilised in the treatment of many types of cancer and neurodegenerative diseases. While their mechanism of action is not fully understood, they are believed to function by blocking the activity of HDACs which ultimately leads to a global hyperacetylation of histones and a concomitant increase in transcription. One of the many genes induced by HDACi is p21(WAF) which plays a major role in cell growth arrest and the induction of apoptosis (Ju *et al.,* 2003).

However, acetylases and deacetylases not only regulate histone function but they also affect the regulation of non-histone proteins. Sterner *et al.* (1979) first showed that HMG1 was a substrate for acetylation, which was later shown to be carried out by CBP (Munshi *et al.*, 1998). Furthermore, acetylation of the coactivator ACTR by CBP was shown to regulate its ability to associate with nuclear receptors. Interestingly, it was reported that CBP acetylates the nuclear import factor Importinα which is involved in the import of many nuclear components (Bannister *et al.*, 2000). Once Impα has dropped its cargo in the nucleus it is re-exported back to the cytoplasm by CAS (Kutay *et al.,* 1997). In the study carried out by Bannister et al., (2000), a large panel of proteins was screened as possible substrates for recombinant CBP. Rch1 (human importinα) and importinα-7 were identified as good substrates *in vitro*. Further work revealed that acetylation occurred on K22 of Rch1 which lies within the importinβ binding domain and acetylation of this residue promoted importinβ binding *in vitro*.

A yeast 2-hybrid screen (Y2-H) identified two novel CBP interacting proteins: Nucleoporin 93 (NUP93) the mouse homologue of the yeast nucleoporin Nic96 which associates with FG repeat proteins on the nuclear side of the NPC and CAS. CAS is a homologue of the yeast Cse1 (Chromosome Segregation Factor) that is highly expressed in proliferating cells and is associated with the mitotic spindle and microtubules. It is also involved in toxin- and TNF-mediated apoptosis and it is highly expressed in many tumours (Scherf *et al.*, 1998). However, CAS is the essential export factor for Impα and mediates its export from the nucleus to the cytoplasm in a RAN-dependent manner. This enables Impα to recycle to the cytoplasm and act as an importer for impβ (Gorlich *et al.*, 1999). Furthermore, Cse1, Nic96 and the yeast homologue of Impα have been shown to associate with active genes in yeast, adding another facet to the story (Casolari *et al.*, 2004).

A yeast two-hybrid assay is a sensitive screen that allows for the identification of protein-protein interactions. Transcription factors generally contain two separable domains, a DNA binding domain (DBD) and a transactivation domain (AD). These domains alone cannot activate transcription in yeast; however, when they interact non-covalently they can activate transcription. Thus, when two proteins containing these domains interact with each other, they form a functional transcription factor. In a typical assay, one protein is expressed containing a functional DBD which is termed the "bait" while the other protein, or "prey", is expressed as a fusion with an AD. pASV3mod is a commonly used AD vector in yeast two-hybrid as it contains the VP16AAD and has a Leu2 selectable marker. pBTM116mod is used as the "bait" vector as it allows the expression of the bacterial repressor DNA binding protein, LexA, which is under the control of the constitutive ADH1 gene promoter. Furthermore, it contains a TRP1 selectable marker. The fusion protein is expressed under the control of the constitutive PGK(PolyGlucoseKinase) promoter. Yeast are transformed with a transcription reporter plasmid containing multiple DNA binding sites specific for the particular DBD being used. Therefore, when the two proteins interact the transcription of the reporter will increase. Using this approach, it is possible to screen for known proteins that interact, mutant proteins that are unable to interact and also to identify novel interacting proteins by screening libraries of AD fusion proteins with a protein of interest fused to a DBD.

This chapter describes experiments that investigate the interaction of CBP with nuclear transport proteins. *In vivo* and *in vitro* studies were carried out to examine whether CBP interacted with CAS and Impα. HDAC inhibitors were employed to test whether acetylation and deacetylation played a role in regulating the subcellular localisation and function of CBP, CAS and Impα.

4.2 CBP-SID interacts with the nuclear export factor CAS and the nucleoporin Nup93

To identify novel CBP binding factors a Y2-H screen of a VP16AAD-fused mouse embryo cDNA library was performed using LexA-CBP 2041-2165 as bait (Matsuda *et al.*, 2004). 5 positive clones were identified, one of which consisted of the pointed domain of Ets-2 (Matsuda *et al.*, 2004). Quantitation of β-galactosidase activity revealed that the clone 1-09 interacted strongly with LexA CBP 1982-2163 whereas clone 5-10 gave a lower but nonetheless significant activation of the reporter (Figure 4.1 A). Sequence analysis revealed two unique cDNAs, which were fused in frame with the VP16 AAD. Database searches demonstrated that

clone 1-09 had 100% identity with the N-terminus (amino acids 1-350) of the mouse homolog of CAS (Brinkmann *et al.*, 1995). This region encompasses the RAN-GTP binding domain of CAS, which is required for complex formation with RAN-GTP. Recent advances have identified the presence of Huntingtin, elongation factor 3, the PR65/A subunit of protein phosphatase 2, TOR (HEAT) repeats within Cse1 which are essential for the interaction with Impα. In its cargo-free state Cse1 consists of N- and C-terminal arches that interact to form a compact ring. However, the arches open via a hinge region located at HEAT repeat 8 to allow the interaction with Impα and RAN-GTP (Cook *et al.,* 2005). Interestingly, we also identified clone 5-10 which we designated mCIP4 (mouse CBP Interacting Protein 4) which was highly homologous to Nucleoporin 93 (Nup93). Nup93 contains a series of heptad repeats, which form the basis of coiled-coil α-helices, within its N-terminus, thereby facilitating protein-protein interactions (Grande *et al.,* 1995). A schematic representation of library fusion proteins, and the parent proteins, indicating known sequence motifs, is shown in Figure 4.1 B.

As the boundaries of the bait sequence used (1982-2163) were extended beyond the minimal SID, we used a series of LexA-CBP fusion proteins to define the minimal sequences capable of binding each protein isolated in the screen. cDNA encoding CAS1 (1-349) was recloned in pASV3 to remove sequences derived from 5'UTR in the original library clones. As shown in Figure 4.2 A, the minimal CBP sequence required for binding CAS1 (1-349) polypeptides corresponded exactly to the boundaries of the SID (2058-2130), suggesting that CAS interacts specifically with the SID.

4.3 Mutations in the SID disrupt the interaction with CAS

NMR studies have determined that complexes involving the p160 AD1 and CBP-SID involve largely hydrophobic interactions between three α-helices (Demarest *et al.,* 2002). In both

SRC1/CBP and ACTR/CBP complexes, a tight 4-helix bundle is formed from 3-helices from CBP and one from the p160 AD1 (Demarest *et al.*, 2002; Waters *et al.*, 2006). This structure may be stabilised by a sequence containing repeats of the sequence QPGM/L (Sheppard *et al.*, 2001). Previous studies have described the effects of amino acid replacements in the SID on binding of SRC1, Ets-2 and E1A (Sheppard *et al.*, 2001; Matsuda *et al.*, 2004). To evaluate how these mutations affect the recruitment of CAS to the SID, we carried out yeast two hybrid experiments. As shown in Figure 4.2 B, the F-2101-P mutation in SID helix-3 completely disrupted CAS interaction with the SID. This mutation also disrupted interaction of Ets-2, E1A and SRC1 with the SID (Matsuda *et al.*, 2004). Similarly, a K-2103-P mutation reduced the interaction of CAS-N and CBP-SID approximately 4-fold, whereas K-2108-A had no effect on the reporter activation. The CAS-N/SID interaction was also disrupted by L-2071/2/5-A, which reduces hydrophobicity of the Cα1 of CBP. This mutation abrogated the binding of the Ets-2 PNT domain to the SID, whereas it only reduced the interaction with SRC1 AD1 (2-fold) (Sheppard *et al.*, 2001; Matsuda *et al.*, 2004). As observed for other SID binding proteins, the Q-2083-R mutation did not affect CAS-N binding. In addition CAS differs from both Ets-2 and SRC1 in that it is more tolerant of the K-2103-P mutation in Helix-3. This differential sensitivity to amino acid substitutions suggests some flexibility in the docking of CAS-N, Ets-2 and SRC1 with the SID.

4.4 Construction of CAS-NΔ244-253

As we have shown that the N-terminus of CAS interacted with CBP-SID we analysed the sequences of various SID binding proteins and found that they contained a conserved leucine-rich motif (Figure 4.3 A). A VP16-AAD-CAS1-349 expression plasmid was generated by recombinant PCR, in which the leucine rich motif had been deleted (CAS-NΔ244-253). The

fragment was digested with HindIII and SACII and cloned into pASV3mod. The construct was verified by DNA sequencing.

4.5 Expression analysis of yeast 2-hybrid constructs

To determine expression of the yeast 2-hybrid constructs, the yeast strain L40 was used as it contains mutations in the genes encoding leucine (leu), tryptophan (trp), and adenine (Ade) allowing it to be selected for on media lacking one of those amino-acids. L40 was transformed (section 2.6.2) with an expression vector encoding pBTM116mod-LexACBP-SID and selected on Synthetic Dextrose minimal medium minus tryptophan (SD – TRP). This allowed for the successful isolation of colonies containing the plasmid as it encoded a functional tryptophan biosynthetic gene. After positive selection the yeast containing CBP-SID were transformed with expression plasmids for pASVmodVP16AAD, pASV3modCAS-N (1-349), pASV3modCAS-NΔ244-253, pASV3modETS2 and pASV3modVP16 respectively. The cells were lysed (section 2.6.3) and then loaded and run on a 12% SDS-PAGE gel. The gel was electroblotted onto nitrocellulose membrane and probed with a mouse monoclonal α-VP16 antibody 1/200 followed by incubation with a mouse HRP conjugated secondary antibody (1/5000). Figure 4.3 B shows that bands of the predicted sizes were observed for CAS-N1-349 and CAS-NΔ244-253 proteins. However, it is unlikely that the difference in expression levels had any affect on the β-gal assay due to the manner in which the experiment was carried out.

4.6 Deletion of a conserved leucine-rich motif in CAS-N abrogates binding to CBP-SID

In order to quantify the interaction between the CAS and CBP fusion proteins in a yeast 2-hybrid assay we performed a quantitative β-galactosidase reporter assay. Yeast cultures containing the desired constructs were grown O/N to OD_{600}(0.8) and lysed as discussed section

2.6.4. 5μl of protein sample was added to each reaction which was initiated by adding 100μl of 4mg/ml ONPG and timing was started. Once a pale-yellow colour was observed 250μl 1M Na_2CO_3 was added which stopped the reaction. The OD was measured at 420nm. The specific activity of each sample was calculated which takes into account all the variables such as time, protein concentration, volume and OD. The specific activity of the β-gal was given in nM product formed/ mg protein/ minute and the results are shown in Figure 4.4. Ets-2 showed a high level of reporter activity indicating a very strong interaction with CBP-SID which verifies work carried out by Matsuda *et al.* (2004). CAS-N 1-349 also interacts quite strongly with CBP-SID (543 Units), but deletion of the leucine-rich motif reduces the reporter activity >10-fold between CAS-N and CBP-SID (42 Units). The value obtained is similar to the value observed for VP16AAD (36 units). Thus it is clear that a leucine-rich motif in the N-terminus of CAS is essential for the interaction with CBP-SID and deletion of this motif disrupts binding between the two proteins.

4.7 Endogenous and overexpressed CAS proteins are expressed in the nucleus and cytoplasm of mammalian cells

Previous reports in the literature indicated that CAS was predominantly a cytoplasmic protein that associated with microtubules. In a subset of adherent cancer and leukemic cells, CAS has been shown to localise to the nucleus. Furthermore, it was demonstrated that inhibition of CAS phosphorylation resulted in a predominantly nuclear form of CAS in HeLa cells (Scherf *et al.*, 1998). Therefore, we wanted to determine if CAS was expressed in panels of immortalised mammalian cell lines and in which subcellular domain it is localised.

Firstly, to facilitate the detection of exogenously expressed CAS a YFP-CAS expression vector was constructed. PCR was used to insert a Ksp1 site at the 3' end of the CAS cDNA using

FLAG-CAS as a substrate. The resulting PCR product was gel purified and digested with BamH1/Ksp1 and ligated into pEYFP(C3). DNA sequencing of positive clones confirmed that the resulting fusion construct, YFP-CAS, was inframe. To confirm that full-length YFP-CAS was expressed, western blot analysis was carried out. HEK293 cells were either transfected with YFP-CAS or untransfected and lysed 48hrs post-transfection. The whole cell lysates were separated on SDS-PAGE gels and immunoblotted with mouse anti-CAS antibody. YFP-CAS was detected as a ~130kDa band, the predicted size for the fusion protein, while an additional band at ~100kDa was observed which corresponds to endogenous CAS (Figure 4.5).

We also investigated via Western blot analysis whether CAS could be detected in the cytoplasm and the nucleus. COS-1 cells were transfected with FLAG-CAS and lysed 48hrs post-transfection under low salt conditions. This yielded a soluble cytosolic fraction and an insoluble nuclear pellet. The cytosolic fraction was removed and the nuclear pellet was lysed under high salt conditions. The two fractions were resolved on SDS-PAGE gels and immunoblotted with mouse anti-FLAG M2 peroxidase conjugated antibody (1/500 dilution, Sigma). As shown in Figure 4.5 B, FLAG-CAS was detected in both the cytosolic and nuclear fractions of COS-1 cells at approximately 100kDa, the expected size for this protein.

4.8 CAS proteins localise to the nucleus and cytoplasm of mammalian cells

As we had shown that CAS proteins were expressed in the nucleus and cytoplasm of mammalian cells, we next examined the subcellular localisation of endogenous and overexpressed CAS proteins via immunofluorescence microscopy.

To determine the subcellular localisation of endogenous CAS, HEK293 cells were seeded on 22mm coverslips which were fixed, permeabilised and incubated with anti-CAS antibody and a mouse anti-FITC conjugated secondary. The nucleus was visualised with Hoechst 33258 stain

which intercalates DNA. Figure 4.6 shows that endogenous CAS proteins display a non-nucleolar, nuclear staining with a lower level of the protein localising to the cytoplasm in HEK293 cells which is in agreement with the observation by Scherf *et. al.* (1998) that CAS localises to the nucleus in adherent cancer cells.

In order to confirm the expression and subcellular localisation of YFP-CAS proteins, HEK293 cells were seeded on 22mm glass coverslips and transfected with 1μg of YFP-CAS using transfast (section 2.4.2). 48hrs post-transfection the cells were fixed and imaged using a Nikon epifluorescence microscope and the location of the nucleus was determined using Hoechst 33258 stain. The subcellular localisation of YFP-CAS was predominantly nuclear, non-nucleolar, with a lower cytoplasmic staining in HEK293 cells.

Therefore, it is clear that both endogenous CAS and YFP-CAS can be detected from whole cell lysates of mammalian cells and that they both localise to the same cellular compartments.

4.9 Overexpressed CAS colocalises with CBP in COS-1 cells

Based on the yeast 2-hybrid experiments we examined whether truncated or full-length CAS co-localised with endogenous or overexpressed CBP *in vivo*. In order to investigate the interaction of CAS and CBP *in vivo,* immunofluorescence studies with CAS and CBP were undertaken.

Figure 4.7 (A and B) shows COS-1 cells that were transfected with either an expression construct encoding CAS-N in the presence or absence of an expression construct encoding CBP. The cells were fixed 48hrs post-transfection and the CAS protein was stained using anti-FLAG and a FITC-conjugated secondary antibody while the CBP was visualised with anti-CBP(A22) and a TRITC conjugated secondary antibody. It is clear that CAS-N and endogenous CBP co-

localised in discrete nuclear foci (approximately 5-25 per cell) which resemble PML bodies. CAS-N also colocalises with ectopically expressed CBP in discrete nuclear foci (Figure 4.7). However, these foci are larger in size and greatly outnumber the foci that were identified when just CAS-N was overexpressed. In Figure 4.7 (C) COS-1 cells were co-transfected with expression constructs encoding full-length CAS and CBP. Overexpressed full-length CAS behaves similar to CAS-N in that it forms nuclear aggregates but they only show partial colocalisation with ectopically expressed CBP. This contrasts to the complete colocalisation of CAS-N and CBP when both proteins are overexpressed. Thus, while CAS-N and CBP accumulate in defined regions of the nucleus, full-length CAS and CBP do not suggesting additional domains in CAS influence its subcellular localisation and interaction with CBP.

4.10 HDAC inhibitors (HDACi) perturb the subcellular localisation of endogenous and overexpressed CAS proteins

CAS has been implicated in the nucleo-cytoplasmic shuttling of Impα in a RAN-GTP dependent manner (Kutay *et al.,* 1997). Interestingly, Impα is acetylated by p300 at Lys22 within the N-terminal Impβ binding domain and this interaction is potentiated by the potent HDAC inhibitor Trichostatin A (TSA) (Bannister *et al.* 2000). Acetylation of this residue was postulated to play a critical role in Impα mediated nuclear transport (Kouzarides, 2000). We investigated whether upregulation of global acetylation levels by the HDAC inhibitors TSA or Sodium Butyrate (NaB) had any effect on the subcellular localisation of endogenous CBP, CAS or Impα proteins.

COS-1 cells were either untreated, treated with vehicle (ethanol) or increasing amounts of TSA (1μM, 5μM, 10μM) or NaB (5mM, 10mM, 20mM) for 18 hours. The cells were then fixed and double immuno-stained with anti-CBP(A22) and anti-CAS. In control cells, endogenous

CAS gives a predominantly diffuse, nuclear stain that is excluded from the nucleoli. On treatment with increasing concentrations of TSA (Figure 4.8) and NaB (Figure 4.9), CAS maintains a diffuse nuclear staining but a subset of CAS proteins appear to accumulate in nuclear aggregates. Endogenous CBP localises to distinct nuclear foci which do not associate with CAS aggregates on HDACi treatment.

We next analysed the effect of TSA on overexpressed CAS proteins in COS-1 cells. COS-1 cells were transfected with an expression vector encoding FLAG-CAS for 30 hours and either untreated or treated with 10μM TSA for a further 18 hours prior to being fixed and stained with antibodies raised against the FLAG epitope. FLAG-CAS displays a diffuse nuclear stain with a lower cytoplasmic concentration of the protein. However, treatment with TSA leads to the formation of nuclear aggregates and a greater proportion of the proteins appears to be cytoplasmic (Figure 4.10). It is also interesting to note that these aggregates do not colocalise with CBP foci.

However, regardless of the failure of CAS and CBP proteins to colocalise, these results suggest that acetylation directly or indirectly affects the localisation of both endogenous and overexpressed CAS proteins.

4.11 TSA and NaB causes an increase in the number of CBP associated PML bodies

While we had shown that CBP and CAS did not colocalise on treatment with TSA a number of questions remained unanswered. (1) Did HDACi cause an increase in the number of CBP foci? (2) were all the foci PML bodies?

Firstly, we examined whether the subcellular localisation of endogenous CBP was affected by TSA or NaB. As CBP is a dynamic component of PML bodies we wanted to see if the CBP association with PML bodies was affected upon addition of HDACi. COS-1 cells were

seeded on 25mm glass coverslips and allowed to adhere before they were either untreated, treated with vehicle ethanol or increasing amounts of TSA (1μM, 5μM, 10μM) or NaB (5mM, 10mM, 20mM) for 18 hours. The cells were then fixed and double immuno-stained with anti-CBP(A22) and anti-PML antibodies. Figure 4.11 shows that in control cells CBP colocalises with PML bodies. However, on treatment with increasing concentrations of TSA or NaB, the number of CBP-associated PML bodies increase. To confirm this observation the total number of CBP-associated PML bodies in each nucleus were quantified under all conditions (n=50 for each condition). The mean number of CBP foci/nucleus was 8.8 in the untreated control population and 9.8 in the vehicle ethanol population. However, the mean numbers increased on addition of 1μM, 5μM, and 10μM TSA to 11.4 18.5, and 26.8 foci/nucleus, respectively. The mean number of foci/nucleus on addition of 5mM, 10mM and 20mM NaB was 16.7, 21.5 and 21.9, respectively. In summary, HDACi increase the number of CBP foci in the nucleus of COS-1 cells and also promote the association of CBP with PML bodies (Figure 4.12).

4.12 The interaction between CAS and CBP is indirect

Kutay *et al.* (1997) demonstrated that CAS was an essential export factor in the nucleo-cytoplasmic shuttling of Impα. Our data suggests an interaction between CBP-SID and CAS-N in yeast and immunofluorescence studies suggested that they both localised to the same nuclear domains. However, it is possible that these observed interactions are indirect as they may be dependent on the formation of a multimeric complex with Impα or activated RAN-GTP. To enable us to identify if CBP and CAS interacted directly *in vitro* a GST-pulldown experiment was carried out.

GST-alone or GST-SID proteins were expressed and purified as described in section 2.5.12. 10% inputs of the GST-SID and GST-alone were run on 10% SDS-PAGE gel and

coomassie stained in order to check expression levels of the proteins (Figure 4.13 A).

pSG5FLAG-CAS, pSG5FLAG-CAS-N, pSG5HIS-Myc-Impα, RANQ69L (a constitutively active RAN) and pSG5FLAG-SRC1 were *in vitro* transcribed and translated in the presence of [S35]-Methionine which allowed for their detection. The expression of the proteins was detected by running 5% (of 50μl total) on a 10% SDS-PAGE gel. The predicted sizes of SRC1, CAS, CAS-N, Impα and RANQ69L are 160kDa, 88kDa, 32kDa, 48kDa and 20kDa respectively. All proteins migrated according to their predicted size based on the amino acid sequence except for Impα which migrates slower than expected at approximately 60kDa (Figure 4.13 B).

Firstly it was necessary to determine if any of the IVT proteins interacted unspecifically with GST. Therefore, GST-alone was incubated with 5μl of IVT SRC1, CAS, CAS-N, Impα or RANQ69L. However, none of the proteins interacted unspecifically as shown in Figure 4.14 A. To ensure that GST-SID was functional we assessed the binding of a known interacting partner SRC1 by incubating IVT SRC1 with GST-SID. Figure 4.14 B shows that SRC1 binds strongly with GST-SID which is consistent with previously published data (Matsuda *et al.* 2004). However, there was no detectable interaction of GST-SID with CAS alone, CAS and RANQ69L or CAS, Impα and Q69L. Similarly, CAS-N alone, CAS-N and RANQ69L or CAS, Impα and RANQ69L failed to interact directly with GST-SID. This suggests that either sequences outside the SID are required for the interaction with CAS or that other factors present in yeast which facilitate interaction were absent in the GST-pulldown. These results also show that Impα does not interact directly with the SID domain of CBP.

In order to determine whether essential factors present within the cell lysate, that may be missing in an *in vitro* experiment such as RANGTP, were necessary for the interaction between CAS and CBP, we carried out a modified GST-pulldown. We have previously shown that CBP-

SID also interacts with the coactivator SRC1 both *in vivo* and *in vitro* using Co-IP and GST-pulldown experiments respectively (Matsuda *et al.* 2004). Therefore, using identical conditions we sought to establish whether full-length CAS interacted with CBP-SID *in vitro* using a modified GST-pulldown experiment. COS-1 cells were transfected with full-length CAS or SRC1 and lysed 48 hours post-transfection in whole cell lysis buffer. The lysate was incubated with equal concentrations of bacterially expressed glutathione purified GST-SID or GST-alone. 10% inputs of the GST-SID and GST-alone were run on 10% SDS-PAGE gel and Coomassie stained in order to check expression levels of the proteins (Figure 4.15 A). After incubation, the protein complexes were analysed by SDS-PAGE and immunoblotted with anti-FLAG antibody for detection of CAS protein that may be bound to either GST-SID or GST-alone. In the top panel of Figure 4.15 (B) full-length CAS is expressed to high levels as it migrates at the expected size (~100Kda) and it does not bind to GST-beads alone. However, in the middle panel, full-length CAS is expressed but it does not bind to GST-SID in this system. To confirm that the experimental conditions were correct, lysates from cells that were transfected with SRC1, a coactivator known to bind to CBP-SID, were incubated with GST-SID. The bottom panel of Figure 4.15 (B) demonstrates that SRC1 is expressed and does bind to bacterially expressed GST-SID.

While yeast 2-hybrid and colocalisation experiments indicate association of CAS-N and CBP, we were unable to detect direct binding of these proteins in GST and IP experiments. This may indicate a) yeast 2-hybrid results are artificial; b) post-translational modifications are absent in the IP experiments; c) the strength of interaction is weaker than that of CBP-SRC1 or d) additional proteins are necessary.

4.13 Co-immunoprecipitations do not detect an interaction between CBP and CAS *in vivo*

In another approach to investigate the interaction between CBP-SID and CAS *in vitro* we decided to carry out a co-immunoprecipitation (Co-IP) of the full-length proteins as the interaction may be dependent on other domains or correct folding of the truncated protein. We also tested whether the presence of TSA had any effect on the interaction between CAS and CBP *in vivo*.

HEK293 were either untransfected (-/+ TSA), transfected with expression vectors for CBP and FLAG-CAS (-/+ TSA) or transfected with expression vectors for CBP and FLAG-SRC1. The cells were incubated for 30hrs prior to the addition of 10 μM TSA and incubated for a further 18 hours before lysis. The Co-IPs were using α-CBP(A22) and carried out as described (section 2.5.2) and the samples were resolved by SDS-PAGE gels before western blotting with α-CBP (A22) 1/500 or α- FLAG 1/100. Figure 4.16 shows that CBP is detected in all input lanes and is immunoprecipitated in all the samples either transfected or untransfected. In addition, treatment with TSA increases the levels of endogenous CBP and overexpressed CBP which may be due to an increase in CBP expression in TSA-dependent manner. The positive control SRC1 is co-immunoprecipitated which suggests that the conditions for the interaction were optimal for this interaction. CAS is also detected in all the input lanes and it appears that it is immunoprecipitated when CBP and CAS are overexpressed. However, CAS and CBP Co-IP in the control sample in which an unspecific LexA antibody is used in the IP reaction. Therefore, due to the high background caused by binding of CAS to the protein A/G beads, we cannot be sure if the interaction between CBP and CAS is specific.

4.14 HDACi treatment of COS-1 cells induces accumulation of Impα at the nuclear periphery

As we had shown that HDACi perturbed the localisation of CBP and CAS we carried out immunofluorescence experiments to assess the effect of HDACi on Impα localisation.

COS-1 cells were either untreated, treated with increasing concentrations of TSA (1μM, 5μM, 10μM) and NaB (5mM, 10mM, 20mM) or vehicle. After 18 hours the cells were harvested and the endogenous proteins visualised by indirect immunofluorescence with antibodies raised against CBP and Impα. Endogenous Impα proteins gave a diffuse cytoplasmic and nuclear stain with a higher concentration of the protein localising to the nuclear envelope. As the TSA (Figure 4.17) and NaB (Figure 4.18) concentration increased Impα became more concentrated at the nuclear envelope. Co-staining for endogenous CBP revealed that some of these CBP foci colocalised with Impα at the nuclear periphery as shown by the high magnification insets.

Therefore, it is clear that HDACi perturb the subcellular localisation of endogenous CBP, CAS and Impα proteins and cause the partial colocalisation of CBP and Impα at the nuclear periphery.

4.15 CBP overexpression leads to the accumulation of endogenous Impα at the nuclear periphery

As a block in HDAC activity induced the accumulation of endogenous Impα at the nuclear periphery, we determined if overexpression of CBP had a similar effect to TSA on the subcellular localisation of Impα. COS-1 cells were seeded on 22mm coverslips and transfected with an expression vector encoding CBP. The cells were incubated for 48 hours prior to being

fixed and double immunostained with antibodies raised against CBP and Impα. Figure 4.19 shows that overexpressed CBP forms nuclear foci which we have shown to be adjacent to PML bodies (Chapter 3). Impα appears to accumulate more strongly at the periphery which is reminiscent to its subcellular localisation in TSA treated cells. Therefore, these results demonstrate that an increase in global acetylation levels induced by HDACi or overexpression of CBP leads to an increase in the accumulation of Impα at the nuclear periphery.

4.16 Association of CBP and Impα *in vivo*

Previous reports have demonstrated that CBP acetylates lysine-22 of Impα *in vitro* (Bannister *et al.*, 2000) while overexpression of p300 leads to the acetylation of Impα *in vivo* (Wang *et al.*, 2004). However, these reports did not address whether Impα associates with CBP *in vivo* and if this association is dependent on cellular acetylation levels. Thus we investigated biochemically whether CBP and Impα were in a complex together and if TSA promoted an association between the two proteins *in vivo* by co-immunoprecipitation.

HEK293 cells were either untransfected or transfected with expression constructs for CBP and Impα and either untreated or treated with 10μM TSA 18hrs prior to harvesting. CBP and Impα were detected in all the input samples. However, an Impα species (represented with *) that migrated slower than the main band was observed in samples where CBP was co-transfected or TSA treated. Based on the experiments carried out by Bannister *et al.* (2000) we suspect this band may be a hyperacetylated form of Impα. CBP was immunoprecipitated from whole cell lysates with α-CBP(A22) coupled to agarose protein A/G beads and western blot analysis was carried out to determine if Impα was co-immunoprecipitated. Figure 4.20 shows that CBP was detected in the input lanes and immunoprecipitated in all the samples, except the α-LexA

negative control sample. Immunoblotting with α-Impα showed that Impα associated with CBP *in vivo* and that this association increased on treatment with TSA. Moreover, CBP associated with the lower Impα species suggesting that CBP preferentially binds hypoacetylated Impα. CBP and Impα did not unspecifically associate in the α-LexA negative control samples. I have also shown, as a positive control, that CBP associated with SRC1.

4.17 Colocalisation of overexpressed CBP and Impα at the nuclear periphery is increased on TSA treatment

As we had demonstrated that overexpressed CBP and Impα were in a complex together and their association increased on TSA treatment we wanted to determine whether they colocalised *in vivo*. COS-1 cells were seeded 22mm coverslips and transfected with an expression vector encoding Impα or co-transfected with expression vectors encoding CBP and Impα. 30 hours post-transfection the cells were either untreated, treated with vehicle or treated with 10μM TSA and incubated for a further 18 hours. The cells were then fixed and double immunostained with antibodies raised against CBP and Impα. As shown in Figure 4.21 overexpressed Impα is a diffuse nuclear protein with a proportion of the protein accumulated in foci which do not colocalise with CBP foci. Interestingly, the levels of nuclear CBP appear to be similar to the levels in untransfected cells suggesting that Impα is not an import factor for CBP. In cells co-expressing CBP and Impα, CBP forms large nuclear foci while Impα displays a nuclear diffuse pattern with a large population of the protein accumulating in nuclear aggregates which associate with the periphery of the nucleus. These aggregates appear to partially colocalise with CBP foci which is in agreement with the Co-IP data. However, in TSA treated cells the diffuse and aggregated populations of Impα proteins associate more strongly with the nuclear periphery. Similarly, a large proportion of the CBP proteins associate with the nuclear periphery and there is

a stronger colocalisation with Impα proteins. This is consistent with the increased interaction between CBP and Impα in TSA treated cells via Co-IP.

4.18 Chapter summary

CBP interacts with a large number of cellular proteins through multiple domains such as CH1, KIX, CRD1, LXXLL motifs and the SID domain. In this study we have identified the nuclear export factor CAS and the nucleoporin, NUP93 as novel CBP-SID binding proteins. The nuclear export factor CAS mediates the nucleo-cytoplasmic shuttling of Impα in a RAN-dependent manner and has been implicated in apoptosis and cell proliferation and gene expression (Kutay *et al.*, 1997, Brinkmann *et al.,* 1995, Casolari *et al.,* 2004). CBP-SID mediates the binding with a large number of proteins such as the p160s, Ets-2, viral proteins and IRF-3 mainly through leucine-rich amphipathic α-helices (Sheppard *et al.*, 2003, Matsuda *et al.,* 2004, Lin *et al.,* 2001). Structural studies of ACTR and SRC-1 in complex with the SID have shown that they form a tight 4-helix bundle (Demarest *et al.,* 2002, Waters *et al.,* 2006). Mutation of conserved leucine residues within the SID have been shown to abrogate binding with SRC-1, ACTR and Ets-2 proteins. Interestingly, we found that the minimal SID was necessary for binding to CAS and that mutation of conserved leucine residues forming part of the LXXLL motif abrogated binding with CAS. This suggests that SID binding proteins such as CAS may share a common mode of binding with the SID although subtle differences remain between the various binding proteins.

Recently, the structure of the yeast homologue of CAS, CSE1, which also mediates the export of yeast Impα, Srp1p to the cytoplasm, was elucidated. Both CSE1 and the importins are HEAT (Huntingtin, elongation factor 3, A subunit of PP2A, and TOR) repeat containing proteins (Matsuura *et al.,* 2005, Cook *et al.,* 2005). HEAT repeats are tandemly arranged curlicue-like proteins that act as molecular scaffolds on which other proteins can assemble. They have been found in condensins and cohesions-associated proteins which are involved in the structural maintenance of chromosomes, such as the TBP-associated protein TIP120 and the budding yeast Mot1p, which is member of the Swi2/Snf2 family of chromatin remodellers (Neuwald *et al.*, 2000). CSE1 HEAT repeats 1-8 form the N-terminal domain while HEAT repeats 13-20 form the C-terminal binding domain and these are separated by a flexible hinge region. In its cargo-free state the N- and C-terminal domains of CSE1 form an arch-like structure preventing the association of RANGTP and Impα. However, upon cargo binding a major conformational change occurs at a hinge region located in HEAT repeat 8 which connects the Impα and RANGTP binding sites and is essential for the association of the three proteins (Cook *et al.*, 2005). Interestingly, amino acids 1-350 of CAS which correspond to HEAT 1-8 were identified in the yeast 2-hybrid screen for CBP-SID interacting proteins. In addition, deletion of a conserved leucine-rich motif which lies within HEAT 6A and the adjacent hinge-region leads to a loss of CBP-SID binding. This region is potentially solvent-exposed and lies close to the flexible HEAT 8, suggesting a role for this region in mediating the binding with CBP-SID. Furthermore, CAS contains a leucine-rich motif resembling the Sα1 helix of SRC-1 which forms a part of a stable 4-helix bundle with the SID (Waters *et al.*, 2006). Mutation of these residues within SRC-1 also abrogated with the SID. This may also suggest that CAS binds to the SID in a similar manner to other SID binding proteins.

The deacetylation of the N-terminal tails of histones was postulated to be the primary role of HDACs in the mammalian cell. The aberrant recruitment of HDACs to gene promoters has been implicated in the pathogenesis of leukemias expressing PML-RAR, PLZF-RAR and the AML1-ETO fusion proteins. HDACi are therefore used to good effect in the treatment of many solid and liquid tumours. While the mode of action is unknown it is predicted to be mediated through an increase in global acetylation levels and the concomitant increase in gene expression.

However, recent evidence suggests that HDACi may act partly through the modulation of non-histone proteins. Deacetylation has been shown to be crucial in regulating the subcellular localisation and function of many non-histone proteins such as p53, Ku70, ACTR and Impα among others (Kalkhoven, 2004). p300 and CBP have been shown to acetylate Impα *in vivo* and *in vitro* respectively (Bannister *et al.*, 2000). Kouzarides, (2000) postulated that acetylation of Impα played a role in regulating the nucleo-cytoplasmic shuttling of Impα. We have shown that blocking acetylation, using the HDACi TSA and NaB, leads to the change in the subcellular localisation of endogenous CAS proteins. However, we could not detect an interaction between CBP and CAS in extracts from mammalian cells or *in vitro* which suggests that either the conditions were suboptimal, the interaction is transient or essential cofactors were not present. Interestingly, two of the leucine residues deleted in CAS, which were part of the leucine-rich motif necessary for interaction with CBP-SID, were shown to be buried and unavailable for binding in the homologous CSE1. However, one of these leucines becomes available for binding when CSE1 is in a complex with Impα and RANGTP (Figure 4.22 and Figure 4.23). Therefore, it may not be possible to detect the interaction between CAS and CBP unless the complex was properly formed.

Treatment of cells with HDACi led to the accumulation of endogenous Impα at the nuclear periphery while endogenous CAS proteins appeared to aggregate in nuclear foci. Similarly, overexpression of CBP which should also lead to an increase in global protein acetylation levels had a similar effect on endogenous Impα proteins. In addition, overexpression of Impα and CBP and treatment with HDACi lead to an apparent increase in their *in vivo* interaction. These results suggest that acetylation plays a critical role in regulating the subcellular localisation of nuclear transport proteins and may affect the nucleo-cytoplasmic shuttling of

crucial proteins necessary in oncogenesis. Furthermore, it suggests that HDACi may target non-histone proteins to mediate their effect on cancer cells.

PML bodies have been implicated in apoptosis, cellular senescence and leukaemogenesis. PML bodies were originally shown to be disrupted into microspeckles in patients expressing the leukemic fusion protein PML-RARα (Weis *et al.,* 1994). In addition, PML-RARα also leads to the mislocalisation of HDACs to retinoic acid response elements (RARE). These are implicated in the pathology of AML which can be treated with high doses of ATRA and HDACi (Weis et al., 1994, Warrell *et al.,* 1998). Interestingly, we found that HDACi gave rise to an increase in PML body number; however, the PML bodies did not display a microspeckled pattern. Moreover, PML body number is known to increase during S-phase (Dellaire *et al.,* 2006) while TSA has been shown to mediate a block in the cell-cycle in S-phase (Papeleu *et al.,* 2003; Toth *et al.,* 2004). This suggests that HDACi may have an indirect effect on PML body number by mediating a block in S-phase. However, we cannot discount the fact that HDACi may also effect their action by regulating the function of PML body-associated proteins and thus cause an increase in the number and size of PML bodies.

From the yeast 2-hybrid screen we also identified the N-terminal 165 amino acids of NUP93 as a novel CBP-SID binding protein. While we did not confirm the interaction between full-length CBP and NUP93, it is interesting to note that NUP93 localises to the nuclear basket of the NPC. The basket contains other NUPs such as NUP98 and NUP153 which have also been shown to interact with CBP via conserved FG repeats which form hydrophobic interactions similar to leucine-rich motifs (Kasper *et al.,* 1999). Indeed, CBP interacts with the N-terminus of NUP98 when it forms part of the NUP98-HOXA9 oncogenic fusion protein expressed in AML patients with the translocation t(7;11)(p15;q15). The FG repeats are required for the transformation of NIH-3T3 cells (Kasper *et al.,* 1999). In addition, Bai *et al.* (2006) demonstrated that the FG-repeats from NUP98 when part of the NUP98-PMX1 and NUP98-HOXC11 leukemic fusion proteins were interchangeable and exhibited dual binding with CBP and HDAC1. This enabled the fusion proteins to act as both trans-activators and trans-repressors and treatment of cells expressing the NUP98-PMX1 fusion protein with TSA mediated a release in transcriptional repression.

Interestingly, recent studies in yeast have shown a direct link between the nuclear periphery, the NPC and gene expression. Ishii *et al.* (2002) demonstrated that CSE1 and the Srp1p, the yeast homologue of Impα, displayed boundary activity that prevented the spread of heterochromatin into the active gene. This was achieved by the tethering of the heterochromatin to the NPC which was mediated through CSE1 and Srp1p binding to NUP2p. Deletion of *nup2* resulted in a loss of boundary activity, highlighting a role for the NPC in gene expression. Further studies, using genomic location analysis, revealed that CSE1, Srp1p, Nup93 along with other nucleoporins and karyopherins associated with highly transcribed genes in *S. cerevisiae*. Interestingly, active genes were shown to localise to the nuclear periphery and the NPC where they associated with SAGA, the histone acetyltransferase complex (Cabal *et al.*, 2006, Taddei *et al.*, 2006). In addition, interference with the ability of these genes to localise to the nuclear periphery resulted in a loss of transcriptional activation (Taddei *et al.*, 2006) but it is not known whether similar mechanisms are present in mammalian cells. Furthermore, it is now believed that genes which need to be rapidly transcribed such as the heat-shock proteins during stress, localise to the periphery of the mammalian nucleus, which is in agreement with the 'gene gating' hypothesis put forward by Blobel, (1986), (Dejean, personal communication).

Chapter 5

To investigate the effect of ARpolyQ expression on the subcellular localisation of CBP and its interacting proteins

5.1 Introduction

Neurodegenerative diseases such as Huntington disease (HD), Kennedy disease (spinal and muscular bulbar atrophy, SMBA) and 6 spinocerebellar ataxias are associated CAG expansions which are translated as poly-glutamine (poly-Q) expansions. These diseases are characterised by the aggregation of poly-Q proteins such as Huntington (htt) protein in Huntington's chorea, and the AR in SMBA. It has been reported that Q-rich proteins can co-aggregate with other poly-Q proteins such as CBP, which has an 18 glutamine stretch in the carboxy terminus, although, it remains unclear whether aggregation of proteins has a role in the pathogenesis of the diseases.

The Htt protein binds CBP poly-Q and this aggregation mislocalises CBP and impairs CBP regulated gene transcription. Nucifora *et al.* (2001) reported that CBP was mislocalised in HD transgenic mice, HD cell culture model and in HD human post-mortem brain. It was demonstrated that htt-mediated neurodegeneration in *Drosophila* in which CBP was mislocalised could be reversed by overexpression of CBP, thereby rescuing poly-Q induced neuronal toxicity. Furthermore, progression of the neurodegenerative phenotype could be halted by treatment with HDAC inhibitors, suggesting that CBP HAT function is essential in the prevention of some neurodegenerative diseases.

Kennedy's disease (X-linked spinal and bulbar muscular atrophy) is a late onset rare inherited disease that is characterised by progressive muscular weakness and atrophy. Like Huntington's disease it is associated with an expansion of polymorphic CAG repeat sequence but in the first exon of the gene encoding the AR. In the normal population the CAG repeat region ranges from 12 to 30 but in patients with Kennedy's disease, the repeats range from 40 to 70 (Butler *et al.*, 1998). AR with an expanded polyglutamine tract has been shown to sequester heat-shock proteins, proteasomal subunits and SRC-1 (Stenoien *et al.*, 1999). McCampbell *et al.*

(2001) reported that CBP was mislocalised in the mouse neuronal cell line MN1 expressing mutant AR. Furthermore, they demonstrated that GAL4-CBP dependent transcription could be impaired by expression of a constitutive AR bearing a 119 glutamine stretch (McCampbell *et al.*, 2000). In a *Drosophila* model of Kennedy's disease it was shown that retinal degeneration and altered histone H4 acetylation levels and transcription could be rescued by CBP (Taylor *et al.*, 2003). However, contrasting reports suggest that CBP is not mislocalised by polyQ inclusions but is degraded by the ubiquitin proteosome pathway (Jiang *et al.*, 2003). In addition, Sopher *et al.* (2004), using samples from transgenic mice expressing either AR wild-type or ARQ100 demonstrated that ARpolyQ interacts with CBP with much higher affinity than wild-type AR. Interestingly, in the affected parts of the brain, such as the motor neurons, the presence of AR aggregates could not be detected. Oral administration of the HDACi, sodium butyrate, to transgenic SMBA mice, ameliorated neurological phenotypes and increased acetylation of histones (Minamiyama *et al.*, 2004).

This chapter describes an investigation to test whether CBP and its interaction proteins are mislocalised in cells expressing the mutant form of the AR with an expanded polyQ tract. The effect of the polyQ expansion on the transcriptional activity of AR and coactivation by CBP is also examined.

5.2 AR polyQ expression perturbs the subcellular localisation of endogenous CBP and PML in a ligand dependent manner

Several reports have suggested that CBP and other co-activators are mislocalised by proteins containing an expanded polyglutamine repeat. Thus, we examined if CBP and PML proteins are mislocalised in cells expressing a mutant AR with an expanded polyglutamine tract. COS-1 cells were seeded on 100mm dishes in DMEM containing dextran/charcoal stripped FCS, to remove all AR ligands, and transfected after 24 hours with expression vectors encoding GFP-AR wild-type (containing 24 glutamine residues, GFP-ARwt) or GFP-AR mutant (containing 77 glutamine residues, GFP-ARQ77). 24 hours post-transfection the cells were either treated with vehicle ethanol or 10^{-8}M Mibolerone, a synthetic analogue of testosterone. 48 hours post-transfection the cells were fixed, permeabilised and stained for endogenous CBP using rabbit anti-CBP and anti-rabbit Alexa 594 or for endogenous PML using rabbit anti-PML (Sigma) and anti-rabbit Alexa 594 and imaged via laser scanning confocal microscopy. Figure 5.1 shows that in vehicle treated control cells, GFPARwt displays a diffuse cytoplasmic distribution in 100% of cells analysed. Similarly, GFP-ARQ77 gives a diffuse cytoplasmic staining but 10% of cells contain cytoplasmic aggregates (Figure 5.2). Under these conditions endogenous CBP was present in PML bodies in untreated cells expressing either GFP-ARwt or GFP-ARQ77.

On treatment with ligand, GFP-ARwt localised to the nucleus and displayed a diffuse pattern of staining in ~83% of cells. However, approximately ~17% of cells displayed a nuclear diffuse pattern of staining although a proportion of this population associated in nuclear aggregates (Figure 5.1 and data not shown). However, CBP did not appear to be mislocalised in cells expressing GFP-ARwt. GFP-ARQ77 expression led to a greater variation in phenotypes in ligand treated cells. In 33% of cells GFP-ARQ77 was nuclear and diffuse while the number of CBP foci appeared to be increased and microspeckled. 25% of cells displayed a nuclear and diffuse staining with a proportion of the proteins associated in nuclear aggregates. In these cells a proportion of the CBP foci were found adjacent to nuclear aggregates. In 42% of cells imaged GFP-ARQ77 displayed a nuclear and diffuse pattern of staining with a subset of the population forming nuclear foci and another associating in cytoplasmic aggregates. In addition, CBP was not mislocalised to the cytoplasm but a proportion of the CBP foci were found adjacent to the GFP-ARwt nuclear aggregates (Figure 5.1, Figure 5.2, Figure 5.3). Interestingly, CBP was shown to be mislocalised to intranuclear inclusions in a transgenic mouse model of Huntington's disease

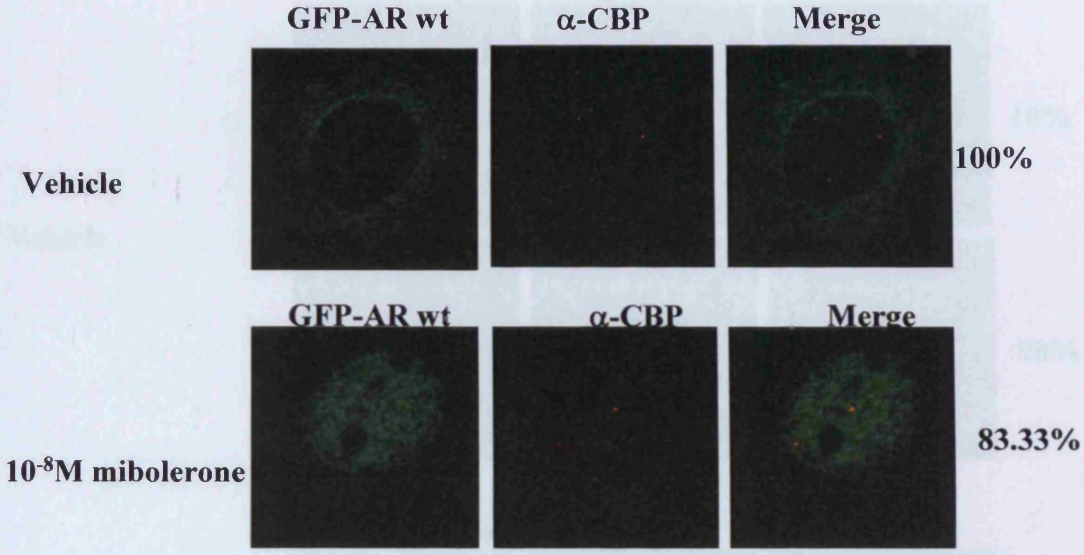

Figure 5.1 Subcellular localisation of GFP-ARwt and endogenous CBP in COS-1 cells. COS-1 cells were seeded on 22mm coverslips at 1 x 10^5 confluency, grown in DMEM with charcoal/dextran stripped FCS and after 24 hours were transfected with GFP-ARwt. 24 hours post-transfection the cells were either treated with vehicle ethanol or treated with 10^{-8}M mibolerone for 24 hours prior to fixation in 4% paraformaldehyde. The cells were permeabilised and stained with antibodies raised against rabbit anti-CBP (red) followed by anti-rabbit Alexa594 conjugated secondary. The % of cells of the total population with that the phenotype is displayed to the right of the images.

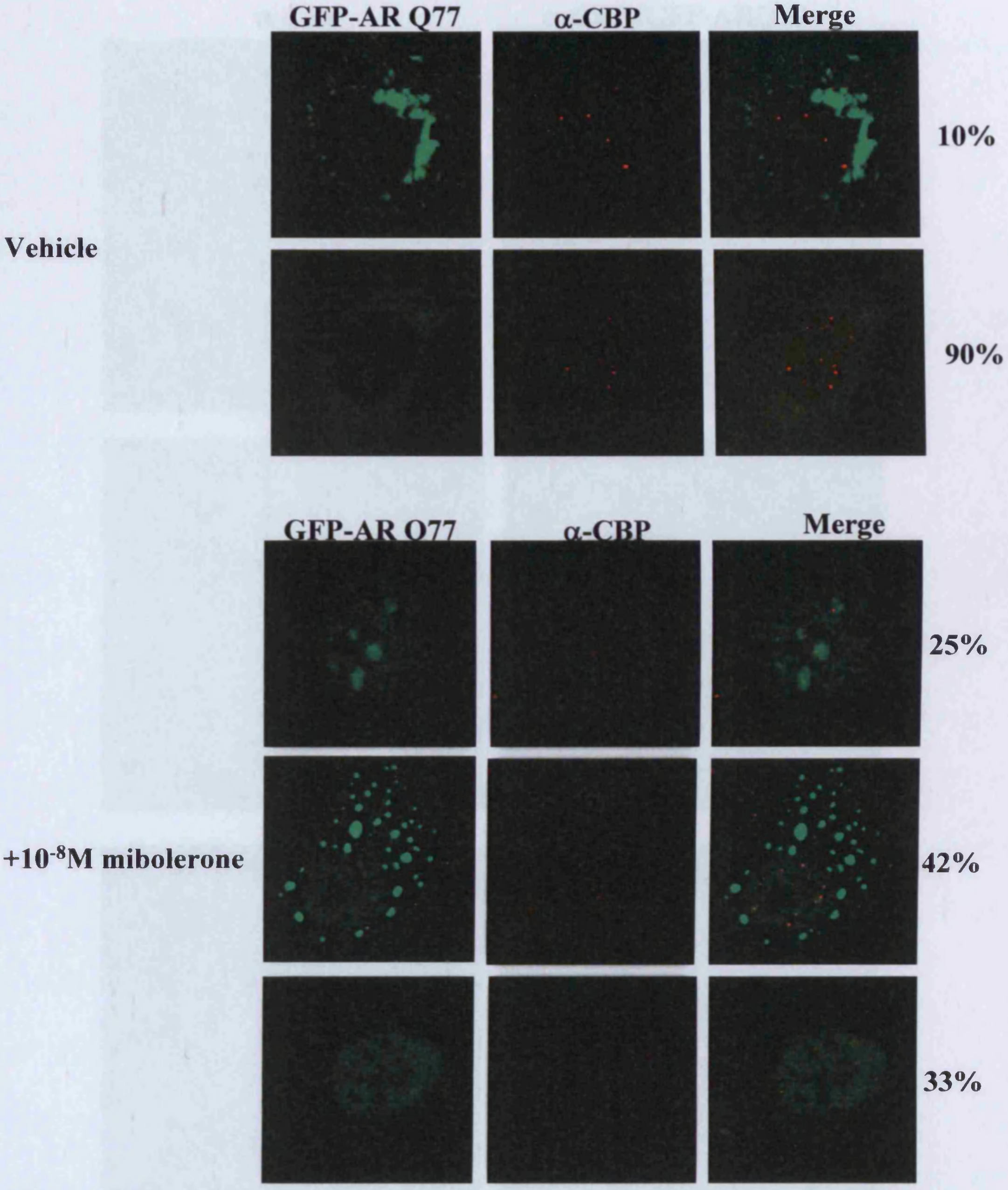
GFP-AR Q77
α-CBP
Merge
10%
Vehicle
90%
GFP-AR Q77
α-CBP
Merge
25%
+10-8M mibolerone
42%
33%

Figure 5.2 Subcellular localisation of GFP-ARQ and endogenous CBP in COS-1 cells. COS-1 cells were seeded on 22mm coverslips at 1×10^5 confluency, grown in DMEM with charcoal/dextran stripped FCS and after 24 hours were transfected with GFP-ARwt. 24 hours post-transfection the cells were either treated with vehicle ethanol or treated with 10^{-8}M mibolerone for 24 hours prior to fixation in 4% paraformaldehyde. The cells were permeabilised and stained with antibodies raised against rabbit anti-CBP (red) followed by anti-rabbit Alexa594 conjugated secondary. The % of cells of the total population with that the phenotype is displayed to the right of the images.

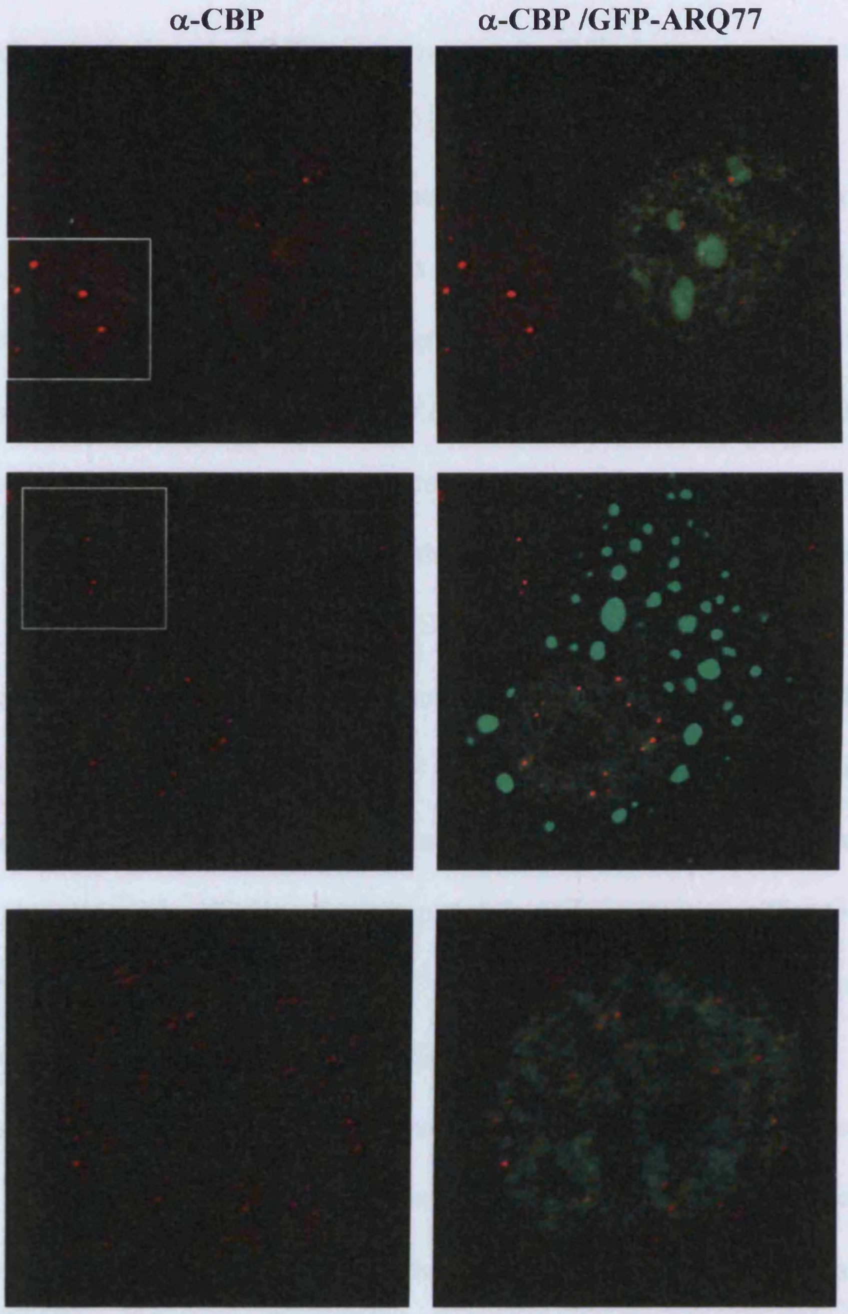

Figure 5.3 GFP-ARQ perturbs the subcellular localisation of endogenous CBP in COS-1 cells. COS-1 cells were seeded on 22mm coverslips at 1 x 10^5 confluency, grown in DMEM with charcoal/dextran stripped FCS and after 24 hours were transfected with GFP-ARQ. 24 hours post-transfection the cells were treated with 10^{-8}M mibolerone for 24 hours prior to fixation in 4% paraformaldehyde. The cells were permeabilised and stained with antibodies raised against rabbit anti-CBP (red) followed by anti-rabbit Alexa594 conjugated secondary antibody. White boxes represent untransfected control cells.

(Steffan *et al.,* 2000). Furthermore, McCampbell *et al.,* (2000) demonstrated that CBP was mislocalised to nuclear inclusions in MN1 (mouse neuronal cell line), transgenic mice and tissue from patients with SMBA.

An expanded polyglutamine tract within the Spinocerebellar ataxia 3 (SCA3)/Machado-Joseph Disease (MJD) protein is implicated in the disease pathology. While the molecular mechanisms of SCA3 are largely unknown it has been shown that it displays many of the features of polyglutamine diseases (Chang *et al.,* 2005). Yasuda *et al.* (1999) demonstrated that SCA3 protein containing a repeat of 79 glutamine residues formed intranuclear inclusions which colocalised with PML bodies. Therefore, the effect of GFP-ARQ77 expression on the integrity of PML bodies was investigated. In COS-1 cells expressing GFP-ARwt, endogenous PML was found to localise to PML bodies and there was no evidence to suggest that the PML body number or structure was perturbed (Figure 5.4 and Figure 5.5). However, in cells expressing GFP-ARQ77, endogenous PML displayed a similar pattern of staining to endogenous CBP. It is clear that PML is also not mislocalised to the cytoplasm in cells expressing either GFP-ARwt or GFP-ARQ77 (Figure 5.5). However, PML body number increased and they appeared much smaller in size compared to cells expressing GFP-ARwt.

Many of the PML microspeckles were found adjacent to GFP-ARQ77 nuclear aggregates which is similar to that observed for endogenous CBP. Interestingly, the pattern of PML distribution in these cells is similar to the subcellular localisation of PML in cells from AML patients expressing the PML-RARα fusion protein. Expression of PML-RARα results in the mislocalisation of PML bodies into microspeckles which is implicated in the pathology of AML. In addition, a common feature of viral infection or interferon treatment is disruption of PML bodies. Muller *et al.,* (1999) demonstrated the disruption of PML bodies in Hela cells expressing the Cauliflower Mosaic Virus IE1 protein. These results suggest that ARQ-mediated disruption of PML bodies may play a role in the pathogenicity of SMBA.

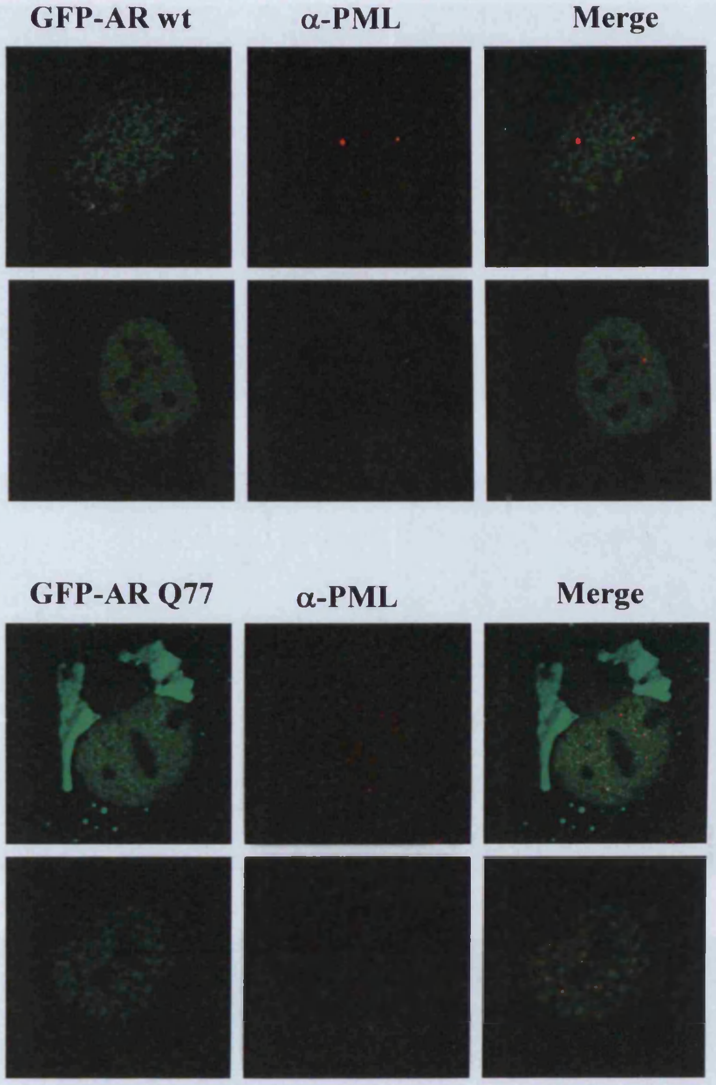

Figure 5.4 Subcellular localisation of GFP-ARwt, GFP-ARQ and endogenous PML in COS-1 cells. COS-1 cells were seeded on 22mm coverslips at 1 x 10^5 confluency, grown in DMEM with charcoal/dextran stripped FCS and after 24 hours were transfected with GFP-ARwt or GFP-ARQ. 24 hours post-transfection the cells were treated with 10^{-8}M mibolerone for 24 hours prior to fixation in 4% paraformaldehyde. The cells were permeabilised and stained with antibodies raised against rabbit anti-PML (red) followed by anti-rabbit Alexa594 conjugated secondary.

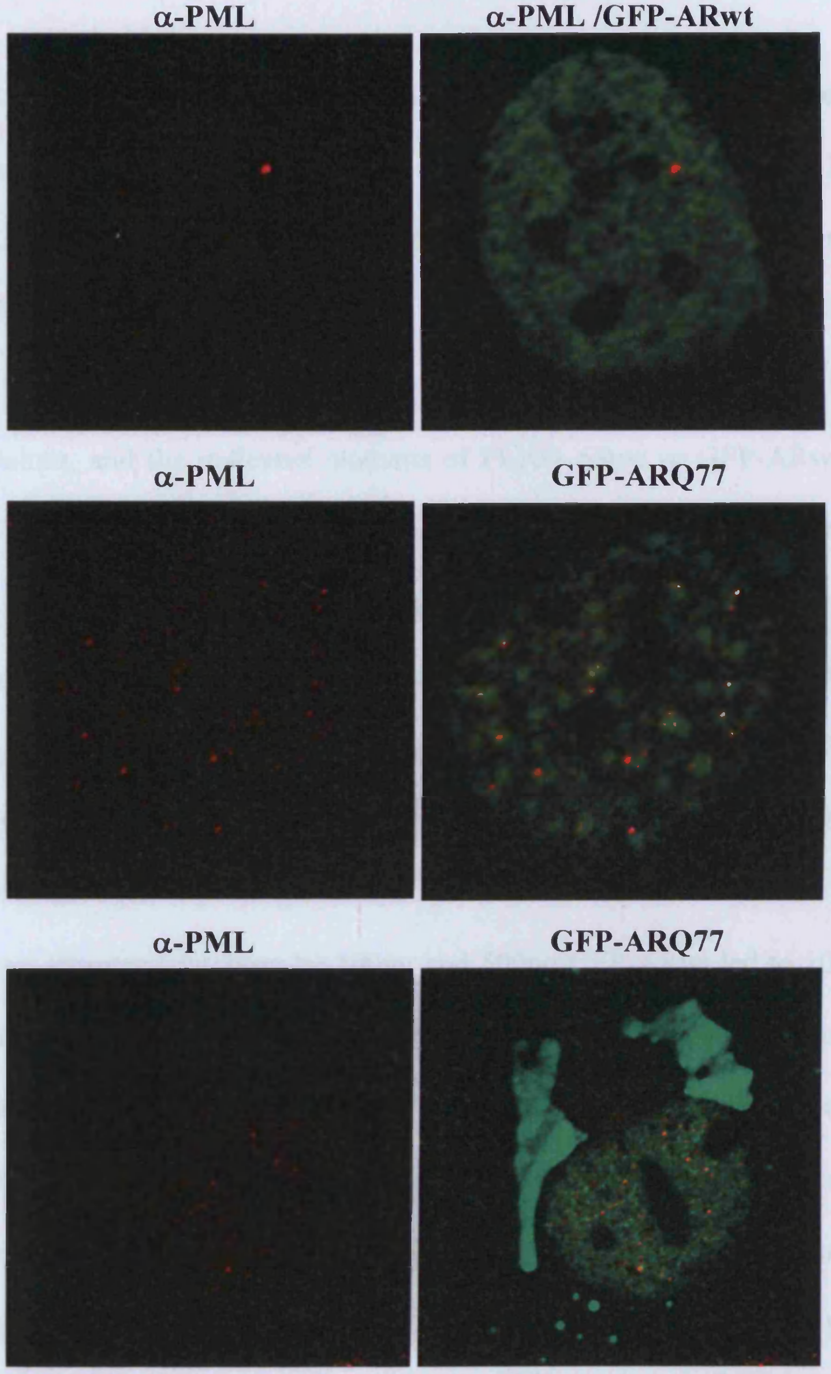

α-PML

α-PML /GFP-ARwt

α-PML

GFP-ARQ77

α-PML

GFP-ARQ77

Figure 5.5 GFP-ARQ expression perturbs PML bodies in COS-1 cells. COS-1 cells were seeded on 22mm coverslips at 1 x 10^5 confluency, grown in DMEM with charcoal/dextran stripped FCS and after 24 hours were transfected with GFP-ARwt or GFP-ARQ. 24 hours post-transfection the cells were treated with 10^{-8}M mibolerone for 24 hours prior to fixation in 4% paraformaldehyde. The cells were permeabilised and stained with antibodies raised against rabbit anti-PML (red) followed by anti-rabbit Alexa594 conjugated secondary antibody.

5.3 FLAG-ARwt and GFP-ARwt activate transcription of a reporter gene construct

To determine if FLAG or GFP-tagged proteins can mediate a normal ligand-dependent response, HEK293 cells were transfected with the AR-responsive MMTV luciferase reporter (gift from C. Bevan). HEK293 cells were seeded in 12 well plates and transfected after 24 hours with 500ng MMTV-luc reporter, 100ng of pCH110 β-galactosidase, which allowed for normalisation of luciferase values, and the indicated amounts of FLAG-ARwt or GFP-ARwt. The cells were incubated for 24 hours and either treated with vehicle ethanol or 10^{-8}M mibolerone for 24 hours. 48 hours post-transfection the luciferase and β-galactosidase activities were measured in duplicate for each cell-free lysate and the Relative Luciferase Activities (RLA) determined for each condition. As shown in Figure 5.6, the RLA value in the absence of transfected AR or CBP was set at 1. FLAG-AR induced MMTV-reporter activity in response to ligand by ~125-150 fold. At the higher amount of transfected plasmid, no further increase was observed.

However, reporter activation by 100ng and 500ng GFP-ARwt led to 10-35 fold increase in reporter activity although the reason for this lower activity is unclear. This suggests that either the GFP-moiety may interfere with the ability of the AR to activate the reporter or expression levels of the GFP-tagged and FLAG-tagged constructs differed. However, the results demonstrate that AR proteins can activate the MMTV reporter in a ligand-dependent fashion consistent with those of Metzger *et al.* (2003) who demonstrated the activation of MMTV-luc by exogenous AR.

5.4 CBP does not rescue ARQ-mediated repression

CBP interacts with the AR and augments AR-dependent transcriptional activation *in vivo* (Aarnisalo *et al.*, 1998). CBP increased the transcriptional activity of a mutant AR devoid of the ligand-binding domain and residues 38-296, which encompasses the glutamine tract. These

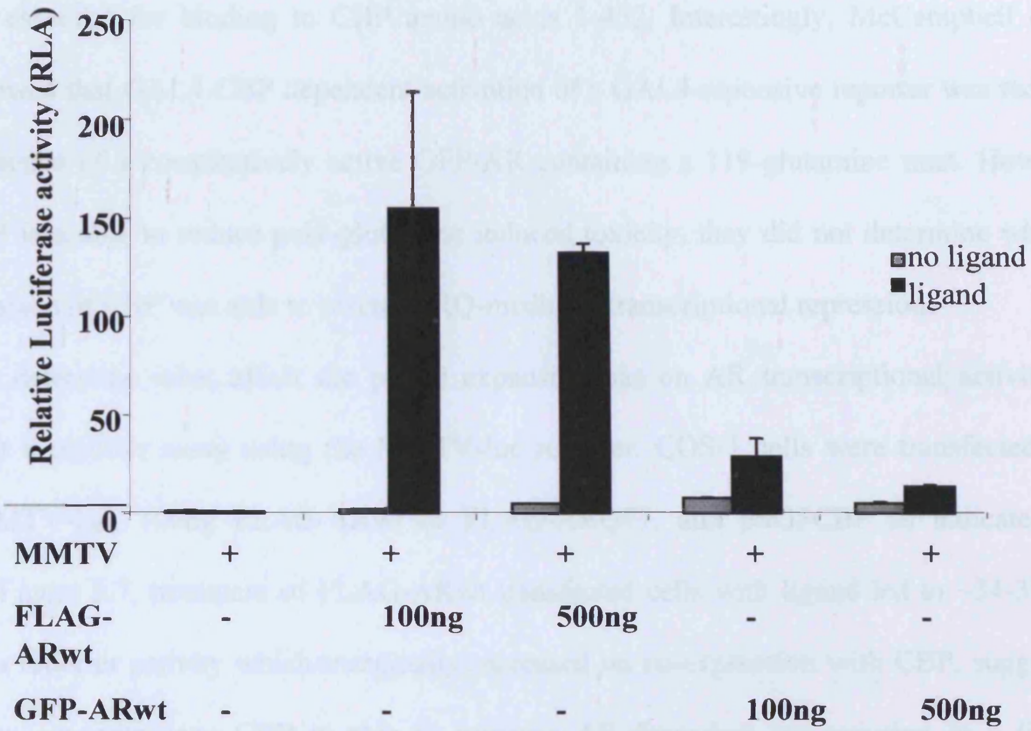

Figure 5.6 FLAG-ARwt and GFP-ARwt activate the MMTV-luc reporter in HEK293 cells. HEK293 cells were grown for 24 hours in DMEM containing charcoal/dextran stripped FCS and transfected in triplicate with 100ng pCH110 β-galactosidase reporter, 500ng MMTV-luc reporter and the indicated amounts of either FLAG-ARwt or GFP-ARwt. The cells were either treated with vehicle ethanol or 10^{-8}M mibolerone for a further 24 hours prior to lysis and the luciferase and β-galactosidase levels measured via a dual assay. The luciferase: β-galactosidase ratios were calculated and plotted as Relative Luciferase Activity (RLA) with the ratio for the reporters MMTV-luc and pCH110 without ligand set to a value of 1. The S.E.M are represented by error bars.

results were re-iterated by Fronsdal *et al.* (1998) who determined that the AR amino acids 333-503 were essential for binding to CBP amino acids 1-452. Interestingly, McCampbell *et al.* (2000) showed that GAL4-CBP dependent activation of a GAL4-reponsive reporter was reduced in the presence of a constitutively active GFP-AR containing a 119-glutamine tract. However, while CBP was able to reduce poly-glutamine induced toxicity, they did not determine whether overexpression of CBP was able to rescue ARQ-mediated transcriptional repression.

To determine what affect the polyQ expansion has on AR transcriptional activity we carried out a reporter assay using the MMTV-luc reporter. COS-1 cells were transfected with 500ng MMTV-luc, 100ng FLAG-ARwt or FLAG-ARQ77, and pSG5CBP as indicated. As shown in Figure 5.7, treatment of FLAG-ARwt transfected cells with ligand led to ~34-38-fold increase in reporter activity which marginally increased on co-expression with CBP, suggesting that at low concentrations CBP is able to increase AR-dependent transcription in a ligand-dependent manner. However, cells transfected with FLAG-ARQ77 only led to ~7-fold activation of the reporter in a ligand-dependent manner and the inability to activate reporter activity was not rescued by overexpression of CBP. In addition, vehicle treated cells led to ~5-8-fold increase in reporter activity under all conditions.

These results show that ligand-dependent ARwt activation of MMTV-luc can be increased by co-expression of CBP. However, CBP overexpression did not rescue the weak activity of ARQ77 on this promoter and the mechanism remains unclear.

5.5 CBP does not rescue ARQ77-mediated transcriptional repression in SY-5Y cells

Studies of ARpolyQ function have focused on cell lines such as HEK293 and COS-7 (Becker *et al.,* 2000). However, neuronal cell lines are more physiologically relevant as Kennedy's disease is primarily associated with neurodegeneration. To compare AR and ARQ77

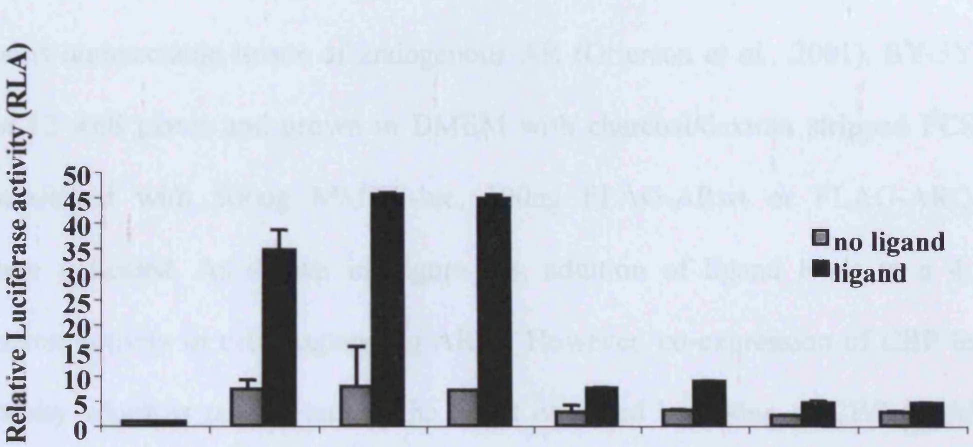

MMTV	+	+	+	+	+	+	+	+
ARwt	-	+	+	+	-	-	-	-
ARQ	-	-	-	-	+	+	+	+
CBP	-	-	10ng	20ng	-	10ng	20ng	50ng

Figure 5.7 FLAG-ARQ represses AR-dependent MMTV-luc reporter activity in COS-1 cells. COS-1 cells were grown for 24 hours in DMEM containing charcoal/dextran stripped FCS and transfected in triplicate with 100ng pCH110 β-galactosidase reporter, 500ng MMTV-luc luciferase reporter, 100ng FLAG-ARwt or FLAG-ARQ where indicated by "+" and the indicated amounts of an expression construct encoding CBP . The cells were either treated with vehicle ethanol or 10^{-8}M mibolerone for a further 24 hours prior to lysis and the luciferase and β-galactosidase levels measured via a dual luciferase assay. The luciferase: β-galactosidase ratios were calculated and plotted as Relative Luciferase Activity (RLA) with the ratio for the reporters MMTV-luc and pCH110 without ligand set to a value of 1. The S.E.M are represented by error bars

transcriptional activation in a neuronal cell line, we used the human neuroblastoma SY-5Y cell line as it contains undetectable levels of endogenous AR (Grierson *et al.,* 2001). SY-5Y cells were seeded in 12 well plates and grown in DMEM with charcoal/dextran stripped FCS. The cells were transfected with 500ng MMTV-luc, 100ng FLAG-ARwt or FLAG-ARQ, and pSG5CBP where indicated. As shown in Figure 5.8, addition of ligand leads to a 4.5-fold increase in reporter activity in cells expressing ARwt. However, co-expression of CBP led to a decrease in activity which is reminiscent to the effect observed by 500ng of CBP on AML-1-mediated transcription i.e. "squelching" (Chapter 3.24). In cells transfected with FLAG-ARQ77 there was a decrease in reporter activity compared to transfection of reporter alone. In addition, co-transfection of increasing amounts of CBP did not lead to a significant increase in reporter activity in a ligand-dependent manner. These results show that ARwt expression results in an increase in reporter activity in a ligand-dependent manner while ARQ77 expression is unable to activate the AR-responsive reporter. Furthermore, it is clear from these results that the concentrations of co-transfected CBP need to be optimised before we can determine whether it can rescue ARQ77-dependent transcription in SY-5Y cells.

5.6 AR-mediated ligand-dependent activation of a GAL4-responsive reporter

McCampbell *et al.* (2000) demonstrated that GAL4-CBP(full-length)-mediated transcription of a GAL4-responsive promoter could be repressed by expression of a constitutively active GFP-ARQ119. We used a modified version of this to determine if CBP-mediated transcriptional activation was unimpaired in cells expressing ARQ77. A GAL4-AD1 fusion protein, which contained the DNA binding domain of the yeast GAL4 transcription factor, and the activation domain of the coactivator SRC1 was used in this experiment. When expressed GAL4-AD1 acts as a potent activator of transcription by recruitment of CBP (Sheppard *et al.,*

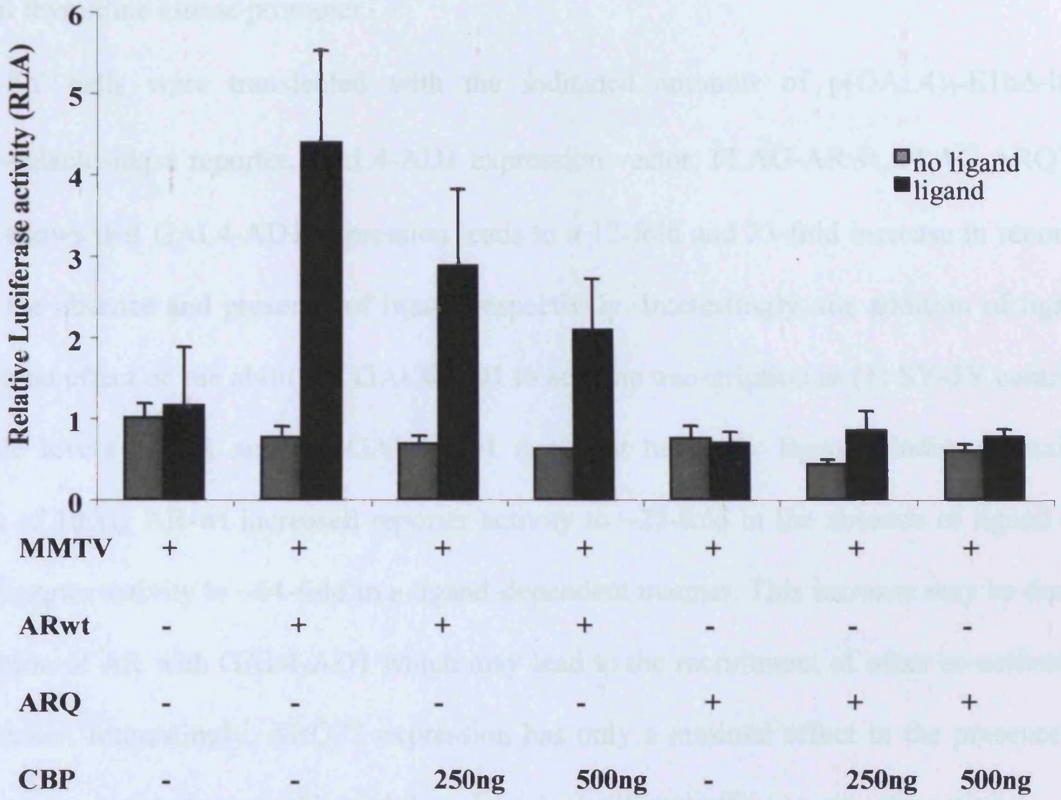

Figure 5.8 FLAG-ARQ represses AR-dependent MMTV-luc reporter activity in SY-5Y cells. SY-5Y cells were grown for 24 hours in DMEM containing charcoal/dextran stripped FCS and transfected in triplicate with 100ng pCH110 β-galactosidase reporter, 500ng MMTV-luc luciferase reporter, 100ng FLAG-ARwt or FLAG-ARQ and the indicated amounts of an expression vector encoding CBP. The cells were either treated with vehicle ethanol or 10^{-8}M mibolerone for a further 24 hours prior to lysis and the luciferase and β-galactosidase levels measured via a dual assay. The luciferase: β-galactosidase ratios were calculated and plotted as Relative Luciferase Activity (RLA) with the ratio for the reporters MMTV-luc and pCH110 without ligand set to a value of 1. The S.E.M are represented by error bars

2001) to the promoter of $p(GAL4)_5$-E1bΔ-luc, which contains 5 GAL4 binding sites upstream of the minimal thymidine kinase promoter.

SY-5Y cells were transfected with the indicated amounts of $p(GAL4)_5$-E1bΔ-luc, pCH110 β-galactosidase reporter, GAL4-AD1 expression vector, FLAG-ARwt, FLAG-ARQ77. Figure 5.9 shows that GAL4-AD1 expression leads to a 12-fold and 23-fold increase in reporter activity in the absence and presence of ligand respectively. Interestingly, the addition of ligand should have no effect on the ability of GAL4-AD1 to activate transcription as (1) SY-5Y contains undetectable levels of AR and (2) GAL4-AD1 does not have any ligand binding domains. Expression of 100ng AR-wt increased reporter activity to ~25-fold in the absence of ligand but increased reporter activity to ~64-fold in a ligand-dependent manner. This increase may be due to the association of AR with GAL4-AD1 which may lead to the recruitment of other co-activators to the promoter. Interestingly, ARQ77 expression has only a minimal effect in the presence of ligand. However, in the absence of ligand there is an insignificant affect on reporter activity.

Similar results were observed in COS-1 cells transfected with the indicated amounts of $p(GAL4)_5$-E1bΔ-luc, pCH110 β-galactosidase reporter, GAL4-AD1 expression vector, FLAG-ARwt or FLAG-ARQ77. Expression of GAL4-AD1 led to both a ligand independent and ligand-dependent increase in reporter activity (Figure 5.10). As in SY-5Y, addition of ARwt led to a ~2600-fold increase in reporter activity in a ligand-dependent manner which may be due to AR recruitment of co-activators to GAL4-promoter. Interestingly, ARQ expression in the absence of ligand led to similar levels of reporter activation when compared to GAL4-AD1 alone. On addition of ligand there was little effect on reporter activity. More experiments are needed to evaluate whether CBP coactivator function is impaired in cells expressing ARQ77.

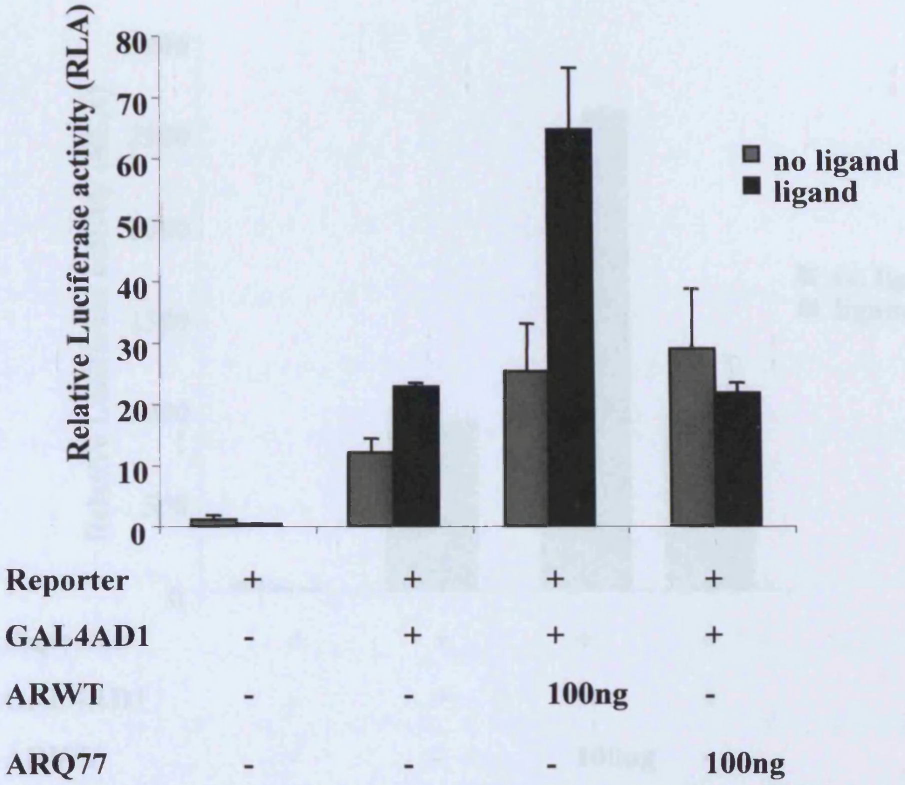

Figure 5.9 FLAG-ARQ represses GAL4-AD1-dependent transcription in SY-5Y cells. SY-5Y cells were grown for 24 hours in DMEM containing charcoal/dextran stripped FCS and transfected in triplicate with 100ng pCH110 β-galactosidase reporter, 500ng p(GAL4)$_5$-E1bΔ-luc luciferase reporter, and the indicated amounts of FLAG-ARwt or FLAG-ARQ. The cells were either treated with vehicle ethanol or 10^{-8}M mibolerone for a further 24 hours prior to lysis and the luciferase and β-galactosidase levels measured via a dual assay. The luciferase: β-galactosidase ratios were calculated and plotted as Relative Luciferase Activity (RLA) with the ratio for the reporters p(GAL4)$_5$-E1bΔ-luc and pCH110 without ligand set to a value of 1. The S.E.M are represented by error bars.

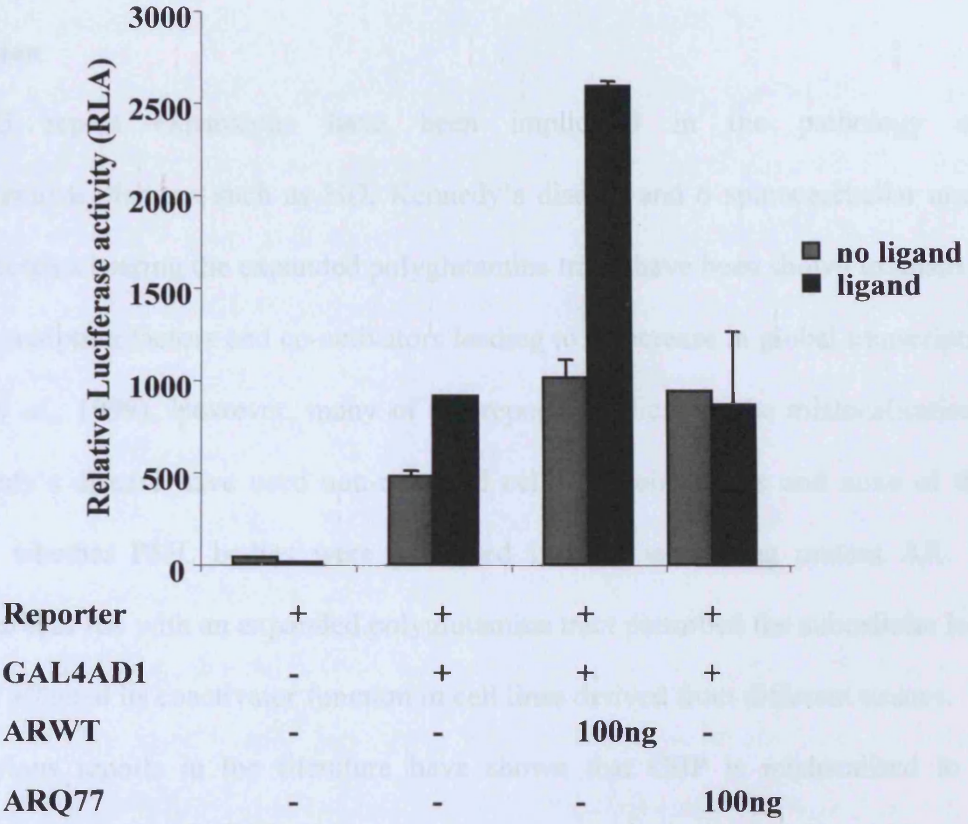

Figure 5.10 FLAG-ARQ represses GAL4-AD1-dependent transcription in COS-1 cells. COS-1 cells were grown for 24 hours in DMEM containing charcoal/dextran stripped FCS and transfected in triplicate with 100ng pCH110 β-galactosidase reporter, 500ng $p(GAL4)_5$-E1bΔ-luc luciferase reporter, and the indicated amounts of FLAG-ARwt or FLAG-ARwt. The cells were either treated with vehicle ethanol or 10^{-8}M mibolerone for a further 24 hours prior to lysis and the luciferase and β-galactosidase levels measured via a dual assay. The luciferase: β-galactosidase ratios were calculated and plotted as Relative Luciferase Activity (RLA) with the ratio for the reporters $p(GAL4)_5$-E1bΔ-luc and pCH110 without ligand set to a value of 1. The S.E.M are represented by error bars

5.7 Discussion

CAG repeat expansions have been implicated in the pathology of many neurodegenerative diseases such as HD, Kennedy's disease and 6 spinocerebellar ataxias. The causative proteins bearing the expanded polyglutamine tracts have been shown to mislocalise and degrade transcription factors and co-activators leading to a decrease in global transcription levels (Stenoien *et al.*, 1999). However, many of the reports implicating the mislocalisation of CBP with Kennedy's disease have used non-neuronal cells in their studies and none of these have determined whether PML bodies were perturbed in cells expressing mutant AR. Thus, we hypothesised that AR with an expanded polyglutamine tract perturbed the subcellular localisation of CBP and affected its coactivator function in cell lines derived from different tissues.

Previous reports in the literature have shown that CBP is mislocalised to ARQ119 aggregates in the nuclei of Hela cells and MN1 mouse neuronal cells (McCampbell *et al.*, 2000). However, in these experiments ARQ119, a constitutively active nuclear protein which did not contain the ligand binding domain, was used to examine the effect of an expanded polyQ tract on AR function. We showed that full-length GFP-AR and GFP-ARQ77 were cytoplasmic proteins in the majority of cells with a subset of the ARQ77 cells displaying cytoplasmic aggregates in a ligand-independent manner. Furthermore, CBP or PML bodies were not perturbed. This is in contrast with the work carried out by Becker *et al.* (2000) who showed that in the absence of ligand ARQ77 forms cytoplasmic aggregates in COS-7 cells. In the presence of ligand, ARQ77 expression resulted in formation of CBP and PML microspeckles in the nuclei of COS-1 cells.

The recruitment of CBP into nuclear aggregates by proteins with an expanded polyQ tract has been shown to reduce CBP coactivator function. In Huntington's disease, mutant Htt expression results in the formation of nuclear aggregates which mislocalise CBP and lead to a reduction in the activation of CBP-responsive genes (Steffan *et al.,* 2000). McCampbell *et al.,* (2000) demonstrated that ARQ119 expression led to a decrease in GAL4-CBP dependent transcription and a reduction in histone H3 acetylation. In addition, the decrease in transcription could be rescued by transfection of exogenous CBP or treatment of the cells with TSA or Nab leading to at least a partial rescue of the mutant phenotype (McCampbell *et al.,* 2000, McCampbell *et al.,* 2001, Minamiyama *et al.,* 2004). We showed that ARwt expression led to a ligand-dependent increase of reporter activity which was modestly enhanced by transfection of CBP. However, overexpression of CBP did not rescue ARQ-mediated transcriptional repression in either COS-1 or SY-5Y cells. This may be due to the inability of ARQ to associate with promoter elements and therefore co-expression of CBP would be unable to rescue any transcriptional inhibition. Alternatively, other co-activators such as SRC-1 which is a potent co-activator of AR-dependent transcription, have been shown to be mislocalised by ARpolyQ and thus overexpression of CBP would have no affect on transcription levels (Stenoien *et al.,* 1999).

As CBP has been shown to be a coactivator of GAL4-AD1 (Shepperd *et al.,* 2001) we examined whether mislocalisation of CBP by ARQ77 had any affect on GAL4-AD1-dependent transcription. ARwt led to an unexpected increase in reporter activity in a ligand-dependent manner which may be due to the recruitment of co-activators to the promoter. However, expression of ARQ77 did not result in an increase in reporter activity compared to GAL4-AD1 alone. This may suggest that not only CBP but other co-activators are being mislocalised or degraded by ARQ77 expression. As the polyglutamine tract lies in the N-terminal coactivator binding domain which is independent from the DNA-binding domain may allow ARQ to associate with DNA leading to the recruitment of co-repressors or the degradation of co-activators and the inhibition of transcription. Future experiments such as ChIP assays would allow us to identify if HDACs and proteasomal subunits are recruited to the promoter of target genes by ARQ. However, GAL4-AD1 reporter activation is similar when expressed alone or in the presence of ARQ77. This suggests that ARQ may not mislocalise coactivators, which would lead to a reduction in reporter activity compared to GAL4-AD1, but prevent further activation by being in a conformational inactive state in the nucleus.

However, it is clear that there are many more experiments needed to fully elucidate the mechanisms of how ARQ disrupts the function of neuronal and non-neuronal cells.

Chapter 6 Concluding Remarks

The subcellular localisation and activity of many PML body-associated proteins has been shown to be regulated by SUMOylation. The CBP paralogue, p300 is SUMOylated which results in the recruitment of HDACs and a decrease in transcriptional activation (Girdwood *et al.,* 2003). In this study, we have shown that endogenous CBP co-localises with PML bodies but overexpressed CBP forms nuclear foci which appear independent from PML bodies and many of which localise to the nuclear periphery over a period of time. Due to the presence of putative SUMOylation sites within the CBP sequence we carried out *in vitro* and *in vivo* experiments which demonstrated that CBP is SUMOylated. Furthermore, we found that SUMOylation has a major affect on the subcellular localisation of CBP. Deletion of the SUMO modification sites resulted in a change in the subcellular localisation of ectopically expressed CBP when compared to the wild-type protein resulting in the appearance of large nuclear aggregates. However, deletion of the C-terminal 543 amino acids led to a diffuse subcellular staining for CBP and an inability of CBP to associate in nuclear foci. In addition, we have shown that expression of CBPΔ998-1087 leads to an increase in the transcriptional activation of AML-1-mediated transcription. CBP SUMOylation has been confirmed by Kuo *et al.* (2005) who further demonstrated that SUMOylation mediates the recruitment of DAXX and HDACs leading to transcriptional repression. Thus, our work suggests that SUMOylation of CBP mediates its ability to form discrete nuclear foci and affects the ability of CBP to act as a coactivator for AML1-mediated transcription. However, our findings suggest that the C-terminus is essential for the ability of CBP to form nuclear foci either through interacting with PML directly or through some other PML-associated protein. Our studies showed for the first time that SUMOylation regulates the subcellular localisation and coactivator function of CBP. Furthermore, our results will hopefully lead to a better understanding of the processes that regulate the subcellular localisation of CBP, which is an integral mediator of cell signalling at the transcriptional level and plays a pivotal role in many cancers and neurodegenerative disorders. It is only in fully understanding the mechanism of CBP-mediated transcriptional activation that we can develop therapies for disease where this process is de-regulated.

CBP acetylates non-histone proteins such as p53, ACTR and Impα which is postulated to regulate their activity. The ability of CBP to interact with a wide variety of cellular proteins is mediated through multiple domains such as the CH1 and the SID. In this study we have identified CAS, which mediates the nucleo-cytoplasmic shuttling of Impα, and the nucleoporin Nup93 as novel CBP-SID binding proteins. Deletion of conserved leucine-rich motifs within CBP-SID and CAS abrogates binding between the two proteins suggesting a semi-conserved mode of binding between CBP-SID interacting proteins. We have also shown that HDACi perturb the subcellular localisation of CAS and increase the number of CBP-associated PML bodies. Furthermore, we have demonstrated that HDACi treatment of cells leads to an increase in the association of Impα and CBP at the nuclear periphery. Figure 6.1 shows the CBP protein interactions at the nuclear periphery and the role of HDACi in the regulation of the subcellular localisation of nuclear transport proteins at the periphery.

Interestingly, studies carried out in S. *cerevisiae* have demonstrated that CSE1 and Srp1p display boundary activity (Ishii *et al.*, 2002) and CSE1 associates with actively transcribing genes at the nuclear periphery (Casolari *et al.*, 2004). These reports coupled with our results suggest that similar mechanisms may be at play in both lower and higher eukaryotic systems and demonstrate a link between the localisation and association of CBP with Impα and CAS, which raises the exciting possibility of functional interactions between transcription factors and transport proteins.

In addition, it is one of the few reported cases in which HDACi have been shown to affect the subcellular localisation of non-histone proteins. HDACi are currently

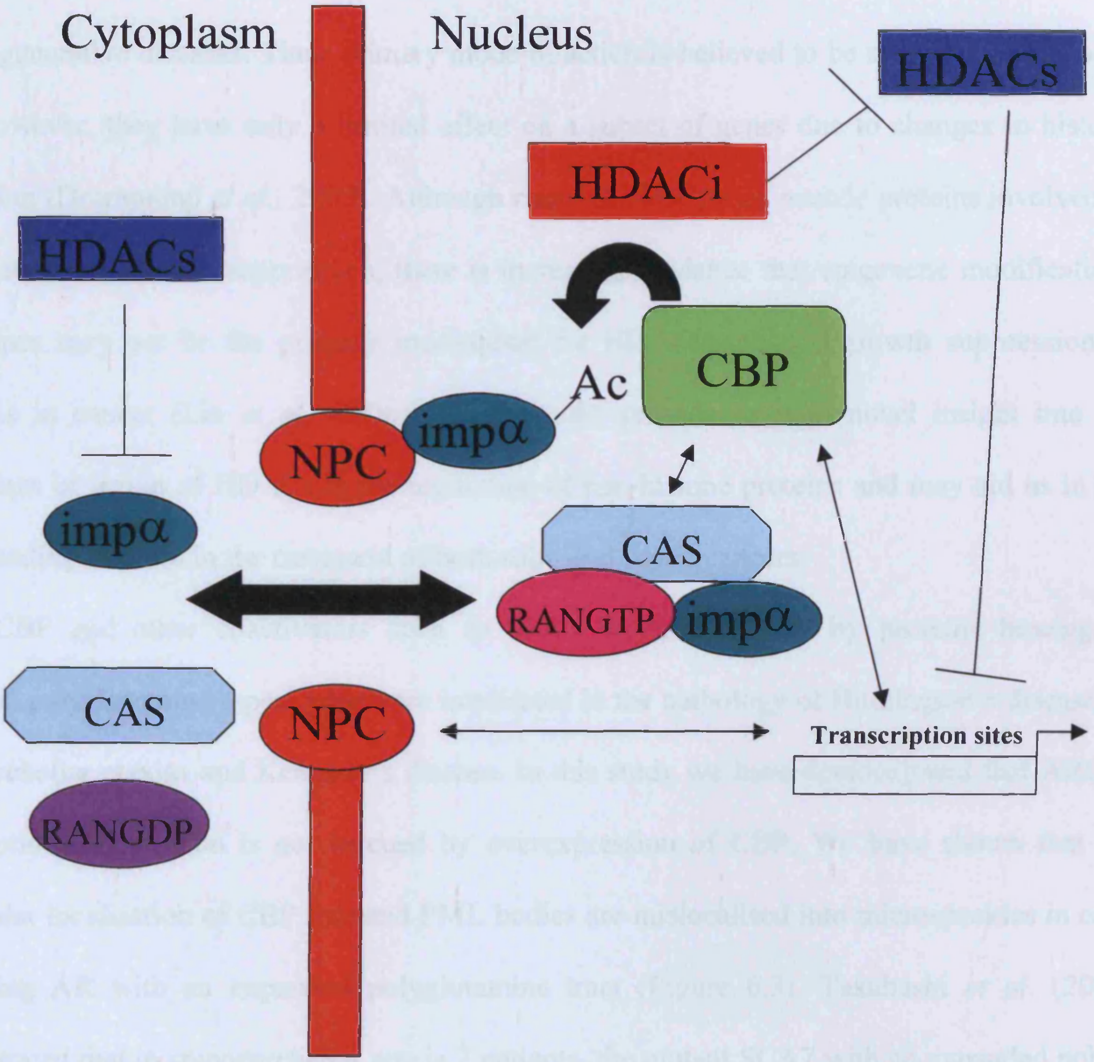
Cytoplasm
Nucleus
HDACs
HDACi
HDACs
CBP
Ac
impα
NPC
impα
CAS
RANGTP
impα
CAS
NPC
Transcription sites
RANGDP

Figure 6.1 Schematic showing the interactions between CBP, nuclear transport proteins and the NPC. In addition, the putative affect of HDACi on the subcellular localisation of these proteins is also indicated.

been used or are in clinical trials for the treatment of a wide variety of cancers and neurodegenerative diseases. Their primary mode of action is believed to be at the transcriptional level, however, they have only a limited effect on a subset of genes due to changes in histone acetylation (Drummond *et al.,* 2005). Although many of these genes encode proteins involved in tumorigenesis or tumour suppression, there is increasing evidence that epigenetic modifications of histones may not be the primary mechanism for HDACi-mediated growth suppression or apoptosis in cancer (Lin *et al.,* 2006). These results provide us with novel insight into the mechanism of action of HDACi in the regulation of non-histone proteins and may aid us in our understanding of these in the treatment of both solid and liquid cancers.

CBP and other coactivators such as SRC1 are mislocalised by proteins bearing an expanded polyglutamine repeat which are implicated in the pathology of Huntington's disease, 6-spinocerebellar ataxias and Kennedy's disease. In this study we have demonstrated that ARQ77 transcriptional repression is not rescued by overexpression of CBP. We have shown that the subcellular localisation of CBP foci and PML bodies are mislocalised into microspeckles in cells expressing AR with an expanded polyglutamine tract (Figure 6.3). Takahashi *et al.* (2002) demonstrated that in spinocerebellar ataxia 7 patients, the mutant SCA7 with an expanded polyQ tract associated in nuclear aggregates that colocalised with PML bodies. In addition, this is similar to the phenotype observed in patients expressing the PML-RAR fusion protein which results in a decrease in the SUMOylation of PML and is implicated in the formation of microspeckles (Muller *et al.,* 1998). Interestingly, treatment of cells with arsenic trioxide (As_2O_3) leads to the degradation of the PML-RARA fusion protein an increase in the SUMOylation of PML and the re-formation of PML bodies. This suggests a possible role for As_2O_3 in the treatment of Kennedy's disease. These results shed light on the mode of action of ARpolyQ and may help in the identification of novel small molecule inhibitors for the treatment of Kennedy's disease.

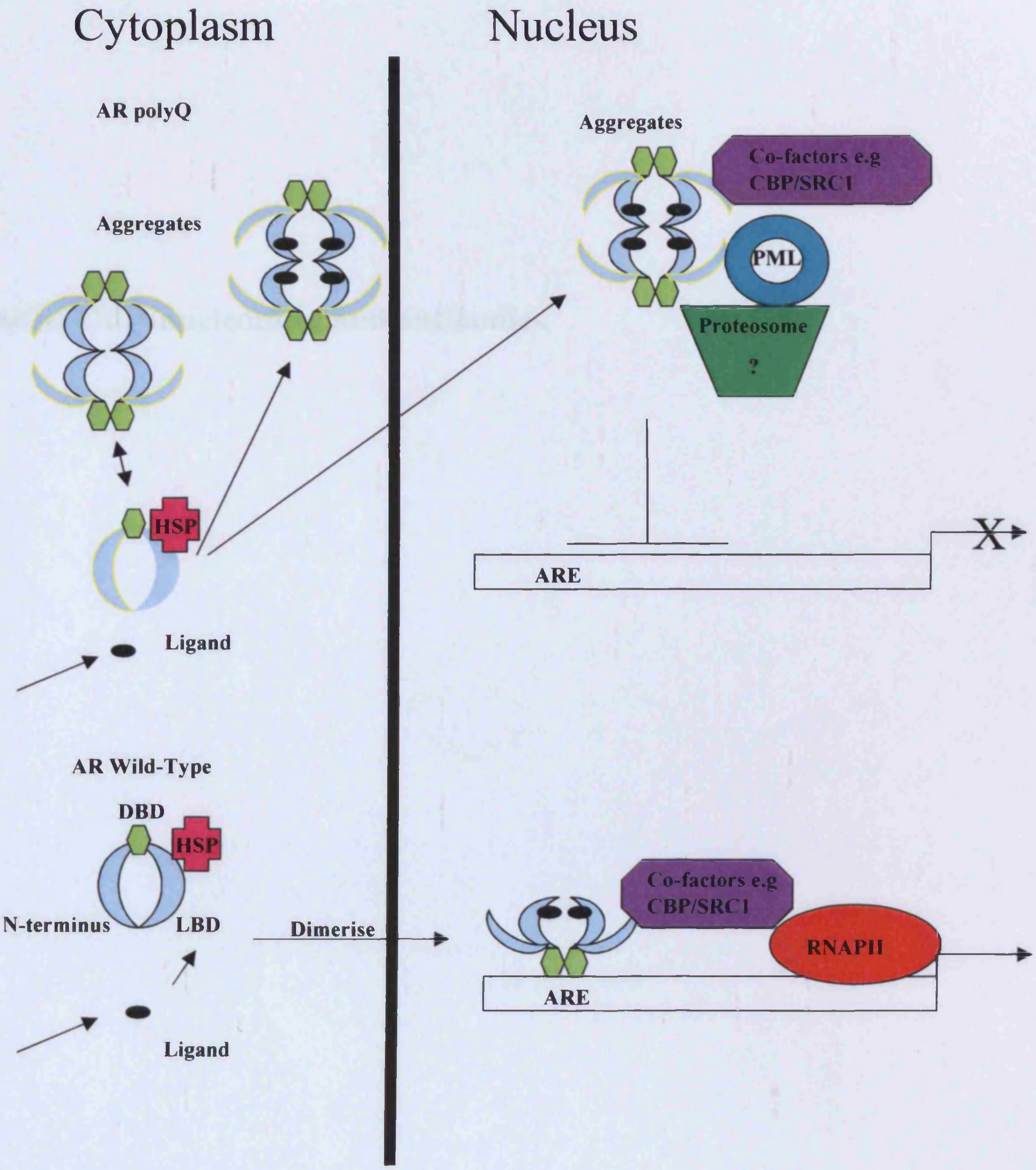
Cytoplasm
Nucleus
AR polyQ
Aggregates
HSP
Ligand
Aggregates
Co-factors e.g CBP/SRC1
PML
Proteosome
?
ARE
X
AR Wild-Type
DBD
HSP
N-terminus
LBD
Ligand
Dimerise
Co-factors e.g CBP/SRC1
RNAPII
ARE

Figure 6.2 Model of the mechanism of action of the wild-type AR and mutant AR polyQ. In the presence of ligand wild-type AR dissociates from the Heat-shock proteins (HSP) and translocates to the nucleus where it recruits co-activators and RNA polymerase II (RNAPII). However, it has been reported that AR polyQ can form aggregates in the nucleus and cytoplasm in the presence or absence of ligand. ARE-Androgen response element, LBD-ligand-binding domain, DBD-DNA binding domain.

Appendix: Oligonucleotides and antibodies

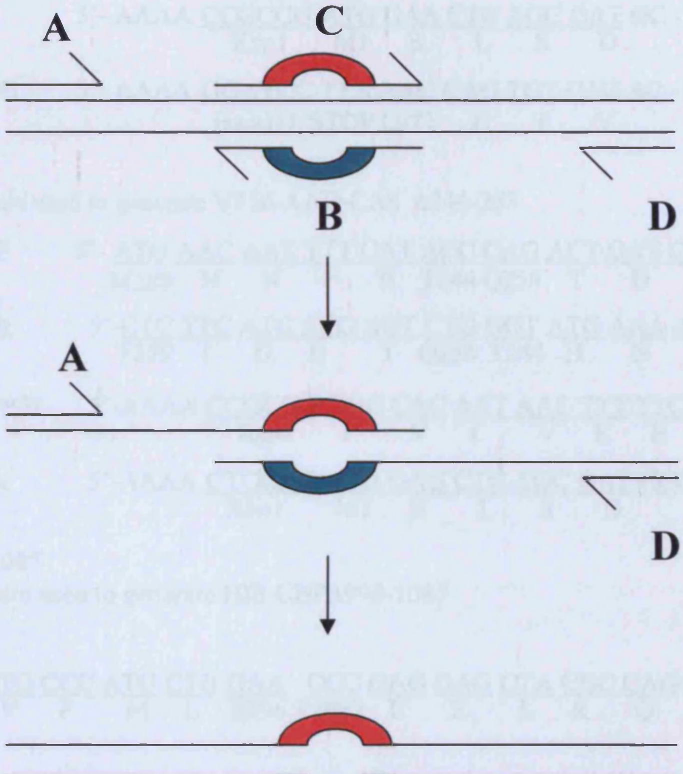

Figure A.1 Schematic of mutagenesis using PCR. DNA is depicted by thin lines (-) while the primers containing the desired mutation or encompassing the region to be deleted are numbered 1 and 2. The first PCR is carried out with primer set A-B and C-D. The second PCR is preformed using the A-D primer set and the two DNA fragments from the first PCR step as template.

YFP-CAS

These primers were used to generate YFP-CAS. Amino acids and restriction enzyme sites are indicated

hCASF-ksp1 5'- AAAA CCGCGG ATG GAA CTC AGC GAT GC -3'
Ksp1 M1 E L S D

hCASR-BamH1 5'- AAAA GGATCC TTA AAG CAG TGT CAC AC -3'
BamH1 STOP L971 L T V

CASΔ244-253

These primers were used to generate VP16-AAD-CAS Δ244-253

hCAS239ΔF 5'- ATG AAC AAT TTT CAT ACC CAG ACT GAT GAT GAA GAG -3'
M288 N N F H T244 Q254 T D D T T

hCAS259ΔR 5'-CTC TTC ATC ATC AGT CTG GGT ATG AAA ATT GTT CAT -3'
T259 T D D T Q254 T244 H N N F M

hCAS382Rnew 5'-AAAA CCGCGG CGG CAC AAT AAC TTT TTC ACA GAT AC-3'
Ksp1 P V I V K E C I

hCAS1Fnew 5'-AAAA CTCGAG ATG GAG CTC AGC GAT GCG -3'
Xho1 M1 E L S D

HIS-CBPΔ998-1087

These primers were used to generate HIS-CBPΔ998-1087

CBP991ΔF

5'-CCC GAT GTG CCC ATG CTG GAA CCC GAG GAG CTA CGC CAG GCA CTT ATG CC-3'
P991 D V P M L E996 P1087 E E L R Q A L M

CBP991ΔR

5'- CAT AAG TGC CTG GCG TAG CTC CTC GGG TTC CAG CAT GGG CAC ATC GGG -3'
M1096 L A Q R L E E P1087 E996 L M P V D P

4472R 5'-TTT TGG TTT GGG GAT TTT CTG-3'
K P K P I K Q4472

CBPHISFnew 5'-AAAA CCGCGG ATG CAC CAC CAC CAC CAC CAC ATG GCC GA-3'
Ksp1 M H H H H H H M1 A

Figure A.2 List of primers used in the cloning of YFP-CAS, VP16-AAD-CASΔ244-253 and HIS-CBPΔ998-1087

	Primer	Sequence
le339	hCASF-ksp1	AAAACCGCGGATGGAACTCAGCGATGC
le340	hCASR-BamH1	AAAAGGATCCTTAAAGCAGTGTCACAC
le341	hCAS481	CGTCATGAATTTAAGTC
le342	hCAS961	CTGGCTTCAGTTTGTGAG
le343	hCAS1438	CTTAAAGCTGACGGTATC
le344	hCAS1921	GAGGAGGCTTTGTTTTTGGTG
le608	hCAS1F new Xho	AAAACTCGAGATGGAGCTCAGCGATGCG
le615	hCAS239F	ATGAACAATTTTCATACCCAGACTGATGATGAAGAG
le616	hCAS259R	CTCTTCATCATCAGTCTGGGTATGAAAATTGTTCAT
le609	hCAS382Rnew	AAAACCGCGGCGGCACAATAACTTTTTCACAGATAC
le613	CASΔH6/H7F	CAGACTGATGATGAAGAGGAAGGGCGAGAAGTTAAAAATGAC
le614	CASΔH6/H7R	CTCATTTTTAACTTCTCGCCCTTCCTCTTCATCATCAGTCTG
le610	CBPFLAGF	AAAACCGCGGCCACCATGGACTACAAGGACGACGACGATAAGATGGCCGAGAACTTGCTGGACG
le642	CBPHISF new	AAAACCGCGGATGCACCACCACCACCACCACATGGCCGA
le626	CBP 4472R	TTTTGGTTTGGGGATTTTCTG
le628	CBP 991F	CCCGATGTGCCCATGCTGGAACCCGAGGAGCTACGCCAGGCACTTATGCC
le629	CBP991R	CATAAGTGCCTGGCGTAGCTCCTCGGGTTCCAGCATGGGCACATCGGG

Table A.3 Table of all primers used and their sequences

	Antibody	Dilution		Antibody	Dilution
1	Rabbit CBP(A22) Santa Cruz	WB:1/500 IF:1/20	17	Anti-Rabbit/mouse/goat FIT/TRITC	1/500
2	Mouse CAS Novocastra	WB:1/25 IF:1/20	18	Anti-Rabbit/mouse/goat Alexa488/594	1/400
3	Mouse Impα BD Biosciences	WB:1/2000 IF:1/100	19	Rabbit LexA Upstate	1/100
4	Mouse FLAG Sigma-Aldrich	WB:1/500 IF:1/100	20	Mouse MAb414 covance	WB:1/5000 IF:1/1000
5	Mouse HA Santa Cruz	WB:1/500 IF:1/100	21	Mouse γ-tubulin Sigma-Aldrich	WB:1/5000
6	PIAS1 (C20) Santa Cruz	WB:1/500 IF:1/100			
7	PIASx α(C20) Santa Cruz	WB:1/500 IF:1/100			
8	PIASγ (F-20) Santa Cruz	WB:1/500 IF:1/100			
9	PIAS3 (H169) Santa Cruz	WB:1/500 IF:1/100			
10	Rabbit SUMO1 (FL-101) Santa Cruz	WB:1/500 IF:1/100			
11	Mouse β-actin Sigma	WB:1/500			
12	Mouse PML (PG-M3) Santa Cruz	WB:1/500 IF:1/100			
13	Rabbit PML (H238) Santa Cruz	WB:1/500 IF:1/10			
14	Goat PML (A20) Santa Cruz	WB1/100			
15	Rabbit GFP Abcam	WB:1/200			
16	Anti-Rabbit/mouse/goat HRP	1/5000			

Table A.1 Table showing the antibodies used for all applications

Plasmid	Source
pGEXDMH-GST-CBPSID	Sheppard et al. 2001
pSG5(PT)CBP	Constructed by Phil Troke, University of Leicester
pGEX	GE Healthcare (Amersham Bioscience)
pcDNA3-MOZ	Dr.D.G Gilliland, Harvard University, U.S.A
pSG5-FLAG-SRC1e	Kalkhoven *et al.* 1998
pCH110	Pharmacia Biotech
FLAGCAS-N	Constructed by Jan Harries, University of Leicester
FLAGCAS	Constructed by Jan Harries, University of Leicester
pETRANQ69L	Dr.C. Dingwell, GSK Ltd., Harlow, Essex, UK
pCDNA3-FLAG-CBP	Dr.Eric Kalkhoven, UMC, Utrecht, Netherlands
pEGFP-SUMO1	Dr.J. Palvimo, University of Helsinki, Finland
pEGFP-SUMO1 G/A	Dr.J. Palvimo, University of Helsinki, Finland
pSG5-ARwt	Dr.A.C.Cato, Forschungszentrum, Karlsruhe, Germany
pSG5-ARQ77	Dr.A.C.Cato, Forschungszentrum, Karlsruhe, Germany
pEYFP-ARwt	Dr.A.C.Cato, Forschungszentrum, Karlsruhe, Germany
pEYFP-ARQ77	Dr.A.C.Cato, Forschungszentrum, Karlsruhe, Germany
pCDNA3FLAGPML IV	Dr.P. Salomoni, MRC toxicology, Leicester
MMTV-luc	Dr.C. Bevan, Imperial College London, UK
pCDNA3-Myc-His-Impα	Bannister *et. al.* 2000

MMTV-PSA	Dr.E.Metzger, Universitat Freiburg, Germany
pASV3-Ets-2	Constructed by Jan Harries, University of Leicester
pASV3-CAS-N	Constructed by Jan Harries, University of Leicester
pBTM116CBP-SID	Constructed by Jan Harries, University of Leicester
pASV3mod	Dr.B. Le Douarain, IGBMC, Illkirch, France
pSG5-TDG	Dr.S.Ali, Imperial College London, UK
pGEX-2T-SUMO1	Prof.R.Hay, University of St.Andrews,Fife, Scotland
pSPORT-PIAS3	ImageClone, MRC Geneservice, Cambridge, UK
pcDNA3.0PT	Constructed by Dr.P.Troke, University of Leicester
pcDNA3-FLAGPIAS1	Dr. V. De Laurenzi, MRC toxicology, Leicester
pcDNA3-HA-SUMO1	Dr. V. De Laurenzi, MRC toxicology, Leicester
pcDNA3-FLAG-SUMO1	Dr. V. De Laurenzi, MRC toxicology, Leicester

Table A.2 Table showing the sources of all plasmids used

References

Aarnisalo P, Palvimo JJ and Janne OA (1998) CREB-binding protein in androgen receptor-mediated signaling. *Proc Natl Acad Sci U S A.* 95(5):2122-7

Adachi H, Katsuno M, Minamiyama M, Waza M, Sang C, Nakagomi Y, Kobayashi Y, Tanaka F, Doyu M, Inukai A, Yoshida M, Hashizume Y and Sobue G (2005) Widespread nuclear and cytoplasmic accumulation of mutant androgen receptor in SBMA patients. *Brain* 128(Pt 3):659-70

Alberts B, Johnson A, Lewis J, Raff M, Roberts K and Walter P (2002) *Molecular biology of the cell*, 4th edition, Garland science

Allfrey VG, Faulkner R, Mirsky AE (1964) Acetylation and methylation of histones and their possible role in the regulation of RNA synthesis *Proc Natl Acad Sci U S A.* 51:786-94

Andrulis ED, Neiman AM, Zappulla DC and Sternglanz R (1998) Perinuclear localization of chromatin facilitates transcriptional silencing. *Nature* 394(6693):592-5

Ascoli CA and Maul GG (1991) Identification of a novel nuclear domain. *J Cell Biol.* 112(5):785-95

Bannister AJ, Miska EA, Gorlich D and Kouzarides T (2000) Acetylation of importin-alpha nuclear import factors by CBP/p300. *Curr Biol.* 10(8):467-70

Bartlett J, Blagojevic J, Carter D, Eskiw C, Fromaget M, Job C, Shamsher M, Trindade IF, Xu M, Cook PR (2006) Specialized transcription factories. *Biochem Soc Symp.* 2006;(73):67-75

Bartsch O, Locher K, Meinecke P, Kress W, Seemanova E, Wagner A, Ostermann K and Rodel G (2002) Molecular studies in 10 cases of Rubinstein-Taybi syndrome, including a mild variant showing a missense mutation in codon 1175 of CREBBP. *J Med Genet.* 39(7):496-501

Baxter J, Merkenschlager M, Fisher AG (2002) Nuclear organisation and gene expression. *Curr Opin Cell Biol.* 14(3):372-6

Bai XT, Gu BW, Yin T, Niu C, Xi XD, Zhang J, Chen Z and Chen SJ (2006) Trans-repressive effect of NUP98-PMX1 on PMX1-regulated c-FOS gene through recruitment of histone deacetylase 1 by FG repeats. *Cancer Res.* 66(9):4584-90

Becker M, Martin E, Schneikert J, Krug HF and Cato AC (2000) Cytoplasmic localization and the choice of ligand determine aggregate formation by androgen receptor with amplified polyglutamine stretch. *J Cell Biol.* 149(2):255-62

Belmont AS, Bignone F and Ts'o PO (1986) The relative intranuclear positions of Barr bodies in XXX non-transformed human fibroblasts. *Exp Cell Res.* 165(1):165-79

Bernardi R, Scaglioni PP, Bergmann S, Horn HF, Vousden KH and Pandolfi PP (2004) PML regulates p53 stability by sequestering Mdm2 to the nucleolus. *Nat Cell Biol.* 6(7):665-72

Best JL, Ganiatsas S, Agarwal S, Changou A, Salomoni P, Shirihai O, Meluh PB, Pandolfi PP and Zon LI (2002) SUMO-1 protease-1 regulates gene transcription through PML. *Mol Cell.* 10(4):843-55

Blobel G (1985) Gene gating: a hypothesis. *Proc Natl Acad Sci U S A.* 82(24):8527-9

Boeger H, Griesenbeck J, Strattan JS and Kornberg RD (2004) Removal of promoter nucleosomes by disassembly rather than sliding in vivo. *Mol Cell.* 14(5):667-73

Boisvert FM, Hendzel MJ and Bazett-Jones DP (2000) Promyelocytic leukemia (PML) nuclear bodies are protein structures that do not accumulate RNA. *J Cell Biol.* 148(2):283-92

Boisvert FM, Kruhlak MJ, Box AK, Hendzel MJ and Bazett-Jones DP (2001) The transcription coactivator CBP is a dynamic component of the promyelocytic leukemia nuclear body. *J Cell Biol.* 152(5):1099-106

Borden KL (2002) Pondering the promyelocytic leukemia protein (PML) puzzle: possible functions for PML nuclear bodies. *Mol Cell Biol.* 22(15):5259-6

Boyes J, Byfield P, Nakatani Y and Ogryzko V (1998) Regulation of activity of the transcription factor GATA-1 by acetylation. *Nature* 396(6711):594-8

Boyle S, Gilchrist S, Bridger JM, Mahy NL, Ellis JA and Bickmore WA (2001) The spatial organization of human chromosomes within the nuclei of normal and emerin-mutant cells. *Hum Mol Genet.* 10(3):211-9

Brinkmann U, Brinkmann E, Gallo M and Pastan I (1995) Cloning and characterization of a cellular apoptosis susceptibility gene, the human homologue to the yeast chromosome segregation gene CSE1. *Proc Natl Acad Sci U S A.* 92(22):10427-31

Brinkmann U, Brinkmann E, Gallo M, Scherf U and Pastan I (1996) Role of CAS, a human homologue to the yeast chromosome segregation gene CSE1, in toxin and tumor necrosis factor mediated apoptosis. *Biochemistry* 35(21):6891-9

Butler R, Leigh PN, McPhaul MJ and Gallo JM (1998) Truncated forms of the androgen receptor are associated with polyglutamine expansion in X-linked spinal and bulbar muscular atrophy *Hum Mol Genet.* 7(1):121-7

Cabal GG, Genovesio A, Rodriguez-Navarro S, Zimmer C, Gadal O, Lesne A, Buc H, Feuerbach-Fournier F, Olivo-Marin JC, Hurt EC and Nehrbass U (2006) SAGA interacting factors confine sub-diffusion of transcribed genes to the nuclear envelope. *Nature* 441(7094):770-3

Casolari JM, Brown CR, Komili S, West J, Hieronymus H and Silver PA (2004) Genome-wide localization of the nuclear transport machinery couples transcriptional status and nuclear organization *Cell* 117(4):427-39

Chalkiadaki A and Talianidis I (2005) SUMO-dependent compartmentalization in promyelocytic leukemia protein nuclear bodies prevents the access of LRH-1 to chromatin. *Mol Cell Biol.* 25(12):5095-105

Chang WH, Cemal CK, Hsu YH, Kuo CL, Nukina N, Chang MH, Hu HT, Li C and Hsieh M (2005) Dynamic expression of Hsp27 in the presence of mutant ataxin-3. *Biochem Biophys Res Commun.* 336(1):258-67

Chauchereau A, Amazit L, Quesne M, Guiochon-Mantel A and Milgrom E (2003) Sumoylation of the progesterone receptor and of the steroid receptor coactivator SRC-1. *J Biol Chem.* 278(14):12335-43

Chen CS, Weng SC, Tseng PH, Lin HP and Chen CS (2005) Histone acetylation-independent effect of histone deacetylase inhibitors on Akt through the reshuffling of protein phosphatase 1 complexes. *J Biol Chem.* 280(46):38879-87

Chrivia JC, Kwok RP, Lamb N, Hagiwara M, Montminy MR and Goodman RH (1993) Phosphorylated CREB binds specifically to the nuclear protein CBP. *Nature* 365(6449):855-9

Cioce M and Lamond AI (2005) Cajal bodies: a long history of discovery. *Annu Rev Cell Dev Biol.* 21:105-31

Cohen HY, Lavu S, Bitterman KJ, Hekking B, Imahiyerobo TA, Miller C, Frye R, Ploegh H, Kessler BM and Sinclair DA (2004) Acetylation of the C terminus of Ku70 by CBP and PCAF controls Bax-mediated apoptosis. *Mol Cell* 13(5):627-38

Cook A, Fernandez E, Lindner D, Ebert J, Schlenstedt G and Conti E (2005) The structure of the nuclear export receptor Cse1 in its cytosolic state reveals a closed conformation incompatible with cargo binding. *Mol Cell.* 18(3):355-67

Cremer T, Kreth G, Koester H, Fink RH, Heintzmann R, Cremer M, Solovei I, Zink D, Cremer C. (2001) Chromosome territories, interchromatin domain compartment, and nuclear matrix: an integrated view of the functional nuclear architecture. *Crit Rev Eukaryot Gene Expr.* 2000:10(2):179-212

Cuthbert GL, Daujat S, Snowden AW, Erdjument-Bromage H, Hagiwara T, Yamada M, Schneider R, Gregory PD, Tempst P, Bannister AJ and Kouzarides T (2004) Histone deimination antagonizes arginine methylation. *Cell* 118(5):545-53

Dahle O, Bakke O and Gabrielsen OS (2004) c-Myb associates with PML in nuclear bodies in hematopoietic cells. *Exp Cell Res.* 297(1):118-26

Daniel JA, Torok MS, Sun ZW, Schieltz D, Allis CD, Yates JR 3rd and Grant PA (2004) Deubiquitination of histone H2B by a yeast acetyltransferase complex regulates transcription. *J Biol Chem.* 279(3):1867-71

Deguchi K, Ayton PM, Carapeti M, Kutok JL, Snyder CS, Williams IR, Cross NC, Glass CK, Cleary ML and Gilliland DG (2005) MOZ-TIF2-induced acute myeloid leukemia requires the MOZ nucleosome binding motif and TIF2-mediated recruitment of CBP. *Cancer Cell* 3(3):259-71

Dellaire G, Ching RW, Dehghani H, Ren Y and Bazett-Jones DP (2006) The number of PML nuclear bodies increases in early S phase by a fission mechanism. *J Cell Sci.* 119(Pt 6):1026-33

Dellaire G, Makarov EM, Cowger JJ, Longman D, Sutherland HG, Luhrmann R, Torchia J and Bickmore WA (2001) Mammalian PRP4 kinase copurifies and interacts with components of both the U5 snRNP and the N-CoR deacetylase complexes. *Mol Cell Biol.* 22(14):5141-56

Demarest SJ, Martinez-Yamout M, Chung J, Chen H, Xu W, Dyson HJ, Evans RM and Wright PE (2002) Mutual synergistic folding in recruitment of CBP/p300 by p160 nuclear receptor coactivators *Nature* 415(6871):549-53

Desterro JM, Rodriguez MS, Kemp GD and Hay RT (1999) Identification of the enzyme required for activation of the small ubiquitin-like protein SUMO-1. *J Biol Chem.* 274(15):10618-24

Di Bacco A, Ouyang J, Lee HY, Catic A, Ploegh H and Gill G (2005) The SUMO-specific protease SENP5 is required for cell division. *Mol Cell Biol.* 26(12):4489-98

Doucas V, Tini M, Egan DA and Evans RM (1999) Modulation of CREB binding protein function by the promyelocytic (PML) oncoprotein suggests a role for nuclear bodies in hormone signaling. *Proc Natl Acad Sci U S A.* 96(6):2627-32

Dover J, Schneider J, Tawiah-Boateng MA, Wood A, Dean K, Johnston M and Shilatifard A (2002) Methylation of histone H3 by COMPASS requires ubiquitination of histone H2B by Rad6. *J Biol Chem.* 277(32):28368-71

Drummond DC, Noble CO, Kirpotin DB, Guo Z, Scott GK and Benz CC (2005) Clinical development of histone deacetylase inhibitors as anticancer agents. *Annu Rev Pharmacol Toxicol.* 45:495-528

Dundr M and Misteli T (2001) Functional architecture in the cell nucleus. *Biochem J.* 356(Pt 2):297-310

Eckner R, Ewen ME, Newsome D, Gerdes M, DeCaprio JA, Lawrence JB and Livingston DM (1994) Molecular cloning and functional analysis of the adenovirus E1A-associated 300-kD protein (p300) reveals a protein with properties of a transcriptional adaptor. *Genes Dev.* 8(8):869-84

Eisenstein M (2005) A look back: finding chromatin's footprints. *Nature Methods* 2:718-718

Fakan S (1994) Perichromatin fibrils are in situ forms of nascent transcripts. *Trends Cell Biol.* 4(3):86-90

Fagioli M, Alcalay M, Tomassoni L, Ferrucci PF, Mencarelli A, Riganelli D, Grignani F, Pozzan T, Nicoletti I, Grignani F and Pelicci PG (1998) Cooperation between the RING + B1-B2 and coiled-coil domains of PML is necessary for its effects on cell survival. *Oncogene* 16(22):2905-13

Felsenfeld G and Groudine M (2003) Controlling the double helix. *Nature.* 421(6921):448-53

Fernandez-Lloris R, Osses N, Jaffray E, Shen LN, Vaughan OA, Girwood D, Bartrons R, Rosa JL, Hay RT and Ventura F (2006) Repression of SOX6 transcriptional activity by SUMO modification. *FEBS Lett.* 580(5):1215-21

Fleischer S, Wiemann S, Will H and Hofmann TG (2006) PML-associated repressor of transcription (PAROT), a novel KRAB-zinc finger repressor, is regulated through association with PML nuclear bodies. *Exp Cell Res.*;312(6):901-12

Fronsdal K, Engedal N, Slagsvold T and Saatcioglu F (1998) CREB binding protein is a coactivator for the androgen receptor and mediates cross-talk with AP-1. *J Biol Chem.* 273(48):31853-9

Fu M, Wang C, Reutens AT, Wang J, Angeletti RH, Siconolfi-Baez L, Ogryzko V, Avantaggiati ML and Pestell RG (2000) p300 and p300/cAMP-response element-binding protein-associated factor acetylate the androgen receptor at sites governing hormone-dependent transactivation. *J Biol Chem.* 275(27):20853-60

Fuchsova B, Novak P, Kafkova J and Hozak P (2002) Nuclear DNA helicase II is recruited to IFN-alpha-activated transcription sites at PML nuclear bodies. *J Cell Biol.* 158(3):463-73

Fuino L, Bali P, Wittmann S, Donapaty S, Guo F, Yamaguchi H, Wang HG, Atadja P and Bhalla K (2003) Histone deacetylase inhibitor LAQ824 down-regulates Her-2 and sensitizes human breast cancer cells to trastuzumab, taxotere, gemcitabine, and epothilone B. *Mol Cancer Ther.* 2(10):971-84

Galy V, Olivo-Marin JC, Scherthan H, Doye V, Rascalou N and Nehrbass U (2000) Nuclear pore complexes in the organization of silent telomeric chromatin. *Nature* 403(6765):108-12

Gaughan L, Logan IR, Cook S, Neal DE and Robson CN (2002) Tip60 and histone deacetylase 1 regulate androgen receptor activity through changes to the acetylation status of the receptor. *J Biol Chem.* 277(29):25904-13

Girdwood D, Bumpass D, Vaughan OA, Thain A, Anderson LA, Snowden AW, Garcia-Wilson E, Perkins ND and Hay RT (2004) P300 transcriptional repression is mediated by SUMO modification *Mol Cell.* 11(4):1043-54

Gorlich D and Kutay U (1997) Transport between the cell nucleus and the cytoplasm. *Annu Rev Cell Dev Biol.* 15:607-6

Grande MA, van der Kraan I, de Jong L and van Driel R (1997) Nuclear distribution of transcription factors in relation to sites of transcription and RNA polymerase II. *J Cell Sci.* 110 (Pt 15):1781-91

Gronroos E, Hellman U, Heldin CH and Ericsson J (2002) Control of Smad7 stability by competition between acetylation and ubiquitination. *Mol Cell.* 10(3):483-93

Grierson AJ, Shaw CE and Miller CC (2001) Androgen induced cell death in SHSY5Y neuroblastoma cells expressing wild-type and spinal bulbar muscular atrophy mutant androgen receptors. *Biochim Biophys Acta.* 1536(1):13-20

Gu W, Shi XL and Roeder RG (1997) Synergistic activation of transcription by CBP and p53. *Nature* 387(6635):819-23

Guillot PV, Xie SQ, Hollinshead M and Pombo A (2004) Fixation-induced redistribution of hyperphosphorylated RNA polymerase II in the nucleus of human cells. *Exp Cell Res.* 295(2):460-8

Hall LL, Smith KP, Byron M and Lawrence JB (2006) Molecular anatomy of a speckle. *Anat Rec A Discov Mol Cell Evol Biol.* Jun 7; [Epub ahead of print]

Hanahan D (1983) Studies on transformation of Escherichia coli with plasmids. *J Mol Biol.* 166(4):557-80

Hardeland U, Steinacher R, Jiricny J and Schar P (2002) Modification of the human thymine-DNA glycosylase by ubiquitin-like proteins facilitates enzymatic turnover. *EMBO J.* 21(6):1456-64

Heery DM, Kalkhoven E, Hoare S and Parker MG (1997) A signature motif in transcriptional co-activators mediates binding to nuclear receptors. *Nature* 387(6634):733-6

Hendzel MJ, Kruhlak MJ and Bazett-Jones DP (1998) Organization of highly acetylated chromatin around sites of heterogeneous nuclear RNA accumulation. *Mol Biol Cell.* 1998 9(9):2491-507

Henry KW, Wyce A, Lo WS, Duggan LJ, Emre NC, Kao CF, Pillus L, Shilatifard A, Osley MA, Berger SL. (2003) Transcriptional activation via sequential histone H2B ubiquitylation and deubiquitylation, mediated by SAGA-associated Ubp8. *Genes Dev.* 17(21):2648-63

Hess-Stumpp H (2005) Histone deacetylase inhibitors and cancer: from cell biology to the clinic. *Eur J Cell Biol.* 84(2-3):109-21

Hockly E, Richon VM, Woodman B, Smith DL, Zhou X, Rosa E, Sathasivam K, Ghazi-Noori S, Mahal A, Lowden PA, Steffan JS, Marsh JL, Thompson LM, Lewis CM, Marks PA and Bates GP (2003) Suberoylanilide hydroxamic acid, a histone deacetylase inhibitor, ameliorates motor deficits in a mouse model of Huntington's disease. *Proc Natl Acad Sci U S A.* 100(4):2041-6

Hood JK and Silver PA (1998) Cse1p is required for export of Srp1p/importin-alpha from the nucleus in Saccharomyces cerevisiae. *J Biol Chem.* 273(52):35142-6

Hubbert C, Guardiola A, Shao R, Kawaguchi Y, Ito A, Nixon A, Yoshida M, Wang XF and Yao TP (2002) HDAC6 is a microtubule-associated deacetylase. *Nature* 417(6887):455-8

Ishii K, Arib G, Lin C, Van Houwe G and Laemmli UK (2002) Chromatin boundaries in budding yeast: the nuclear pore connection. *Cell* 109(5):551-62

Ishov AM, Sotnikov AG, Negorev D, Vladimirova OV, Neff N, Kamitani T, Yeh ET, Strauss JF 3rd and Maul GG (1999) PML is critical for ND10 formation and recruits the PML-interacting protein daxx to this nuclear structure when modified by SUMO-1. *J Cell Biol.* 147(2):221-34

Ito A, Kawaguchi Y, Lai CH, Kovacs JJ, Higashimoto Y, Appella E and Yao TP (2002) MDM2-HDAC1-mediated deacetylation of p53 is required for its degradation. *EMBO J.* 21(22):6236-45

Jacobs EY, Frey MR, Wu W, Ingledue TC, Gebuhr TC, Gao L, Marzluff WF and Matera AG (1999) Coiled bodies preferentially associate with U4, U11, and U12 small nuclear RNA genes in interphase HeLa cells but not with U6 and U7 genes. *Mol Biol Cell.* 10(5):1653-63

Jang MS, Ryu SW and Kim E Modification of Daxx by small ubiquitin-related modifier-1. *Biochem Biophys Res Commun.* 295(2):495-500

Jensen K, Shiels C and Freemont PS (2001) PML protein isoforms and the RBCC/TRIM motif. *Oncogene* 20(49):7223-33

Jenuwein T and Allis CD (2001) Translating the histone code. *Science* 293(5532):1074-80

Jeong JW, Bae MK, Ahn MY, Kim SH, Sohn TK, Bae MH, Yoo MA, Song EJ, Lee KJ and Kim KW (2002) Regulation and destabilization of HIF-1alpha by ARD1-mediated acetylation. *Cell* 111(5):709-20

Jiang H, Nucifora FC Jr, Ross CA and DeFranco DB (2003) Cell death triggered by polyglutamine-expanded huntingtin in a neuronal cell line is associated with degradation of CREB-binding protein. *Hum Mol Genet.* 12(1):1-12

Johnson C, Primorac D, McKinstry M, McNeil J, Rowe D and Lawrence JB (2000) Tracking COL1A1 RNA in osteogenesis imperfecta. splice-defective transcripts initiate transport from the gene but are retained within the SC35 domain. *J Cell Biol.* 150(3):417-32

Johnson ES (2004) Protein modification by SUMO. *Annu Rev Biochem.* 73:355-82

Ju R and Muller MT (2003) Histone deacetylase inhibitors activate p21(WAF1) expression via ATM. *Cancer Res.* 63(11):2891-7

Kagey MH, Melhuish TA, Wotton D (2003) The polycomb protein Pc2 is a SUMO E3 Cell 113(1):127-37

Kalkhoven, E (2004) CBP and p300: HATs for different occasions. *Biochem Pharmacol.* 68(6):1145-55

Kalkhoven E, Teunissen H, Houweling A, Verrijzer CP and Zantema A (2002) The PHD type zinc finger is an integral part of the CBP acetyltransferase domain. *Mol Cell Biol.* 22(7):1961-70

Kamitani T, Kito K, Nguyen HP, Wada H, Fukuda-Kamitani T and Yeh ET (1998) dentification of three major sentrinization sites in PML. *J Biol Chem.* 273(41):26675-82

Kasper LH, Brindle PK, Schnabel CA, Pritchard CE, Cleary ML and van Deursen JM CREB binding protein interacts with nucleoporin-specific FG repeats that activate transcription and mediate NUP98-HOXA9 oncogenicity. *Mol Cell Biol.* 19(1):764-76

Kataoka N, Yong J, Kim VN, Velazquez F, Perkinson RA, Wang F, and Dreyfuss G (2000) Pre-mRNA splicing imprints mRNA in the nucleus with a novel RNA-binding protein that persists in the cytoplasm. *Mol Cell.* 6(3):673-82

Katsuno M, Adachi H, Doyu M, Minamiyama M, Sang C, Kobayashi Y, Inukai A and Sobue G (2003) Leuprorelin rescues polyglutamine-dependent phenotypes in a transgenic mouse model of spinal and bulbar muscular atrophy. *Nat Med.* 9(6):768-73

Kindle KB, Troke PJ, Collins HM, Matsuda S, Bossi D, Bellodi C, Kalkhoven E, Salomoni P, Pelicci PG, Minucci S and Heery DM (2005) MOZ-TIF2 inhibits transcription by nuclear receptors and p53 by impairment of CBP function. *Mol Cell Biol.* 25(3):988-1002

Kitabayashi I, Aikawa Y, Nguyen LA, Yokoyama A and Ohki M (2001) Activation of AML1-mediated transcription by MOZ and inhibition by the MOZ-CBP fusion protein. *EMBO J.* 20(24):7184-96

Kitabayashi I, Yokoyama A, Shimizu K and Ohki M (1998) Interaction and functional cooperation of the leukemia-associated factors AML1 and p300 in myeloid cell differentiation. *EMBO J.* 17(11):2994-3004

Kotaja N, Karvonen U, Janne OA and Palvimo JJ (2002) PIAS proteins modulate transcription factors by functioning as SUMO-1 ligases. *Mol Cell Biol.* 22(14):5222-34

Kouzarides T (2000) Acetylation: a regulatory modification to rival phosphorylation? *EMBO J.* 19(6):1176-9

Kuo HY, Chang CC, Jeng JC, Hu HM, Lin DY, Maul GG, Kwok RP and Shih HM (2005) SUMO modification negatively modulates the transcriptional activity of CREB-binding protein via the recruitment of Daxx. *Proc Natl Acad Sci U S A.* 102(47):16973-8

Kutay U, Bischoff FR, Kostka S, Kraft R and Gorlich D (1997) Export of importin alpha from the nucleus is mediated by a specific nuclear transport factor. *Cell* 90(6):1061-71

Laemmli UK (1970) Cleavage of structural proteins during the assembly of the head of bacteriophage T4. *Nature.* 227(5259):680-5

Lallemand-Breitenbach V, Zhu J, Puvion F, Koken M, Honore N, Doubeikovsky A, Duprez E, Pandolfi PP, Puvion E, Freemont P and de The H (2001) Role of promyelocytic leukemia (PML) sumolation in nuclear body formation, 11S proteasome recruitment, and As2O3-induced PML or PML/retinoic acid receptor alpha degradation. *J Exp Med.* 193(12):1361-71

LaMorte VJ, Dyck JA, Ochs RL and Evans RM (1998) Localization of nascent RNA and CREB binding protein with the PML-containing nuclear body. *Proc Natl Acad Sci U S A.* 95(9):4991-6

Laroche T, Martin SG, Gotta M, Gorham HC, Pryde FE, Louis EJ and Gasser SM (1998) Mutation of yeast Ku genes disrupts the subnuclear organization of telomeres. *Curr Biol.* 8(11):653-6

Lavau C, Du C, Thirman M and Zeleznik-Le N (2000) Chromatin-related properties of CBP fused to MLL generate a myelodysplastic-like syndrome that evolves into myeloid leukemia. *EMBO J.* 19(17):4655-64

Le XF, Yang P and Chang KS (1996) Analysis of the growth and transformation suppressor domains of promyelocytic leukemia gene, PML. *J Biol Chem.* 271(1):130-5

Lee H, Quinn JC, Prasanth KV, Swiss VA, Economides KD, Camacho MM, Spector DL and Abate-Shen C (2006) PIAS1 confers DNA-binding specificity on the Msx1 homeoprotein. *Genes Dev.* 20(7):784-94

Lee JH, Cook JR, Yang ZH, Mirochnitchenko O, Gunderson SI, Felix AM, Herth N, Hoffmann R, Pestka S (2005) PRMT7, a new protein arginine methyltransferase that synthesizes symmetric dimethylarginine. *J Biol Chem.* 280(5):3656-64

Li SJ and Hochstrasser M (1999) A new protease required for cell-cycle progression in yeast. *Nature.* 398(6724):246-51

Lin HY, Chen CS, Lin SP, Weng JR and Chen CS (2006) Targeting histone deacetylase in cancer therapy. *Med Res Rev.* 26(4):397-413

Lin RJ, Sternsdorf T, Tini M and Evans RM (2001) Transcriptional regulation in acute promyelocytic leukemia. *Oncogene* 20(49):7204-15

Lindemann RK, Gabrielli B and Johnstone RW (2004) Histone-deacetylase inhibitors for the treatment of cancer. *Cell Cycle* 3(6):779-88

Long J, Wang G, Matsuura I, He D and Liu F (2004) Activation of Smad transcriptional activity by protein inhibitor of activated STAT3 (PIAS3). *Proc Natl Acad Sci U S A*. 101(1):99-10

Lorente M, Perez C, Sanchez C, Donohoe M, Shi Y and Vidal (2006) Homeotic transformations of the axial skeleton of YY1 mutant mice and genetic interaction with the Polycomb group gene Ring1/Ring1A. *Mech Dev*. 123(4):312-20

Luciani JJ, Depetris D, Usson Y, Metzler-Guillemain C, Mignon-Ravix C, Mitchell MJ, Megarbane A, Sarda P, Sirma H, Moncla A, Feunteun J, Mattei MG (2006) PML nuclear bodies are highly organised DNA-protein structures with a function in heterochromatin remodelling at the G2 phase. *J Cell Sci.* 119(Pt 12):2518-31

Luger K, Mader AW, Richmond RK, Sargent DF and Richmond TJ (1997) Crystal structure of the nucleosome core particle at 2.8 A resolution. *Nature* 389(6648):251-60

Luo J, Nikolaev AY, Imai S, Chen D, Su F, Shiloh A, Guarente L and Gu W (2001) Negative control of p53 by Sir2alpha promotes cell survival under stress. *Cell* 107(2):137-48

Mahy NL, Perry PE and Bickmore WA (2002) Gene density and transcription influence the localization of chromatin outside of chromosome territories detectable by FISH. *J Cell Biol.* 159(5):753-63

Manning ET, Ikehara T, Ito T, Kadonaga JT and Kraus WL (2001) p300 forms a stable, template-committed complex with chromatin: role for the bromodomain.
Mol Cell Biol. 21(12):3876-87

Markiewicz E, Dechat T, Foisner R, Quinlan RA and Hutchison CJ (2002) Lamin A/C binding protein LAP2alpha is required for nuclear anchorage of retinoblastoma protein. *Mol Biol Cell.* 13(12):4401-13

Matsuda S, Harries JC, Viskaduraki M, Troke PJ, Kindle KB, Ryan C and Heery DM (2004) A Conserved alpha-helical motif mediates the binding of diverse nuclear proteins to the SRC1 interaction domain of CBP. *J Biol Chem.* 279(14):14055-64

Matsuura Y and Stewart M (2004) Structural basis for the assembly of a nuclear export complex. *Nature* 432(7019):872-7

Mayeda A, Badolato J, Kobayashi R, Zhang MQ, Gardiner EM and Krainer AR (1999) Purification and characterization of human RNPS1: a general activator of pre-mRNA splicing. *EMBO J.* 18(16):4560-70

McCampbell A, Taye AA, Whitty L, Penney E, Steffan JS and Fischbeck KH (2001) Histone deacetylase inhibitors reduce polyglutamine toxicity. *Proc Natl Acad Sci U S A.* 98(26):15179-84

McCampbell A, Taylor JP, Taye AA, Robitschek J, Li M, Walcott J, Merry D, Chai Y, Paulson H, Sobue G and Fischbeck KH (2000) CREB-binding protein sequestration by expanded polyglutamine *Hum Mol Genet.* 9(14):2197-202

Metivier R, Penot G, Hubner MR, Reid G, Brand H, Kos M and Gannon F (2003) Estrogen receptor-alpha directs ordered, cyclical, and combinatorial recruitment of cofactors on a natural target promoter *Cell* 115(6):751-63

Metzger E, Muller JM, Ferrari S, Buettner R and Schule R (2003) A novel inducible transactivation domain in the androgen receptor: implications for PRK in prostate cancer. *EMBO J.* 22(2):270-80

Minamiyama M, Katsuno M, Adachi H, Waza M, Sang C, Kobayashi Y, Tanaka F, Doyu M, Inukai A and Sobue G (2004) Sodium butyrate ameliorates phenotypic expression in a transgenic mouse model of spinal and bulbar muscular atrophy.*Hum Mol Genet.* 13(11):1183-92

Moller A, Sirma H. Hofmann TG, Rueffer S, Klimczak E, Droge W, Will H and Schmitz ML (2003) PML is required for homeodomain-interacting protein kinase 2 (HIPK2)-mediated p53 phosphorylation and cell cycle arrest but is dispensable for the formation of HIPK domains.*Cancer Res.* 63(15):4310-4

Muller S and Dejean A (1999) Viral immediate-early proteins abrogate the modification by SUMO-1 of PML and Sp100 proteins, correlating with nuclear body disruption. *J Virol.* 73(6):5137-43

Munshi N, Merika M, Yie J, Senger K, Chen G and Thanos D (1998) Acetylation of HMG I(Y) by CBP turns off IFN beta expression by disrupting the enhanceosome. *Mol Cell.* 2(4):457-67

Muratani M, Gerlich D, Janicki SM, Gebhard M, Eils R and Spector DL (2002) Metabolic-energy-dependent movement of PML bodies within the mammalian cell nucleus. *Nat Cell Biol.* 4(2):106-10

Nabetani A, Yokoyama O and Ishikawa F (2004) Localization of hRad9, hHus1, hRad1, and hRad17 and caffeine-sensitive DNA replication at the alternative lengthening of telomeres-associated promyelocytic leukemia body. *J Biol Chem.* 279(24):25849-57

Nakagawa K and Yokosawa H (2002) PIAS3 induces SUMO-1 modification and transcriptional repression of IRF-1. *FEBS Lett.* 530(1-3):204-8

Narlikar GJ, Fan HY and Kingston RE (2002) Cooperation between complexes that regulate chromatin structure and transcription. *Cell* 108(4):475-87

Nathan D, Ingvarsdottir K, Sterner DE, Bylebyl GR, Dokmanovic M, Dorsey JA, Whelan KA, Krsmanovic M, Lane WS, Meluh PB, Johnson ES and Berger SL (2006) Histone sumoylation is a negative regulator in Saccharomyces cerevisiae and shows dynamic interplay with positive-acting histone modifications. *Genes Dev.* 20(8):966-76

Neuwald AF and Hirano T (2000) HEAT repeats associated with condensins, cohesins, and other complexes involved in chromosome-related functions. *Genome Res.* 10(10):1445-52

Nielsen SJ, Schneider R, Bauer UM, Bannister AJ, Morrison A, O'Carroll D, Firestein R, Cleary M, Jenuwein T, Herrera RE, Kouzarides T (2001) Rb targets histone H3 methylation and HP1 to promoters. *Nature* 412(6846):561-5

North BJ, Marshall BL, Borra MT, Denu JM and Verdin E (2003) The human Sir2 ortholog, SIRT2, is an NAD+-dependent tubulin deacetylase. *Mol Cell.* 11(2):437-44

Nucifora FC Jr, Sasaki M, Peters MF, Huang H, Cooper JK, Yamada M, Takahashi H, Tsuji S, Troncoso J, Dawson VL, Dawson TM and Ross CA (2001) Interference by huntingtin and atrophin-1 with cbp-mediated transcription leading to cellular toxicity. *Science* 291(5512):2423-8

Ogryzko VV, Brinkmann E, Howard BH, Pastan I and Brinkmann U (1997) Antisense inhibition of CAS, the human homologue of the yeast chromosome segregation gene CSE1, interferes with mitosis in HeLa cells. *Biochemistry* 36(31):9493-500

Osborne CS, Chakalova L, Brown KE, Carter D, Horton A, Debrand E, Goyenechea B, Mitchell JA, Lopes S, Reik W and Fraser P. (2004) Active genes dynamically colocalize to shared sites of ongoing transcription. *Nat Genet.* 36(10):1065-71

Owerbach D, McKay EM, Yeh ET, Gabbay KH and Bohren KM (2005) A proline-90 residue unique to SUMO-4 prevents maturation and sumoylation. *Biochem Biophys Res Commun.* 337(2):517-20

Pickart CM (2001) Mechanisms underlying ubiquitination. *Annu Rev Biochem.* 70:503-33

Papeleu P, Loyer P, Vanhaecke T, Elaut G, Geerts A, Guguen-Guillouzo C and Rogiers V (2003) Trichostatin A induces differential cell cycle arrests but does not induce apoptosis in primary cultures of mitogen-stimulated rat hepatocytes.*J Hepatol.* 39(3):374-82

Peterson CL and Laniel MA (2004) Histones and histone modifications. *Curr Biol.* 14(14):R546-51

Petrij F, Giles RH, Dauwerse HG, Saris JJ, Hennekam RC, Masuno M, Tommerup N, van Ommen GJ, Goodman RH, Peters DJ, et al (1995) Rubinstein-Taybi syndrome caused by mutations in the transcriptional co-activator CBP. *Nature* 376(6538):348-51

Pombo A, Cuello P, Schul W, Yoon JB, Roeder RG, Cook PR and Murphy S (1998) Regional and temporal specialization in the nucleus: a transcriptionally-active nuclear domain rich in PTF, Oct1 and PIKA antigens associates with specific chromosomes early in the cell cycle. *EMBO J.* 17(6):1768-78

Pombo A, Jackson DA, Hollinshead M, Wang Z, Roeder RG and Cook PR (1999) Regional specialization in human nuclei: visualization of discrete sites of transcription by RNA polymerase III.*EMBO J.* 18(8):2241-53

Ragvin A, Valvatne H, Erdal S, Arskog V, Tufteland KR, Breen K, OYan AM, Eberharter A, Gibson TJ, Becker PB and Aasland R (2004) Nucleosome binding by the bromodomain and PHD finger of the transcriptional cofactor p300. *J Mol Biol.* 337(4):773-88

Reverter D and Lima CD (2005) Insights into E3 ligase activity revealed by a SUMO-RanGAP1-Ubc9-Nup358 complex. *Nature* 435(7042):687-92

Rice JC, Nishioka K, Sarma K, Steward R, Reinberg D and Allis CD (2002) Mitotic-specific methylation of histone H4 Lys 20 follows increased PR-Set7 expression and its localization to mitotic chromosomes. *Genes Dev.* 16(17):2225-30

Riquelme C, Barthel KK and Liu X (2006) SUMO-1 modification of MEF2A regulates its transcriptional activity. *J Cell Mol Med.* 10(1):132-44.

Rodriguez MS, Desterro JM, Lain S, Midgley CA, Lane DP and Hay RT (1999) SUMO-1 modification activates the transcriptional response of p53. *EMBO J.* 18(22):6455-61

Roeder RG (1996) The role of general initiation factors in transcription by RNA polymerase II. *Trends Biochem Sci.* 21(9):327-35

Ross S, Best JL, Zon LI and Gill G (2002) SUMO-1 modification represses Sp3 transcriptional activation and modulates its subnuclear localization. *Mol Cell.* 10(4):831-42

Ryan CM, Harries JC, Kindle KB, Collins HM and Heery DM (2006) Functional interaction of CREB binding protein (CBP) with nuclear transport proteins and modulation by HDAC inhibitors. *Cell Cycle* 5(18):2146-52

Sachdev S, Bruhn L, Sieber H, Pichler A, Melchior F, Grosschedl R (2001) PIASy, a nuclear matrix-associated SUMO E3 ligase, represses LEF1 activity by sequestration into nuclear bodies. *Genes Dev* 15(23):3088-103

Saitoh H and Hinchey J (2000) Functional heterogeneity of small ubiquitin-related protein modifiers SUMO-1 versus SUMO-2/3. *J Biol Chem.* 275(9):6252-8

Saitoh N, Uchimura Y, Tachibana T, Sugahara S, Saitoh H and Mitsuyoshi N (2006) In situ SUMOylation analysis reveals a modulatory role of RanBP2 in the nuclear rim and PML bodies. *Exp Cell Res.* 312(8):1418-30

Sambrook J and Russell DW (1989) Molecular cloning a laboratory manual *CSHL press* 1st edition

Santos-Rosa H and Caldas C (2005) Chromatin modifier enzymes, the histone code and cancer. *Eur J Cancer.* 41(16):2381-402

Scherf U, Kalab P, Dasso M, Pastan I and Brinkmann U (1998) The hCSE1/CAS protein is phosphorylated by HeLa extracts and MEK-1: MEK-1 phosphorylation may modulate the intracellular localization of CAS. *Biochem Biophys Res Commun.* 250(3):623-8

Scherf U, Pastan I, Willingham MC and Brinkmann U (1996) The human CAS protein which is homologous to the CSE1 yeast chromosome segregation gene product is associated with microtubules and mitotic spindle. *Proc Natl Acad Sci U S A* 93(7):2670-4

Schmidt D and Muller S (2002) Members of the PIAS family act as SUMO ligases for c-Jun and p53 and repress p53 activity. *Proc Natl Acad Sci U S A*. 99(5):2872-7

Schneider J, Dover J, Johnston M and Shilatifard A (2004) Global proteomic analysis of *S. cerevisiae* (GPS) to identify proteins required for histone modifications. *Methods Enzymol.* 2004;377:227-34

Sheppard HM, Harries JC, Hussain S, Bevan C and Heery DM (2001) Analysis of the steroid receptor coactivator 1 (SRC1)-CREB binding protein interaction interface and its importance for the function of SRC1. *Mol Cell Biol.* 21(1):39-50

Shi Y, Lan F, Matson C, Mulligan P, Whetstine JR, Cole PA, Casero RA, Shi Y (2004) Histone demethylation mediated by the nuclear amine oxidase homolog LSD1. *Cell* 119(7):941-53

Shiels C, Islam SA, Vatcheva R, Sasieni P, Sternberg MJ, Freemont PS, Sheer D (2001) PML bodies associate specifically with the MHC gene cluster in interphase nuclei. *J Cell Sci.* 114(Pt 20):3705-16

Shiio Y and Eisenman RN. (2003) Histone sumoylation is associated with transcriptional repression. *Proc Natl Acad Sci U S A.* 100(23):13225-30

Shopland LS, Johnson CV, Byron M, McNeil J and Lawrence JB (2003) Clustering of multiple specific genes and gene-rich R-bands around SC-35 domains: evidence for local euchromatic neighborhoods. *J Cell Biol.* 162(6):981-90

Song J, Durrin LK, Wilkinson TA, Krontiris TG and Chen Y (2004) identification of a SUMO-binding motif that recognizes SUMO-modified proteins. *Proc Natl Acad Sci U S A.* 101(40):14373-8

Song CZ, Keller K, Chen Y, Murata K and Stamatoyannopoulos G (2002) Transcription coactivator CBP has direct DNA binding activity and stimulates transcription factor DNA binding through small domains. *Biochem Biophys Res Commun.* 296(1):118-24

Sopher BL, Thomas PS Jr, LaFevre-Bernt MA, Holm IE, Wilke SA, Ware CB, Jin LW, Libby RT, Ellerby LM and La Spada AR (2004) Androgen receptor YAC transgenic mice recapitulate SBMA motor neuronopathy and implicate VEGF164 in the motor neuron degeneration. *Neuron* 41(5):687-99

Spector DL (2003) The dynamics of chromosome organization and gene regulation. *Annu Rev Biochem.* 72:573-608

Steffan JS, Bodai L, Pallos J, Poelman M, McCampbell A, Apostol BL, Kazantsev A, Schmidt E, Zhu YZ, Greenwald M, Kurokawa R, Housman DE, Jackson GR, Marsh JL and Thompson LM (2001) Histone deacetylase inhibitors arrest polyglutamine-dependent neurodegeneration in Drosophila. *Nature* 413(6857):739-43

Steffan JS, Kazantsev A, Spasic-Boskovic O, Greenwald M, Zhu YZ, Gohler H, Wanker EE, Bates GP, Housman DE and Thompson LM (2000) The Huntington's disease protein interacts with p53 and CREB-binding protein and represses transcription. *Proc Natl Acad Sci U S A.* 97(12):6763-8

Stenoien DL, Cummings CJ, Adams HP, Mancini MG, Patel K, DeMartino GN, Marcelli M, Weigel NL and Mancini MA (1999) Polyglutamine-expanded androgen receptors form aggregates that sequester heat shock proteins, proteasome components and SRC-1, and are suppressed by the HDJ-2 chaperone. *Hum Mol Genet.* 8(5):731-41

Sterner R, Vidali G, Allfrey VG (1979) Studies of acetylation and deacetylation in high mobility group proteins. Identification of the sites of acetylation in HMG-1. *J Biol Chem.* 254(22):11577-83

Sternsdorf T, Jensen K and Will H (1997) Evidence for covalent modification of the nuclear dot-associated proteins PML and Sp100 by PIC1/SUMO-1. *J Cell Biol.* 139(7):1621-34

Strahl BD, Briggs SD, Brame CJ, Caldwell JA, Koh SS, Ma H, Cook RG, Shabanowitz J, Hunt DF, Stallcup MR, Allis CD (2001) Methylation of histone H4 at arginine 3 occurs in vivo and is mediated by the nuclear receptor coactivator PRMT1. *Curr Biol.* 11(12):996-1000

Subramanian C, Opipari AW Jr, Bian X, Castle VP and Kwok RP (2005) Ku70 acetylation mediates neuroblastoma cell death induced by histone deacetylase inhibitors. *Proc Natl Acad Sci U S A.* 102(13):4842-7

Sun J, Xu H, Subramony SH and Hebert MD (2005) Interactions between coilin and PIASy partially link Cajal bodies to PML bodies. *J Cell Sci.* 118(Pt 21):4995-5003

Taddei A, Van Houwe G, Hediger F, Kalck V, Cubizolles F, Schober H and Gasser SM (2006) Nuclear pore association confers optimal expression levels for an inducible yeast gene. *Nature* 441(7094):774-8

Takahashi H, Hatakeyama S, Saitoh H and Nakayama KI (2005) Noncovalent SUMO-1 binding activity of thymine DNA glycosylase (TDG) is required for its SUMO-1 modification and colocalization with the promyelocytic leukemia protein. *J Biol Chem.* 280(7):5611-21

Tatham MH, Jaffray E, Vaughan OA, Desterro JM, Botting CH, Naismith JH and Hay RT (2001) Polymeric chains of SUMO-2 and SUMO-3 are conjugated to protein substrates by SAE1/SAE2 and Ubc9. *J Biol Chem.* 276(38):35368-74

Taylor JP, Taye AA, Campbell C, Kazemi-Esfarjani P, Fischbeck KH and Min KT (2003) Aberrant histone acetylation, altered transcription, and retinal degeneration in a Drosophila model of polyglutamine disease are rescued by CREB-binding protein. *Genes Dev.* 17(12):1463-8

Thomas MC and Chiang CM (2006) The general transcription machinery and general cofactors. *Crit Rev Biochem Mol Biol.* 41(3):105-78

Tong JK, Hassig CA, Schnitzler GR, Kingston RE and Schreiber SL (1998) Chromatin deacetylation by an ATP-dependent nucleosome remodelling complex. *Nature* 395(6705):917-21

Toth KF, Knoch TA, Wachsmuth M, Frank-Stohr M, Stohr M, Bacher CP, Muller G and Rippe K (2004) Trichostatin A-induced histone acetylation causes decondensation of interphase chromatin. *J Cell Sci.* 117(Pt 18):4277-87

Trask B, van den Engh G, Pinkel D, Mullikin J, Waldman F, van Dekken H and Gray J (1988) Fluorescence in situ hybridization to interphase cell nuclei in suspension allows flow cytometric analysis of chromosome content and microscopic analysis of nuclear organization. *Hum Genet.* 78(3):251-9

Troke PJ, Kindle KB, Collins HM, Heery DM (2006) MOZ fusion proteins in acute myeloid leukaemia. *Biochem Soc Symp.* 2006;(73):23-39

Tsai MJ and O'Malley BW (1994) Molecular mechanisms of action of steroid/thyroid receptor superfamily members. *Annu Rev Biochem.* 63:451-86

Vassileva MT and Matunis MJ (2004) SUMO modification of heterogeneous nuclear ribonucleoproteins. *Mol Cell Biol.* 24(9):3623-32

Vaziri H, Dessain SK, Ng Eaton E, Imai SI, Frye RA, Pandita TK, Guarente L and Weinberg RA (2001) hSIR2(SIRT1) functions as an NAD-dependent p53 deacetylase. *Cell* 107(2):149-59

Vertegaal AC, Ogg SC, Jaffray E, Rodriguez MS, Hay RT, Andersen JS, Mann M and Lamond AI (2004) A proteomic study of SUMO-2 target proteins. *J Biol Chem.* 279(32):33791-8

Volpi EV, Chevret E, Jones T, Vatcheva R, Williamson J, Beck S, Campbell RD, Goldsworthy M, Powis SH, Ragoussis J, Trowsdale J and Sheer D (2000) Large-scale chromatin organization of the major histocompatibility complex and other regions of human chromosome 6 and its response to interferon in interphase nuclei. *J Cell Sci.* 113 (Pt 9):1565-76

Wang R, Cherukuri P and Luo J (2005) Activation of Stat3 sequence-specific DNA binding and transcription by p300/CREB-binding protein-mediated acetylation *J Biol Chem.* 280(12):11528-34

Wang W, Yang X, Kawai T, Lopez de Silanes I, Mazan-Mamczarz K, Chen P, Chook YM, Quensel C, Kohler M and Gorospe M (2004) AMP-activated protein kinase-regulated phosphorylation and acetylation of importin alpha1: involvement in the nuclear import of RNA-binding protein HuR. *J Biol Chem.* 279(46):48376-884

Warrell RP Jr, He LZ, Richon V, Calleja E and Pandolfi PP (1998) Therapeutic targeting of transcription in acute promyelocytic leukemia by use of an inhibitor of histone deacetylase. *J Natl Cancer Inst.* 90(21):1621-5

Waters L, Yue B, Veverka V, Renshaw P, Bramham J, Matsuda S, Frenkiel T, Kelly G, Muskett F, Carr M and Heery DM (2006) Structural diversity in p160/CREB-binding protein coactivator complexes. *J Biol Chem.* 281(21):14787-95

Weger S, Hammer E, Engstler M (2003) The DNA topoisomerase I binding protein topors as a novel cellular target for SUMO-1 modification: characterization of domains necessary for subcellular localization and sumolation. *Exp Cell Res.* 290(1):13-27

Weis K, Rambaud S, Lavau C, Jansen J, Carvalho T, Carmo-Fonseca M, Lamond A and Dejean A (1994) Retinoic acid regulates aberrant nuclear localization of PML-RAR alpha in acute promyelocytic leukemia cells. *Cell* 76(2):345-56

Williams RR, Broad S, Sheer D and Ragoussis J (2002) Subchromosomal positioning of the epidermal differentiation complex (EDC) in keratinocyte and lymphoblast interphase nuclei. *Exp Cell Res.* 272(2):163-75

Yang SH and Sharrocks AD (2004) SUMO promotes HDAC-mediated transcriptional repression. *Mol Cell.* 13(4):611-7

Yao YL, Yang WM and Seto E (2001) Regulation of transcription factor YY1 by acetylation and deacetylation. *Mol Cell Biol.* 21(17):5979-91

Yasuda S, Inoue K, Hirabayashi M, Higashiyama H, Yamamoto Y, Fuyuhiro H, Komure O, Tanaka F, Sobue G, Tsuchiya K, Hamada K, Sasaki H, Takeda K, Ichijo H and Kakizuka A (2003) Triggering of neuronal cell death by accumulation of activated SEK1 on nuclear polyglutamine aggregations in PML bodies. *Genes Cells.* 4(12):743-56

Yu C, Rahmani M, Almenara J, Subler M, Krystal G, Conrad D, Varticovski L, Dent P and Grant S (2003) Histone deacetylase inhibitors promote STI571-mediated apoptosis in STI571-sensitive and -resistant Bcr/Abl+ human myeloid leukemia cells. *Cancer Res.* 63(9):2118-26

Zeitlin SG, Barber CM, Allis CD, Sullivan KF. (2001) Differential regulation of CENP-A and histone H3 phosphorylation in G2/M. *J Cell Sci.* 114(Pt 4):653-61

Zhang W, Kadam S, Emerson BM and Bieker JJ (2001) Site-specific acetylation by p300 or CREB binding protein regulates erythroid Kruppel-like factor transcriptional activity via its interaction with the SWI-SNF complex. *Mol Cell Biol.* 21(7):2413-22

Zimber A, Nguyen QD, Gespach C (2004) Nuclear bodies and compartments: functional roles and cellular signalling in health and disease. *Cell Signal.* 16(10):1085-104

Publication List

Ryan C, Harries JC, Kindle KB, Collins HM and Heery DM (2006) Functional Interaction of CREB Binding Protein (CBP) with Nuclear Transport Proteins and Modulation by HDAC Inhibitors *Cell Cycle* 5(18):2146-52

Collins HM, Kindle KB, Matsuda S, Ryan C, Troke PJ, Kalkhoven E and Heery DM (2006) MOZ-TIF2 alters cofactor recruitment and histone modification at the RARbeta2 promoter: differential effects of MOZ fusion proteins on CBP- and MOZ-dependent activators. *J Biol Chem.* 281(25):17124-33

Kumar AP, Ryan C, Cordy V and Reynolds WF (2005) Inducible nitric oxide synthase expression is inhibited by myeloperoxidase.
Nitric Oxide 13(1):42-53

Matsuda S, Harries JC, Viskaduraki M, Troke PJ, Kindle KB, Ryan C and Heery DM (2004) A Conserved alpha-helical motif mediates the binding of diverse nuclear proteins to the SRC1 interaction domain of CBP. *J Biol Chem.* 279(14):14055-64

Ryan C, Kindle KB, Collins HM and Heery DM (2006) SUMOylation affects the subcellular localisation and transcriptional activity of CBP *(in preparation)*

Functional Interaction of CREB Binding Protein (CBP) with Nuclear Transport Proteins and Modulation by HDAC Inhibitors

Colm Ryan, Janet C. Harries, Karin B. Kindle, Hilary M. Collins & David M. Heery*

School of Pharmacy, University Park, University of Nottingham, Nottingham NG7 2RD, United Kingdom.

Phone: 00-44-115-951-5087
Fax: 00-44-115-846-6249
email : david.heery@nottingham.ac.uk

*Corresponding author

Abstract

Nuclear transport proteins such as CSE1, NUP93 and Importinα have recently been shown to be chromatin-associated proteins in yeast, which have unexpected functions in gene regulation. Here we report interactions between the mammalian histone acetyltransferase CBP with nuclear transport proteins CAS (a CSE1 homologue) and Importin-α (Impα) and NUP93. CAS was found to bind the SRC1 interaction domain (SID) of CBP via a leucine-rich motif in the N-terminus of the protein, that is conserved in other SID-binding proteins. Co-immunoprecipitation experiments also revealed that CBP and Impα proteins form a complex. As Impα is a known acetylation target of CBP/p300, and is recycled to the cytoplasm via the exportin CAS, we investigated whether HDAC inhibitors would alter the subcellular localisation of these proteins. Treatment of COS-1 cells with the HDAC inhibitors trichostatin A or sodium butyrate resulted in sequestration of Impα in the nuclear envelope, accumulation of CAS in nuclear aggregates, and an increased number of CBP-containing PML bodies per cell. In addition, HDACi treatment appeared to enhance the association of Impα and CBP in co-immunoprecipitation experiments. Our results provide evidence for novel functional

interactions between the chromatin modification enzyme CBP and nuclear transport proteins in mammalian cells.

Introduction

CBP and p300 are protein acetyltransferases that function as transcriptional coactivators for a wide range of DNA binding transcription factors. Recruitment of CBP to gene promoters results in chromatin modification, chiefly by acetylation of lysine residues in histone N-terminal tails[1]. In addition to histones, CBP/p300 proteins acetylate a number of chromatin-associated proteins such as p53,[2] TFIIE, TFIIF,[3] Ku70,[4] MyoD,[5] and ACTR.[6] However, it has also been reported that CBP acetylates the nuclear import factors Importinα (Impα) and Impα-7.[7] The implications of this are unclear, and may suggest that CBP regulates other nuclear processes such as nucleo-cytoplasmic shuttling of importins[8] or alternatively, may indicate a role of nuclear transport proteins in transcriptional regulation in mammalian cells.

The interaction of CBP and p300 with diverse nuclear proteins is facilitated by multiple subdomains, including LXXLL motifs, CH1, KIX, bromodomain, CRD1, CH3 and SID. These domains display both distinct and overlapping substrate-binding specificities.[1] For example, the SRC1 Interaction domain (SID) mediates binding to the p160 coactivators[9] as well as transcription factors Ets-2 and IRF3, and viral proteins such as Tax and E1A.[10] These proteins share a conserved leucine-rich amphipathic α-helix that is critical for interactions with the SID.[10] Recent structural studies of the CBP-SID domain in complex with p160 AD1 domains or IRF3 revealed that complex formation induces folding, although structural diversity was observed between different complexes.[11-13]

To identify novel CBP-SID binding proteins we performed a yeast 2-hybrid screen of a mouse embryo cDNA library.[10] We report here the identification of interactions between CBP and nuclear transport proteins. Our findings suggest a role for protein acetylation in controlling functional interactions between CBP and nuclear transport machinery.

Materials and Methods

Plasmid Expression Vectors

The following plasmids used in this study have been described previously; DBD LexA-CBP series 1982–2163, 1982–2130, 1982–2111, 1982–2100, 1982–2080, 2000–2163, 2017–2163, 2041–2163, 2041–2130, 2058–2163, 2058–2130, and 2073–2163; DBD LexA-CBP SID (2058–2130) mutant series, L2071A/L2072A/ L2075A, Q2082R, F2101P, K2103A, K2103P, K2108A, Q2117A/P2118A, pSG5CBP,[9] pSG5-HIS-Myc-Impα,[7] pQE30-HIS-CAS,[14] pEYFP-CBP.[15] The following plasmids were generous gifts and have been described previously; pASV3, pASV3-mouse embryonic cDNA library.[16]

cDNA sequences flanked by appropriate restriction enzyme sites were generated by PCR using *Elongase* (Invitrogen) or KOD HiFi (Novagen) and cloned in frame into a modified version of the pASV3 vector[16] to generate VP16-acidic activation domain (AAD) fusion proteins. All constructs generated in this study were verified by sequence analysis.

(i) pASV3(mod)CAS-NΔ244-255. PCRs were carried out using pSG5CAS-N (amino acids 1-349) with CASXho1F and delta reverse primers and the delta forward and CAS382Ksp1R primers. The products were combined by recombinant PCR. The resulting fragment was digested with Xho1 and Ksp1 restriction enzymes and cloned into pASV(mod). CASXho1F 5'-AAAACTCGAGATGGAGCTCAGCGATGCG-3'; delta reverse 5'-CTCTTCATCATCAGTCTGGGTATGAAAATTGTTCAT-3'; delta forward 5'-ATGAACAATTTTCATACCCAGACTGATGATGAAGAG-3'; CAS382Ksp1R 5'-AAAACCGCGGCGGCACAATAACTTTTTCACAGATAC-3'.

Yeast Methods

The yeast two-hybrid screen was carried out essentially as described previously.[16] *Saccharomyces cerevisiae* L40 cells expressing DBD-LexA-CBP (1982–2163) were transformed with the pASV3 mouse embryo cDNA library using a modified lithium acetate transformation method.[16] Transformants were initially selected for L-leucine and L-tryptophan prototrophy on dropout medium resulting in the recovery of 1.5 x 10^6 library clones. The library was then re-plated (10-fold) onto dropout medium with selection for L-leucine, L-tryptophan, and L-histidine prototrophy, and resistance to either 10 mM or 20mM 3-aminotriazole (3-AT), to select bait-interacting clones. Colonies capable of growth on 3-AT and showing strong activation of the secondary reporter (β-galactosidase) were subjected to further analysis. The putative positives from the first round of selection were cultured in the presence of L-tryptophan to eliminate the bait plasmid, followed by rescue of pASV3 library (LEU2) plasmids in *E. coli* HB101 (*leuB-*) by complementation on M9 minimal medium containing 100 μg/ml ampicillin, and lacking L-leucine.[16] *Bona fide* positive clones were selected by retransformation of fresh L40 pBTM116-CBP 1982–2163 and testing for 3-AT resistance and β-galactosidase activity. Quantitative β-galactosidase assays were carried out in duplicate, in three separate experiments, as previously described and reporter activities are expressed as nmol of substrate transformed/min/mg protein extract; data shown the mean of three experiments.[9,16] The expression of fusion proteins in cell-free extracts was monitored by Western blotting using antibodies (Autogen BioClear) directed against VP16 (sc-7545).

Co-immunoprecipitations and Western blotting

HEK293 cells were seeded at a density of 2 x 10^5 cells per ml in 10-cm dishes, and transfected with 10μg of either pSG5-HIS-Myc-Impα vector, or pSG5-FLAG-SRC1e in addition to 10 μg of pSG5-CBP. 48 hours post-transfection whole cell extracts were prepared as follows: cell pellets were washed twice in 0.5 ml of cold phosphate-buffered saline and lysed in 400μl of lysis buffer (50 mM Tris-HCl, pH 7.5; 150 mM NaCl; 0.5% Nonidet P-40, 0.1% SDS), and fresh protease and phosphatase inhibitors. The extract was homogenised ~15 times using 19G needle and incubated at 0 °C for 30 min. The lysate was then pre-cleared for 30 min at 4 °C with 20 μl of protein-A/G PLUS-agarose beads (Autogen Bioclear, sc-2003) and subsequently centrifuged at 10 krpm, 4 °C, for 10 min. To prepare an immuno-affinity matrix, 5μl anti-Impα antibody was incubated with 20 μl of packed volume protein-A/G PLUS-agarose beads (Autogen Bioclear, sc-2003) at 0°C. Impα proteins were purified using the preprepared 20 μl mix of protein-A/G PLUS-agarose beads (Autogen Bioclear, sc-2003) and anti-Impα on a rotating wheel overnight at 4 °C for 2 hours, followed by three washes in 0.5 ml of lysis buffer. Proteins bound to the beads were separated by SDS-PAGE (6% acrylamide for CBP, 12% acrylamide for Impα proteins), transferred to nitrocellulose and detected by Western blotting. Impα proteins were detected using a 1:1000 dilution of α-Impα monoclonal antibody followed by a 1:5000 dilution of secondary α-mouse IgG-HRP (Autogen Bioclear, sc-2954). For detection of co-purified CBP, α-CBP (A-22) rabbit polyclonal (Autogen Bioclear, sc-583) was used, in conjunction with a 1:5000 dilution of anti-rabbit IgG-HRP (Autogen Bioclear, sc-2004).

Immunofluorescence

COS-1 cells were plated onto coverslips in six-well plates at $1x10^5$ to $3x10^5$ cells/well and, where appropriate, transfected 24 hours later using TransFast (Promega) according to the manufacturer's protocol. After 48 hours, the cells were fixed in 4% paraformaldehyde and permeabilised with 0.2% Triton X-100. The cells were washed and, after blocking in 3% bovine serum albumin– PBS, incubated with primary antibodies (1:50 dilution for overexpressed proteins, 1:10 for CBP, 1:30 for PML, 1:100 for Impα and 1:25 for CAS). After incubation for 1 hour, the cells were washed and incubated with the secondary antibody (1:400 dilution). The samples were viewed with a fluorescence microscope (Zeiss Axiovert 200 M) or a confocal laser-scanning microscope (Zeiss LSM510).

Results

CAS associates with the C-terminus of CBP

To identify novel CBP-binding factors we performed a yeast-2-hybrid screen of a VP16AAD-fused mouse embryo cDNA library using LexA-CBP 2041-2165 as bait.[10] Several strongly interacting clones were identified including the *pointed* domain of Ets-2.[10] Sequence analysis of another positive clone identified the N-terminus ($\alpha\alpha$s 1-349) of the mouse homolog of human cellular apoptosis susceptibility protein CAS (clone 1-09),[17] which has been reported to function in recycling of Importin-α from the nucleus to the cytoplasm.[14,18,19,20] This region of CAS was reported to be required for complex formation with RAN-GTP. A second interacting clone was identified as nucleoporin Nup93, a mammalian homologue of the *S.cerevisiae* nucleoporin Nic96 (data not shown). The identified region corresponded to the N-terminal 165 amino acids of Nup93, which contains heptad repeats similar to coiled-coil or leucine-zipper motifs.[21] However, in this study, we focused on the potential interaction between CBP and CAS proteins.

As the boundaries of the bait sequence used (1982-2163) in the screen extended beyond what is now known to be the minimal SID, a series of LexA-CBP fusion proteins were used to define the minimal sequences capable of binding each protein isolated in the screen. The sequence encoding the CAS N-terminus (1-349) was PCR amplified to remove sequences derived from 5'UTR in the original library clones and then recloned into pASV3. As shown in Figure 1B, deletion analysis indicated that the minimal CBP sequence for CAS-N binding was located between amino acids 2058 and 2130.

Mutations in the SID disrupt CAS binding

NMR studies have determined that complexes involving the p160 AD1 and CBP-SID involves largely hydrophobic interactions involving a tight 4-helix bundle formed from three α-helices in CBP SID (Cα1, Cα2 Cα3)[11,12] and a conserved leucine-rich α-helix present in p160 family members and other SID-binding proteins.[10] However, we previously reported differential effects of mutations within the SID on binding SRC1, Ets-2 and E1A,[9,10] suggesting that the complexes formed may have topological differences. To determine the sequence requirements for CAS interaction with the SID, we carried out yeast two hybrid experiments with a panel of LexA-SID proteins containing various amino acid replacement mutations. As shown in Figure 1C, a F-2101-P mutation in Cα3 completely disrupted CAS interaction with the SID, as previously observed for Ets-2, E1A and SRC1.[10] This is likely to be due to the role of F-2101 in stabilising the complex, as it lies at the hydrophobic core of the 4-helix bundle in CBP/160 complexes.[11] The K-2103-P mutation reduced the reporter activation due to binding of CAS-N and SID by approximately 4-fold, (Fig. 1C) in contrast to Ets-2 and SRC1, which are unable to bind SID proteins containing this mutation.[10] As previously observed for SRC1, K-2108-A had little effect on the CAS/ SID interaction (Fig. 1C), in contrast to the binding of the Ets-2 *pointed* domain.[10] The CAS-N/SID interaction was also disrupted by L-2071/2/5-A, which reduces hydrophobicity of the Cα1 of CBP. A similar effect was observed previously for the binding of the Ets-2 PNT domain to the SID, but not SRC1 AD1, which was only moderately affected (2-fold reduction in reporter activity). [9,10] As observed for other SID binding proteins, Q-2083-R mutation did not adversely affect CAS-N binding. However, CAS differs from both Ets-2 and SRC1 in that it is more tolerant of the K-2103-P mutation in Cα3. Taken together, our results indicate differential sensitivities of CAS and other SID-binding proteins to amino acid substitutions in Cα1 and Cα3. This suggests structural flexibility in the docking of CAS, Ets-2 and SRC1 proteins with CBP, consistent with the observation that of different topologies of the CBP SID in complex with p160s or IRF3.[11-13]

Sequence comparisons revealed that the N-terminus of CAS contains a sequence showing homology to the LLXXLXXLL motif present in p160s and other SID binding proteins (residues 244-255; Fig. 1D). To determine if this leucine-rich motif of CAS was necessary for the interaction between CAS and CBP, we generated a VP16-AAD CAS-N fusion in which the leucine-rich sequence had been deleted. Reporter assays were carried out in a yeast L40 strain coexpressing CAS-NΔ244-255 and LexA-CBP SID. As shown in Fig. 1D, deletion of the leucine-rich motif abrogates binding of CAS-N to the CBP SID. Thus, the association between CAS and CBP appears to require a conserved leucine-rich motif.

CBP co-localises with CAS *in vivo*

To determine whether CBP and the N-terminus of CAS interact *in vivo*, COS-1 cells were transfected with a vector expressing residues 1-349 of CAS (FLAG-CAS-N). The majority of transfected cells showed predominant localisation of FLAG-CAS-N proteins to the nucleus with exclusion from nucleolar regions (Fig. 1E). A proportion of the nuclear FLAG-CAS-N proteins were observed to be present in subnuclear foci, resembling PML bodies. Co-staining for endogenous CBP detected co-localisation of CBP and CAS-N at some of these foci, suggesting that some CAS proteins may associate with CBP at PML bodies (Fig. 1E; upper panels). In addition, ectopic expression of CBP with FLAG-CAS-N vectors detected a strong co-localisation of these proteins in subnuclear foci (Fig. 1E; lower panels and data not shown). However, we were unable to unambiguously detect co-immunoprecipitation of full length CAS and CBP, due to non-specific binding of the CAS protein with protein A/G beads in controls (data not shown).

HDAC inhibitors perturb the subcellular distribution of CBP and CAS proteins.

CAS has been implicated in the nucleo-cytoplasmic shuttling of Impα in a RAN-GTP dependent manner. [14,18-20] Interestingly, Impα is acetylated by p300 at Lys22 within the N-terminal Impβ binding domain and this interaction is potentiated by the potent HDAC inhibitor Trichostatin A, TSA. [7,9] Acetylation of this residue was postulated to play a critical role in Impα-mediated nuclear transport.[8] We investigated whether upregulation of global acetylation levels by treating cells with the HDAC inhibitors trichostatin A (TSA) or sodium butyrate (NaB), or over-expression of CBP, had any effect on the subcellular localisation of endogenous Impα and CAS proteins. COS-1 cells were treated with vehicle, 10μM TSA or 20mM NaB. After 18hrs cells were harvested and the endogenous proteins visualised by indirect immunofluorescence with antibodies raised against CBP and CAS. As shown in Figure 2A, endogenous CAS gives a predominantly diffuse, nuclear stain that is excluded from nucleoli. Treatment with increasing concentrations of TSA or NaB was found to drive a proportion of CAS proteins into nuclear aggregates. This contrasts to vehicle-treated cells, in which endogenous CAS displayed a diffuse and predominantly nuclear distribution. However, we did not detect a strong colocalisation between the observed CAS aggregates and PML bodies in HDACi-treated cells (Fig 2A; merge).

Endogenous CBP was found to remain associated with PML bodies in COS-1 cells treated with HDACi (Figs. 2&3). However, we noted that the number of PML bodies appeared to increase after HDACi treatment (Fig. 3A). To confirm this observation, CBP and PML foci were immunostained and quantified in untreated, vehicle-treated, TSA-treated or NaB-treated cells (n=50 for each condition; Fig. 3B). The mean number of CBP foci/nucleus was 8.8 in the untreated control population and 9.8 in the vehicle ethanol population. However, the mean numbers increased on addition of 1μM, 5μM, and 10μM TSA to 11.4, 18.5, and 26.8 foci/nucleus, respectively (Fig. 3B). The mean number of foci/nucleus on addition of 5mM, 10mM and 20mM NaB was 16.7, 21.5 and 21.9, respectively (Fig. 3B). In summary, these results indicate that treatment of COS-1 cells with HDACi compounds increases the number of CBP/PML foci in the nucleus.

Importinα accumulates at the nuclear periphery following HDACi treatment

CAS is involved in the nucleo-cytoplasmic shuttling of Impα and it has been suggested that this process was regulated by p300 via acetylation.[8] Therefore, we investigated the effect of HDACi compounds on the subcellular localisation of Impα. COS1 cells were treated with vehicle, or increasing concentrations of TSA or NaB for 18hrs prior to fixation and staining with antibodies to detect endogenous CBP and Impα. Endogenous Impα was predominantly cytoplasmic in control cells, with a lower detection of Impα in the nucleus (Fig. 4A). However, cells treated with TSA (Fig.4A) or

NaB (data not shown) showed high levels of Impα at the nuclear envelope. This coincided with an increased detection of CBP-containing PML bodies at the nuclear envelope.

As inhibitors of HDAC activity perturbed the subcellular localisation of Impα, we investigated whether over-expression of CBP had a similar effect. COS-1 cells were transfected with an expression vector encoding CBP and stained for endogenous Impα. As observed with HDACi treatment, cells over-expressing CBP displayed a high level of Impα staining at the nuclear periphery, consistent with the hypothesis that acetylation of Impα modulates its subcellular distribution (Fig. 4B).

CBP association with Importin-α is stimulated by TSA

While Impα is acetylated by p300 *in vitro*,[7] it is not known whether Impα interacts with HAT proteins directly *in vivo*. As our results indicate that HDACi treatment can induce partial co-localisation of CBP and Impα proteins at the nuclear periphery, we investigated whether CBP and Impα proteins form *in vivo* complexes, using co-immunoprecipitation experiments. HEK293 cells were transfected with expression constructs for CBP and Impα and either untreated or treated with 10μM TSA for 18hrs prior to harvesting. CBP proteins were successfully precipitated with α-CBP, but not control antibody (Fig. 4C). Western blots using an antibody specific for Impα showed that Impα proteins co-precipitated with CBP, indicating that these proteins can exist in a complex *in vivo*. Treatment of cells with TSA increased the amount of Impα protein bound to CBP, indicating that acetylation may regulate the interaction of these proteins. Interestingly, a higher molecular weight band that cross-reacted with the Impα antibody was also detected (Fig. 4C; indicated with asterix). This was only observed in cells that overexpressed CBP, and may correspond to a hyperacetylated form of Impα as observed previously.[7]

TSA treatment induces co-localisation of CBP and Impα at the nuclear periphery

To test whether TSA treatment had any effect on the subcellular localisation of ectopic Impα and CBP, COS-1 expressing both proteins were treated with TSA or vehicle and subjected to immunostaining. Over-expression of Impα resulted in a dramatic increase in the amount of protein detected in the nucleus (Fig.4D) as compared to endogenous Impα (Fig. 4A). Moreover, coexpression of both Impα and CBP drove a subset of the Impα proteins into nuclear aggregates some of which partially colocalised with CBP foci. Treatment of COS-1 cells over-expressing Impα and CBP with TSA led to the redistribution and colocalisation of the two proteins at the nuclear periphery, consistent with the effects of TSA on endogenous proteins. Taken together, these data suggest that CBP and Impα proteins can coexist in nuclear complexes, suggesting functional interactions between transcription regulator and nuclear transport factors.

Discussion

In this study we have identified components of the nuclear transport machinery as novel CBP-interacting partners. The C-terminus of CBP contains a domain conserved in p300 (SID/IbiD), which mediates interaction with the p160s, Ets-2, IRFs and viral proteins. [9,10,22-25] We have shown here that CAS, a homolog of the yeast exportin CSE1p, is a novel binding partner for the SID. CAS/CSE1p is a member of the β–karyopherin family of exportins, involved in nucleocytoplasmic shuttling of Impα. CAS is also implicated in cellular apoptosis, chromosome segregation and gene regulation.[26] The crystal structure of CSE1 in complex with Impα and RAN-GTP has shown it to be a right-handed superhelix of 20 HEAT repeats.[27] HEAT repeats (huntingtin, elongation factor 3, A subunit of PP2A and TOR) are evolutionarily conserved motifs consisting of pairs of anti-parallel α-helices that are an important structural feature of karyopherins.[28] CSE1 is comprised of N- and C-terminal domains containing HEAT 1-8 and HEAT 13-20 are separated by a flexible hinge region (HEAT 9-12). These domains (or arches) form a ring that wraps around the armadillo (ARM) repeats in the N-terminus of Impα, and RAN-GTP.[27] The CAS sequence isolated in our screen for SID binding proteins consists of amino acids 1-350 corresponding to the N-terminal domain HEAT 1-8.

Amino acid substitutions in the SID were found to have differential effects on the binding of CAS (Fig. 1C), SRC1 and Ets2[10] suggesting subtle differences in the docking of different partners to the SID. This is consistent with observations that the SID can adopt different topologies in complex with p160 proteins[11,12] or IRF3.[13] In common with p160s and other SID binding proteins, CAS contains a leucine-rich sequence resembling the Sα1 helix of SRC1, which forms a stable 4-helix bundle with the SID.[11] Deletion of this sequence disrupted binding of CAS-N and CBP-SID in yeast 2-hybrid assays. Based on the structure of the yeast CSE1 protein, the SID-binding motif lies in the hinge between the HEAT 6 A and B helices. This region is potentially solvent exposed and is close to the region that undergoes a major conformational change on binding of cargo.[29]

Interestingly, in addition to CAS, we also detected an interaction between the SID and the N-terminal 165 amino acids of NUP93 (Figure 1 A), which localises to the nuclear basket of the nuclear pore complex. While the interaction between full length CBP and NUP93 remains to be confirmed, we note that CBP has previously been shown to bind the nucleoporins NUP98 and NUP153, which are also located within the basket structure of the nuclear pore complex. This interaction is mediated via FG repeat sequences, another hydrophobic repeat motif, which are a feature of a subfamily of nucleoporins. Indeed, in acute myeloid leukaemia resulting from the t(7;11)(p15;q15) translocation, it has been shown that binding of CBP to FG repeats is required for oncogenicity of the HOX9-NUP98 fusion protein.[30] The N-terminus region of NUP93, which contains leucine-containing heptad repeat sequences, appears to mediate binding to CBP via the SID. Interestingly, this region is released from the nucleoporin-associated core during apoptosis due to the presence of a caspase cleavage site (154-DALD-157) implying it may have additional functions in the nucleoplasm.[31]

HDACs play an essential role in regulating the cell-cycle, apoptosis and differentiation, at least in part through deacetylation of the N-terminal tails of histones. Aberrant recruitment of HDACs to the gene promoters by leukemogenic fusion proteins such as PML-RAR, PLZF-RAR and AML1-ETO has been implicated in the pathogenesis of many types of leukemias and cancers. Consequently, HDAC inhibitors are currently in clinical trials as anti-cancer agents.[32] While the mode of action of HDAC inhibitors as anticancer agents is unknown, it is likely to involve direct modulation of gene expression as HDACi treatment of cells increases global histone acetylation. However, the effects of HDACi compounds on the acetylation status on non-histone proteins are poorly understood, although it has been shown that HDACi treatment increases acetylation of Impα.[27] Here we have shown that treatment of COS-1 cells with TSA or NaB has a dramatic effect on the subcellular localisation of Impα, and also alters subcellular distribution of CAS and CBP. This observation suggests that HDACi compounds may pleiotropic effects that may combine to inhibit the growth of cancer cells. The observation that HDACi compounds induce an increase in the average number of PML bodies per cell also suggests a role for acetylation in regulating the formation of this compartment. Many proteins that are associated with PML bodies (including CBP) are posttranslationally modified by conjugation of SUMO the small ubiquitin like modifier protein. This modification occurs at lysine residues, which are also subject to acetylation, methylation and ubiquitination which impacts on the function, subcellular location and stability of the substrate proteins. HDACi compounds are likely to disrupt the balance of lysine modifications in the nuclear proteome.

PML body disruption has been implicated in the pathogenesis of acute promyelocytic leukaemia (APL), due to expression of PML-RAR fusion proteins. PML-RAR behaves as a dominant inhibitor of retinoic acid receptor target genes, due to multimerisation and recruitment of HDAC-containing corepressor complexes. This can be relieved in part by treatment with a combination of high doses of all trans retinoic acid and HDACi compounds. Another consequence of expression of PML-RAR is the disruption of PML bodies, as recently observed in murine fibroblasts.[33] It is possible that HDACi compounds may prevent reversible acetylation of proteins that assemble at PML bodies.

Recent studies in yeast have established clear link between nuclear transport proteins, nuclear organisation and gene transcription. Association of promoters with the nucleoporins has been observed to be an early event in gene activation in yeast. [34,35]

Moreover, components of the histone acetyltransferase SAGA complex have been shown to be involved in both transcription and mRNA export, and associate with nucleoporins. Nuclear transport proteins including CSE1 and Nic96 (homologues of CAS and NuP93, respectively) have been shown to be chromatin-associated proteins enriched at highly transcribed genes.[36] Yeast CSE1 has also been shown to function as function as a boundary insulator, which may depend on tethering to the nuclear pore.[37,38] Our findings provide evidence for an association of a mammalian histone acetyltransferase CBP with nuclear transport factors CAS and Impα, and the nucleoporin NUP93, raising the possibility that similar mechanisms of gene regulation exist in mammalian cells.

Acknowledgements

We are grateful to Andy Bannister, Tony Kouzarides, Regine Losson, Pierre Chambon, Eric Kalkhoven, Dirk Gorlich, for gifts of reagents. This work was supported by Wellcome Trust Senior Fellowship awarded to DMH (grant no. 054401/Z/98/B). CMR was supported by the BBSRC and the Department of Biochemistry, University of Leicester. HMC was supported by grants from Cancer Research UK and Leukemia Research Fund.

References

1. Kalkhoven E, CBP and p300: HATs for different occasions. Biochem. Pharmacol. 2004 68(6):1145-55.

2. Gu W, Roeder RG. Activation of p53 sequence-specific DNA binding by acetylation of the p53 C-terminal domain. Cell 1997 90(4):595-606

3. Imhof A, Yang XJ, Ogryzko VV, Nakatani Y, Wolffe AP, Ge H. Acetylation of general transcription factors by histone acetyltransferases, Curr. Biol. 1997 7(9):689-92.

4. Cohen HY, Lavu S, Bitterman KJ, Hekking H, Imahiyerobo TA, Miller C, Frye R, Ploegh H, Kessler BM, Sinclair DA. Acetylation of the C terminus of Ku70 by CBP and PCAF controls Bax-mediated apoptosis. Mol. Cell. 2004 13(5):627-38.

5. Polesskaya A, Duquet A, Naguibneva I, Weise C, Vervisch A, Bengal E, Hucho F, Robin P, Harel-Bellan A. CREB-binding protein/p300 activates MyoD by acetylation. J. Biol. Chem. 2000 275(44):34359-64.

6. Chen H, Lin RJ, Xie W, Wilpitz D, Evans RM. Regulation of hormone-induced histone hyperacetylation and gene activation via acetylation of an acetylase. Cell 1999 98(5):675-86.

7. Bannister AJ, Miska EA, Gorlich D, Kouzarides T. Acetylation of importin-alpha nuclear import factors by CBP/p300. Curr. Biol. 2000 10(8):467-70.

8. Kouzarides T. Acetylation: a regulatory modification to rival phosphorylation? EMBO J. 2000 19(6):1176-9.

9. Sheppard HM, Matsuda S, Harries JC, Kindle KB, Heery DM. Transcriptional activation by estrogen receptor (ERalpha) and steroid receptor coactivator (SRC1) involves distinct mechanisms in yeast and mammalian cells. J. Mol. Endocrinol. 2003 30(3):411-22.

10. Matsuda S, Harries JC, Viskaduraki M, Troke PJ, Kindle KB, Ryan C, Heery DM, A Conserved alpha-helical motif mediates the binding of diverse nuclear proteins to the SRC1 interaction domain of CBP, J. Biol. Chem. 2004 279(14):14055-64.

11. Waters L, Yue B, Ververka V, Renshaw P, Bramham J, Matsuda S, Frenkiel T, Kelly G, Muskett F, Carr M, Heery DM. Structural diversity in p160/CREB binding protein coactivator complexes. J. Biol. Chem. 2006 281(21):14787-95

12. Demarest SJ, Martinez-Yamout M, Chung J, Chen H, Xu W, Dyson HJ, Evans RM, P.E. Wright PE. Mutual synergistic folding in recruitment of CBP/p300 by p160 nuclear receptor coactivators. Nature 2002 415(6871):549-53.

13. Qin BY, Liu C, Srinath H, Lam SS, Correia JJ, Derynck R, Lin R. Crystal structure of IRF-3 in complex with CBP Structure 2005 13,1269-1277

14. Kutay U, Bischoff FR, Kostka S, Kraft R, Gorlich D. Export of importin alpha from the nucleus is mediated by a specific nuclear transport factor. Cell 1997 90(6):1061-71

15. Kindle KB, Troke PJ, Collins HM, Matsuda S, Bossi D, Bellodi C, Kalkhoven E, P. Salomoni P, Pelicci PG, Minucci S, Heery DM. MOZ-TIF2 inhibits transcription by nuclear receptors and p53 by impairment of CBP function. Mol. Cell. Biol. 2005 25(3):988-1002.

16. Le Douarin B, Heery DM, Gaudon C, vom Baur E, Losson R. Yeast two-hybrid screening for proteins that interact with nuclear hormone receptors. Methods Mol. Biol. 2001 176:227-48.

17. Brinkmann U, Brinkmann E, Gallo M, Pastan I. Cloning and characterization of a cellular apoptosis susceptibility gene, the human homologue to the yeast chromosome segregation gene CSE1. Proc. Natl. Acad. Sci. U. S. A. 1995 92(22):10427-31.

18. Kunzler M, Hurt EC. Cse1p functions as the nuclear export receptor for importin alpha in yeast. FEBS Lett. 1998 433(3):185-90.

19. Solsbacher J, Maurer P, Bischoff FR, Schlenstedt G. Cse1p is involved in export of yeast importin alpha from the nucleus. Mol. Cell. Biol. 1998 18(11):6805-15.

20. Hood JK, Silver PA, Cse1p is required for export of Srp1p/importin-alpha from the nucleus in Saccharomyces cerevisiae, J. Biol. Chem. 1998 273(52):35142-6

21. Grandi P, Schlaich N, Tekotte H, Hurt EC, Functional interaction of Nic96p with a core nucleoporin complex consisting of Nsp1p, Nup49p and a novel protein Nup57p, EMBO J. 1995 14(1):76-87.

22. Kalkhoven E, Valentine JE , Heery DM, Parker MG. isoforms of steroid receptor co-activator 1 differ in their ability to potentiate transcription by the oestrogen receptor. EMBO J. 1998 17, 232-243

23. McInerney EM, Rose DW, Flynn SE, Westin S, Mullen TM, Krones A, J. Inostroza J, Torchia J, Nolte RT, Assa-Munt N, Milburn MV, Glass CK, Rosenfeld MG. Determinants of coactivator LXXLL motif specificity in nuclear receptor transcriptional activation. Genes Dev. 1998 12(21):3357-68

24. Lin CH, Hare BJ, Wagner G, Harrison SC, Maniatis T, Fraenkel E. A small domain of CBP/p300 binds diverse proteins: solution structure and functional studies. Mol. Cell. 2001 8, 581-590.

25. Livengood JA, Scoggin KE, Van Orden K, McBryant SJ, Edayathumangalam RS, Laybourn PJ, Nyborg JK. p53 Transcriptional activity is mediated through the SRC1-interacting domain of CBP/p300. J. Biol. Chem. 2002 277, 9054-9061.

26. Brinkmann U, Brinkmann E, Gallo M, Scherf U, Pastan I. Role of CAS, a human homologue to the yeast chromosome segregation gene CSE1, in toxin and tumor necrosis factor mediated apoptosis. Biochemistry 1996 35(21):6891-9.

27. Matsuura Y, Stewart M. Structural basis for the assembly of a nuclear export complex. Nature 2004 432(7019):872-7.

28. Goldfarb DS, Corbett AH, Mason DA, Harreman MT, Adam SA. Importin alpha: a multipurpose nuclear-transport receptor. Trends Cell Biol. 2004 14(9):505-14.

29. Cook A, Fernandez E, Lindner D, Ebert J, Schlenstedt G, Conti E. The structure of the nuclear export receptor Cse1 in its cytosolic state reveals a closed conformation incompatible with cargo binding. Mol. Cell. 2005 18(3):355-67.

30. Kasper LH, Brindle PK, Schnabel CA, Pritchard CE, Cleary ML, van Deursen JM. CREB binding protein interacts with nucleoporin-specific FG repeats that activate transcription and mediate NUP98-HOXA9 oncogenicity. Mol. Cell. Biol. 1999 19(1):764-76.

31. Patre M, Tabbert A, Hermann D, Walczak H, Rackwitz HR, Cordes VC, Ferrando-May E. Caspases target only two architectural components within the core structure of the nuclear pore complex. J. Biol. Chem. 2006 281(2):1296-304

32. Choi Y, Elagib KE, Goldfarb AN. AML-1-ETO-Mediated erythroid inhibition: new paradigms for differentiation blockade by a leukemic fusion protein. Crit Rev Eukaryot Gene Expr. 2005 15(3):207-16.

33. Bellodi C, Kindle K, Bernassola F, Dinsdale D, Cossarizza A, Melino G, Heery D, Salomoni P. Cytoplasmic function of mutant promyelocytic leukemia (PML) and PML-retinoic acid receptor-alpha. J. Biol. Chem. 2006 281(20):14465-73.

34. Schmid M, Arib G, Laemmli C, Nishikawa J, Durussel T, Laemmli UK. Nup-PI: the nucleopore-promoter interaction of genes in yeast. Mol. Cell. 2006 21(3):379-91.

35. A. Taddei A, G. Van Houwe G, F. Hediger F, V. Kalck V, F. Cubizolles F, H. Schober H, S.M. Gasser SM. Nuclear pore association confers optimal expression levels for an inducible yeast gene. Nature 2006 441(7094):774-8

36. Casolari JM, Brown CR, Komili S, West J, Hieronymus H, Silver PA. Genome-wide localization of the nuclear transport machinery couples transcriptional status and nuclear organization. Cell (2004) 117(4):427-39.

37. Ishii K, Arib G, Lin C, Van Houwe G, Laemmli UK. Chromatin boundaries in budding yeast: the nuclear pore connection. Cell 2002 109(5):551-62.

38. Ishii K, Laemmli UK. Structural and dynamic functions establish chromatin domains. Mol. Cell. 2003 11(1):237-48.

Figure Legends

Figure 1. CBP-SID interacts with the nuclear export factor CAS (A) Quantitative β-galactosidase assays showing reporter activities in cell-free extracts of *S.cerevisiae* L40 expressing DBD LexA-CBP 1982-2163 with VP16 acidic domain (AAD) or CAS-N 1-349. Schematic representation of CAS-N isolated in the yeast two-hybrid screen and the full length protein. Shaded boxes refer to coding sequence; un-shaded boxes correspond to sequence derived from the 5'-UTR or intronic sequence in the cDNA. Ran Binding Domain (RBD), Heptad Repeats (HR)[21] (B) Yeast two-hybrid interaction of AAD-CAS (1-349) with a series of DBD LexA-CBP fusion proteins. Reporter assays were carried out as in A). A schematic representation of the CBP sequence 2058-2163 is shown, indicating four putative αHelices H1 to H4 (black boxes) and the QPGM/L repeat sequences (black triangles). (C) Yeast two-hybrid interaction between CAS-N and a series of LexA-CBP-SID fusion constructs containing point mutations. CBP sequences are represented schematically, and the black box denotes the minimal SID as previously described. (D) Yeast two-hybrid interaction of DBD lexA-CBP with CAS-N and CAS-NΔ244-255. (E) COS1 cells were transiently transfected with FLAGCAS-N (green) and stained after 48Hrs for endogenous CBP (red) (F) COS-1 cells were transfected with CAS-N and pSG5CBP and harvested after 48 hrs. Yellow denotes co-localisation.

Figure 2. HDACi perturbs the subcellular localisation of CBP and CAS proteins. (A) COS-1 cells were either treated with vehicle (ethanol) or treated with 10μM TSA or 10mM NaB for 18hrs before harvesting. Epifluorescence microscopy showing the subcellular localisation of endogenous CAS (green) and endogenous CBP (red).

Figure 3. Endogenous CBP and PML colocalise after treatment with HDACi. (A) COS-1 cells were treated with vehicle (ethanol), treated with 10μM TSA or 10mM NaB for 18 hrs prior to being fixed in 4% paraformaldehyde. The cells were co-stained for endogenous CBP (green) and PML (red) proteins. (B) Quantification of the number of PML bodies in untreated cells or cells treated with vehicle (ethanol), 1μM TSA, 5μM TSA, 10μM TSA, 5mM NaB, 10mM NaB or 20mM NaB. For each condition the total number of PML bodies were counted in 50 cells (n=50).

Figure 4. HDACi modulate the interaction between Impα and CBP proteins

(A) COS-1 cells were either treated with vehicle (ethanol) or treated with 10μM TSA 18hrs prior to fixation in 4% paraformaldehyde. The cells were stained with antibodies specific for Impα (green) and CBP (red). (B) COS1 cells were transfected with an expression vector encoding CBP and stained with antibodies raised against Impα (green) and CBP (red). (C) HEK293 cells were either untransfected or transfected with expression constructs for CBP and Impα. The cells were then treated with 10μM TSA 18hrs prior to being harvested. CBP was immunoprecipitated and the blots were probed for Impα and CBP proteins. (Asterisks denotes probable hyperacetylated form of Impα). (D) COS-1 cells were transfected with an expression vector encoding Impα alone or co-transfected with pSG5CBP. 18hrs prior to being harvested the cells were incubated with or without 10μM TSA and after fixation, were stained for Impα (green) and CBP (red) proteins.

FIGURE 1

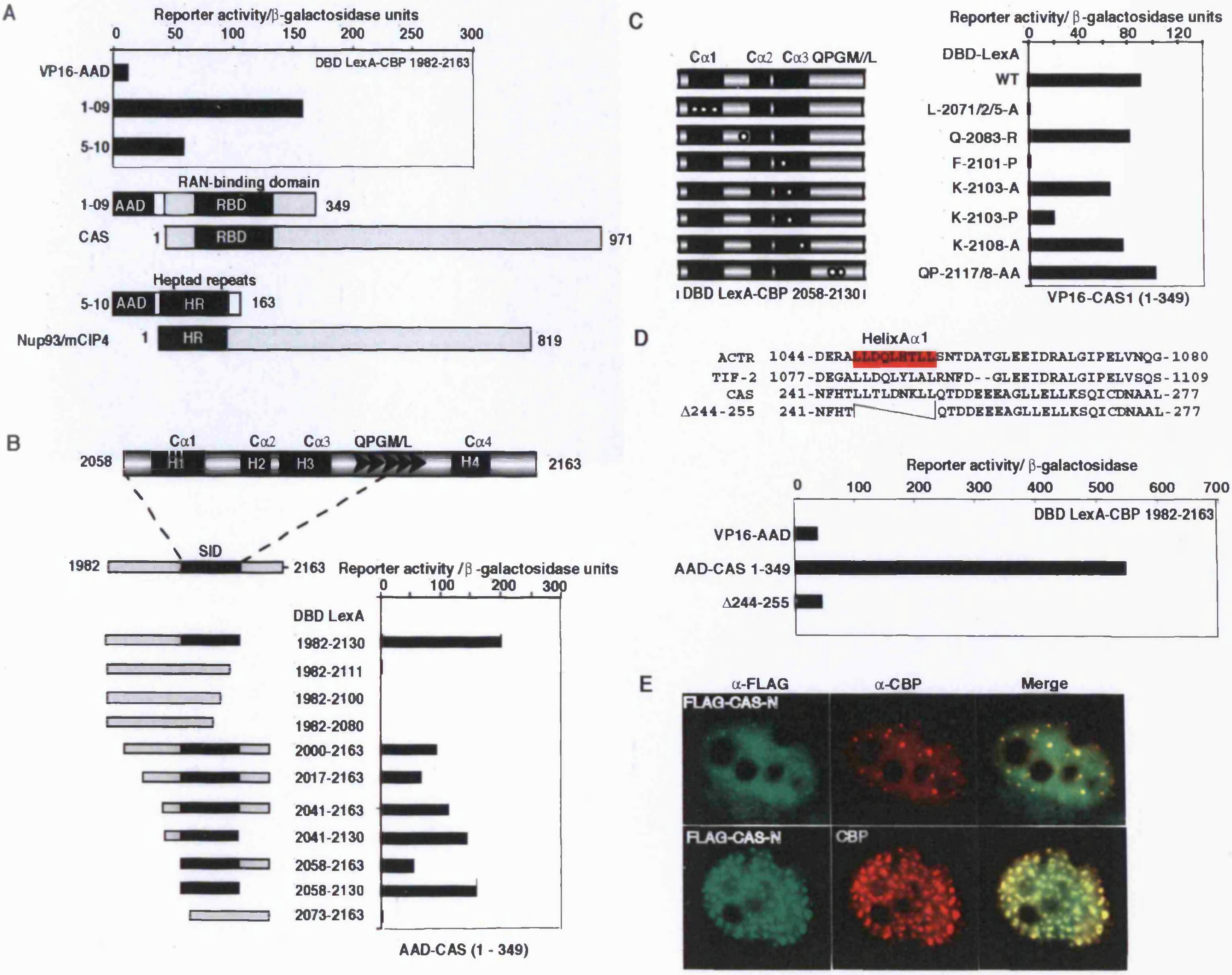
A
Reporter activity/β-galactosidase units
0
50
100
150
200
250
300
DBD LexA-CBP 1982-2163
VP16-AAD
1-09
5-10
RAN-binding domain
1-09
AAD
RBD
349
CAS
1
RBD
971
Heptad repeats
5-10
AAD
HR
163
Nup93/mCIP4
1
HR
819
B
Cα1
Cα2
Cα3
QPGM/L
Cα4
2058
H1
H2
H3
H4
2163
SID
1982
2163
Reporter activity /β -galactosidase units
0
100
200
300
DBD LexA
1982-2130
1982-2111
1982-2100
1982-2080
2000-2163
2017-2163
2041-2163
2041-2130
2058-2163
2058-2130
2073-2163
AAD-CAS (1 - 349)
C
Cα1
Cα2
Cα3
QPGM/L
DBD LexA-CBP 2058-2130
Reporter activity/ β -galactosidase units
0
40
80
120
DBD-LexA
WT
L-2071/2/5-A
Q-2083-R
F-2101-P
K-2103-A
K-2103-P
K-2108-A
QP-2117/8-AA
VP16-CAS1 (1-349)
D
HelixAα1
ACTR 1044-DERALLDQLHTLLSNTDATGLEEIDRALGIPELVNQG-1080
TIF-2 1077-DEGALLDQLYLALRNFD--GLEEIDRALGIPELVSQS-1109
CAS 241-NFHTLLTLDNKLLQTDDEEEAGLLELLKSQICDNAAL-277
Δ244-255 241-NFHT QTDDEEEAGLLELLKSQICDNAAL-277
Reporter activity/ β-galactosidase
0
100
200
300
400
500
600
700
DBD LexA-CBP 1982-2163
VP16-AAD
AAD-CAS 1-349
Δ244-255
E
α-FLAG
α-CBP
Merge
FLAG-CAS-N
FLAG-CAS-N
CBP

Figure 2

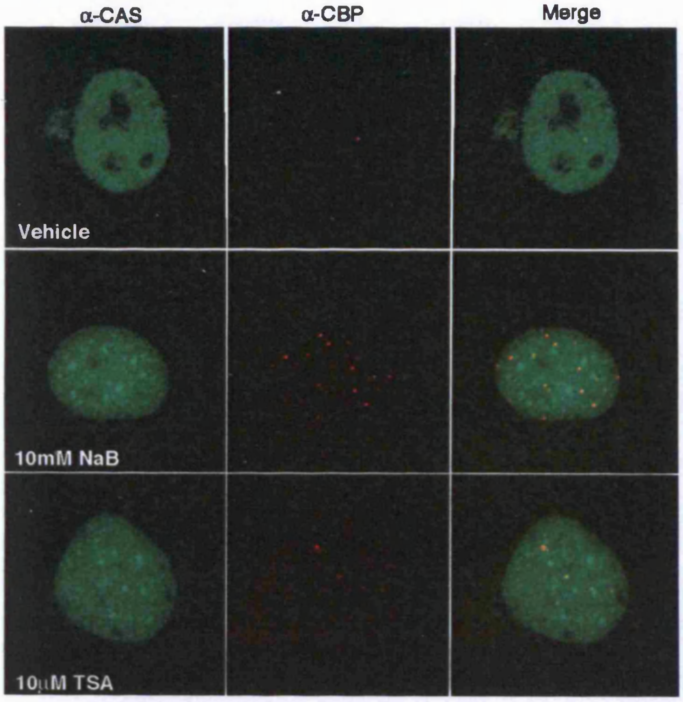
α-CAS
α-CBP
Merge
Vehicle
10mM NaB
10μM TSA

Figure 3

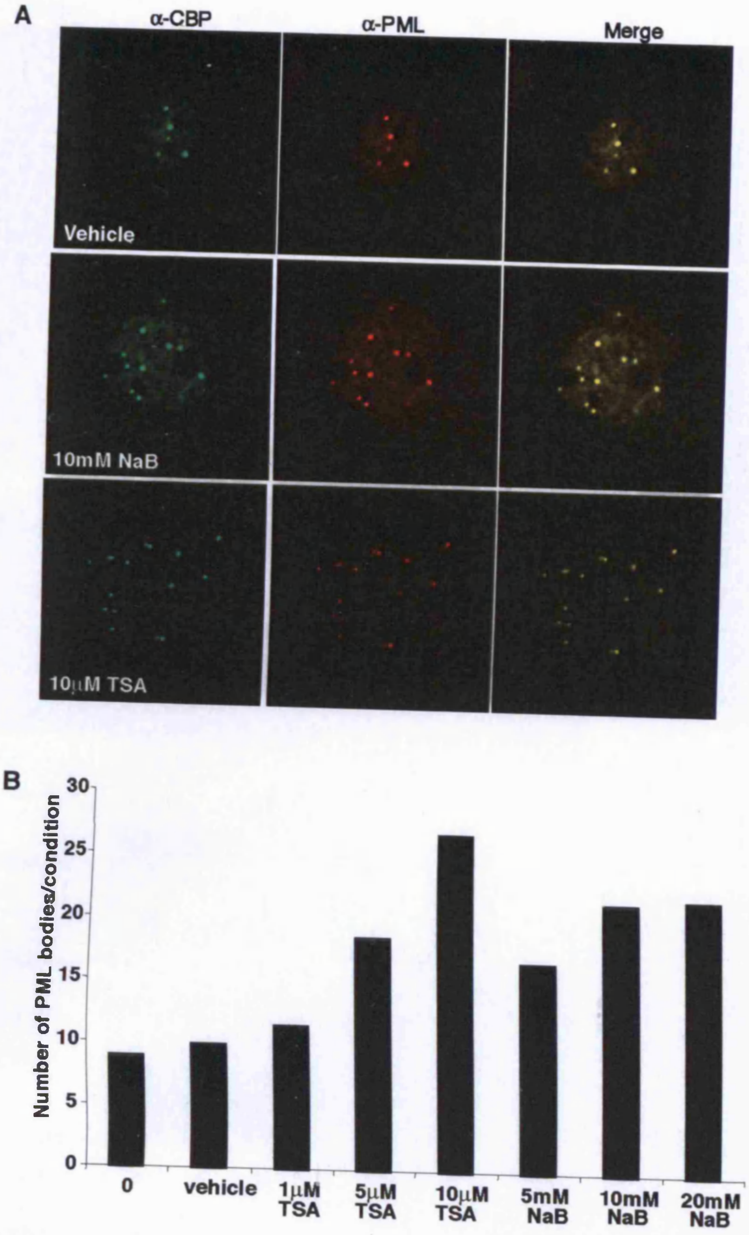
A
α-CBP
α-PML
Merge
Vehicle
10mM NaB
10μM TSA
B
Number of PML bodies/condition
0
5
10
15
20
25
30
0
vehicle
1μM TSA
5μM TSA
10μM TSA
5mM NaB
10mM NaB
20mM NaB

Figure 4

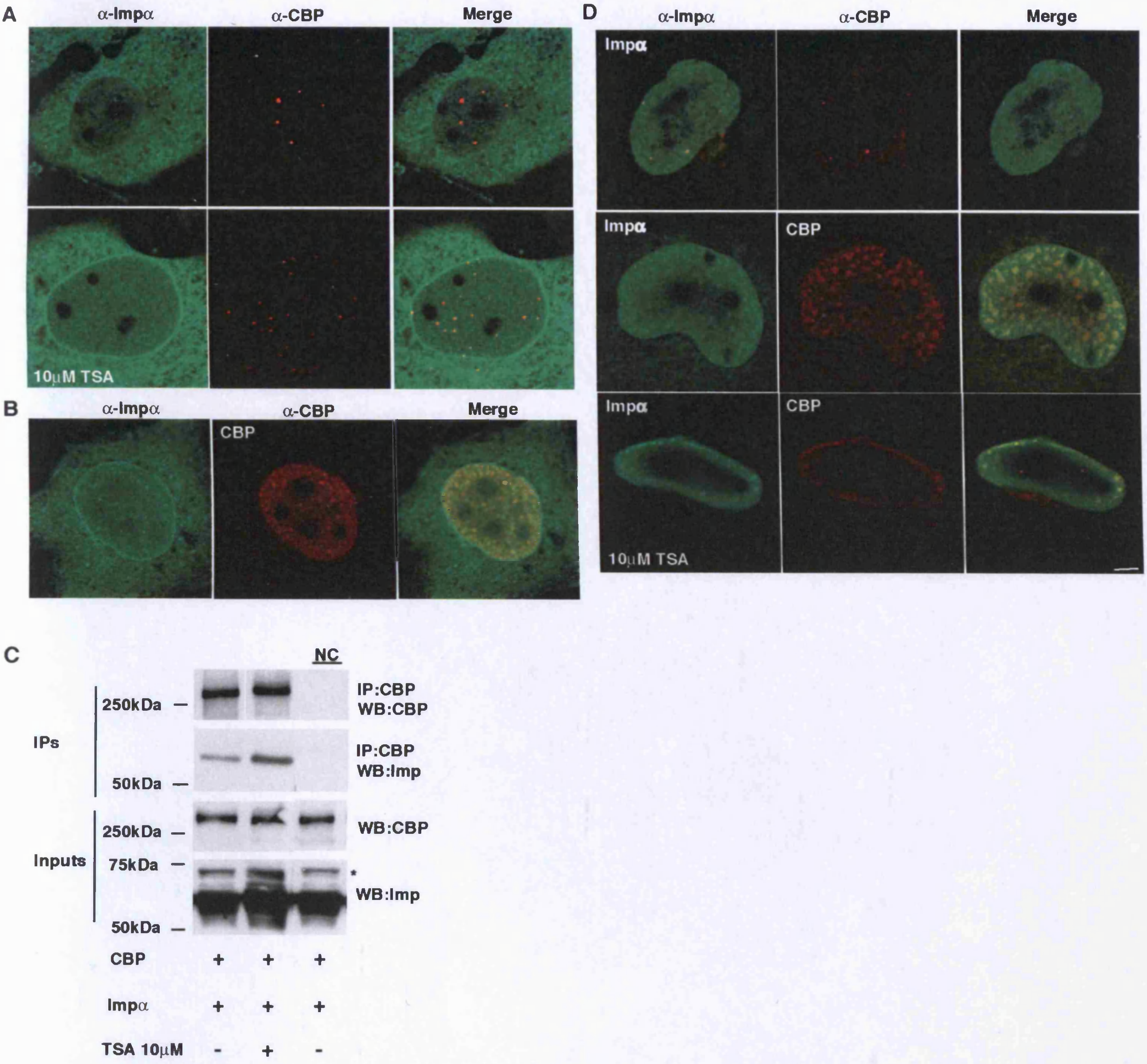
A
α-Impα
α-CBP
Merge
10μM TSA
B
α-Impα
α-CBP
CBP
Merge
C
NC
IPs
250kDa
50kDa
IP:CBP
WB:CBP
IP:CBP
WB:Imp
Inputs
250kDa
75kDa
50kDa
WB:CBP
*
WB:Imp
CBP + + +
Impα + + +
TSA 10μM - + -
D
α-Impα
α-CBP
Merge
Impα
Impα
CBP
Impα
CBP
10μM TSA